

Characterization of phage-host interactions in
Stenotrophomonas maltophilia

by

Jaclyn Grace McCutcheon

A thesis submitted in partial fulfillment of the requirements for the degree of

Doctor of Philosophy

in

Molecular Biology and Genetics

Department of Biological Sciences
University of Alberta

© Jaclyn Grace McCutcheon, 2022

Abstract

Bacteriophages are highly abundant viruses that replicate within and effectively kill specific target bacterial hosts. The specificity of phages to their host relies on the presence of the correct cell surface receptor that is recognized by phage receptor binding proteins. These properties make phages desirable as an alternative to antibiotics for the treatment of multidrug resistant bacterial infections, a concept termed phage therapy that has gained renewed interest in recent years. One such bacterium of concern is *Stenotrophomonas maltophilia*, a Gram-negative opportunistic pathogen that is rapidly increasing in prevalence in hospital and community-acquired infections worldwide, due largely to its numerous innate antibiotic resistance mechanisms. To further develop phage therapy against *S. maltophilia* and address an overlooked aspect of phage characterization, I have identified the cellular surface receptor for eight *S. maltophilia* phages. Seven phages with Siphoviridae morphologies adhere to the major pilin subunit of the type IV pilus, a virulence factor that aids in motility, adherence to surfaces and biofilm formation. The eighth phage was identified to putatively interact with the TonB-dependent iron uptake protein, CirA, as a novel phage receptor. To further assess two of these phages as therapeutic candidates, I analyzed their complete genome sequences and phenotypic properties. Phage AXL1 was identified to encode resistance to the frontline antibiotic combination trimethoprim-sulfamethoxazole, whereas AXL3 is a novel virulent phage and candidate for genetic engineering. Additionally, I investigated the lack of in vivo data for *S. maltophilia* and show that type IV pili-binding phage DLP3 rescues *Galleria mellonella* larvae from lethal *S. maltophilia* infection. Further investigation into the mechanism of host interactions for the type IV pili binding phages identified the surface exposed $\alpha\beta$ -loop of the major pilin protein as a structural region important for phage binding, as well as two tail proteins in phage

DLP2 as putative receptor binding proteins for cross-genera bacterial infection. The identification of bacterial virulence factors as host receptors makes these phages promising candidates for an anti-virulence phage therapy strategy in which phage treatment creates a selective pressure for bacterial avirulence if phage resistant mutants arise.

Preface

Content from Chapter 1 as well as a portion of Chapter 7 were published as JG McCutcheon and JJ Dennis “The potential of phage therapy against the emerging opportunistic pathogen *Stenotrophomonas maltophilia*,” 2021 *Viruses*, volume 13, article 1057 (doi.org/10.3390/v13061057). I reviewed the published literature and drafted the manuscript including all figures and tables. JJ Dennis assisted in manuscript editing.

Chapter 2 of this thesis was published as JG McCutcheon, DL Peters, and JJ Dennis “Identification and characterization of the type IV pili as the cellular receptor of broad host range *Stenotrophomonas maltophilia* bacteriophages DLP1 and DLP2,” 2018 *Viruses*, volume 10, article 338 (doi:10.3390/v10060338). I collected and analyzed the data presented in this publication and drafted the manuscript, apart from the bioinformatic analyses in Figure 4 and the supplementary material and accompanying text that were performed and written by DL Peters and are not included in this thesis. JJ Dennis supervised this project and contributed to conceptualization, manuscript composition and editing.

Chapter 3 includes original unpublished research and some published data conducted by JG McCutcheon. A portion of Figure 3-1 was published in DL Peters, JG McCutcheon, P Stothard and JJ Dennis “Novel *Stenotrophomonas maltophilia* temperate phage DLP4 is capable of lysogenic conversion,” 2019 *BMC Genomics*, volume 20, article 300 (doi.org/10.1186/s12864-019-5674-5) as my contribution to the paper. A portion of Figure 3-1 and the entirety of Figure 3-13 along with the corresponding text was published in DL Peters, JG McCutcheon, and JJ Dennis “Characterization of novel broad-host-range bacteriophage DLP3 specific to *Stenotrophomonas maltophilia* as a potential therapeutic agent,” 2020 *Frontiers in Microbiology*, volume 11, article 6 (doi:10.3389/fmicb.2020.01358) as my contribution to the published paper.

Chapter 4 of this thesis and a portion of Figure 3-1 was published as JG McCutcheon, A Lin, and JJ Dennis “Isolation and characterization of the novel bacteriophage AXL3 against *Stenotrophomonas maltophilia*,” 2020 *International Journal of Molecular Sciences*, volume 21, article 6338 (doi:10.3390/ijms21176338). A Lin isolated phage AXL3 and conducted preliminary host range analysis. I collected and analyzed the data presented in this publication

and drafted the manuscript. JJ Dennis supervised this project and contributed to conceptualization and manuscript editing.

Chapter 5 of this thesis and a portion of Figure 3-1 was published as JG McCutcheon, A Lin, and JJ Dennis “Characterization of *Stenotrophomonas maltophilia* phage AXL1 as a member of the genus *Pamexvirus* encoding resistance to trimethoprim-sulfamethoxazole,” 2022 *Scientific Reports*, volume 12, article 10299 (doi:10.1038/s41598-022-14025-z). A Lin isolated phage AXL1 and conducted preliminary host range analysis. I collected and analyzed the data presented in this publication and drafted the manuscript. JJ Dennis supervised this project and contributed to conceptualization and manuscript editing.

The data and analysis presented in Chapter 6 is original research conducted by JG McCutcheon and is unpublished.

Acknowledgements

I would first like to thank my supervisor Dr. Jonathan Dennis. You welcomed me into your lab as a quiet undergraduate student from MacEwan University and gave me the opportunities to grow into the scientist, mentor, and leader I am today. I am incredibly grateful for all your support and encouragement of even my wildest ideas, and for believing in my abilities when I doubted myself. My accomplishments these past six years would not have been possible without your mentorship.

Thank you to my committee members, Dr. Lisa Stein and Dr. Dominic Sauvageau, for your wisdom, guidance and encouragement throughout my degree, as well as Dr. Tracy Raivio and Dr. Kimberley Harcombe for your support and for generously writing me reference letters.

Thank you to the talented staff at the Molecular Biology Service Unit, the Advanced Microscopy Facility, the Biological Sciences Storeroom, and the administrative staff in the department for research support. I would also like to thank NSERC, Alberta Innovates, the Government of Alberta, Novartis Pharmaceuticals Inc., and numerous University of Alberta donors for their generous funding that together gave me the freedom to discover research that I love without added financial stress.

Thank you to the past and present members of the Dennis and Raivio labs for the helpful scientific discussions and office chats. I learned from and mentored some amazing people in the past six years, and I am a better scientist and person for having known every one of you. To Dr. Danielle Peters, Dr. Randi Guest, and Dr. Fatima Kamal, your accomplishments, guidance, and mentorship gave me the confidence to pursue a PhD and I am grateful for the friendship you showed me. To Carly Davis, Marta Ruest and Brittany Supina, I could not have made it through the last few years without your friendship and all the pep talks. I can't wait to see what you accomplish. Grad school during a global pandemic was no joke and we survived it together.

Thank you to my friends and family for their unwavering love and support at every step of the way, even when you had no idea what my research entailed. To my parents, you set me up for success and believed in me. Monica and Mariam Takla, you were my biggest cheerleaders during both the ups and the downs, and I am so thankful for our trio.

Finally, thank you to Greg. You kept me grounded, gave me perspective, and reminded me to explore a world outside of the lab. And of course, to my cat Aurora, whose careful supervision made writing this thesis a little less stressful.

Table of Contents

CHAPTER 1 - Introduction	1
Introduction	2
<i>Stenotrophomonas maltophilia</i>	2
Clinical prevalence and significance	4
<i>S. maltophilia</i> virulence factors	6
Antimicrobial resistance mechanisms of <i>S. maltophilia</i>	11
Phage Therapy	13
Bacteriophages.....	13
Phage-bacterial host interactions	16
Clinical data using phages	18
Phage therapy strategies	19
<i>S. maltophilia</i> Phages	21
<i>S. maltophilia</i> phage characteristics	22
Potential of phage therapy for <i>S. maltophilia</i>	35
Thesis Objectives	35
CHAPTER 2 - Identification and characterization of type IV pili as the cellular receptor of broad host range <i>Stenotrophomonas maltophilia</i> bacteriophages DLP1 and DLP2	37
Objectives.....	38
Materials and Methods	38
Bacterial strains, phages, and growth conditions	38
Transposon mutant library receptor screen	40
Phage plaquing assays	40
Construction of $\Delta pilA$ <i>S. maltophilia</i> D1585 and 280 mutants	41
Complementation of pilus mutants.....	45

Transmission electron microscopy	45
Twitching motility assay	46
Results and Discussion.....	46
<i>P. aeruginosa</i> PA01 type IV pilus mutants are resistant to DLP1 infection	46
Complementation in <i>P. aeruginosa</i> restores DLP1 infectivity.....	50
Deletion of <i>pilA</i> in <i>S. maltophilia</i> D1585 prevents DLP1 and DLP2 infection	56
Deletion of <i>pilA</i> in <i>S. maltophilia</i> 280 prevents DLP2 infection.....	58
Conclusions	61
Acknowledgements	62
CHAPTER 3 - Identification of the type IV pilus as a common receptor for	
<i>Stenotrophomonas maltophilia</i> bacteriophages and the potential for anti-virulence phage	
therapy	63
Objectives.....	64
Materials and Methods	64
Bacterial strains, bacteriophages and growth conditions.....	64
Host range analysis	66
Phage plaquing assays	67
Mutant construction.....	67
Transmission electron microscopy (TEM)	70
Phage resistant mutant isolation and genome sequencing.....	70
Twitching motility	71
Bioinformatics	72
Complementation of D1571 <i>pilQ</i> ⁻	72
<i>Galleria mellonella</i> killing and phage rescue assays.....	73
<i>Lemna minor</i> virulence assay	74
Results and Discussion.....	74

Phage <i>S. maltophilia</i> host ranges	74
Type IV pili receptor identification	77
Analysis of the DLP5 phage receptor	81
<i>Xanthomonas</i> spp. phage susceptibility	85
<i>S. maltophilia</i> type IV pili as virulence factors and phage rescue in <i>G. mellonella</i>	89
Investigation of the DLP6 receptor	96
Conclusions	102
Acknowledgements	102
CHAPTER 4 - Isolation and characterization of the novel bacteriophage AXL3 against <i>Stenotrophomonas maltophilia</i>.....	103
Objectives.....	104
Materials and Methods	104
Bacterial strains and growth conditions.....	104
Phage isolation, propagation, and host range	104
Transmission electron microscopy	106
Determining phage lifecycle.....	106
One-step phage growth curve	107
Growth reduction assay	107
Phage plaquing assays	108
Phage DNA isolation, RFLP analysis, and sequencing.....	108
Bioinformatic analysis.....	109
Results and Discussion.....	111
Isolation, morphology, and host range	111
Genomic characterization	114
DNA replication and repair module	123

Virion Morphogenesis Module.....	126
Lysis module.....	127
Conclusions	130
Acknowledgments.....	130
CHAPTER 5 - Characterization of <i>Stenotrophomonas maltophilia</i> phage AXL1 as a member of the genus <i>Pamexvirus</i> encoding resistance to trimethoprim-sulfamethoxazole	
Objectives.....	132
Materials and Methods	132
Bacterial strains and growth conditions.....	132
Phage isolation, propagation and host range analysis	133
Transmission electron microscopy	134
One-step growth curve.....	134
Growth reduction assay and phage lifestyle analysis	135
Twitching motility	135
Phage DNA isolation, RFLP analysis and genome sequencing	136
Bioinformatic analysis	136
Proteomic analysis of virion-associated proteins	137
Antibacterial susceptibility checkerboard assays	138
Results	139
AXL1 phage physical characteristics	139
Genomic characterization.....	143
DNA replication, repair, and packaging module.....	147
Structural proteins within the virion morphogenesis module.....	159
YbiA operon	160
Lysis module.....	162

Lifestyle analysis	163
AXL1-encoded DHFR contributes to host resistance to trimethoprim	163
Discussion	167
Acknowledgements	170
CHAPTER 6 - Investigating the host interactions of type IV pili-binding bacteriophages of <i>Stenotrophomonas maltophilia</i>.....	171
Objectives.....	172
Materials and Methods	172
Bacterial strains, bacteriophages and growth conditions.....	172
Cloning and modification of <i>S. maltophilia pilA1</i> genes.....	174
Twitching motility	178
DLP2 training on PA01	179
Bioinformatics	179
Phage receptor binding protein swapping	180
Results and Discussion.....	180
Investigation of phage binding sites on PilA1 of the type IV pilus.....	180
Prediction of phage receptor binding proteins.....	186
Examining putative phage RBPs	191
Conclusions	194
Acknowledgements	195
CHAPTER 7 - Conclusions and future directions	196
Summary	197
Future Directions.....	198
DLP6 receptor confirmation.....	198
Role of type IV pili in <i>S. maltophilia</i> virulence	199

Phage engineering: expanding phage host range by RBP swapping	202
Perspectives on <i>S. maltophilia</i> phage therapy	205
Significance	209
Appendix – Genomic characterization of <i>Xanthomonas</i> phage HXX.....	210
Objectives.....	211
Materials and Methods	211
Bacterial strains, growth conditions and phage propagation	211
HXX DNA isolation and genome sequencing.....	212
Bioinformatics	212
Results and Discussion.....	213
HXX_Dennis host range.....	213
Genomic characterization	213
Bibliography	222

List of Tables

Table 1-1: <i>S. maltophilia</i> phage characteristics.	26
Table 2-1: List of bacterial strains, phages, and plasmids used in this study.	39
Table 2-2: Primers used in this study.....	43
Table 2-3: Characteristics of <i>P. aeruginosa</i> PA01 transposon mutants.	48
Table 2-4: <i>P. aeruginosa</i> PA01 genes involved in type IV pilus biogenesis and DLP1 phage infection identified by a transposon mutant library screen.	49
Table 2-5: Summary of DLP1 and DLP2 phage susceptibility of cross complemented <i>pilA</i> mutants.	61
Table 3-1: Bacterial strains and plasmids used in this study.	65
Table 3-2: Primers used in this study.....	68
Table 5-1: Strains and plasmids used in this study.....	132
Table 5-2: <i>S. maltophilia</i> clinical isolates susceptible to AXL1.....	141
Table 5-3: Genome annotations for AXL1 obtained from BLASTp and CD-search data.	149
Table 5-4: The conserved domains found in 83 AXL1 proteins.	156
Table 5-5: Virion-associated proteins identified by proteomic analysis of CsCl-purified AXL1 virions.	161
Table 5-6: Minimum inhibitory concentrations (MICs) of trimethoprim (μg/mL) in <i>E. coli</i> DH5α and <i>S. maltophilia</i> clinical isolates expressing AXL1 <i>dhfr</i> in the presence of 32 μg/mL sulfamethoxazole.	164
Table 6-1: Bacterial strains and plasmids used in this study.	173
Table 6-2: Primers used in this study.....	175
Table 6-3: Summary of putative phage RBPs tested for broadened host infectivity in new phages.	193
Table A-1: Host range analysis of <i>Xanthomonas</i> phage HXX_Dennis on clinical <i>S. maltophilia</i> isolates.....	214

List of Figures

Figure 1-1: Transmission electron micrograph of <i>S. maltophilia</i> cell attacked by phages.....	3
Figure 1-2: <i>S. maltophilia</i> pathogenicity and antibiotic resistance mechanisms.....	7
Figure 1-3: Prophage prevalence in 47 complete <i>S. maltophilia</i> genomes.....	14
Figure 1-4: <i>S. maltophilia</i> phage phylogenetic tree.....	34
Figure 2-1: Infection of <i>P. aeruginosa</i> PA01 expressing varying pilin subunits by DLP1 and DLP2.....	51
Figure 2-2: DLP1 interacts with pili on the cell surface of wildtype <i>S. maltophilia</i> D1585 and <i>P. aeruginosa</i> PA01.....	52
Figure 2-3: Twitching motility is partially restored in cross-genera complemented <i>P. aeruginosa</i> PA01 pilin mutants.....	54
Figure 2-4: Infection of <i>S. maltophilia</i> D1585 expressing varying pilin subunits by DLP1 and DLP2.....	58
Figure 2-5: Infection of <i>S. maltophilia</i> 280 expressing varying pilin subunits by DLP1 and DLP2.....	60
Figure 3-1: <i>S. maltophilia</i> bacteriophages require functional type IV pili for infection.....	79
Figure 3-2: Deletion of <i>pilT</i> in <i>S. maltophilia</i> D1585 produces hyperpiliated cells.....	80
Figure 3-3: DLP1 and DLP2 bacteriophages require a functional type IV pilus for infection.....	80
Figure 3-4: Truncation of PilQ in D1571 provides resistance to DLP5 and DLP3.....	84
Figure 3-5: <i>S. maltophilia</i> phages DLP3 and DLP5 require a type IV pilus for infection.....	85
Figure 3-6: DLP5 requires cell-mediated pilus retraction for successful infection.....	85
Figure 3-7: <i>Xanthomonas</i> phage HXX uses the type IV pilus as its receptor.....	88
Figure 3-8: Virulence of <i>Xanthomonas</i> spp. in <i>Lemna minor</i>	89
Figure 3-9: <i>S. maltophilia</i> type IV pilin gene cluster compared to related phytopathogen <i>Xylella fastidiosa</i> and pathogen <i>P. aeruginosa</i>	90
Figure 3-10: Role of the type IV pilus in virulence of <i>S. maltophilia</i> strain 280 in <i>G. mellonella</i>	91
Figure 3-11: Role of type IV pili or fimbriae in virulence of <i>S. maltophilia</i> strain D1585 in <i>G. mellonella</i>	92
Figure 3-12: Role of type IV pili and fimbriae in virulence of <i>S. maltophilia</i> strain ATCC13637 in <i>G. mellonella</i>	93

Figure 3-13: Effect of DLP3 on the virulence of D1571 in <i>G. mellonella</i>	95
Figure 3-14: Phage susceptibility of <i>S. maltophilia</i> D1571 DLP6 resistant mutant.	97
Figure 3-15: <i>S. maltophilia</i> D1571 gene mutations in DLP6 resistant isolates.	98
Figure 3-16: Putative Fur-box and promoter sequence upstream of D1571 <i>cirA</i> gene.	100
Figure 3-17: Transmission electron micrographs of <i>S. maltophilia</i> D1571 in the presence of phage DLP6.	101
Figure 4-1: Transmission electron micrograph of AXL3.	111
Figure 4-2: Infection dynamics of AXL3 on <i>S. maltophilia</i> strain D1585.	113
Figure 4-3: Circularized genomic map of AXL3.	114
Figure 4-4: Restriction digests of AXL3 gDNA show evidence of base modification.	116
Figure 4-5: Network representation of AXL3 phylogeny.	117
Figure 5-1: AXL1 phage morphology.	140
Figure 5-2: Infection dynamics of AXL1 on <i>S. maltophilia</i> strain D1585.	142
Figure 5-3: Temperature stability of AXL1 virions.	143
Figure 5-4: Circularized genomic map of AXL1.	144
Figure 5-5: Comparative genome alignment of AXL1 and phages of the <i>Pamexvirus</i> genus. ..	146
Figure 5-6: Restriction digests of AXL1 gDNA.	147
Figure 5-7: AXL1-encoded dihydrofolate reductase functions to increase trimethoprim resistance in <i>S. maltophilia</i> in the presence of sulfamethoxazole.	167
Figure 6-1: Effect of internal <i>pilA1</i> truncation on twitching motility in <i>S. maltophilia</i> 280.	182
Figure 6-2: <i>S. maltophilia</i> pilins exhibit sequence heterogeneity and a conserved structure.	183
Figure 6-3: Amino acids 77 and 79 affect phage infection in <i>S. maltophilia</i> D1585.	185
Figure 6-4: <i>S. maltophilia</i> type IV pilin gene cluster organization.	188
Figure 6-5: Comparative genome alignment of type IV pili-binding <i>S. maltophilia</i> phages.	189
Figure 6-6: Percent identity matrix of type IV pili phage tail proteins containing a phage-tail_3 domain.	189
Figure 6-7: Comparative genomic alignment of related phages, DLP1 and DLP2, to AXL3.	190
Figure 6-8: Schematic of phage RBP swapping in phage progeny without genetic engineering.	192
Figure 6-9: Effect of exogenous putative RBPs in progeny phage on host susceptibility.	194
Figure 7-1: Deletion of <i>pilA2</i> does not affect phage infection.	201

List of Abbreviations

AA	amino acid
ABC	ATP binding cassette
AHL	<i>N</i> -acyl homoserine lactone
bp or kb	base pair or kilobase pair
CANWARD	Canadian Ward Surveillance
CBCRRR	Canadian <i>Burkholderia cepacia</i> complex Research and Referral Repository
c-di-GMP	cyclic diguanylate monophosphate
CD-Search	conserved domain search
CDS	coding domain sequence
CF	cystic fibrosis
CFU	colony forming units
Cm	chloramphenicol
CYPHY	CYstic Fibrosis bacterioPHage Study at Yale
°C	degrees Celsius
DNA	deoxyribonucleic acid
dsDNA	double-stranded deoxyribonucleic acid
DSF	diffusible signal factor
DUF	domain of unknown function
eIND	expanded access Investigational New Drug
g, mg, µg, ng	grams, milligrams, micrograms, nanograms
gDNA	genomic DNA
gp	gene product
h	hour
IAA	indole-3-acetic acid
ICU	intensive care unit
ID	identity
IPATH	Innovative Phage Applications and Therapeutics

ISCR	insertion sequence common region
kV	kilovolt
L, mL, μ l	liter, millilitre, microliter
LB	Lennox broth
MFS	major facilitator superfamily
min	minute
mM or M	millimolar or molar
MOI	multiplicity of infection
MUSCLE	MUltiple Sequence Comparison by Log Expectation
N/A	not applicable
NCBI	National Center for Biotechnology Information
nm	nanometer
NSERC	Natural Sciences and Engineering Research Council
OD	optical density
ORF	open reading frame
PAS	phage antibiotic synergy
PCR	polymerase chain reaction
PFU	plaque forming units
PTLB	phage tail-like bacteriocins
RBS	ribosome binding site
RBP	receptor binding protein
RFLP	restriction fragment length polymorphism
RND	resistance-nodulation-cell-division
s	seconds
SM	suspension medium
Smc	<i>Stenotrophomonas maltophilia</i> complex
SNP	single nucleotide polymorphism
ssDNA	single-stranded deoxyribonucleic acid

T2SS	type II secretion system
T4SS	type IV secretion system
T4P	type IV pilus
TAILOR	Tailored Antibacterials and Innovative Laboratories for Phage (Φ) Research
Tc	tetracycline
TEM	transmission electron microscopy
TMP/SMX	trimethoprim/sulfamethoxazole
Tp	trimethoprim
tRNA	transfer ribonucleic acid

CHAPTER 1 - Introduction

A version of this chapter has been published as:

McCutcheon JG, Dennis JJ. 2021. The potential of phage therapy against the emerging opportunistic pathogen *Stenotrophomonas maltophilia*. *Viruses*. 13:1057. doi.org/10.3390/v13061057. Impact factor (IF): 5.048

Introduction

The increasing prevalence of broad-spectrum antimicrobial resistance in bacterial infections worldwide is a global health concern. Use and misuse of antimicrobials have driven the evolution of resistant bacteria and the effectiveness of current antibiotics against bacterial pathogens is rapidly declining, created the risk of a post-antibiotic era in the near future; reports estimate that antimicrobial resistant bacterial infections will cause 10 million deaths annually worldwide by the year 2050 with significant socio-economic impacts if alternative treatment options are not discovered [1,2].

Stenotrophomonas maltophilia is one bacterium of concern that is emerging as a multidrug resistant opportunistic nosocomial pathogen. *S. maltophilia* infections are difficult to treat with conventional antibiotics due to numerous chromosomally encoded antimicrobial resistance mechanisms [3]. The use of bacterial viruses, or bacteriophages, as an alternative treatment is an attractive option due to the specificity of these viruses to their host. In this chapter I will first briefly summarize the current existing research on *S. maltophilia* pathogenicity mechanisms and then examine the potential of phage therapy as an alternative treatment option to antibiotics in light of the extreme antibiotic resistance of this bacterial pathogen.

Stenotrophomonas maltophilia

S. maltophilia is a Gram-negative obligate aerobe that is motile due to the presence of polar flagella, as well as type IV pili that aid in twitching motility and biofilm formation [3–5] (Figure 1-1). This bacteria is ubiquitous in the environment, often having beneficial interactions with plants, both on their surface and in the rhizosphere [6]. First isolated as *Bacterium bookeri* in 1943 by J. L. Edwards, this species was originally named *Pseudomonas maltophilia* by Hugh and Ryschenko in 1961 [7], followed by controversial reclassification into the genus *Xanthomonas* in 1983 [8] before finally being given its own genus in 1993 [9]. *S. maltophilia* is now one of 23 species in the genus *Stenotrophomonas* currently listed in the NCBI taxonomy browser. Strains with 16S rRNA gene sequence similarities greater than 99.0% have been grouped into the '*S. maltophilia* complex' (Smc) to encompass the genetic heterogeneity and diversity of these bacteria [10].

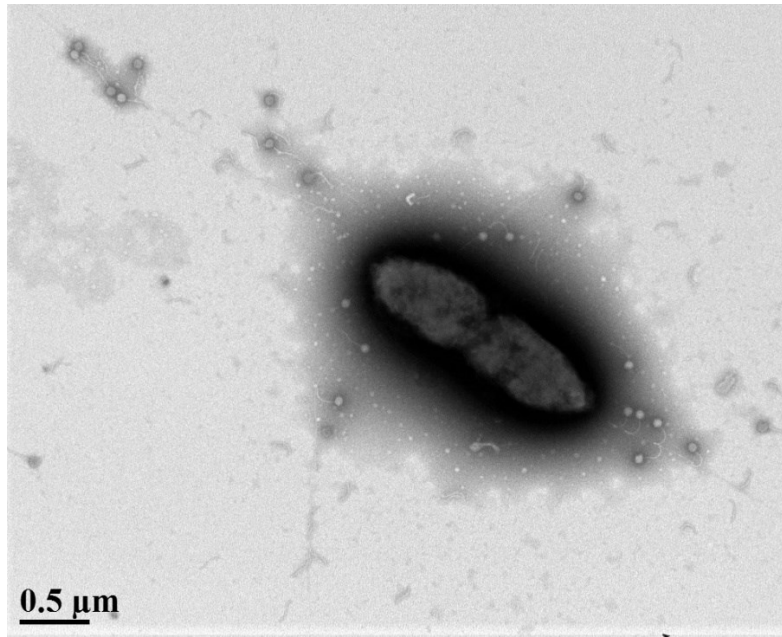


Figure 1-1: Transmission electron micrograph of *S. maltophilia* cell attacked by phages. *S. maltophilia* strain D1585 with numerous DLP1 bacteriophage [11] virions binding to type IV pili that are protruding from the cell. Cells and phage were stained with 2% phosphotungstic acid and visualized at 18,000-fold magnification by transmission electron microscopy. (TEM: McCutcheon, J. G. and Oatway, A.; University of Alberta).

The genus name *Stenotrophomonas*, translating as “narrow one who feeds,” was meant to reflect the perceived limited nutritional spectrum of these bacteria, however further research has demonstrated the vast metabolic diversity and intraspecific heterogeneity within this genus [6,12]. We now know that *S. maltophilia* bacteria are capable of utilizing a wide range of carbon sources, have an intrinsic resistance to heavy metals, and tolerate nutrient-poor environments, allowing them to survive and persist in many undesirable conditions [3,6,13]. In addition to the ability to metabolize a variety of organic compounds, such as phenolics and xenobiotics, *Stenotrophomonas* species are not phytopathogenic, unlike the closely related genera *Xanthomonas* and *Xylella*, and can promote plant productivity via the expression of the plant growth hormone indole-3-acetic acid (IAA) [6]. These properties make *S. maltophilia* a desirable candidate for the bioremediation of soil contaminated with heavy metals or pesticides and for

biotechnical applications in agriculture to promote plant productivity [6,13–15], however, the ability of *S. maltophilia* to cause disease in humans discourages their use in agriculture [6,13].

Clinical prevalence and significance

S. maltophilia is the most prominent species within this genus and is of rising concern due to its ability to cause human disease [3,6]. The significant genetic and phenotypic heterogeneity within *S. maltophilia* populations allows these bacteria to adapt rapidly under changing selective pressures in both a clinical and environmental setting [3,5,10,13,16]. This high genetic diversity can be observed even between isolates from the same hospital [17], with higher mutation frequencies observed in clinical isolates compared to those from environmental sources [18]. Global surveillance programs began tracking the prevalence and clinical significance of *S. maltophilia* in the late 1990s; the frequency of *S. maltophilia* occurrence among bacterial isolates from all sources ranged from 0.8% to 1.4% during 1997 to 2003 time period and increased to prevalence rates of 1.3% to 1.68% in the years 2007 to 2013 [19]. Current data from the Canadian Ward Surveillance Study (CANWARD) identified *S. maltophilia* at a frequency of 2.98% in the nearly 3,000 pathogens isolated from hospitalized patients in the year 2018 [20]. These data suggest an increasing trend in *S. maltophilia* infections in recent years.

Recently, a comprehensive genome-based phylogenetic analysis of an international collection of 1,305 Smc isolates from 22 countries, 87% of which were from clinical origin, was undertaken to understand the global population structure of the Smc, identify human-associated lineages, and the potential for global and local spread [21]. The genome collection clustered into 23 monophyletic lineages named Sgn1-Sgn4 and Sm1-Sm18, with lineage Sgn4 most distantly related to the rest of the strains. The largest lineage was Sm6 and comprises the highest rate of human-associated strains. Key virulence and antibiotic resistance genes, including multiple efflux pumps, were found in all lineages, however some genes were unequally distributed. Notably, through genetic diversity analysis the authors identified hospital-linked clusters of strains collected within short time intervals, suggesting potential direct or indirect human-to-human transmission. Although average nucleotide identity between the 23 lineages clearly distinguishes them, the authors note that it is also below the threshold considered to define a

species, suggesting further studies to revise the taxonomic assignments and nomenclature for this group are required [21].

Numerous virulence factors including biofilm formation and the secretion of hydrolytic enzymes that allow environmental *S. maltophilia* isolates to colonize plant surfaces and compete with other soil microbes are also important for colonization of medical devices and patients [6]. Listed by the World Health Organization as one of the leading drug-resistant nosocomial pathogens worldwide [22], this opportunistic pathogen is rapidly increasing in prevalence in nosocomial and community-acquired infections worldwide, passing easily between immunocompromised patients and health care providers through direct contact and cough-generated aerosols [3]. A recent ranking of the top ten most serious multidrug resistant bacteria affecting critically ill patients in intensive care units specifically also included trimethoprim-sulfamethoxazole resistant *S. maltophilia* as a medium priority pathogen [23]. Most commonly associated with respiratory infections, including pneumonia and acute exacerbations of chronic obstructive pulmonary disease, *S. maltophilia* can also cause severe bacteremia, meningitis, endocarditis, osteomyelitis, endophthalmitis, biliary sepsis, and catheter-related bacteremia/septicemia [3]. Numerous risk factors for *S. maltophilia* infection include chronic respiratory disease, the presence of indwelling devices, underlying malignancy, a compromised immune system, prior use of antibiotics, and prolonged hospital or ICU stay [3,24]. *S. maltophilia* can adhere to and form biofilms on plastic surfaces, allowing colonization of many humid hospital surfaces, as well as intravenous cannulae, prosthetic devices and nebulizers [3,19]. In response to starvation or stress, these bacteria are also able to form ultramicrocells that can pass through 0.2 μm filters similar to point-of-use water filtration used in hospital showers, potentially becoming a source for hospital-acquired infection [25]. In addition, tolerance to antiseptics and hydrogen peroxide-based disinfectants is provided by the presence of *qacEΔ1* and *katA* genes in many isolates [3,21,26,27], making *S. maltophilia* well-equipped to persist and spread in hospital settings.

Patients with cystic fibrosis are at greater risk for *S. maltophilia* infections than the general population with prevalence increasing significantly in recent decades [28,29]; data collected in 2019 by Cystic Fibrosis Canada and the Cystic Fibrosis Foundation shows that *S. maltophilia* were present in the airways of 14% and 11.9% of patients with cystic fibrosis in Canada and the USA, respectively [28,30]. Although the pathogenicity of *S. maltophilia* and its

role as a colonizer of cystic fibrosis lungs or causative agent of disease has been unclear [3,31,32], retrospective studies indicate that this bacterium is a marker of lung disease severity [32–34]. *S. maltophilia* isolates are highly immunostimulatory and have been shown to significantly increase expression of the potent pro-inflammatory cytokine TNF- α in a murine lung, likely contributing to airway inflammation and the development of pneumonia [35]. Of particular concern is the interaction between *S. maltophilia* and other pathogens in polymicrobial infections of the cystic fibrosis lung, specifically *Pseudomonas aeruginosa*, one of the most prominent pathogens found in cystic fibrosis patients [32,34,36,37]. Studies show cooperativity between these bacterial species, with each bacterium benefitting from the presence of the other. Reports indicate that polymicrobial infection with *S. maltophilia* and *P. aeruginosa* in patients with cystic fibrosis may increase virulence, as patients with co-infections had significantly higher mortality rates than those with monoculture infections [38]. Early studies in vitro showed that *S. maltophilia* can encourage growth of *P. aeruginosa* in the presence of β -lactam antibiotics due to secretion of β -lactamases, indirectly contributing to disease progression [37]. Additionally, interspecies communication has been observed to occur through quorum sensing; *S. maltophilia*-produced diffusible signal factor (DSF) is recognized by *P. aeruginosa*, resulting in significantly altered biofilm structure and virulence factor expression, including increased tolerance to cationic antimicrobial peptides [39]. Although no *S. maltophilia* strain has been reported to produce an *N*-acyl homoserine lactone (AHL) quorum sensing signaling molecule, *S. maltophilia* is also capable of sensing *P. aeruginosa*-produced (AHL) using its LuxR solo SmoR (Smlt1839) protein, leading to changes in virulence factors such as swarming motility [40]. This synergy can also be observed in vivo; co-microbial infections with *P. aeruginosa* resulted in significantly higher *S. maltophilia* bacterial loads in the murine lung and this increase was directly correlated with live *P. aeruginosa* cell density [36].

***S. maltophilia* virulence factors**

Although *S. maltophilia* is not considered a highly virulent pathogen to healthy individuals, increasing nosocomial infection rates are of concern. Pathogenesis of infections caused by this bacterium involves numerous virulence factors and the ability to form biofilms on abiotic surfaces and host cells [3,41]. Production of virulence factors has been linked to iron availability in the infection environment; under iron-restricted conditions or in a ferric uptake

regulator *fur* mutant, *S. maltophilia* K279a produces more dense biofilms, increased amounts of exopolysaccharide and DSF, and is more virulent than in wildtype or iron-rich conditions [42]. This is concerning because in the lung iron is not biologically available due to lactoferrin sequestration, potentially contributing to increased pathogenicity of *S. maltophilia* infections [42,43]. Analyses of early whole genome sequencing data of *S. maltophilia* strain K279a identified numerous putative virulence and antimicrobial resistance genes by homology to known factors in other pathogens [44]. Research has since sought to characterize cell-associated and extracellular virulence factor mechanisms and their role in the pathogenesis of *S. maltophilia*. Specifically, research into the mechanisms of adherence to and colonization of medical devices and epithelial cells, which allows the formation of antibiotic and immune resistant biofilms that are characteristic of *S. maltophilia* infections and disease progression, is of utmost importance [3,41,45]. The main virulence factors and antibiotic resistance mechanisms in *S. maltophilia* discussed below are summarized in Figure 1-2.

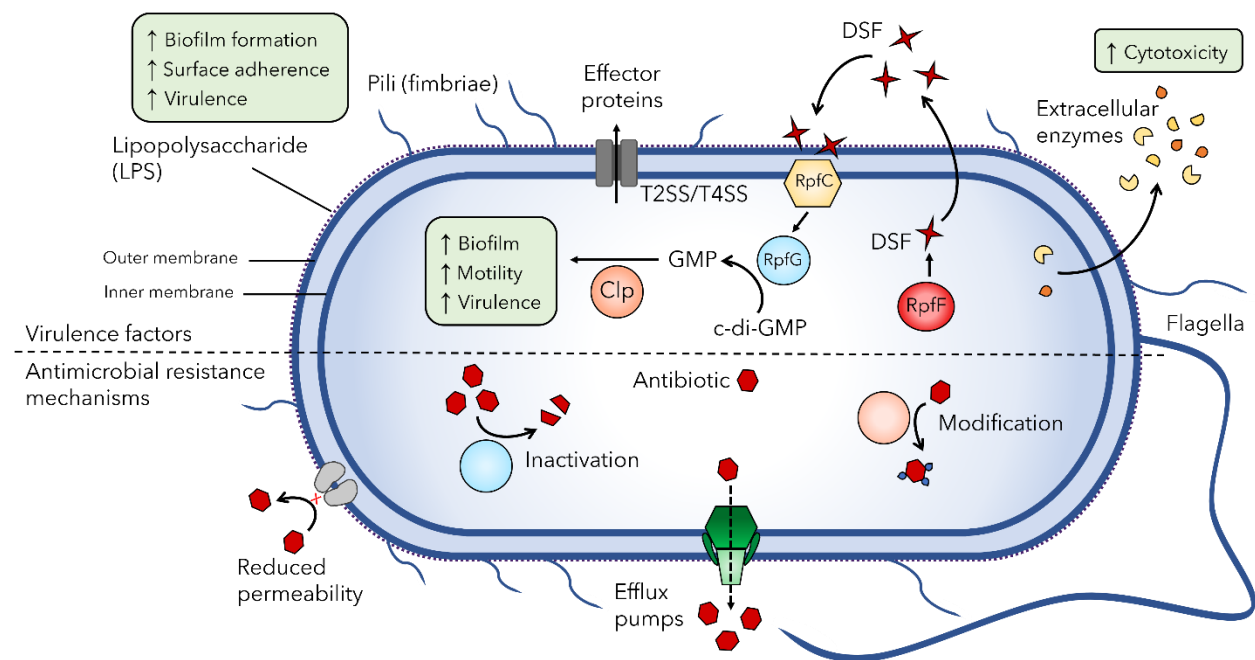


Figure 1-2: *S. maltophilia* pathogenicity and antibiotic resistance mechanisms. *S. maltophilia* encodes many virulence factors that contribute to its pathogenicity. Hydrolytic enzymes (yellow and orange shapes) released from the cell and secreted effector proteins contribute to cytotoxicity. Surface structures such as LPS, flagella, type IV pili, and SMF-1 fimbriae help the bacterium adhere to surfaces and form antibiotic resistant biofilm communities,

contributing to increased virulence. Quorum sensing via diffusible signal factors (DSF, red stars) induces downstream gene expression shown to increase biofilm, motility and virulence factors described. The extreme multidrug resistance of this bacterium is due to numerous mechanisms, including reduced membrane permeability, numerous chromosomally encoded efflux pumps, β -lactamases and aminoglycoside-modifying enzymes. Antibiotic molecules are represented by red hexagons.

S. maltophilia isolates express numerous cell-associated virulence factors on their surface. The outer lipopolysaccharide (LPS) layer of *S. maltophilia* is structurally diverse between strains [35,46] and plays an important role in colonization and virulence in a host; research has shown that *spgM* mutants deficient in the assembly of O-polysaccharide are unable to colonize rat lungs and are completely avirulent in this animal model, showing no histopathological changes [47]. Additionally, *spgM* mutants were susceptible to complement-mediated killing, exhibiting increased sensitivity to human serum compared to wildtype [47]. The *rmlBACD* and *xanAB* operons that are involved in synthesis of lipopolysaccharide and exopolysaccharide also contribute to biofilm formation, with defective LPS production associated with decreased biofilm formation on hydrophobic surfaces [48]. Motility and fimbriae structures are also important for virulence and contribute to the formation of biofilms through adherence. The flagella is an important immunogenic structure that is found at the pole of the cell and is responsible for swimming motility [48,49]. Studies show that the *S. maltophilia* flagella plays a role in adherence to abiotic plastic surfaces [49] as well as mouse tracheal mucus [50], and flagella-deficient mutants have significantly reduced adherence to human bronchial epithelial cell monolayers obtained from cystic fibrosis patients [51]. We identified three *fliC* flagellin genes encoded in tandem in many *S. maltophilia* genomes, including our sequenced strains. Deletion of all three genes abolishes swimming motility in *S. maltophilia* strain 280 (data not shown) but does not affect its ability to survive in human serum (data not shown; serum susceptibility assay conducted by MSc student Marta Ruest). A recent publication examined the effect of non-polar deletions of the three genes in all combinations on flagella function and morphology [52]. Single and double mutants displayed different flagellar morphologies and reduced swimming motility, suggesting that the flagellins are not redundant and their composition affects filament morphology and function. Differential expression of these flagellin

subunits therefore likely contributes to host evasion, however this was not explored in their study. The type 1 fimbriae SMF-1 is also implicated in adhesion to epithelial cells [53]. This adhesion, as well as adherence to abiotic surfaces, was inhibited by anti-SMF-1 antibodies. Also involved in haemagglutination and biofilm formation, SMF-1 fimbriae were identified in all clinical isolates tested [53], and were absent from *S. maltophilia* isolates of environmental origin [54], suggesting a role in respiratory tract infection in cystic fibrosis patients. Lastly, the type IV pilus is an important virulence factor on the bacterial cell surface that plays a role in motility, adherence to biotic and abiotic surfaces, and biofilm formation in many bacterial pathogens [55]. In *S. maltophilia*, type IV pili-mediated twitching motility has been correlated with increased biofilm mass in cystic fibrosis isolates [5,48] and although the majority of clinical isolates are twitching positive [5,56], the role of type IV pili in virulence has not been studied in depth in *S. maltophilia*.

Numerous secreted enzymes and proteins have been studied for their contribution to *S. maltophilia* pathogenesis as extracellular virulence factors. These include proteases, lipases, phospholipases, esterases, nucleases, haemolysins, cytotoxins, and siderophores [3,41,44]. The production of these enzymes provides a competitive advantage in unfavourable conditions, such as the rhizosphere, but also contributes to cytotoxicity [6,41,57]. The major protease StmPr1 that is associated with tissue destruction and evasion of host defense mechanisms [58], along with serine proteases StmPr2 and StmPr3, were recently shown to be substrates of the Xps type II secretion system (T2SS) in *S. maltophilia* [59–61]. These secreted proteases are largely responsible for Xps-mediated detrimental morphological and cytotoxic effects on lung epithelial cells, demonstrating the significance of the Xps T2SS in *S. maltophilia* pathogenesis.

Recently, *S. maltophilia* has also been found to encode a VirB/VirD4 type IVA secretion system (T4SS) that is highly conserved within the species [62,63]. T4SSs are diverse systems found in both Gram-positive and Gram-negative bacteria, functioning to deliver DNA and/or effector proteins into eukaryotic or bacterial targets [64]. The *S. maltophilia* T4SS was found to promote both an antiapoptotic effect in lung epithelial cells as well as a proapoptotic effect on macrophages in a contact-dependent manner, likely due to the secretion of different effector proteins [62]. This system was also shown to give *S. maltophilia* a competitive growth advantage against other bacteria, including *Escherichia coli*, *Klebsiella pneumoniae*, and *P. aeruginosa*, due to the targeted bacterial cell killing through the secretion of effector toxins [62,63]. The role

of the *S. maltophilia* T4SS in establishing infections as well as interacting with other pathogens in coinfections warrants further investigation.

Regulation of the expression of numerous *S. maltophilia* virulence factors is in part controlled by quorum sensing via the diffusible signal factor (DSF) system. First described in the related bacterial species *Xanthomonas campestris* pv. *campestris* as a regulator of virulence [65], research shows that the DSF quorum sensing system also controls many virulence-related phenotypes in *S. maltophilia* [66–69]. Stimulated RpfF synthesizes DSFs such as cis- Δ^2 -11-methyl-2-dodecenoic acid that is released to the extracellular environment; the sensor kinase RpfC detects accumulated DSF and induces the cytoplasmic regulator RpfG to degrade cyclic diguanylate monophosphate (c-di-GMP) to GMP, activating the transcriptional regulator Clp to stimulate virulence gene expression [70] (Figure 1-2). The effects of deletion of *rpfF* in *S. maltophilia* K279a and resultant loss of DSF production are pleiotropic, causing reductions in virulence and motility and changes in biofilm formation [66]. These effects could be reversed with *rpfF* complementation in trans or supplementation with DSF. In addition, DSF can stimulate the production and secretion of outer membrane vesicles found to contain the putative quorum sensing factor Ax21 among other proteins [71,72]. *S. maltophilia* secreted outer membrane vesicles are shown to have cytotoxic effects on human lung epithelial cells, stimulating the expression of proinflammatory cytokines and chemokines [73]. The putative diffusible signal Ax21 also has pleiotropic effects, with Ax21-deficient mutants exhibiting decreased motility, biofilm formation, tolerance to tobramycin and virulence compared to their wildtype counterparts [74]. Additionally, Ax21 abundance was shown to be directly proportional to mortality in a zebrafish model [45]. Motility deficits could be restored to wildtype levels in the presence of exogenous Ax21, consistent with the putative function as a signal molecule involved in cell-to-cell communication [74], however further investigation is needed.

As described above, cross talk between *S. maltophilia* and *P. aeruginosa* quorum sensing systems has significant implications for the clinical outcome of cystic fibrosis patients that have polymicrobial infections [38], therefore quorum quenching remains a strong therapeutic potential for further research. Although *S. maltophilia* isolates have the genetic potential for numerous virulence mechanisms, more research on the functionality of many of these virulence factors beyond homology relationships is needed to understand their role in *S. maltophilia* pathogenicity.

Antimicrobial resistance mechanisms of *S. maltophilia*

The rise in *S. maltophilia* infections worldwide is largely due to its intrinsic resistance to numerous frontline antibiotics. *S. maltophilia* exhibits resistance to a wide range of structurally unrelated antibiotics, including β -lactam antibiotics, macrolides, cephalosporins, aminoglycosides, carbapenems, chloramphenicol, tetracyclines and polymyxins [3]. This resistance is attributed to multiple intrinsic and acquired antibiotic resistance mechanisms including reduced membrane permeability, numerous chromosomally encoded efflux pumps, β -lactamases, and aminoglycoside-modifying enzymes (Figure 1-2).

Typical of Gram-negative bacteria, *S. maltophilia* isolates exhibit reduced membrane permeability due to the rigid structure of their cell envelope that provides protection against the passive diffusion of antibiotics [75]. A major contributor to the high level of multidrug resistance observed in *S. maltophilia* strains is the numerous efflux pumps that mediate the active extrusion of multiple classes of antimicrobials across the largely impenetrable cell envelope. Multidrug efflux pumps form a tripartite double membrane-spanning channel consisting of an inner membrane protein that binds the substrate, an outer membrane porin, and a membrane fusion protein that connects the inner and outer membrane proteins in the periplasmic space [76]. Over a dozen efflux pumps have been identified in *S. maltophilia*, with the majority belonging to the resistance-nodulation-cell-division (RND) family [44]. These include SmeABC [77], SmeDEF [78,79], SmeGH [80], SmeJK [81], SmeMN [44], SmeOP [82], SmeVWX [83] and SmeYZ [84], the molecular mechanism for each characterized, with the exception of SmeMN. Two ATP binding cassette (ABC) family efflux pumps, SmrA [85] and MacABCsm [86], and one major facilitator superfamily (MFS) efflux pump, EmrCABsm [87] have also been characterized in *S. maltophilia*. The final efflux pump identified in this bacterium is FuaABC and contributes to fusaric acid resistance [88]. Collectively, these efflux pumps provide intrinsic and adaptive resistance to the antibiotics listed above [19,89].

Antimicrobial resistance in *S. maltophilia* is more elegant than simple upregulation of efflux pumps. These bacteria encode a plethora of drug resistance mechanisms targeted to specific classes of antibiotics, many of which are antibiotic modifying enzymes. Resistance to β -lactam antibiotics in *S. maltophilia* is largely determined by two chromosomally encoded inducible β -lactamases, L1 and L2 [3,19,90]. L1 is a broad spectrum Zn^{2+} -dependent metallo- β -lactamase and L2 is a clavulanic acid-sensitive cephalosporinase, both of which are regulated by

AmpR, a transcriptional regulator located upstream of L2 [90]. The presence of a TEM-type β -lactamase encoded on a mobilizable TnI-like transposon has also been reported in the genomes of clinical isolates of *S. maltophilia* [91]. Aminoglycoside resistance is primarily due to aminoglycoside-modifying enzymes, in addition to the efflux pumps SmeABC, SmeOP, SmeYZ, and MacABCsm in *S. maltophilia* [19]. Three of these enzymes have been characterized in *S. maltophilia* to date. These include the aminoglycoside acetyltransferases AAC(6')-Iz [92] and AAC(6')-Iak [93], and the aminoglycoside phosphotransferase APH(3')-IIc [94].

Unlike other bacteria, quinolone resistant *S. maltophilia* isolates do not carry mutations in their topoisomerases [95]. Instead, low level resistance to quinolones stems from a chromosomal resistance gene, *smqnr*, encoding a pentapeptide repeat protein that protects the DNA gyrase and topoisomerase IV from inhibition by quinolones [96,97]. Additional quinolone resistance is largely provided by efflux pumps, including SmeDEF and SmeVWX [98,99]. The current recommended treatment for *S. maltophilia* infections is trimethoprim/sulfamethoxazole (TMP/SMX), and although susceptibility remains high, resistance to this antibiotic is increasing [100]. This is due to the presence of the sulfonamide resistance genes *sul1* carried by class 1 integrons and *sul2* associated with insertion sequence common region (ISCR) elements [26,101,102]. Dihydrofolate reductase encoding *dfrA* genes have also been found in Class 1 integrons and contribute to increased TMP/SMX resistance [100]. Additional TMP/SMX resistance in *S. maltophilia* is attributed to the efflux pumps SmeDEF, SmeOP, and SmeYZ. The choice of TMP/SMX as the recommended frontline treatment for *S. maltophilia* infections is also problematic due to the potential sulfonamide allergies in patients and cross-reactivity with other drugs limiting its use [103].

The majority of antimicrobial resistance genes in *S. maltophilia* are not associated with mobile genetic elements, however intrinsic resistance via multidrug efflux pumps and aminoglycoside-modifying enzymes are widespread, with several families of efflux pumps ubiquitously present in *S. maltophilia* strains of all 23 lineages identified by Gröschel et al. [21]. The inability to control *S. maltophilia* infections due to this intrinsic and adaptive multi-drug resistance as well as range of virulence factors increases mortality and morbidity and exemplifies the need for alternative treatments to combat this antibiotic resistant bacterium.

Phage Therapy

Bacteriophages

The pathogenicity and prevalence of *S. maltophilia* infections worldwide combined with the high level of antimicrobial resistance in these bacteria emphasizes the need for alternative treatments. Phage therapy is one promising treatment option under development. Bacteriophages, or phages for short, are bacterial viruses that recognize and bind to a specific host bacterium by recognition of a cell surface receptor to infect and kill the target bacterial species. Discovered over a century ago, phages were first used therapeutically to treat bacterial dysentery and cholera [104,105], however, controversy surrounding the efficacy of phage therapy combined with the discovery of broad-spectrum antibiotics in the 1940s meant that phages were no longer considered a viable treatment option in the West [106]. Research and application of phage therapy continued in Eastern European countries, however, with active phage therapy treatment centers such as the Eliava Institute in Tbilisi, Georgia and the Ludwik Hirszfeld Institute in Wrocław, Poland existing to this day [104,105].

Most phages undergo one of two replication cycles within a bacterial host cell following attachment of the viral particle to the bacterial cell surface [107]. Virulent phages replicate via the lytic cycle; the phage injects its genetic material into the cytoplasm and hijacks host cell metabolism to express phage genes and replicate its genome, followed by assembly of progeny virions that are released into the surrounding environment after phage-induced cell lysis. A successful infection by a virulent phage will release tens to hundreds of progeny phages that can infect surrounding bacterial cells, leading to exponential propagation. In contrast, temperate phages are capable of lysogeny, in which the phage genome integrates into the bacterial chromosome as a stable prophage or exists as a circular “phagemid” and lays dormant, replicating with the bacterial genome and passing vertically to daughter cells through bacterial cell division. In response to host cell stress or environmental cues, the prophage excises from the bacterial chromosome and resumes the lytic cycle to release progeny virions from the cell. Prophages naturally exist in approximately half of sequenced bacteria, with many strains containing multiple intact or partial prophages that can constitute 10–20% of a bacterial genome [108–110]. To determine the prevalence of intact prophages and prophage remnants in *S. maltophilia* specifically, an updated version of PHAST [111,112] was used to identify putative

prophage regions present in sequenced *S. maltophilia* strains with complete genomes in the NCBI database (February 2021). Of these 47 isolates, 23 are of clinical origin, 20 are from environmental sources and four are of unknown origin. Within the 47 unique genomes analyzed, 188 prophage regions were identified with 78 predicted to be intact prophages (Figure 1-3). Strain FDAARGOS_1044 (accession: NZ_LS483377.1) was predicted to have the most prophage regions with 11, three of which were classified as intact, six as incomplete, and two as questionable, whereas only one strain, AA1 (accession: NZ_CP018756.1), had zero predicted prophage regions. Although many bacteria have phage defense systems to protect against phage predation and possibly prophage integration, these systems, including CRISPR-Cas immunity, have not yet been characterized in *S. maltophilia* [113–115], potentially contributing to the high prevalence of prophage DNA in their genomes.

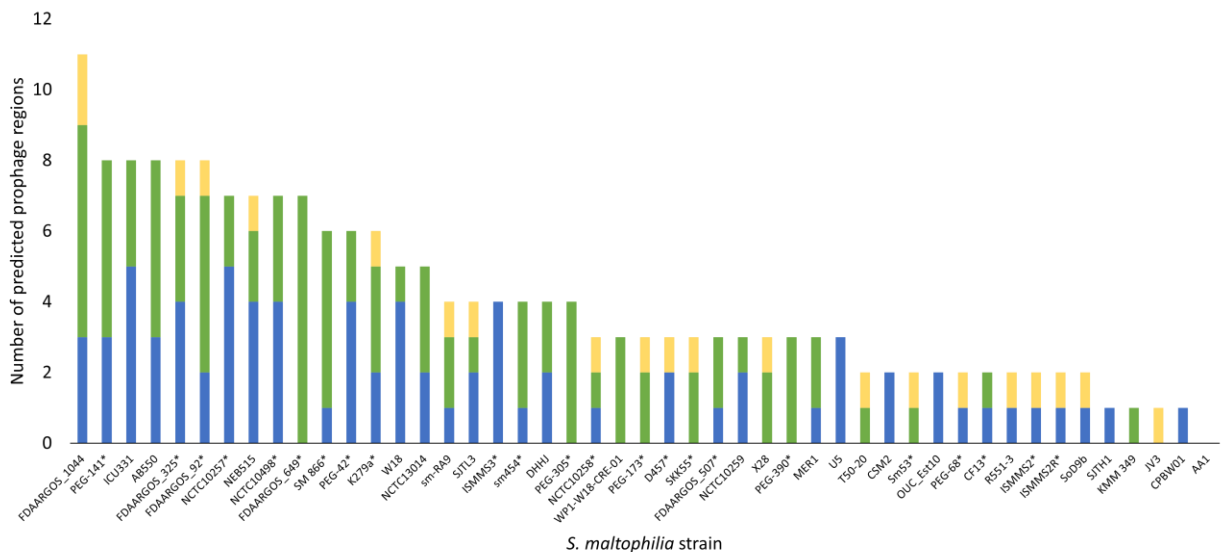


Figure 1-3: Prophage prevalence in 47 complete *S. maltophilia* genomes. Stacked bar graph showing the number of predicted prophage regions present in each *S. maltophilia* genome ranging from zero to eleven as determined by an updated version of PHAST [111,112]. Prophage regions are classified as intact (blue), incomplete (green) or questionable (yellow). Strains with * are clinical isolates and the remainder are environmental isolates, with the exception of FDAARGOS_1044, ICU331, NCTC13014, and NCTC10259 that are of unknown origin.

The high prevalence of prophages in bacterial genomes suggests that phages have played an important role in bacterial evolution [110,116]. Prophages may alter cell physiology and manipulate host metabolism by introducing new DNA that encodes novel functions. The integration of prophages affects the architecture of the bacterial genome and can account for a large portion of strain-to-strain genetic variation within a single species and in many cases, this contributes to the fitness of bacterial pathogens such as *Streptococcus pyogenes* [116,117] and shiga-toxin producing *E. coli* [118,119]. Temperate phages encoding accessory genes, or moron genes, can increase the host virulence or resistance to antibiotics during the lysogenic state, known as lysogenic conversion [116,120]. Additionally, prophages may transfer genes between bacteria by specialized transduction, potentially spreading antibiotic resistance or increasing bacterial virulence. Due to this, temperate phages are not considered as therapeutic candidates, however with advances in genetic techniques, discussed in Chapter 7, these highly abundant temperate phages may be engineered to become suitable for therapeutic use.

There are numerous benefits to using phages therapeutically over antibiotics. As the most abundant biological entity in the biosphere at an estimated 10^{31} particles [121], phages are naturally occurring in the environment and therefore may be easily isolated for characterization. The majority of phages isolated from the environment using the current techniques are tailed phages belonging to the Class *Caudoviricetes* [122,123]. Unlike broad spectrum antibiotics, phages are generally regarded as specific to a single bacterial species, due largely to the recognition of specific bacterial surface receptors. The use of phage therapy therefore does not harm beneficial bacterial flora or impose the risk of secondary *Clostridium difficile* bacterial infections due to depletion of the patient's natural microbiome as observed following antibiotic treatment [124]. The specificity of phages can also be viewed as a negative due to the time needed to find a phage active against a specific strain, however, with advances in genetic engineering, the construction of broad host range phages is possible [125,126]. Phages have also recently been found to play a role in the structure and function of a healthy gut microbiome [127,128], with an estimated 31 billion phages transcytosed across the epithelial cell layers of the gut each day [129], and elicit limited or no host immune response [123]. Finally, the mechanism of action in phages differs from antibiotics, making phages effective against multidrug resistant bacteria, and production of phage enzymes such as exo-polymer depolymerases allows phages to penetrate bacterial biofilms that inherently have increased drug resistance [124].

Phage-bacterial host interactions

The first stage of phage infection is adsorption to the cell surface, which requires the presence of a surface receptor that is recognized and bound by phage receptor binding proteins. This crucial interaction controls the host specificity of a phage and plays a large role in determining its host range, making this a key piece of knowledge for the use of phages therapeutically [130,131]. The bacterial cell surface is decorated with numerous diverse structures that can function as phage receptors, ranging from proteinaceous substrates to polysaccharide moieties [130]. Many phage receptors that have been documented in the literature have been compiled into the Phage Receptor Database (PhReD; <https://portal.bio-conversion.org>), which currently lists 561 phage receptors across 83 bacterial hosts [130]. The most common phage receptors identified in Gram-positive bacteria are the peptidoglycan or cell wall teichoic acids. In Gram-negative hosts, numerous structures in the cell wall have been identified as phage receptors. A common receptor is the lipopolysaccharide (LPS) layer, a complex polymer of fatty acids and monosaccharides that consists of three parts: lipid A at the cell membrane, the core polysaccharide, and the distal O-polysaccharide (O-antigen) [130,132]. Phages have been described to bind both the O-antigen, present in smooth bacteria, and core region of the LPS. Phages that interact with the more highly conserved core region often have broader host ranges, capable of infecting smooth and rough bacteria or mutants, which lack the O-antigen [132]. Conversely, because the O-polysaccharide is highly variable, O-antigen specific phages often have more narrow host ranges. In some cases, such as *E. coli* phages T4 and T5 [130], phages bind reversibly to the LPS as a primary receptor for host recognition and navigate the cell surface to bind irreversibly to their secondary receptor, initiating genome injection into the host cell. These secondary receptors can be a variety of outer membrane proteins, for example OmpA, OmpC, LamB, or iron-uptake proteins such as FhuA, that have been documented for *E. coli* phages [130].

Finally, bacterial structures separate from the cell wall, including capsule and motility structures such as pili and flagella, are documented as phage receptors. Central to the research presented in this thesis is the type IV pilus, a virulence factor on the cell surface of numerous bacterial pathogens, including *P. aeruginosa* and *Neisseria gonorrhoeae* [133]. Assembly of this dynamic structure involves the expression of over 40 genes, the machinery of which is highly conserved. The pilus itself is composed of a group of minor pilins that prime the assembly of the

major pilin subunit; the polymerization and depolymerization of the major pilins by the action of opposing cytoplasmic ATPases controls a form of bacterial surface translocation called twitching motility [134]. Phages that bind to the type IV pilus often rely on this dynamic movement of cell-mediated pilus retraction for successful phage infection, as documented for the *P. aeruginosa* dsDNA phages PO4, B3, D3112, and filamentous ssDNA phage Pf1 [135]. Type IV pili and F-pili have also been described as receptors for ssRNA viruses [136,137].

Despite the significance of receptors for phage propagation, the identification of cell surface receptors is often an overlooked aspect of phage characterization. This is likely due to the labour and time intensive methods typically required for receptor identification [131]. Classic techniques involve genomic comparison of phage sensitive wildtype strains to phage resistant mutants via whole genome sequencing of spontaneous resistant mutants, as described in Chapter 3. Follow-up gene knockout and complementation experiments can confirm the receptor identified. More high throughput, comprehensive screening methods using transposon mutant libraries, described in Chapter 2, can identify receptors and other phage resistance mechanisms in an unbiased manner [131]. Promising new technologies using barcoded transposons, CRISPR interference, and dual-barcoded shotgun expression library sequencing have enabled the construction of quantitative genome-wide screens to rapidly identify genes providing phage resistance when disrupted, underexpressed, or overexpressed, respectively [138]. Although these techniques require optimization in new bacterial species and initial library construction is expensive, they offer an improvement in speed and can provide a global view of phage resistance compared to traditional methods.

The other molecular determinant of phage-host interactions are the phage receptor binding proteins (RBPs). Most well characterized in the tailed bacteriophages, RBPs are typically present at the distal end of the tail as tail fibres, tail spikes, or tail tip proteins [139]. Although most phages use a single RBP, polyvalent phages can encode numerous RBPs for recognition and binding of more than one receptor, as discovered in the *Salmonella* phage SP6 that expresses two RBPs on a V-shaped structure that changes orientation depending on the host species encountered [140]. Likewise, *E. coli* phage phi92 assembles a baseplate tail structure resembling an open Swiss army knife, with each phage particle carrying five different tail spike and tail fibre proteins to allow infection of nonencapsulated *E. coli* and *Salmonella* serovars with distinct O-antigens [141]. Alteration to phage host range can also arise from mutations in genes

encoding RBPs from as little as a single point mutation [142]. These mutations can also lead to expansion of host receptor binding, as observed during Lambda phage evolution experiments where mutations in the host specificity J protein allowed binding of a new receptor, OmpF, in addition to the ancestral receptor, LamB [143]. Further information on the molecular mechanisms of phage-host interactions is reviewed in Nobrega et al. 2018 [139] and de Jonge et al. 2019 [144].

Clinical data using phages

The rising antibiotic resistance crisis has led to increased interest in phage therapy in North America. In the last 15 years, nearly a dozen human clinical trials have been conducted to test the safety and efficacy of phages against numerous pathogens [145]. These trials have included single phage treatments as well as cocktails against priority pathogens, including *P. aeruginosa*, *Staphylococcus aureus* and *E. coli*. The majority of trials administered phages topically at the site of infection or orally, however intraoperative and intravenous routes were also used. Overall, the outcomes from these trials suggest that phage therapy is tolerable, as few adverse effects were reported, however, the data from these trials are limited.

We have observed an increase not only in the number of approved phage therapy clinical trials in recent years, but also in the number of compassionate use single patient cases treated with phages under expanded access Investigational New Drug (eIND) applications in the United States [146]. This is largely due to the creation of the first phage therapy center in North America in 2018, the Center for Innovative Phage Applications and Therapeutics (IPATH) affiliated with the University of San Diego School of Medicine in California, USA, and its role in helping patients access phage therapy. A review of the first ten cases of phage therapy conducted by IPATH revealed the safety and feasibility of intravenous phage treatment for a number of bacterial species and infection sites [146]. Adverse effects were rarely observed following phage administration and phages were successful in treating eight out of the ten patients; however, all patients were treated simultaneously with antibiotics, making it difficult to determine the effectiveness of phage treatment alone. These personalized phage therapy case studies have provided valuable empirical data and while the clinical data on phage therapy to date is promising, more translational research and controlled trials are needed. To address this issue, additional phage therapy centers in the USA have emerged, including Tailored Antibacterials

and Innovative Laboratories for Phage (Φ) Research (TAILOR) at Baylor College of Medicine in Texas and the Center for Phage Research and Therapy at Yale University. These centers have focused on personalized phage therapy on a case-by-case basis. Additionally, a Phase II CYstic Fibrosis bacterioPHage Study at Yale (CYPHY) is currently recruiting patients to evaluate the safety and effectiveness of phage therapy in reducing sputum bacterial load in cystic fibrosis patients with *P. aeruginosa* lung infections (Clinical trial: NCT04684641).

For a comprehensive overview on the most recent compassionate use case reports and clinical data on phage therapy, see reviews by Luong et al. and Aslam et al. [145,146]. Additionally, Chan et al. summarize the therapeutic use of phages in cystic fibrosis cases specifically [147]. It should be noted that no human cases to date have included phage treatment for *S. maltophilia* infections.

Phage therapy strategies

Recent research has sought to determine strategies for effective delivery of phages to the site of infection, as well as combat challenges of administering phages. Although there are many options for the delivery of phages, such as inhalation, topical application, and intravenous injection, there are potential complications surrounding phage penetration of tissues and the inactivation of phage particles due to protein instability or clearance by the immune system [145,148,149].

To address this, researchers are investigating encapsulation of phages within protective polymer or lipid matrices that increase phage stability and retention and can allow controlled release in vivo [148–150]. Encapsulation of phages provides a protective barrier, allowing phage particles to withstand adverse storage and physiological conditions, and penetrate deeper in the body while allowing controlled release at the site of infection [148,150]. Using pH-responsive microencapsulation of *E. coli* bacteriophages, Vinner et al. [151] show phage protection against the gastric acid environment of the stomach and effective release of phages at higher pH, as found in the intestine, while maintaining effective lytic ability against actively growing *E. coli*. Additionally, entrapment of phages within liposome has been shown to provide 100% protection against phage neutralizing antibodies and maintain the killing ability of the phages against *K. pneumoniae* in vitro as well as within macrophages, demonstrating the potential to treat intracellular pathogens [152]. Further study using a liposomal entrapped phage cocktail to treat

K. pneumoniae in a murine burn model showed increased phage retention time in vivo resulting in increased efficacy compared to free phage [153]. This research helps overcome major manufacturing, formulation, and delivery challenges of phage therapy.

Beyond delivery of phages to the site of infection, one of the major obstacles to developing effective phage therapies is the evolution of phage resistance arising in the bacterial host during the course of treatment. To overcome this, researchers suggest the use of phage cocktails that combine multiple phage isolates targeting different surface receptors to reduce the likelihood and speed of phage resistance evolving in a population, rather than single phage treatments [131]. These carefully designed phage mixtures decrease the risk of resistance arising to all phages in the mixture and broaden the lytic spectrum of a single treatment to target multiple bacterial strains, or in some cases species. For example, Yang et al. [154] designed a phage cocktail that is effective against a broad panel of *P. aeruginosa* clinical isolates using phages that target full-length and truncated O-antigen mutants, effectively constraining the emergence of phage resistance observed when using the phages individually. A similar approach to intelligent phage cocktail design was used against *Acinetobacter baumannii* with a mixture of phages that bind to both capsulated and uncapsulated cells to effectively control emergent resistant mutants [155]. The application of phages in combination with selected antibiotics can also increase the production and/or killing activity of phages, a phenomenon termed phage antibiotic synergy (PAS) [156]. Specifically, subinhibitory concentrations of antibiotics that lead to changes in cell morphology due to affected cell wall synthesis and cell division have been shown to increase the activity of phages targeting *E. coli* [156], *Burkholderia cepacia* [157], and *P. aeruginosa* [158], and combination phage and antibiotic treatments led to decreased mortality in a *Galleria mellonella* model [157] and increased biofilm clearance [158] compared to phage treatment alone. These examples demonstrate that carefully designed combinations of phages alone or together with antibiotics can increase the efficacy of phage therapy.

Another strategy is to harness the inevitable phage resistance that will arise by driving the evolution of a less fit bacterial population. Termed an anti-virulence strategy or phage steering [159–161], the use of phages that bind bacterial surface proteins that are important to pathogenicity or colonization of a host, such as pili, flagella, LPS, or capsule, can select for reduced virulence of the bacterial host due to mutation of the phage surface receptor. In addition to selecting for decreased bacterial virulence, surface receptor mutations in response to phage

predation can also re-sensitize multidrug resistant bacteria to antibiotics. Recent research has shown that loss of capsule in *A. baumannii* in response to phage pressure not only decreased the virulence of resistant mutants, but also led to susceptibility to human complement system, beta-lactam antibiotics, and phages with non-capsule receptors [162]. A subsequent pre-clinical study in a murine model of severe *A. baumannii* bacteraemia confirmed these results in vivo, demonstrating the superior bactericidal effect of this phage in combination with the antibiotic ceftazidime compared to either agent individually [163]. Similarly, a phage targeting the outer membrane protein of a *P. aeruginosa* multidrug efflux pump produced an evolutionary trade-off whereby phage resistance resulted in increased sensitivity to several classes of antibiotics [164]; this phage was later used in combination with antibiotics to successfully treat a patient's life-threatening aortic graft infection [165]. Alternatively, phages may encode proteins that directly affect host cell virulence, such as the Tip protein of *Pseudomonas* phage D3112 that inhibits type IV pili-mediated twitching motility through interaction with the ATPase required for pili assembly [166]. A new family of small c-di-GMP interfering peptides known as YIPs have also been identified in PB1-like *Pseudomonas* phages that affect c-di-GMP regulated virulence processes such as motility and biofilm formation [167]. Intelligent design of cocktails containing phages that interfere with or bind important virulence factors or antimicrobial resistance proteins shows great promise as a strategy, as phage resistant mutants that arise will be more susceptible to secondary antimicrobial treatments and clearance by the immune system.

S. maltophilia Phages

Interest in *S. maltophilia* phage research has increased in recent years, coinciding with rising infection prevalence. At the beginning of this research project, only 16 dsDNA phages, six of which were isolated by the Dennis lab, and five ssDNA phages were described in the literature against *S. maltophilia*. At the time of writing, there are now an additional 41 dsDNA phages deposited in Genbank, some with associated publications describing the phage characterization including two phages described in this thesis, AXL3 (Chapter 4) [115] and AXL1 (Chapter 5) [168]. The following section summarizes the general features of these 57 dsDNA phages, with focus on their genetic diversity.

S. maltophilia phage characteristics

Phages against *S. maltophilia* were first described in 1973, when this bacterium was believed to be a species of *Pseudomonas*. Early research investigated phages as genetic tools to study the genetic maps of different species of *Pseudomonas* using transduction. This led to isolation of the phage M6 that was induced as a prophage from *P. maltophilia* strain 6 [169]. A host range mutant, M6a, was isolated by plating high titre M6 lysate on *P. aeruginosa* and further study revealed that it is a general transducing phage, however, this variant was unable to infect the original *P. maltophilia* hosts, therefore interspecies transductions were unable to be performed. No further research on phages as genetic tools for *S. maltophilia* has been described since phage M6.

In the 21st century, research on *S. maltophilia* phages shifted its focus to the isolation and characterization of phages for therapeutic applications. From 2005 to 2014, 35 *S. maltophilia* phages were mentioned in the literature, however only nine phages were functionally characterized [170–176]. Three of these phages had confirmed temperate lifecycles while the remaining six are virulent (Table 1-1). Most notably, a translated abstract of a journal article published by a group of researchers from China described the first in vivo use of phage against *S. maltophilia* [175]. Using a mouse infection model, all *S. maltophilia* infected mice survived to seven days post-infection when treated with SM1 phage. Although lifestyle was not mentioned, the resistant mutation rate was low, at 10^{-10} , suggesting SM1 may be virulent.

Over the next five years, *S. maltophilia* phage research was mainly limited to phages discovered in the Dennis lab, highlight in bold in Table 1-1. These include virulent phages DLP1 and DLP2 that are both capable of infecting across taxonomic orders and lysing *P. aeruginosa* [11], the divergent T4-like virulent phage and sole myovirus in our lab, DLP6 [177], novel virulent phage AXL3 (Chapter 4) [115], temperate phages DLP3 and DLP5 that are maintained as phagemids during host cell lysogeny [178,179], and the related phages DLP4 [114] and AXL1 (Chapter 5) [168] that encode functional trimethoprim resistance genes. Further characterization of these eight phages is the focus of this thesis, and includes the second in vivo use of phages against *S. maltophilia* using phage DLP3 to rescue infected *G. mellonella* larvae (Chapter 3) [178]. During this period, a separate study was also published using virulent phages to treat a corrosion-producing *S. maltophilia* strain isolated from a petroleum pipeline in Iran [180]. Two unnamed phages were isolated from surrounding wastewater and electron microscopy showed

that both had a Siphoviridae morphology with unusually long tails over 400 nm long. Phage treatment reduced bacterial growth by 50% in vitro, however, no further information was provided and these phages are not included in Table 1-1. This study provides an example of the potential industrial application of *S. maltophilia* phages to treat biocorrosion in addition to human therapy.

From 2020 onwards, genomic sequencing of *S. maltophilia* phages has skyrocketed, however associated functional characterization of these sequenced phages is lacking. The majority of sequenced *S. maltophilia* phages were produced by students in a BICH464 Phage Genomics undergraduate course at Texas A&M University, in which individual phage genomes are assembled, annotated, and submitted to Genbank along with a corresponding genome announcement that contains transmission electron microscopy data. A total of 17 *S. maltophilia* phages have been documented from this program, with the first letter of each name corresponding to the phage morphology (ie. Ponderosa is a Podoviridae phage). An additional group of researchers from China have also contributed numerous *S. maltophilia* phage genomes to Genbank with few having associated publications that contain experimental functional characterization. These include 13 phages named with the prefix BUCT (Table 1-1). Interestingly, a single virulent myovirus, Ps15, has been characterized for phage therapy against ocular infections caused by *S. maltophilia* [181].

One of the final noteworthy *S. maltophilia* phages functionally characterized to date is Φ SHP3, a B3-like transposable Siphoviridae phage with a small genome of 37.6 kb [182]. In addition to the conserved genes Mor, GemA, TnpA, and TnpB widely distributed in transposable phages, Φ SHP3 also encodes a functional RdgC exonuclease protein that possibly plays a role in phage recombination. Investigation into the regulation of its lytic-lysogenic switch suggested that the SOS response may play a role due to the presence of LexA and CpxR binding motifs [182]. Further characterization of Φ SHP3 as the first transposable phage of *S. maltophilia* will provide information on the role phages play in the genetic heterogeneity of *S. maltophilia* and may become a powerful tool for genetic manipulation in this species.

While not useful for therapeutic applications, numerous filamentous phages have also been described in *S. maltophilia*. Filamentous phages in the family *Inoviridae* are characterized by their unique morphology, small single-stranded DNA genomes, and chronic infection cycle whereby progeny virions are continuously released without killing the host. In 2006, Hagemann

et al. discovered a self-replicating DNA molecule in genome preparations of a clinical *S. maltophilia* strain [183]. Sequencing of the extra-chromosomal DNA molecule revealed a 6,709 bp linear genome encoding seven proteins, including a putative Zonula occludens-like toxin (zot) with sequence identity to the Zot toxins of *Xylella* and *Vibrio cholerae*. The authors named this novel filamentous phage Φ SMA9 based on resemblance of the size and gene organization of the DNA molecule to the replicative form of other filamentous phages [183]. Several filamentous phages have since been identified in environmental *S. maltophilia* isolates. In 2012 and 2013, a second group detailed their findings of the novel *Inoviridae* phages Φ SHP1 and Φ SHP2 isolated from the environmental *S. maltophilia* strains P2 and P28 [184,185]. Electron microscopy of Φ SHP1 showed filamentous structures approximately 2.1 μ m long. Sequencing of the 6,867 bp genome previously isolated in its replicative form as pSH1 revealed ten putative ORFs including a predicted Zot-like toxin [184]. Electron microscopy of Φ SHP2 revealed filamentous particles 0.8 μ m long that contained single-stranded DNA [185]. Sequencing of the replicative form, pSH2, revealed similarities to Φ SHP1 and Φ SMA9, including a Zot-like toxin gene present in the 5,819 bp length genome. Two additional filamentous phages were identified in 2014 from an environmental isolate, *S. maltophilia* strain Khak84, as extrachromosomal genetic elements [186]. Sequencing revealed two contigs approximately 7 kb in size with similar gene organization and homology to other filamentous *Inoviridae* phages. Both genomes encode 11 putative ORFs, including zot-like genes. Recent investigation of microbial genomic sequencing data has identified a vast heterogeneity and widespread distribution of *Inoviridae* phages that were previously underappreciated [187]. Filamentous phages are abundant in other human pathogens, such as *P. aeruginosa* [188], and have been shown to increase the virulence of their bacterial host and interact with the human immune system during infection [189,190], prompting concern into the role of filamentous phages in *S. maltophilia* pathogenicity. Although all five filamentous phages identified in *S. maltophilia* strains to date encode a Zot-like protein, the sequences are divergent and further research is needed to determine the functionality of these proteins as toxins and whether they affect host virulence [191].

In addition to harnessing active phages for their antimicrobial properties, individual phage proteins have also been characterized for use against antibiotic resistant bacteria, including *S. maltophilia*. Phages encode enzymes called endolysins or lysozymes that degrade the peptidoglycan of the bacterial cell wall from within during the final stage of the phage lytic

replication cycle, causing host cell lysis [192]. Research has shown that endolysins can also be effective when applied externally to the cell. In 2006, Lee and colleagues characterized a *Xanthomonas oryzae* phage lysozyme, Lys411, and found it active against not only its host species, but it also had even stronger activity against *S. maltophilia* [193]. The number of *S. maltophilia* strains Lys411 is active against was not indicated and no follow-up studies have been published, meaning the potential of this enzyme for therapeutic control of *S. maltophilia* infections is unknown. Bacterial genomes may also carry gene clusters that encode phage tail-like bacteriocins (PTLBs). These large protein complexes resemble the tails of Siphoviridae and Myoviridae phage particles and have bactericidal activity against bacteria related to the producing strain [194]. Two PTLBs have been identified in *S. maltophilia*, maltocin P28 and S16 [185,195]. Liu and colleagues identified maltocin P28 as phage tail-like particles in electron micrographs of filamentous phage Φ SHP2; purification of these particles indicated that they contained no genetic material but had antimicrobial activity against both environmental and clinical *S. maltophilia* isolates [185]. In 2019, the same group of researchers published on a second maltocin, S16, that had broad antibacterial activity against 62 out of 86 *S. maltophilia* strains tested and remarkably eight out of 14 *E. coli* strains [195]. The authors suggest that maltocins are widespread in *S. maltophilia*, possibly providing a range of novel antimicrobial alternatives to antibiotics yet to be discovered.

Table 1-1 lists the 65 *S. maltophilia* phages and phage elements identified to date, with unique features noted. For many phages without transmission electron micrographs, morphology of the phage is predicted based on its genome. The eight phages isolated in the Dennis lab and the topic of this thesis are bolded.

Table 1-1: *S. maltophilia* phage characteristics.

Phage	Source; isolation strain	Genome length (bp)	GC (%)	Morphology	Taxonomy	Lifestyle	Unique features	Reference; Accession if applicable
M6	<i>P. maltophilia</i> ^a 6	-	-	Siphoviridae	-	Temperate	Transducing phage Host range: 4/50 strains Host range mutant, M6a, is capable of infecting <i>P. aeruginosa</i>	[169]
ΦSMA5	Sputum; <i>S. maltophilia</i> T39	~250 kb ^b	-	Myoviridae	-	Virulent	Broad host range: 61/87 strains Burst size: 95 phage/cell DNA is restriction enzyme resistant	[170]
Smp14	Sewage; <i>S. maltophilia</i> T14	~160 kb ^c	53.3 ^c	Myoviridae	<i>Tequatrovirus</i>	Virulent	T4-like phage Moderate host range: 37/87 strains Adsorbs to poles of cells Burst size: ~150 phage/cell DNA is restriction enzyme resistant	[171] DQ364602
S1	Environmental <i>S. maltophilia</i> CECT 4793	40,287	63.7	Siphoviridae	-	Temperate	Narrow host range: 4/26 strains Encodes putative GspM protein involved in host type II secretion system Burst size: ~75 phage/cell 48 ORFs	[172] NC_011589
S3	Sewage; <i>S. maltophilia</i> E539	~33 kb ^b	-	Myoviridae	-	Virulent	Moderate host range: 12/26 strains Burst size: ~100 phage/cell Short eclipse period of 30 min DNA is restriction enzyme resistant	[172]
S4	Sewage; <i>S. maltophilia</i> F227	~200 kb ^b	-	Siphoviridae	-	Temperate	Broad host range: 18/26 strains Burst size: ~80 phage/cell DNA is restriction enzyme resistant	[172]
IME13	Sewage; clinical <i>S. maltophilia</i>	162,327	41.2	Myoviridae ^d	<i>Tulanevirus</i>	Virulent	Large burst size: >3,000 phage/cell Produces three plaque sizes 182 ORFs; 15 tRNAs	[173] JX306041

IME15	Sewage; clinical <i>S. maltophilia</i>	38,513	53.7	Podoviridae ^d	<i>Teseptimavirus</i> IME15	Virulent	T7-like phage Burst size >100 phage/cell 45 ORFs	[174] JX872508
SM1	Sewage; <i>S. maltophilia</i>	~50 kb ^b	-	Myoviridae	-	-	Large burst size: 187 phage/cell <i>In vivo</i> mouse trials show 100% of SM1 treated mice surviving past day 7	[175]
Smp131	Clinical <i>S. maltophilia</i> T13	33,525	65.0	Myoviridae	<i>Simpcentum-</i> <i>virus</i> Smp131	Temperate	P2-like phage Narrow host range: 3/86 strains 47 ORFs	[176] JQ809663
DLP1	Red Deer River sediment; clinical <i>S. maltophilia</i> D1585	42,887	53.7	Siphoviridae	<i>Septimatrevirus</i>	Virulent	Host range includes <i>P. aeruginosa</i> Uses type IV pilus as host receptor 57 ORFs	[11,160] KR537872 Chapter 2
DLP2	Blue flax soil; clinical <i>S. maltophilia</i> D1585	42,593	53.7	Siphoviridae	<i>Septimatrevirus</i> kakheti25	Virulent	Host range includes <i>P. aeruginosa</i> Uses type IV pilus as host receptor 58 ORFs	[11,160] KR537871 Chapter 2
DLP3	Empty soil; clinical <i>S. maltophilia</i> D1571	96,852	58.3	Siphoviridae	<i>Delepquinta-</i> <i>virus</i>	Temperate	Uses type IV pilus as host receptor Broad host range: 22/29 strains Therapeutically active in D1571 infected <i>G. mellonella</i> larvae Causes lysogenic conversion Encodes functional erythromycin resistance protein DNA is restriction enzyme resistant 148 ORFs; 5 tRNAs	[178] MT110073 Chapter 3
DLP4	Planter soil; clinical <i>S. maltophilia</i> D1585	63,945	65.1	Siphoviridae	<i>Pamexvirus</i>	Temperate	Moderate host range: 14/27 strains Uses type IV pilus as host receptor Causes lysogenic conversion Encodes functional trimethoprim resistance protein (DHFR) DNA is restriction enzyme resistant 82 ORFs; 1 tRNA	[114] MG018224 Chapter 3

DLP5	Empty soil; clinical <i>S. maltophilia</i> D1614	96,542	58.4	Siphoviridae	<i>Delepquinta-virus</i>	Temperate (phagemid)	Narrow host range: 5/27 strains Uses type IV pilus as host receptor Causes lysogenic conversion Encodes putative erythromycin resistance protein DNA is restriction enzyme resistant 149 ORFs; 5 tRNAs	[179] NC_042082 Chapter 3
DLP6	Planter soil; clinical <i>S. maltophilia</i> D1571	168,489	55.8	Myoviridae	<i>Ackermann-viridae</i> (Family)	Virulent	Moderate host range: 13/27 strains Likely uses CirA iron uptake protein as host receptor Divergent T4-like virus Encodes a transposase DNA is restriction enzyme resistant 241 ORFs; 30 tRNAs	[177] KU682439 Chapter 3
AXL3	Empty soil; clinical <i>S. maltophilia</i> D1585	47,545	63.3	Siphoviridae	<i>Axeltriavirus</i> (proposed genus)	Virulent	Narrow host range: 5/29 strains Uses type IV pilus as host receptor Long infection cycle Burst size: 38 phages/cell DNA is restriction enzyme resistant 65 ORFs	[115] MT536174 Chapters 3 & 4
Ponderosa	Water sample; <i>S. maltophilia</i> ATCC 17807	42,612	60.0	Podoviridae	<i>Okabevirinae</i> (Subfamily)	-	T7-like phage 54 ORFs	[196] MK903280
Pokken	Water sample; <i>S. maltophilia</i> ATCC 17807	76,239	55.1	Podoviridae	<i>Pokkenvirus</i> pokken	-	N4-like phage Encodes virion RNA polymerase 92 ORFs; 5 tRNAs	[197] MN062186
Moby	Wastewater; <i>S. maltophilia</i> ATCC 17807	159,365	54.1	Myoviridae	<i>Menderavirus</i> moby	-	T4-like phage 271 ORFs; 24 tRNAs	[198] MN095772
Mendera	Wastewater; <i>S. maltophilia</i> ATCC 17807	159,961	54.0	Myoviridae	<i>Menderavirus</i> mendera	-	T4-like phage 287 ORFs; 23 tRNAs	[199] MN098328
BUCT548	Sewage; <i>S. maltophilia</i> 824	62,354	56.3	Siphoviridae	-	-	Broad host range: 11/13 strains Burst size: 134 phages/cell 102 ORFs; 1 tRNA	[200] MN937349
ΦSHP3	<i>S. maltophilia</i> c31	37,611	65.3	Siphoviridae	-	Temperate	Transposable phage Moderate host range: 20/83 strains 51 ORFs	[182] MT872956
IME-SM1	Hospital sewage	159,514	54.1	Myoviridae ^d	<i>Menderavirus</i> IMESM1	-	T4-like phage 254 ORFs; 20 tRNAs	NC_054952

YB07	-	159,862	54.1	Myoviridae ^d	<i>Menderavirus</i> IMESM1	-	T4-like phage 257 ORFs	MK580972
BUCT555	Hospital sewage; <i>S.</i> <i>maltophilia</i> 1207	39,440	61.4	Podoviridae	-	Virulent	Narrow host range: 2/13 strains Burst size: 204 phages/cell 57 ORFs	[201] MW291508
Salva	Soil; <i>S.</i> <i>maltophilia</i>	60,789	56.4	Siphoviridae	-	-	102 ORFs; 1 tRNA	[202] MW393850
BUCT609	Sewage; <i>S.</i> <i>maltophilia</i> 3015	43,145	58.3	Podoviridae ^d	<i>Okabevirinae</i> (Subfamily)	-	T7-like phage 56 ORFs	MW960043
BUCT603	Sewage; <i>S.</i> <i>maltophilia</i> 118	44,912	63.7	Siphoviridae ^d	-	-	64 ORFs	MW934263
BUCT598	Hospital sewage; <i>S.</i> <i>maltophilia</i> 826	43,581	60.0	Podoviridae	<i>Okabevirinae</i> (Subfamily)	-	T7-like phage Narrow host range: 3/11 Burst size: 165 phages/cell Stable across pH range 2-10 55 ORFs	[203] MW831865
BUCT608	-	160,122	54.1	Myoviridae ^d	<i>Menderavirus</i> IMESM1	-	T4-like phage 266 ORFs; 19 tRNAs	MZ398248
BUCT626	-	61,662	56.2	Siphoviridae ^d	-	-	98 ORFs; 1 tRNA	MZ398241
BUCT627	-	61,860	56.3	Siphoviridae ^d	-	-	98 ORFs; 1 tRNA	MZ398240
Marzo	Wastewater; <i>S.</i> <i>maltophilia</i> ATCC 17807	159,384	54.0	Myoviridae	<i>Menderavirus</i>	-	T4-like phage 268 ORFs; 23 tRNAs; 1 tmRNA	[204] MZ326868
Silvanus	Soil, horse pasture; <i>S.</i> <i>maltophilia</i> ATCC 51331	45,678	58.4	Siphoviridae	-	-	68 ORFs	[205] MZ326867
Philippe	Soil; <i>S.</i> <i>maltophilia</i> ATCC 17807	74,717	54.3	Podoviridae	<i>Schitoviridae</i> (Family)	-	N4-like phage Encodes virion RNA polymerase 95 ORFs; 6 tRNAs	[206] MZ326861
Sonora	Topsoil; <i>S.</i> <i>maltophilia</i> ATCC 51331	63,825	63.0	Siphoviridae	-	-	97 ORFs	[207] MZ326860
Siara	Wastewater; <i>S.</i> <i>maltophilia</i> ATCC 17807	61,427	56.5	Siphoviridae	-	-	100 ORFs; 3 tRNAs	[208] MZ326859

Pepon	Wastewater; <i>S. maltophilia</i> ATCC 17807	42,532	60.0	Podoviridae	<i>Okabevirinae</i> (Subfamily)	-	T7-like phage Large plaques of 8 mm diameter with 1 mm halo 53 ORFs	[209] MZ326858
Piffle	Wastewater; <i>S. maltophilia</i> ATCC 17807	76,332	54.9	Podoviridae	<i>Pokkenvirus</i>	-	N4-like phage Encodes virion RNA polymerase 90 ORFs; 6 tRNAs	[210] MZ326857
Paxi	Pondwater; <i>S. maltophilia</i> ATCC 17807	74,962	54.6	Podoviridae	<i>Pokkenvirus</i>	-	N4-like phage Encodes virion RNA polymerase 89 ORFs; 5 tRNAs	[211] MZ326856
Ptah	Wastewater; <i>S. maltophilia</i> ATCC 17807	42,593	61.8	Podoviridae	<i>Okabevirinae</i> (Subfamily)	-	T7-like phage 56 ORFs	[212] MZ326854
Suso	Freshwater; <i>S. maltophilia</i> ATCC 17807	44,659	67.4	Siphoviridae	-	-	69 ORFs	[213] MZ326866
Summit	Weaning foal swab; <i>S. maltophilia</i> ATCC 17807	95,728	58.5	Siphoviridae	<i>Delepquinta-virus</i>	Temperate (predicted)	Encodes ParB protein 147 ORFs; 5 tRNAs 1 predicted amber suppressor tRNA	[214] MZ326862
Suzuki	Freshwater; <i>S. maltophilia</i> ATCC 17807	56,042	62.6	Siphoviridae	<i>Sanovirus</i>	-	Genetic similarity to <i>Xylella</i> phages 83 ORFs	[215] MZ326855
TS-10	Sewage; <i>S. maltophilia</i>	42,931	59.9	Podoviridae ^d	<i>Okabevirinae</i> (Subfamily)	-	T7-like phage 53 ORFs	OK018136
P15	-	43,707*	60.2	Podoviridae ^d	<i>Okabevirinae</i> (Subfamily)	-	T7-like phage 57 ORFs	OK490494
ytsc_ply20 08005c	-	42,318	63.0	Siphoviridae ^d	-	-	54 ORFs	OK562670
AXL1	Soil; <i>S. maltophilia</i> D1585	63,962	67.3	Siphoviridae	<i>Pamexvirus</i>	Virulent	Moderate host range: 14/30 strains Burst size: 58 phages/cell Long infection cycle Encodes a functional trimethoprim resistance gene, <i>dhfr</i> 83 ORFs	[168] OL674541 Chapter 5
SM171	Hospital wastewater; <i>S. maltophilia</i> 2355	44,514	67.3	Siphoviridae	-	-	59 ORFs	MZ611865

C121	Cave sediment; <i>S. maltophilia</i> YCR3A-1	73,045	49.8	Podoviridae ^d	<i>Schitoviridae</i> (Family)	-	N4-like phage Encodes virion RNA polymerase 98 ORFs	OM158235
Ps15	Wastewater; <i>S. maltophilia</i> AP143	161,350	54.2	Myoviridae	<i>Menderavirus</i>	Virulent	T4-like phage Broad host range: 22/24 strains 21 ocular isolates susceptible Burst size: ~52 phages/cell 276 ORFs; 24 tRNAs	OL702939
BUCT705	Hospital sewage; <i>S. maltophilia</i>	50,665	50.7	Siphoviridae ^d	<i>Webevirus</i>	-	Genetic similarity to <i>Klebsiella</i> phages 84 ORFs	OM735690
BUCT703	Hospital sewage; <i>S. maltophilia</i>	43,221	59.7	Podoviridae ^d	<i>Okabevirinae</i> (Subfamily)	-	T7-like phage 50 ORFs	OM735688
BUCT702	Hospital sewage; <i>S. maltophilia</i>	34,535	37.6	Siphoviridae ^d	-	Temperate (predicted)	Encodes recombinase/integrase 44 ORFs	OM735687
BUCT700	Hospital sewage; <i>S. maltophilia</i>	43,214	59.7	Podoviridae ^d	<i>Okabevirinae</i> (Subfamily)	-	T7-like phage 55 ORFs	OM735686
BUCT603 B1	Hospital sewage; <i>S. maltophilia</i> R118-1	44,592	63.6	Siphoviridae ^d	-	-	62 ORFs	OM913894
Filamentous phages								
ΦSMA9	Clinical <i>S. maltophilia</i> c5	6,907	62.4	Inoviridae	<i>Staminivirus</i> SMA9	Chronic	Encodes zot-like protein 7 ORFs	[183] NC_007189
ΦSHP1	Environmental <i>S. maltophilia</i> P2	6,867	61.1	Inoviridae	<i>Psecadovirus</i> PSH1	Chronic	Encodes zot-like protein 10 ORFs	[184] NC_010429
ΦSHP2	-	5,819	61.5	Inoviridae	-	Chronic	Encodes zot-like protein 9 ORFs	[185] NC_015586
ΦSMA6	Environmental <i>S. maltophilia</i> Khak84	7,648	62.6	Inoviridae	<i>Scuticavirus</i> SMA6	Chronic	Encodes zot-like protein and putative conjugal transfer protein 11 ORFs	[186] HG315669

ΦSMA7	Environmental <i>S. maltophilia</i> Khak84	7,069	62.3	Inoviridae	<i>Subteminivirus</i> SMA7	Chronic	Encodes zot-like protein 11 ORFs	[186] HG007973
Phage-derived antimicrobials and PTLBs								
Lys411 lysozyme	<i>Xanthomonas</i> <i>oryzae</i> phage ΦXo411	537	54.2	-	-	-	No holin required for export to periplasm 124,400 U/mg activity against <i>S.</i> <i>maltophilia</i>	[193] DQ408365
Maltocin P28	<i>S. maltophilia</i> P28	19,919	66.2	-	-	-	Bactericidal activity: 38/81 strains R-type pyocin structure Mitomycin C inducible, thermolabile, proteinase K sensitive 23 ORFs.	[185] KC787694
Maltocin S16	<i>S. maltophilia</i> S16	19,658	66.3	-	-	-	Bactericidal activity: 62/86 <i>S.</i> <i>maltophilia</i> strains, 8/14 <i>E. coli</i> strains Mitomycin C inducible, thermolabile, insensitive to proteases Binds LPS as surface receptor 23 ORFs.	[195] MH703584

^a Genus was previously classified as *Pseudomonas maltophilia*, which is now known as *Stenotrophomonas maltophilia*.

^b Estimated genome size based on PFGE; no sequencing data available.

^c Estimated genome size and GC content based on PFGE and HPLC; 16 kb fragment containing morphogenesis genes sequenced.

^d Morphology is speculated based on genome characteristics in the absence of electron microscopy.

In summary, 62 phages have been isolated and characterized against *S. maltophilia*, with their key features described in Table 1-1. Five of these phages belong to the family *Inoviridae*, each encoding a putative Zot-like toxin, and are not useful for therapy, however they may play ecological roles and influence the pathogenicity of their host. The remaining 57 phages belong to the Class *Caudoviricetes* as tailed phages with dsDNA genomes; these are further classified by morphology with 27 Siphoviridae phages having long, non-contractile tails, 16 Podoviridae phages have short, non-contractile tails, and 14 Myoviridae phages have long, contractile tails. Of these, 18 morphologies were predicted based on their genomes. These phages were isolated from a range of sources, primarily from wastewater/sewage (31 phages) or soil (13 phages).

Of the 57 dsDNA phages, 52 have genome sequencing data available. Phylogenetic analysis of these phage proteomes using ViPTree [216] shows the extreme diversity found within the *S. maltophilia* phages isolated to date (Figure 1-4). Seven phages belonging to the *Menderavirus* genus and Smp14 group together in the same clade and represent many of the T4-like *S. maltophilia* phages, with the exception of DLP6. Similarly, T7-like phage IME15 shares limited protein similarity with the remaining T7-like phages, BUCT598, P15, BUCT700, BUCT703, BUCT609, TS-10, Ptah, Ponderosa and Pepon; these examples highlight the diversity present with the T4-like and T7-like groups of phages. Numerous N4-like phages encoding virion RNA polymerases are also present, belonging to the *Pokkenvirus* genus or unclassified genera within the *Schitoviridae* Family (Figure 1-4). Few additional *S. maltophilia* phages have also been namesakes for phage genera, namely *Delepquintavirus*, *Simpcentumvirus*, and the newly proposed *Axeltriavirus*. Many of the remaining phages share low protein sequence similarity with each other as well as with phages infecting other bacterial species, and phages such as Silvanus and S1 may even belong to new genera, as well as phages Siara, Salva, BUCT626, BUCT627, and BUCT548 as members of their own genus. The extreme diversity within *S. maltophilia* phages is promising for the creation of effective broad-range phage cocktails, as well as the study of novel phage biology mechanisms.

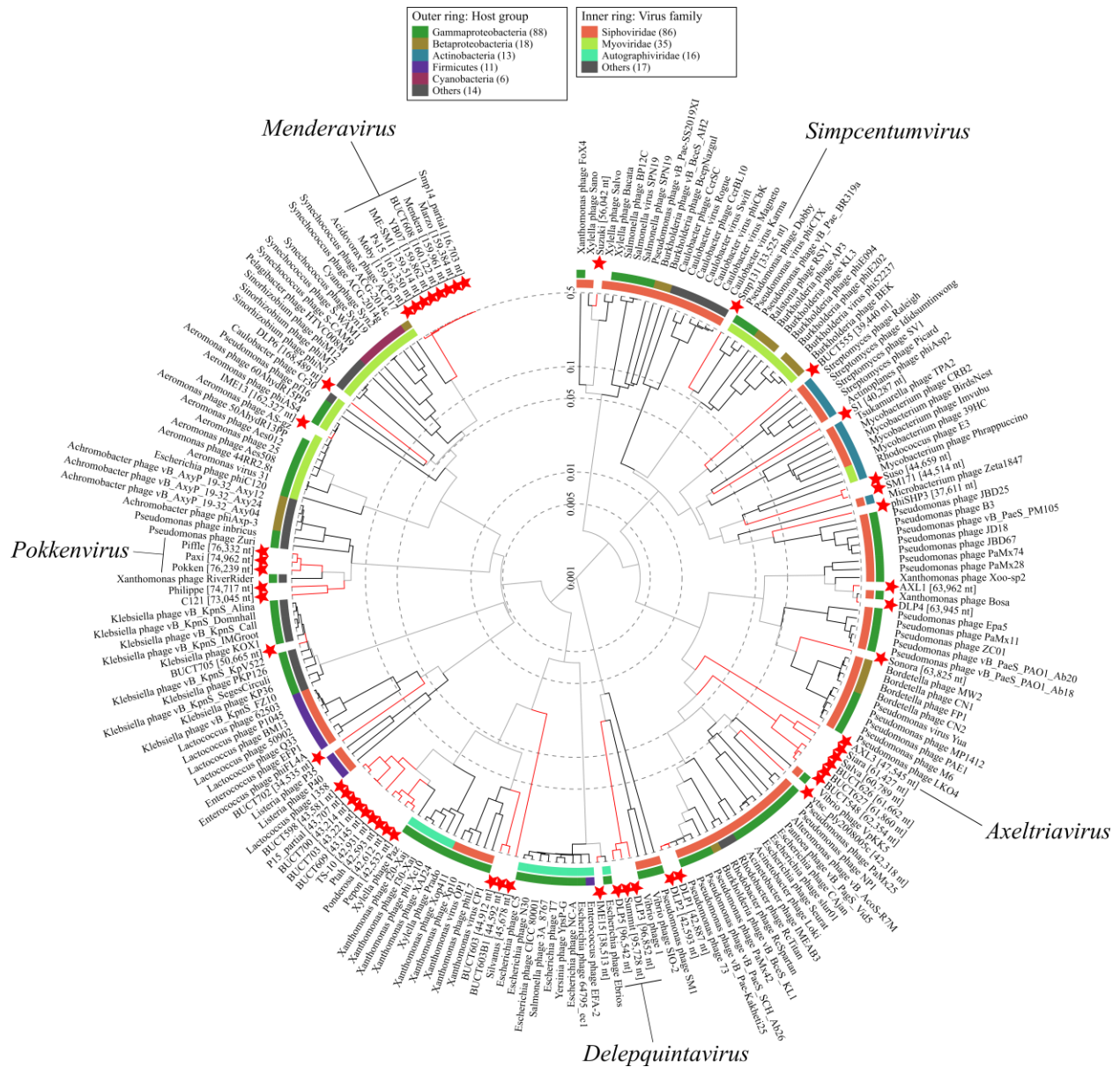


Figure 1-4: *S. maltophilia* phage phylogenetic tree. The results of ViPTree analysis using a protein distance metric based on normalized tBLASTx scores plotted on a log scale. This tree includes 206 dsDNA phages, including 52 *S. maltophilia* phages with genome sequencing data highlighted with red stars. Related phages chosen for inclusion were selected as the top ten phages with the highest genome similarity S_G scores for each of the 52 *S. maltophilia* phages. Phage genera named after *S. maltophilia* phages are labeled. Tree was generated using the ViPTree server [216].

Potential of phage therapy for *S. maltophilia*

Of the *S. maltophilia* phages with experimentally confirmed lifecycles, 12 are virulent and potentially desirable for therapeutic use, while eight are temperate and capable of lysogeny, and in the case of phage Φ SHP3, transposition. The 12 virulent phages, Φ SMA5, Smp14, S3, IME13, IME15, DLP1, DLP2, DLP6, AXL3, BUCT555, AXL1, and Ps15, isolated and characterized for their potential use in phage therapy are diverse (Figure 1-4). For some phages with genomic sequencing and characterization, lifestyle was not determined, which is essential prior to use in therapy. Based on genome sequencing data alone, only two newly sequenced phages may be temperate; phage Summit encodes a ParB protein and is related to phages DLP3 and DLP5 that have been experimentally confirmed as temperate and capable of replicating as a phagemid during the lysogenic cycle. BUCT702 is a novel phage encoding a recombinase protein that likely functions as an integrase. Although no experimental data regarding host range, lifecycle, or phage infection dynamics were provided to evaluate the suitability of the 34 remaining phages for therapeutic use, we may putatively classify these phages as virulent based on the absence of lysogeny related genes such as those encoding integrases, repressors, or recombinases. Overall, the seemingly large proportion of globally distributed, highly diverse virulent phages for *S. maltophilia* is promising for the creation of broad-host range phage cocktails for therapy. However, characterization in recent years is deficient in the physiological characterization of these phages, specifically in phage infection dynamics and phage-host interactions. Electron microscopy of Smp14 revealed a Myoviridae morphology and phage particles were observed binding to the poles of the host cells [171]. No receptor was identified, however, based on their observations it is likely that Smp14 interacts with polar structures such as the flagella or type IV pili that may have been retracted during imaging. Beyond this observation, no phage receptors have been identified for *S. maltophilia* phages in the literature, a key feature for design of phage cocktails limiting the emergence of resistant mutants.

Thesis Objectives

Although identification of phage receptors for individual phages can be time consuming, characterizing the receptors for *S. maltophilia* phages will inform their use as therapeutics in effective phage cocktails, emphasizing the need for routine receptor identification. The objectives of my thesis therefore center around characterizing the initial phage-host interaction

that dictates a phage's host range, as well as genomic and functional characterization of novel phages isolated by our group.

More specifically, I describe the first identification of a receptor for *S. maltophilia* phages in Chapter 2, using the broad host range phages DLP1 and DLP2. In Chapter 3 I examine the receptor for six additional *S. maltophilia* phages and a single *Xanthomonas* phage and investigate the concept of an anti-virulence phage therapy strategy via reduced fitness and/or virulence in phage resistant mutants. To determine the suitability of two novel phages, AXL3 and AXL1, for use in this anti-virulence strategy, I complete the genomic and functional characterizations for these phages in Chapters 4 and 5. Finally, in Chapter 6 I examine the phage-host interactions identified in Chapters 2 and 3 in more detail, specifically analyzing phage binding sites on the type IV pilus receptor and putative receptor binding proteins of each phage to inform their future use in genetic engineering and phage cocktail design.

CHAPTER 2 - Identification and characterization of type IV pili as the cellular receptor of broad host range *Stenotrophomonas maltophilia* bacteriophages DLP1 and DLP2

A version of this chapter has been published as:

McCutcheon JG, Peters DL, Dennis JJ. 2018. Identification and characterization of the type IV pili as the cellular receptor of broad host range *Stenotrophomonas maltophilia* bacteriophages DLP1 and DLP2. *Viruses*. 10:338. doi:10.3390/v10060338. IF: 5.048

Objectives

Bacteriophages DLP1 and DLP2 are capable of infecting both *Stenotrophomonas maltophilia* and *Pseudomonas aeruginosa* strains, two highly antibiotic resistant bacterial pathogens that are often found together in polymicrobial infections in the lungs of patients with cystic fibrosis [217]. As phages typically exhibit host ranges limited to one bacterial species, this unique ability suggests that DLP1 and DLP2 may be good candidate phages for use in phage therapy, as their unusually broad host ranges would minimize the number of different phages needed in one treatment. The specificity of phages for their hosts relies on irreversible binding to host receptors, therefore, the objective of this study is to identify the cell surface receptor used by both phages to explain their unusual cross-order infectivity. Understanding the mechanism of attachment for these phages will inform their use as therapeutic agents.

Materials and Methods

Bacterial strains, phages, and growth conditions

Bacterial strains, bacteriophages and plasmids used in this study are listed in Table 2-1. The *S. maltophilia* strain D1585 was acquired from the Canadian *Burkholderia cepacia* complex Research and Referral Repository (Vancouver, BC) and *S. maltophilia* strain 280 was gifted from The Provincial Laboratory for Public Health - North (Microbiology), Alberta Health Services. The mini-Tn5-*luxCDABE* *P. aeruginosa* PA01 mutant library used for the receptor screen was a kind gift from S. Lewenza [218]. Additional PA01 mutants were obtained from the University of Washington *P. aeruginosa* transposon mutant library constructed with either an IS*phoA*/hah or IS*lacZ*/hah Tn5 IS50L derivative transposon [219,220]. *P. aeruginosa* and *S. maltophilia* strains were grown aerobically overnight at 30°C on half-strength Luria Bertani (½ LB) solid medium or in ½ LB broth with shaking at 225 rpm, and *Escherichia coli* strains were grown at 37°C in full LB, unless otherwise noted. When plasmid maintenance was required, media was supplemented with antibiotics at the following final concentrations (µg per mL): gentamicin (Gm), 10 for *E. coli* and 35 for *P. aeruginosa*; chloramphenicol (Cm), 35 for *E. coli* and *S. maltophilia* D1585 and 75 for *S. maltophilia* 280; and tetracycline (Tc), 10 for *E. coli*, 50 for 280, and 100 for D1585.

Table 2-1: List of bacterial strains, phages, and plasmids used in this study.

Bacterial Strain	Genotype or Description	Source
<i>P. aeruginosa</i> PA01	Wildtype host for DLP1	[221]
<i>S. maltophilia</i> D1585	Wildtype host for DLP1 and DLP2	CBCRRR*
D1585 $\Delta pilA$	Clean deletion of <i>pilA</i> in D1585	This study
<i>S. maltophilia</i> 280	Wildtype host for DLP2	PLPHN/AHS**
280 $\Delta pilA$	Clean deletion of <i>pilA</i> in 280	This study
<i>E. coli</i> S17-1	Conjugative donor strain	[222]
<i>E. coli</i> DH5 α	Host for plasmid cloning	[223]
Phage		
DLP1	Lytic phage	Accession: KR537872.1 [11]
DLP2	Lytic phage	Accession: KR537871.1 [11]
E79	Lytic <i>Pseudomonas</i> phage	Accession: MH536736.1 [224,225]
Plasmids		
pBBR1MCS	Broad-host range cloning vector, Cm ^R	[226]
pD1585 <i>pilA</i>	pBBR1MCS carrying D1585 <i>pilA</i> , Cm ^R	This study
pPA01 <i>pilA</i>	pBBR1MCS carrying PA01 <i>pilA</i> , Cm ^R	This study
p280 <i>pilA</i>	pBBR1MCS carrying 280 <i>pilA</i> , Gm ^R	This study
pD1585 <i>pilE</i>	pBBR1MCS carrying D1585 <i>pilE</i> , Cm ^R	This study
pPA01 <i>pilE</i>	pBBR1MCS carrying PA01 <i>pilE</i> , Cm ^R	This study
pUCP22	Broad-host range cloning vector, Gm ^R	[227]
pUCP(D1585 <i>pilA</i>)	pUCP22 carrying D1585 <i>pilA</i> , Gm ^R	This study
pUCP(PA01 <i>pilA</i>)	pUCP22 carrying PA01 <i>pilA</i> , Gm ^R	This study
pUCP(280 <i>pilA</i>)	pUCP22 carrying 280 <i>pilA</i> , Gm ^R	This study
pUCP(D1585 <i>pilE</i>)	pUCP22 carrying D1585 <i>pilE</i> , Gm ^R	This study
pUCP(PA01 <i>pilE</i>)	pUCP22 carrying PA01 <i>pilE</i> , Gm ^R	This study
pEX18Tc	Tc ^R , <i>oriT</i> , <i>sacB</i> , gene replacement vector	[228]
pD1585 $\Delta pilA$	pEX18Tc, 2 kb $\Delta pilA$ D1585 region	This study
p280 $\Delta pilA$	pEX18Tc, 2 kb $\Delta pilA$ 280 region	This study

*Canadian *Burkholderia cepacia* complex Research and Referral Repository. **Provincial Laboratory for Public Health - North, Alberta Health Services.

Bacteriophages DLP1 and DLP2 were previously isolated on *S. maltophilia* strain D1585 and partially characterized, with the results subsequently reported [11]. DLP1 and DLP2 have Siphoviridae morphologies and are both capable of infecting across taxonomic orders, lysing different strains of *S. maltophilia* in addition to *P. aeruginosa*. Bacteriophage E79 is a virulent phage having a Myoviridae morphology and infects *P. aeruginosa* strains [224,225]. Propagation of DLP1, DLP2, and E79 were performed using soft agar overlays as previously described [11]. Briefly, 100 µl of culture was incubated with 100 µl of phage for 20 minutes, mixed with 3 ml of 0.7% ½ LB top agar, and overlaid onto plates of ½ LB solid media [229]. Plates were incubated at 30°C overnight until plaques formed. Plates with confluent lysis were used to make high titre stocks by overlaying with 3 mL of modified suspension medium (SM) (50 mM Tris-HCl pH 7.5, 100 mM NaCl, 10 mM MgSO₄), collecting the top agar and incubating for 30 min at room temperature on a platform rocker with 20 µL chloroform per plate. The supernatant was collected after centrifugation for 5 min at 10,000 × g and filter sterilized using a Millex-HA 0.45 µm syringe-driven filter unit (Millipore, Billerica, MA) and stored at 4°C. Titre of stocks was obtained using serial dilutions of phage stock into SM in the soft agar overlay technique with *S. maltophilia* D1585 for DLP1 and DLP2, and *P. aeruginosa* PA01 for E79.

Transposon mutant library receptor screen

A 2,242 member *P. aeruginosa* PA01 random-insertion mini-Tn5-*luxCDABE* transposon mutant library [218] was screened for resistance to DLP1 phage infection using a spotting assay. 100 µL overnight culture was spread on ½ LB solid medium and allowed to dry. 10 µL of DLP1 was spotted in duplicate, as well as 10 µL of phage E79 and ½ LB as positive and negative controls, respectively. Plates were incubated overnight at 30°C and examined for absence of DLP1 clearing the following day. High titer phage stocks of 10¹⁰ pfu/mL were used.

Phage plaquing assays

DLP1 and DLP2 plaquing ability was determined by spotting on bacterial soft agar overlays. Briefly, 100 µL of overnight culture was mixed with 3 mL of 0.7% ½ LB top agar,

overlaid onto ½ LB plates with or without antibiotics and allowed to dry at room temperature for 30 min. Phage stocks were standardized to 10¹⁰ PFU/mL on *S. maltophilia* D1585 and tenfold serially diluted in SM to 10³ PFU/mL. 5 µL of each dilution was spotted onto the prepared plates and incubated for 18 h at 30°C. Each experiment was repeated in biological and technical triplicate.

Construction of Δ *pilA* *S. maltophilia* D1585 and 280 mutants

The major pilin subunit, *pilA*, was identified in *S. maltophilia* D1585 by sequence homology to *pilA* in *P. aeruginosa* PA01 using Geneious (10.1.3) [230], and was subsequently used to identify the *pilA* ortholog in *S. maltophilia* 280. The amino acid sequence percent identity of pilin subunits were compared using MUSCLE [231,232]. The *S. maltophilia* D1585 and 280 clean deletion *pilA* mutants were constructed by allelic exchange [233] as described below, using primers listed in Table 2-2.

Two separate PCRs were performed to amplify DNA fragments 1,096 bp and 955 bp in length, corresponding to regions upstream and downstream of the *pilA* gene in D1585, respectively, with 30 nucleotides of overlap at the 3' and 5' ends. Primers were designed from a 6,361 bp contig containing the *pilA* gene, as the D1585 genome assembly is currently incomplete. The sequence upstream to the region to be deleted was amplified from D1585 genomic DNA using primers *SmpilAupF* and *SmpilAupR-OE*. The sequence downstream of the deletion was amplified from D1585 genomic DNA using primers *SmpilAdownF-OE* and *SmpilAdownR*. Primers to delete *pilA* in *S. maltophilia* 280 were designed similarly from a 111,798 bp contig containing *pilA*, as the 280 genome assembly is also incomplete. The region upstream of the deletion was amplified from 280 genomic DNA using primers *280pilAupR* and *280pilAupF-OE*, producing a 1,074 bp product. The downstream region was amplified using primers *280pilAdownR-OE* and *280pilAdownF*, producing a 1,146 bp product. The PCR mixture contained 50 ng D1585 genomic DNA, 0.5 µM of each primer, 0.2 mM dNTPs, 3% DMSO and 1 × GC Buffer (New England Biolabs, Mississauga, Ontario, Canada) in sterile milliQ water and was heated for 3 minutes at 98°C before the addition of 1 U of Phusion High-Fidelity DNA Polymerase (New England Biolabs) per reaction. The reactions were then processed for 35 cycles of 15 s at 98°C, 30 s at 57.4°C for D1585 or 66.7°C for 280, and 30 s at 72°C before a

final extension of 10 min at 72°C. The PCR products were purified using a QIAquick PCR purification kit (Qiagen, Inc., Germantown, MD, USA).

Overlap extension PCR [234] was used to join the upstream and downstream PCR products, creating a 2,021 bp template for D1585 and a 2,190 bp template for 280. Briefly, a 1:1 ratio of upstream and downstream template was added to a PCR mixture lacking primers and processed for 3 min at 98°C, during which time Phusion polymerase was added, followed by 35 cycles of 15 s at 98°C, 30 s at 67.8°C for D1585 and 65.3°C for 280, and 1 min at 72°C before a final extension of 10 min at 72°C. A 1:1 ratio of primers *SmpilA*upF and *SmpilA*downR or *280pilA*upR and *280pilA*downF was added to the reaction after 10 cycles, which allowed the upstream and downstream templates to prime off their 30 bp overlap. The ~2 kb products were purified from a 1% agarose gel using a Gene Clean II kit (MP Biomedicals, Santa Ana, CA, USA) and digested with *SalI* and *HindIII* Fast Digest restriction endonucleases (Thermo Scientific, Waltham, MA, USA). The fragments were cloned into pEX18Tc, yielding pD1585Δ*pilA* containing a 444 bp in-frame deletion within the 477 bp D1585 *pilA* gene and p280Δ*pilA* containing a 372 bp in-frame deletion within the 414 bp 280 *pilA* gene as confirmed by Sanger sequencing. The deletion vectors were transformed into the mobilizing *E. coli* strain S17-1 and the plasmids were transferred into D1585 or 280 by conjugation as described previously, in a 1:10 donor to recipient ratio [235]. Single crossover D1585 transconjugants carrying pD1585Δ*pilA* in their chromosome were selected on LB agar containing 100 µg/mL tetracycline and merodiploid status was verified by PCR using *pilA* specific primers, *SmpilAF* and *SmpilAR* lacking restriction enzyme tails. Single crossover 280 transconjugants carrying p280Δ*pilA* were selected on LB agar containing 50 µg/mL tetracycline and merodiploid status was verified by PCR using *pilA* specific primers, *280pilAF* and *280pilAR* lacking restriction enzyme tails. Positive transconjugants were grown in the absence of tetracycline for 2 h to allow for a second crossover and screened on LB agar containing 10% (w/v) sucrose. Sucrose-resistant colonies appearing after 48 h incubation at 37°C were screened for the presence of the *pilA* deletion using the *pilA* specific primer pairs.

Table 2-2: Primers used in this study.

Primer name	Sequence (5' – 3')	Function
<i>SmpilA</i> upF	GTAT <u>GTTCGAC</u> GCCAATCGC CCCTATGCTGG	Anneals 1,047 to 1,028 bp upstream to the D1585 <i>pilA</i> start codon, <i>Sall</i> site underlined
<i>SmpilA</i> upR-OE	ATGGGATTAGCAGCCAGA GCACAGGATCGGTCTGG	The 20 nucleotides at the 3' end anneal to the seven codons following the D1585 <i>pilA</i> start codon and the first 15 nucleotides in bold overlap with the 5' end of the downstream fragment
<i>SmpilA</i> downF-OE	CCGATCCTGTGCTCTGGC TGCTAATCCCATCTGGA	The first 15 nucleotides in bold overlap with the 3' end of the upstream fragment, the last 20 nucleotides at the 3' end anneal to the last three codons in D1585 <i>pilA</i> and 11 bp following the stop codon
<i>SmpilA</i> downR	CCTC <u>AAGCTT</u> CCCCAACCA CCTTGTTCTGC	Anneals 902 to 921 bp downstream to the D1585 <i>pilA</i> stop codon, <i>HindIII</i> site underlined
280 <i>pilA</i> upR	GCCCA <u>AAGCTT</u> CATGTTTAC GATCATCTGGG	Anneals 1,046 to 1,027 bp upstream to the 280 <i>pilA</i> start codon on the reverse strand. <i>HindIII</i> site underlined.
280 <i>pilA</i> upF-OE	GGCGTACTTCTTCAGCAT TTTGGTACATCCCCAAG	The 20 nucleotides at the 3' end anneal to the 280 <i>pilA</i> start codon and 17 bp upstream, and the first 15 nucleotides in bold overlap with the 5' end of the downstream fragment.
280 <i>pilA</i> downR-OE	GGATGTACCAAAATGCTG AAGAAGTACGCCCCGAC	The first 15 nucleotides in bold overlap with the 3' end of the upstream fragment, and the last 20 nucleotides at the 3' end anneal to seven out of 12 codons upstream of the 280 <i>pilA</i> stop codon
280 <i>pilA</i> downF	GGCAG <u>TTCGAC</u> GGAAGTTGA TCTCGTCCAGC	Anneals 1,082 to 1,063 bp downstream of the 280 <i>pilA</i> stop codon. <i>Sall</i> site underlined.

<i>PapilAF</i>	GCGT <u>GTCGACCC</u> AGTTTCC TTGATCGTGGC	Anneals upstream of PA01 <i>pilA</i> gene. <i>Sall</i> site underlined.
<i>PapilAR</i>	GCCG <u>AAGCTT</u> GAGGAACCC AATCACAACGG	Anneals downstream of PA01 <i>pilA</i> gene. <i>HindIII</i> site underlined.
<i>PapilEF</i>	CCGAG <u>GATCC</u> GATCGAGAA AGAACAGCCCC	Anneals upstream of the PA01 <i>pilE</i> gene. <i>BamHI</i> site underlined.
<i>PapilER</i>	GCGG <u>AAGCTT</u> GCGGGAGG AGAACATTACCT	Anneals downstream of the PA01 <i>pilE</i> gene. <i>HindIII</i> site underlined.
<i>SmpilAF</i>	CCAAG <u>TCGACCC</u> ATCCGTG AAATAGCTGCC	Anneals upstream of D1585 <i>pilA</i> start codon. <i>Sall</i> site underlined.
<i>SmpilAR</i>	CGCC <u>AAGCTT</u> ACGAGCCGA CAAAAGAAAGGC	Anneals downstream of D1585 <i>pilA</i> stop codon. <i>HindIII</i> site underlined.
<i>SmpilEF</i>	GTCT <u>GTCGACC</u> AGTAACCC CAGTGCGAGGA	Anneals upstream of the D1585 <i>pilE</i> gene. <i>Sall</i> site underlined.
<i>SmpilER</i>	GCCC <u>AAGCTT</u> CTAACCGGC TGAGCTATTCG	Anneals downstream of the D1585 <i>pilE</i> gene. <i>HindIII</i> site underlined.
<i>280pilAF</i>	GCAAG <u>TCGACC</u> AGACCGAT CCTGTGCTCTG	Anneals upstream of the 280 <i>pilA</i> gene. <i>Sall</i> site underlined.
<i>280pilAR</i>	GACCA <u>AAGCTT</u> CCCCTAGTT CGCTTCATGGC	Anneals downstream of the 280 <i>pilA</i> gene. <i>HindIII</i> site underlined.

Complementation of pilus mutants

The *pilA* and *pilE* genes were amplified from *P. aeruginosa* PA01 by colony PCR using primer pairs *PapilAF* and *PapilAR*, and *PapilEF* and *PapilER* respectively, and from *S. maltophilia* D1585 genomic DNA by PCR using primer pairs *SmpilAF* and *SmpilAR*, and *SmpilEF* and *SmpilER*, as listed in Table 2-2. The *pilA* gene was amplified from *S. maltophilia* 280 genomic DNA by PCR using primer pairs *280pilAF* and *280pilAR*. The resulting products were digested with *SaII* and *HindIII*, or *BamHI* and *HindIII* Fast Digest restriction endonucleases (Thermo Scientific) and ligated using T4 DNA ligase (NEB) into the vector pUCP22 [30] for expression in PA01, or pBBR1MCS [29] for expression in D1585 and 280. The resulting constructs as listed in Table 2-1 were verified by Sanger sequencing and subcloned into electrocompetent *E. coli* DH5 α before transforming *P. aeruginosa* PA01 and *S. maltophilia* D1585 and 280 mutants by electroporation.

Electrocompetent *P. aeruginosa* PA01 cells were prepared as described by Choi et al. (2006) [236] with some modifications. Briefly, overnight cultures of PA01 grown in LB at 37°C were harvested by centrifugation for 5 min at 8,000 \times g and were washed 3 times with 300 mM sucrose. The cell pellet was resuspended in the remaining 300 mM sucrose and competent cells were stored in 100 μ l aliquots at –80°C prior to use. Electrocompetent *S. maltophilia* D1585 and 280 cells were prepared as described by Ye et al. (2014) [237]. Overnight cultures were subcultured and grown to an optical density at 600 nm (OD₆₀₀) of 1.0 in LB at 37°C and placed on ice for 30 min. The chilled cells were harvested by centrifugation for 5 min at 4,000 \times g and 4°C and washed 3 times with ice-cold 10% glycerol (v/v). The competent cells were resuspended in residual 10% glycerol and stored in 100 μ L aliquots at –80°C prior to use. Electrocompetent *E. coli* DH5 α cells were prepared similarly to *S. maltophilia*, however subcultures were grown to an OD₆₀₀ of 0.5 – 0.7 at 37°C.

Transmission electron microscopy

Bacterial samples were prepared for electron microscopy as follows. Overnight cultures were diluted 1:20 in fresh ½ LB broth and grown to an OD₆₀₀ of 0.3 - 0.6 at 30°C with shaking. 1 mL of subculture was harvested at 15,000 \times g, fixed in EM fixative (2.5% glutaraldehyde, 2% paraformaldehyde, 0.1 M phosphate buffer, pH 7.2) for 30 min, and resuspended in 1 \times phosphate-buffered saline (PBS), pH 7.4. For visualization of bacteria, a carbon-coated copper

grid was incubated with 10 µL of sample for 2 min and stained with 2% phosphotungstic acid (PTA) for 10 s. To visualize phage binding, the bacterial samples were mixed in a 1:2 ratio with high titre 10^{10} pfu/mL phage stock for 2 min. 10 µL of this mixture was incubated on the copper grid for 4 min, followed by staining with 2% PTA. Transmission electron micrographs were captured using a Philips/FEI (Morgagni) transmission electron microscope with charge-coupled device camera at 80 kV (University of Alberta Department of Biological Sciences Advanced Microscopy Facility).

Twitching motility assay

Twitching motility assays were used as an indirect measurement of type IV pili function. A single bacterial colony was suspended in 100 µL LB broth and stab inoculated with a toothpick through a 3 mm thick LB agar layer (1% agar), containing 0.3% porcine mucin or antibiotic where indicated, to the bottom of the petri dish and incubated with humidity at 37°C for 24 h for PA01 [238] or 72 h for D1585 [16]. Twitching motility zones between the agar and petri dish interface were visualized by gently removing the agar and staining each plate with 1% (w/v) crystal violet for 30 min followed by rinsing excess stain away with water. Stained twitching zone areas were measured using ImageJ software (NIH, Bethesda, MD, USA) [239]. Each strain was tested in biological and technical triplicate and average twitching area was calculated from the nine twitching zones.

Results and Discussion

***P. aeruginosa* PA01 type IV pilus mutants are resistant to DLP1 infection**

Bacteriophage DLP1 is a broad host range phage capable of lysing eight out of 27 *S. maltophilia* and two out of 19 *P. aeruginosa* strains tested, one being the reference strain PA01 [11]. A spotting screen of 2,242 PA01 mutants with random mini-Tn5-*luxCDABE* transposon insertions causing polar mutations [218] identified 27 mutants (Table 2-3) with insertions in 12 different genes that were resistant to DLP1 infection (Table 2-4). Ten of the 12 genes disrupted are directly involved in type IV pilus biogenesis, including both structural components, *pilB*, *pilE*, *pilT*, *pilV*, *pilY1*, and *fimV*, and regulatory components, *pilJ*, *pilR*, *pilS*, and *algR*. The two

additional genes, *PA1241* and *PA2806*, encode a probable transcriptional regulator belonging to the TetR family and a conserved hypothetical protein with homology to QueF, an NADPH-dependent 7-cyano-7-deazaguanine reductase enzyme involved in queuosine biosynthesis, respectively, that have unknown functions related to pilus biogenesis. Although the pilus related genes identified in the mutant library cover only a fraction of the over 40 genes involved in type IV pilus biogenesis and function in *P. aeruginosa* [134], there were no other pilus mutants in the library to screen for DLP1 sensitivity.

To better identify the type IV pilus as the receptor for DLP1 infection of PA01, additional PA01 pilus mutants were obtained [219,220] and screened. These included transposon mutants of the major pilin subunit PilA, the outer membrane pore subunit PilQ, and additional structural subunits PilF, PilN and PilU (Tables 2-3, 2-4). As expected, these mutants were also resistant to DLP1 infection, however the *pilU* mutant was not. Similar results have been observed following infection of mutant *P. aeruginosa* strains PA01 and PAK by another pilus-dependent Siphoviridae bacteriophage, P04; the unpiliated *pilB* and hyperpilated *pilT* mutants are resistant to phage infection, whereas the hyperpilated *pilU* mutant remains susceptible [135]. These genes encode the three ATPases that are responsible for extension and retraction of the type IV pilus; PilB is involved in polymerization of pilin subunits, and PilT and PilU are involved in depolymerization [240]. Assembly and disassembly of the pilus allows bacteria to move across a surface, a process known as twitching motility. While PilT and PilU appear to have similar functions, only *pilU* mutants have the unusual combination of pilus-specific phage susceptibility and loss of twitching motility [135,240]. Assessment of twitching motility in each of the 27 DLP1 resistant PA01 mutants, as well as the *pilU* mutant, revealed that all lack a twitching zone and therefore functional pili, with the exception of the *PA2806* mutant. These findings mirror what others have observed for pilus-specific phages P04, B3, and D3112 [135], and support the hypothesis that DLP1 uses the type IV pilus for first contact with its host and requires a pilus functionally capable of retraction in order to infect.

Table 2-3: Characteristics of *P. aeruginosa* PA01 transposon mutants.

Mutant ID/ Strain Name	Gene affected	Transposon	Genome Insertion Position	DLP1 lysis	Source
PW8621	<i>pilA</i>	<i>lacZ-hah</i>	5069310	-	[219]
PW8622	<i>pilA</i>	<i>phoA-hah</i>	5069368	-	[219]
PA01_lux_18_G2	<i>pilB</i>	<i>mini-Tn5-luxCDABE</i>	5069913	-	[218]
PA01_lux_50_H10	<i>pilB</i>	<i>mini-Tn5-luxCDABE</i>	5071244	-	[218]
PA01_lux_67_D1	<i>pilB</i>	<i>mini-Tn5-luxCDABE</i>	5070860	-	[218]
PA01_lux_97_B10	<i>pilB</i>	<i>mini-Tn5-luxCDABE</i>	5070077	-	[218]
PA01_lux_38_F5	<i>pilE</i>	<i>mini-Tn5-luxCDABE</i>	5104853	-	[218]
PA01_lux_41_C7	<i>pilE</i>	<i>mini-Tn5-luxCDABE</i>	5104839	-	[218]
PA01_lux_50_D5	<i>pilE</i>	<i>mini-Tn5-luxCDABE</i>	5104869	-	[218]
PW7438	<i>pilF</i>	<i>phoA-hah</i>	4264656	-	[219]
PA01_lux_44_E9	<i>pilJ</i>	<i>mini-Tn5-luxCDABE</i>	452821	-	[218]
PW9471	<i>pilN</i>	<i>phoA-hah</i>	5679378	-	[219]
PW9465	<i>pilQ</i>	<i>phoA-hah</i>	5676840	-	[219]
PW9466	<i>pilQ</i>	<i>phoA-hah</i>	5676900	-	[219]
PA01_lux_80_E5	<i>pilR</i>	<i>mini-Tn5-luxCDABE</i>	5096068	-	[218]
PA01_lux_18_G4	<i>pilS</i>	<i>mini-Tn5-luxCDABE</i>	5094527	-	[218]
PA01_lux_42_D11	<i>pilS</i>	<i>mini-Tn5-luxCDABE</i>	5094527	-	[218]
PA01_lux_53_B6	<i>pilS</i>	<i>mini-Tn5-luxCDABE</i>	5094527	-	[218]
PA01_lux_80_C7	<i>pilS</i>	<i>mini-Tn5-luxCDABE</i>	5094527	-	[218]
PA01_lux_32_G12	<i>pilT</i>	<i>mini-Tn5-luxCDABE</i>	436863	-	[218]
PA01_lux_46_D4	<i>pilT</i>	<i>mini-Tn5-luxCDABE</i>	436504	-	[218]
PW1730	<i>pilU</i>	<i>lacZ-hah</i>	438793	+	[219]
PA01_lux_19_D2	<i>pilV</i>	<i>mini-Tn5-luxCDABE</i>	5098940	-	[218]
PA01_lux_73_C10	<i>pilV</i>	<i>mini-Tn5-luxCDABE</i>	5099241	-	[218]
PA01_lux_20_D4	<i>pilY1</i>	<i>mini-Tn5-luxCDABE</i>	5101178	-	[218]

PA01_lux_51_H7	<i>pilY1</i>	<i>mini-Tn5-luxCDABE</i>	5102516	-	[218]
PA01_lux_82_C12	<i>pilY1</i>	<i>mini-Tn5-luxCDABE</i>	5102516	-	[218]
PA01_lux_97_G2	<i>pilY1</i>	<i>mini-Tn5-luxCDABE</i>	5100755	-	[218]
PA01_lux_67_E3	<i>fimV</i>	<i>mini-Tn5-luxCDABE</i>	3496099	+/-	[218]
PA01_lux_20_D1	<i>fimV</i>	<i>mini-Tn5-luxCDABE</i>	3497859	+/-	[218]
PA01_lux_21_F1	<i>fimV</i>	<i>mini-Tn5-luxCDABE</i>	3496114	+/-	[218]
PA01_lux_97_D2	<i>algR</i>	<i>mini-Tn5-luxCDABE</i>	5923165	+/-	[218]
PA01_lux_50_H9	<i>PA2806</i>	<i>mini-Tn5-luxCDABE</i>	3160973	-	[218]
PA01_lux_39_G8	<i>PA1241</i>	<i>mini-Tn5-luxCDABE</i>	1343199	-	[218]

DLP1 lysis: +, phage sensitivity; -, phage resistance; +/-, DLP1 low efficiency of plating

More information on strains is available at <http://pseudomutant.pseudomonas.com> for *mini-Tn5-luxCDABE* mutants and <http://www.gs.washington.edu/labs/manoil/libraryindex.htm> for *lacZ-hah* and *phoA-hah* mutants.

Table 2-4: *P. aeruginosa* PA01 genes involved in type IV pilus biogenesis and DLP1 phage infection identified by a transposon mutant library screen.

Number of mutants	Gene affected	Function	DLP1 lysis	Source
2	<i>pilA</i>	Major pilin subunit	-	[219]
4	<i>pilB</i>	Cytoplasmic ATPase/pilin polymerase	-	[218]
3	<i>pilE</i>	Minor pilin subunit	-	[218]
1	<i>pilF</i>	Outer membrane pilotin; controls secretin localization	-	[219]
1	<i>pilJ</i>	Involved in pilus assembly	-	[218]
1	<i>pilN</i>	Inner membrane assembly protein	-	[219]
2	<i>pilQ</i>	Secretin monomer; forms outer membrane pore	-	[219]
1	<i>pilR</i>	Cytoplasmic response regulator of two-component system; regulates PilA expression	-	[218]

4	<i>pilS</i>	Inner membrane histidine kinase of two component system; regulates PilA expression	-	[218]
2	<i>pilT</i>	Cytoplasmic ATPase; pilin depolymerase	-	[218]
1	<i>pilU</i>	Cytoplasmic ATPase; regulation of pilus retraction	+	[219]
2	<i>pilV</i>	Minor pilin subunit	-	[218]
4	<i>pilY1</i>	Possible adhesin; regulates pilus retraction	-	[218]
3	<i>fimV</i>	Inner membrane protein; aids in secretin assembly	+/-	[218]
1	<i>algR</i>	Regulates expression of minor pilin operon	+/-	[218]
1	<i>PA2806</i>	Conserved hypothetical protein	-	[218]
1	<i>PA1241</i>	Probable transcriptional regulator	-	[218]

Strain characteristics: +, phage sensitivity; -, phage resistance; +/-, DLP1 low efficiency of plating

Complementation in *P. aeruginosa* restores DLP1 infectivity

To confirm that PA01 mutants were resistant to DLP1 infection due to their lack of pili, the two major subunit *pilA* and three minor subunit *pilE* mutants were chosen as hosts for complementation analysis and to assess DLP1 infectivity via phage plaquing assays. In PA01, *pilE* is the seventh gene in the minor pilin operon and *pilA* is transcribed as a single gene, therefore polar mutations are not a concern for complementation of these mutants. Wildtype PA01 is susceptible to DLP1, clearing at 10^9 PFU/mL, but not DLP2 (Figure 2-1). Both *pilA* mutants, PW8621 and PW8622, are resistant to DLP1 infection and when transformed with the endogenous PA01 *pilA* gene, exhibit restored susceptibility to DLP1 infection. DLP1 deposited on bacterial lawns of the complemented *pilA* mutants produce clear spots comparable to wildtype levels. The same effect was observed for each of the three PA01 *pilE* mutants transformed with pUCP22 carrying the endogenous *pilE* gene (Figure 2-1). In comparison, transformation of each mutant with an empty pUCP22 vector did not restore DLP1 infection and no lysis of the bacterial lawn was observed. As confirmation that DLP1 binds type IV pili expressed on the surface of PA01, transmission electron microscopy (TEM) was used to visualize this interaction. Imaging of log phase PA01 cells mixed with high titre DLP1 showed phage particles near the cell surface

that appeared to interact with the base of a pilus via the phage tail (Figure 2-2A). This observation, along with complementation restoring phage infectivity, confirms the pilus as phage DLP1's initial point of attachment to *P. aeruginosa* PA01.

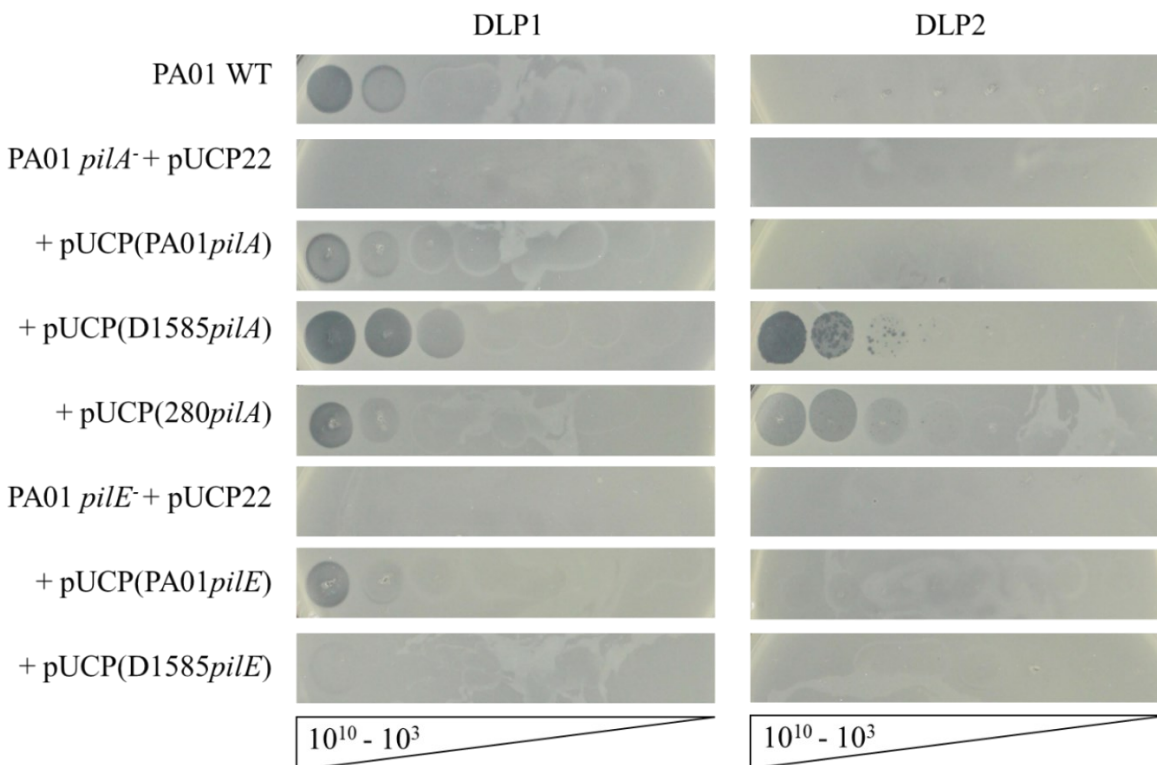


Figure 2-1: Infection of *P. aeruginosa* PA01 expressing varying pilin subunits by DLP1 and DLP2. PA01 wildtype (WT) is susceptible to DLP1, while the PA01 *pilA* PW8621 and *pilE* PA01_lux_41_C7 mutants are resistant to infection. Complementation of PA01 mutants with the endogenous genes restores DLP1 infectivity to wildtype levels, clearing at 10⁹ PFU/ml. Cross-genera complementation with the *S. maltophilia* D1585 *pilA* gene restores infection by DLP1, clearing at 10⁸ PFU/mL, and allows DLP2 plaquing at 10⁷ PFU/mL. Complementation with the D1585 *pilE* gene allows partial DLP1 infection. Cross-genera complementation with the *S. maltophilia* 280 *pilA* gene also allows DLP2 infection at 10⁸ PFU/mL and partially restores DLP1 infectivity. Images are representative of three biological replicates, each with three technical replicates. Similar results were observed for the additional *pilA* and *pilE* mutants when complemented.

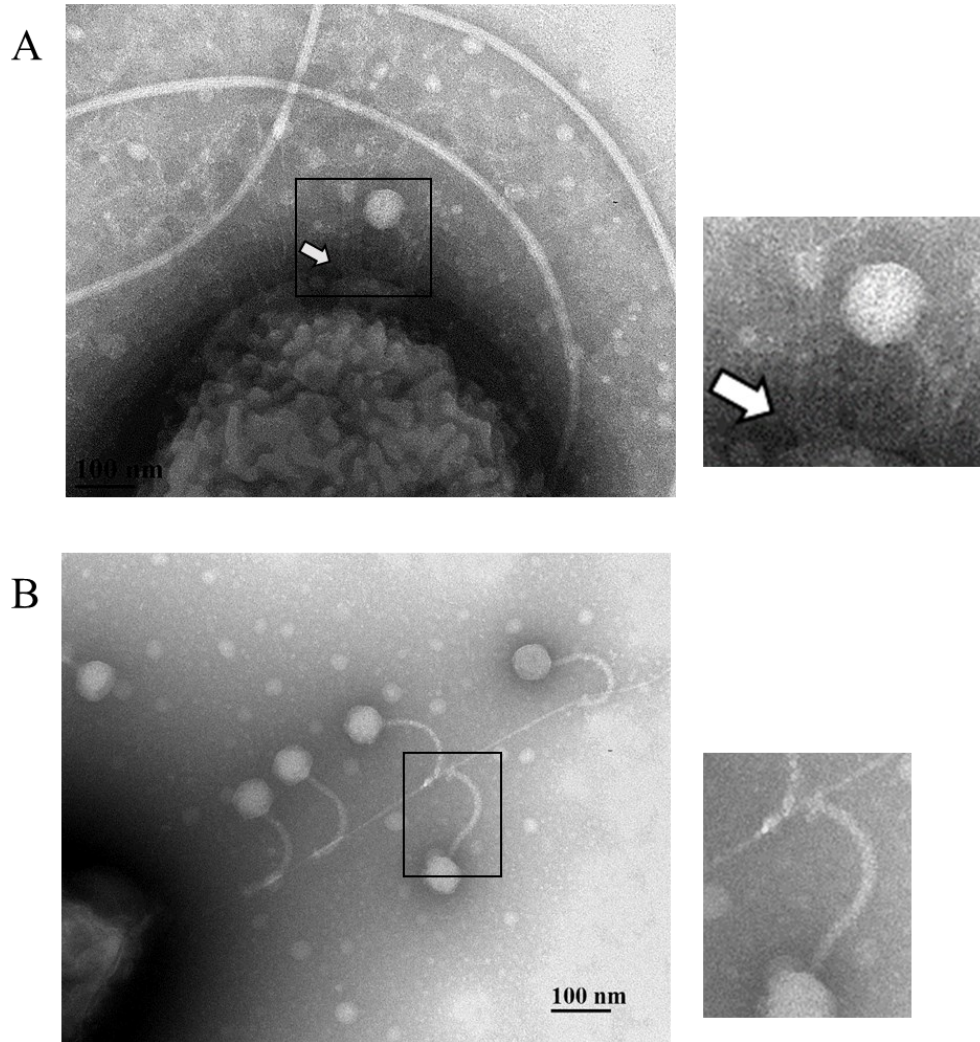


Figure 2-2: DLP1 interacts with pili on the cell surface of wildtype *S. maltophilia* D1585 and *P. aeruginosa* PA01. Electron micrographs showing (A) multiple pili projecting from the pole of a PA01 cell with a single DLP1 phage interacting with the base of a pilus (arrow) and (B) five DLP1 phage binding a single pili extending from the pole of a D1585 cell. Boxed images show larger views of phage-pili interactions. Cells and phage were stained with 2% phosphotungstic acid and visualized at 110,000-fold magnification by transmission electron microscopy.

To ascertain whether DLP1 also uses the type IV pilus as the first point of contact with its *S. maltophilia* hosts, we performed cross-genera complementation experiments using the PA01 minor pilin, *pilE*, and major pilin, *pilA*, orthologs in strain D1585 expressed in the respective PA01 mutant. Both DLP1 and DLP2 were isolated on *S. maltophilia* strain D1585, and out of the

27 strains tested, both phages infect D1585 with equally high efficiency, producing plaques when spotted at 10^3 PFU/mL [11]. Therefore, we describe D1585 as the major host for DLP1 and DLP2 in our *S. maltophilia* strain collection. Similar to complementation with the endogenous PA01 genes, cross-genera complementation of the PA01 *pilA* mutants PW8621 and PW8622 with D1585 *pilA* also restored DLP1 infection. Exposure of these cross-genera complemented PA01 mutants to DLP1 produced infection at the same efficiency of plating as wildtype PA01; however, DLP1 appears to clear the bacterial lawn expressing D1585 *pilA* more effectively (Figure 2-1). DLP1 infects *S. maltophilia* D1585 at higher efficiency of plating, plaquing at 10^3 PFU/mL, as compared to *P. aeruginosa* PA01 that DLP1 is unable to infect at a PFU/mL lower than 10^8 . It is likely that DLP1 binds amino acids in the PilA of D1585 with more affinity than the PilA of PA01. Therefore, expression of the D1585 *pilA* subunit in a *pilA* deficient PA01 strain permits more efficient DLP1 receptor binding and infection, resulting in more clear spots in the bacterial lawn.

Alternatively, cross-genera complementation of the three PA01 *pilE* mutants with D1585 *pilE* produces only partial infection by DLP1, showing a slightly thinned lawn at 10^{10} PFU/mL (Figure 2-1). The *pilE* gene encodes one of four minor pilin subunits in *P. aeruginosa* that assemble together at the tip of the pilus, along with FimU and PilY1, to prime pilus assembly [241]. *P. aeruginosa* strains express one of five major type IV pilin alleles with an associated set of minor pilin alleles [242,243]. Studies have shown that the minor pilin genes are compatible with major pilins of the same group, but do not function as well when expressed with a heterologous major pilin [243]. Because the PA01 and D1585 PilA subunits and PilE subunits share only 51% and 43% amino acid sequence identity, respectively, it is possible that the major pilin *pilA* subunits are sufficiently different between *P. aeruginosa* PA01 and *S. maltophilia* D1585 that the D1585 PilE minor subunit does not have high affinity for the PA01 PilA major subunit. This may decrease the association between the minor pilin priming complex and PilA such that the pilus does not assemble proficiently, resulting in decreased piliation or inefficient pilus extension and decreased phage infection, as observed, due to loss of receptor expression. Examination of twitching motility in each of the complemented strains supports this hypothesis, showing that pili function is reduced by approximately 61% and 58% for D1585 *pilA* and *pilE* cross-genera complementation respectively, compared to complementation with the PA01 endogenous subunits (Figure 2-3). Although the overall pili function is similar between D1585

pilE and *pilA* complemented PA01 mutants, differences in phage infectivity may be explained by changes in amino acids between the foreign and endogenous subunits. This is similar to observations by Giltner et al. 2011; *P. aeruginosa* PA01 Group II *pilE* mutants complemented with a PA14 Group III *pilE* gene in trans decreased twitching motility by 9% relative to endogenous complementation [243]. Because the amino acid sequence identity of PA01 and D1585 PilE subunits is lower than PA01 and PA14 PilE products that share 51% amino acid identity, our substantial decrease in twitching motility is likely due to the inefficient assembly of D1585 PilE with the PA01 pilin subunits.

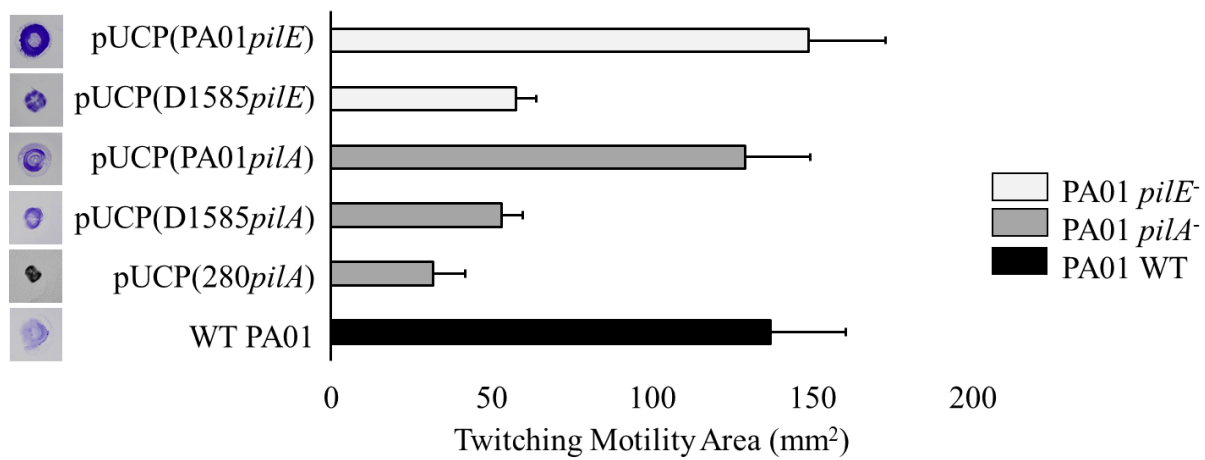


Figure 2-3: Twitching motility is partially restored in cross-genera complemented *P. aeruginosa* PA01 pilin mutants. PA01, its *pilA* PW8621 and *pilE* PA01_lux_41_C7 mutants and their respective complemented strains were stab inoculated through 1% ½ LB agar and incubated for 24 h at 37°C. Twitching zones were visualized with 1% crystal violet and measured using ImageJ [42]. Complementation with the endogenous PA01 genes restored twitching to wildtype, while cross-genera complementation only partially restored motility. Representative twitching zones are shown on the left and the average area of the twitching zones from nine replicates are shown on the right including error bars showing standard deviation.

A second *S. maltophilia* phage, DLP2, was tested against the *pilA* cross-genera complemented strains PW8621 and PW8622 carrying D1585 *pilA* on pUCP22. DLP2 is another broad host range phage that is capable of infecting nine out of 27 *S. maltophilia* strains, including D1585, and two out of 19 *P. aeruginosa* strains, although PA01 is not one of them [11]. Phage

spotting shows that DLP2 can infect *pilA* deficient PA01 mutants expressing the D1585 *pilA* gene, clearing the bacterial lawn at 10^9 PFU/mL (Figure 2-1). This is not entirely surprising given that DLP2 can infect two different strains of *P. aeruginosa*, HER1004 and 14,715 [11], suggesting that there are no intracellular blocks to phage infection across these genera once a primary receptor for DLP2 is expressed on the cell surface. DLP1 and DLP2 are closely related phages, sharing a high degree of sequence identity over their genomes [11]. Because both are capable of infecting *S. maltophilia* D1585 as a major host, it is possible if not probable that they share the same receptor. These results suggest that DLP2 also uses the type IV pilus as the primary receptor for infection of D1585, requiring only the D1585 major pilin expressed in trans to infect the previously resistant strain, *P. aeruginosa* PA01. However, it is then unclear why the host ranges of DLP1 and DLP2 differ, and how these two phages adhere to pilin subunits of different hosts if they both do adhere to the PilA subunit to infect D1585. Rescue of phage infection through cross-genera complementation of the major pilin subunit also suggests that the pre-pilin signal cleavage sequence of D1585 pilins is conserved and recognized by *P. aeruginosa* pre-pilin peptidase, allowing proficient assembly of mature pilins sufficient for phage recognition and infection.

Based upon the similarity between pilin subunits and the highly conserved nature of type IV pili assembly machinery, heterologous expression of type IV pilins has been used to analyze structure-function relationships of pili in numerous pathogenic bacteria. Research shows that *P. aeruginosa* can assemble exogenous pilins from species including *Dichelobacter nodosus*, *Moraxella bovis*, *Neisseria gonorrhoeae*, and *Escherichia coli* [244–247]. Heterologous expression of pili subunits restores pili function and associated phenotypes, such as natural competence and phage binding [248–250]. For example, the major pilin subunit PilA from *P. aeruginosa* can be successfully expressed and assembled into functional type IV pili in *N. gonorrhoeae*, and is sufficient for *P. aeruginosa* specific phage PO4 binding, determined through transmission electron microscopy [251]. In contrast to our cross-genera complementation, many of these studies use retraction-deficient *pilT*⁻ strains of *P. aeruginosa* to compensate for low steady-state expression of pili. However, such a technique would inhibit DLP1 and DLP2 infection of the host, as these phages appear to require pili retraction by the host to reach the cell surface. While pilin sequences vary within species, the type IV pilus assembly machinery is widely conserved at the nucleotide level, providing relaxed specificity for the

heterologous expression of pilin proteins from distantly related species [243]. This insensitivity to sequence changes in PilA provides an evolutionary benefit to the cell, allowing the incorporation of a wide range of pilins for antigenic variation and functional diversity.

Deletion of *pilA* in *S. maltophilia* D1585 prevents DLP1 and DLP2 infection

Following on the results obtained from cross-genera complementation that implicate the type IV pilus in D1585 as the receptor for DLP1 and DLP2, the major subunit *pilA* ortholog was deleted in *S. maltophilia* D1585 using overlap-extension PCR and allele exchange to create a clean deletion. Sanger sequencing confirmed the in-frame clean deletion and twitching motility was subsequently examined in both wildtype D1585 and the $\Delta pilA$ mutant to analyze pili function. D1585 wildtype produces a small zone of twitching, averaging $25 \pm 10 \text{ mm}^2$ after 72 h incubation at 37°C. This twitching zone is absent in the D1585 $\Delta pilA$ mutant, indicating that the mutant cannot assemble functional type IV pili, and suggests that the deleted gene encodes the major type IV pilin subunit in D1585. While the sizes of twitching motility zones vary greatly in both clinical and environmental *S. maltophilia* strains [5,16], our D1585 wildtype strain did not consistently produce twitching zones. To further confirm that the D1585 $\Delta pilA$ mutant was incapable of twitching motility, we induced pili expression in both the wildtype and mutant strains by adding mucin to the media. Mucin is a major component of mucus produced in the lungs where *S. maltophilia* can colonize and has been shown to increase the expression of type IV pili in *P. aeruginosa* resulting in increased twitching motility zones [252]. The addition of 0.3% mucin to the twitching motility plates increased D1585 wildtype twitching zones to approximately $41 \pm 14 \text{ mm}^2$ after only 24 h incubation. This increase in motility, while also inconsistent, was completely absent in the $\Delta pilA$ mutant, indicating that the mutant does not express functional pili.

Assessment of phage plaquing ability on the constructed D1585 $\Delta pilA$ mutant by spot assay shows that this mutant is resistant to infection by DLP1 and DLP2, displaying an absence of clearing and cell lysis at high phage titre (Figure 2-4). Complementation of the mutant with the endogenous D1585 *pilA* gene restored infection by DLP1 and DLP2 to wildtype levels, each producing plaques at 10^3 PFU/mL. Transformation of D1585 $\Delta pilA$ with an empty pBBR1MCS vector did not restore phage infection and no change in bacterial growth in each phage spot was observed. In contrast to the original characterization of DLP1 by Peters et al. (2015) [11], high

titre phage stocks of 10^{10} PFU/mL were able to clear the bacterial lawn and plaque formation was no longer delayed. We suspect that the efficiency of DLP1 infection has increased since its original isolation due to repeated propagation on the *S. maltophilia* host D1585 under laboratory conditions. These results confirm the identification of the type IV pilus as the primary receptor for DLP1 and DLP2 infection of their shared host, D1585. Because DLP1 can infect both D1585 and PA01 via adherence to the type IV pilus, we hypothesized that expression of the exogenous PA01 *pilA* gene in our D1585 $\Delta pilA$ mutant should restore DLP1 binding and infection, similar to the reverse situation as described above. As expected, cross-genera complementation of the D1585 $\Delta pilA$ mutant with the PA01 *pilA* gene produced less efficient DLP1 infection, forming plaques when spotted with 10^7 PFU/mL DLP1 (Figure 2-4). Surprisingly, DLP2 was also capable of low-level infection of D1585 $\Delta pilA$ expressing the PA01 major pilin subunit; DLP2 produced plaques at 10^9 PFU/mL, approximately 10^2 -fold lower efficiency than DLP1. While DLP2 is unable to infect wildtype PA01, it is possible that the PA01 PilA subunit is assembled differently in D1585 to expose different phage binding sites and enable low levels of DLP2 infection. Alternatively, PA01 PilA may interact with the pilus priming minor pilin subunits of D1585 as efficiently as the endogenous major subunit, perhaps permitting DLP2 to recognize pili via the minor pilins and reach a surface secondary receptor for partial infection. Twitching motility analysis of the complemented D1585 mutant yielded no changes in motility compared to the low levels observed in wildtype D1585 (data not shown).

TEM visualization of log phase D1585 cells mixed with high titre DLP1 confirmed that DLP1 binds the type IV pilus of D1585. The *S. maltophilia* D1585 viewed expressed multiple pili from their poles, however the pilus morphology differed from *P. aeruginosa* PA01; D1585 pili were longer and thicker than the fine projections viewed on PA01 (Figure 2). Cells mixed with DLP1 clearly showed phage particles distributed tail first along D1585 type IV pilus filaments, with phage appearing to attach to the sides of the pili via the tail baseplate, confirming that DLP1's initial point of attachment to *S. maltophilia* D1585 is the type IV pilus (Figure 2B). In addition to PA01 pili being finer than those of D1585, they were also on average shorter. It is possible that the length of the pili affects the susceptibility of these strains to DLP1 and DLP2. Attempts to visualize DLP2 binding the pili of D1585 were unsuccessful.

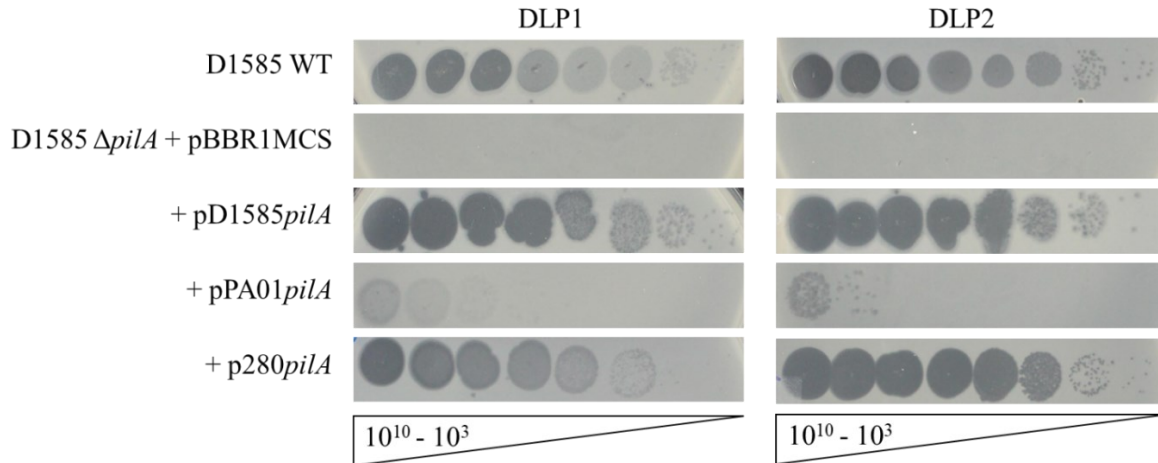


Figure 2-4: Infection of *S. maltophilia* D1585 expressing varying pilin subunits by DLP1 and DLP2. D1585 wildtype (WT) is susceptible to DLP1 and DLP2, while the D1585 $\Delta pilA$ mutant is resistant to both phages. Complementation of D1585 $\Delta pilA$ with the endogenous *pilA* gene restores DLP1 and DLP2 infectivity to wildtype levels, each plaquing at 10^3 PFU/ml. Cross-genera complementation with the *P. aeruginosa* PA01 *pilA* gene restores partial infection by DLP1 and DLP2, plaquing at 10^7 and 10^9 respectively. Cross-species complementation with the *S. maltophilia* 280 *pilA* gene restores DLP2 infection to wildtype levels, and partially restores DLP1 infectivity, showing plaquing at 10^5 . Images are representative of three biological replicates, each with three technical replicates.

Deletion of *pilA* in *S. maltophilia* 280 prevents DLP2 infection

As described above, DLP1 and DLP2 infection of *S. maltophilia* D1585 relies on the presence of the type IV pilus for cell surface attachment. To verify that DLP2 uses the type IV pili across its host range and possibly explain differences in the host ranges of DLP1 and DLP2, we examined the *S. maltophilia* strain 280 that is highly susceptible to DLP2 but not DLP1. *S. maltophilia* 280 expresses functional pili, demonstrated by a twitching motility zone area of approximately 155 mm^2 , 6-fold greater than D1585, following 72 h incubation (Figure 2-5A). This twitching zone also increased in size similarly to D1585 when examined on media containing 0.3% mucin, increasing to $250 \pm 22 \text{ mm}^2$ after 24 h incubation. Log phase 280 cells viewed by TEM revealed long pili projections from the sides of the cells rather than from the poles (data not shown). These pili were similar in length and diameter to *S. maltophilia* strain

D1585, however, attempts to visualize DLP2 interacting with 280 pili or the cell surface have been unsuccessful due to difficulties in preparing clean samples expressing pili.

A 280 $\Delta pilA$ mutant was also constructed using overlap extension PCR and allele exchange to delete the D1585 major pilin subunit *pilA* ortholog. Sanger sequencing of the 1 kb regions flanking the deletion confirmed the in-frame clean deletion and assessment of twitching motility on $\frac{1}{2}$ LB and $\frac{1}{2}$ LB supplemented with 0.3% mucin revealed the absence of a twitching zone, consistent with a lack of the PilA major pilin subunit and a non-functional type IV pilus. Exposure of the 280 $\Delta pilA$ mutant to bacteriophage DLP2 via spot assay showed no evidence of cell lysis, indicating that this mutant is resistant to DLP2 infection, similar to D1585 $\Delta pilA$ (Figure 2-5B). Complementation of 280 $\Delta pilA$ with the endogenous *pilA* gene restored DLP2 infection to near wildtype levels, producing plaques at 10^7 PFU/mL as compared to 10^5 PFU/mL on wildtype. These results confirm that DLP2 uses the type IV pilus as its cell surface receptor for infection of *S. maltophilia* 280 in addition to strain D1585.

Similar to cross-genera complementation of the PA01 *pilA* mutant with the D1585 *pilA* gene, expression of the exogenous D1585 *pilA* gene in our 280 $\Delta pilA$ mutant permitted infection by DLP2 as well as DLP1, plaquing at 10^5 PFU/mL and 10^8 PFU/mL respectively (Figure 2-5B). The reverse complementation of D1585 $\Delta pilA$ with the 280 *pilA* also restores DLP1 and DLP2 infection to near wildtype levels, with DLP2 infecting more efficiently (Figure 2-4, Table 2-5). Cross-genera complementation of 280 $\Delta pilA$ with the *P. aeruginosa* PA01 *pilA* gene did not restore infection by either DLP1 or DLP2. This is contrary to the reverse complementation of PA01 *pilA* mutants with the 280 *pilA* gene that shows partial infection by DLP2 as well as DLP1 (Figure 2-1, Table 2-5). These observations suggest that the *P. aeruginosa* PA01 PilA subunit does not assemble proficiently with the *S. maltophilia* 280 type IV pili machinery, whereas the more closely related D1585 PilA subunit can be assembled correctly to allow pili function and phage infection. The amino acid sequence identity between 280 and PA01 PilA subunits is lower than 280 and D1585 PilA, sharing 48% and 67% sequence identity respectively. Additionally, the twitching motility zone of 280 $\Delta pilA$ carrying pPA01*pilA* is reduced by 80% relative to wildtype 280, compared to complementation with the D1585 or endogenous *pilA* gene restoring twitching motility to 52% and 29% of wildtype respectively (Figure 2-5A).

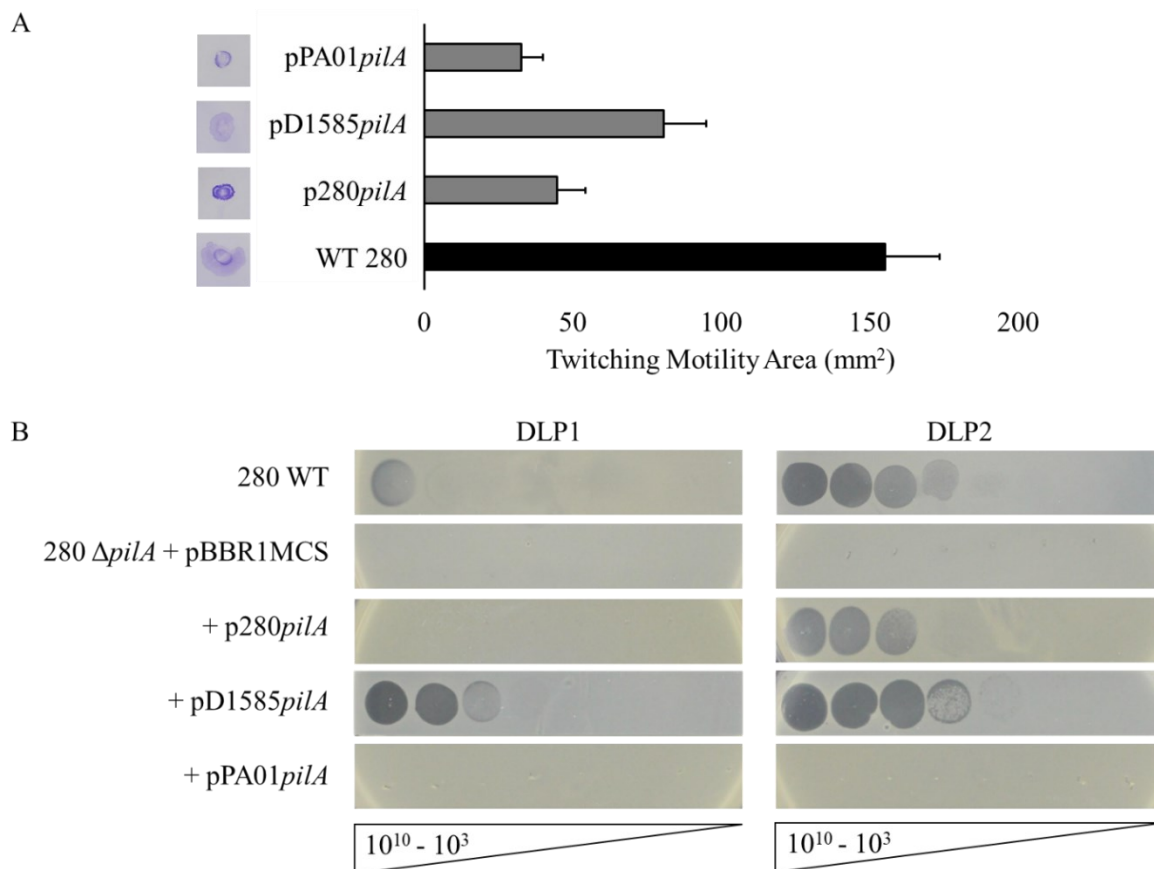


Figure 2-5: Infection of *S. maltophilia* 280 expressing varying pilin subunits by DLP1 and DLP2. (A) Twitching motility of the 280 Δ *pilA* mutant complemented with the PA01, D1585 or endogenous 280 *pilA* is not restored to wildtype levels and is not correlated with phage susceptibility. Representative twitching zones are shown on the left and the average area of the twitching zones from nine replicates are shown on the right. (B) 280 wildtype (WT) is susceptible to DLP2, while the 280 Δ *pilA* mutant is resistant. Complementation of 280 Δ *pilA* with the endogenous *pilA* gene restores DLP2 infectivity to near wildtype levels, plaquing at 10⁷ PFU/ml. Cross-species complementation with the *S. maltophilia* D1585 *pilA* gene restores DLP2 infectivity to wildtype levels, plaquing at 10⁵ PFU/mL, and allows partial DLP1 infectivity, showing plaquing at 10⁸ PFU/mL. Cross-genera complementation with the *P. aeruginosa* PA01 *pilA* gene does not restore phage infection. Images are representative of three biological replicates, each with three technical replicates.

While inefficient pilin assembly in foreign backgrounds may explain changes in phage susceptibility, it is also possible that *S. maltophilia* 280 modifies its surface pili to become

unrecognizable by some bacteriophages, such as DLP1. Studies of pilus-specific phage in *P. aeruginosa* have revealed that surface modification of pili via glycosylation can protect the bacteria from phage infection by masking potential binding sites, without creating disadvantageous phenotypes through changes to pilin sequence [253]. Although this modification protects *P. aeruginosa* from infection by most phages, some phages such as DMS3 have developed the ability to bind glycosylated pili and bypass this bacterial defense mechanism [253]. If *S. maltophilia* strain 280 has a modification system for its pili, this modification may mask DLP1's binding site by steric hindrance, however expressing the 280 *pilA* gene in a PA01 or D1585 background that lacks this modification system allows DLP1 to recognize a new motif for host recognition, resulting in more efficient infection than expression in 280 (Table 2-5).

Table 2-5: Summary of DLP1 and DLP2 phage susceptibility of cross complemented *pilA* mutants.

Strain + DLP1	Pilin Complement		
	pPA01 <i>pilA</i>	pD1585 <i>pilA</i>	p280 <i>pilA</i>
<i>P. aeruginosa</i> PA01 <i>pilA</i> ⁻	10 ⁹	10 ⁸	10 ⁹
<i>S. maltophilia</i> D1585 Δ <i>pilA</i>	10 ⁷	10 ³	10 ⁵
<i>S. maltophilia</i> 280 Δ <i>pilA</i>	-	10 ⁸	-
Strain + DLP2	pPA01 <i>pilA</i>	pD1585 <i>pilA</i>	p280 <i>pilA</i>
	pPA01 <i>pilA</i>	pD1585 <i>pilA</i>	p280 <i>pilA</i>
<i>P. aeruginosa</i> PA01 <i>pilA</i> ⁻	-	10 ⁷	10 ⁸
<i>S. maltophilia</i> D1585 Δ <i>pilA</i>	10 ⁹	10 ³	10 ³
<i>S. maltophilia</i> 280 Δ <i>pilA</i>	-	10 ⁵	10 ⁷

Darker shading indicates increased susceptibility to phages: □ no infection, □ clearing at 10⁹, □ plaquing at 10⁹, □ clearing at 10⁸, □ plaquing at 10⁷, □ plaquing at 10⁵, □ plaquing at 10³.

Conclusions

The type IV pilus is a common receptor for many *P. aeruginosa* specific phages, including PO4 [254], F116 [255], DMS3 [256], MP22 [257], and MPK7 [258], however this study is the first to identify the type IV pilus as the surface receptor for phages that infect *S.*

maltophilia and is the first described receptor for phages infecting this bacterium. The type IV pilus is a well characterized virulence factor in many bacteria, including *P. aeruginosa* and *N. gonorrhoeae*, involved in surface motility, biofilm formation, and adherence to mammalian cells and surfaces [134]. The results presented identify the type IV pilus as the primary receptor for both DLP1 and DLP2, with implications for phage therapy. Several studies have shown the ability of bacteriophages to increase bacterial virulence through moron genes encoded by the phage, however phages may also provide a selective pressure against bacteria expressing specific virulence factors [259]. Although bacteria may become resistant to phages through the modification of phage receptors, when the phage receptor is a virulence factor such as lipopolysaccharide or type IV pili, this mutation provides resistance at the cost of lowered virulence and reduced fitness compared to non-resistant cells [259]. Therapy targeting bacterial virulence factors has been termed an “anti-virulence strategy” [159] and such a strategy using an antibiotic in combination with a phage targeting a *P. aeruginosa* efflux pump responsible for antibiotic resistance has been used successfully to treat a patient’s life-threatening aortic infection [164,165]. Therefore, the application of “anti-virulence” phages such as DLP1 and DLP2 may prove to be an effective therapy for clearing *S. maltophilia* and *P. aeruginosa* infections, while potentially reducing the virulence of resistant mutants that may arise.

Acknowledgements

I would like to thank Arlene Oatway from the University of Alberta Department of Biological Sciences Advanced Microscopy Facility for assistance with electron microscopy. We also thank Shawn Lewenza from the University of Calgary for gifting the PA01 transposon mutant library, as well as the Canadian Burkholderia cepacia complex Research and Referral Repository (CBCCRRR, Vancouver, BC, Canada) and The Provincial Laboratory for Public Health—North (Microbiology), Alberta Health Services, for gifts of the *S. maltophilia* strains used in this study. I was kindly supported by a CGS-M scholarship award from NSERC, and a summer studentship from Alberta Innovates—Health Solutions during this research.

CHAPTER 3 - Identification of the type IV pilus as a common receptor for *Stenotrophomonas maltophilia* bacteriophages and the potential for anti-virulence phage therapy

Some data included in Figures 3-1 and 3-13 has been published within:

Peters DL, **McCutcheon JG**, Stothard P, Dennis JJ. 2019. Novel *Stenotrophomonas maltophilia* temperate phage DLP4 is capable of lysogenic conversion. *BMC Genomics*. 20:300. doi.org/10.1186/s12864-019-5674-5. IF: 3.969

Peters DL, **McCutcheon JG**, Dennis JJ. 2020. Characterization of novel broad-host-range bacteriophage DLP3 specific to *Stenotrophomonas maltophilia* as a potential therapeutic agent. *Front Microbiol*. 11:6. doi:10.3389/fmicb.2020.01358. IF: 5.640

McCutcheon JG, Lin A, Dennis JJ. 2020. Isolation and characterization of the novel bacteriophage AXL3 against *Stenotrophomonas maltophilia*. *Int J Mol Sci*. 21:6338. doi:10.3390/ijms21176338. IF: 5.924

McCutcheon JG, Lin A, Dennis JJ. 2022. Characterization of *Stenotrophomonas maltophilia* phage AXL1 as a member of the genus *Pamexvirus* encoding resistance to trimethoprim-sulfamethoxazole. *Sci Rep*. 12:10299. doi:10.1038/s41598-022-14025-z. IF: 5.516

Objectives

The identification of phage receptors is an often overlooked but essential aspect of phage characterization [131]. This knowledge improves our understanding of phage-host interactions and informs the design of effective therapeutic phage cocktails. To better understand the interaction of *S. maltophilia* phages and their hosts, the objectives of this chapter are to identify the receptors for the additional six bacteriophages against *S. maltophilia* in our lab, as well as further examine the role of type IV pili in *S. maltophilia* host virulence to inform an anti-virulence phage therapy strategy. Identifying additional phage receptors for this bacterial pathogen will aid in the construction of effective phage cocktails containing multiple phages targeting different receptors, as well as provide further information on the evolution between *S. maltophilia* and its viral predators.

Materials and Methods

Bacterial strains, bacteriophages and growth conditions

Bacterial strains and plasmids used in this study are listed below and in Tables 3-1, 3-2 and 3-3. The 30 phenotypically distinct *S. maltophilia* clinical isolates used for host range analysis were grown aerobically overnight at 30°C on half-strength Lennox (½ LB; 10 g/L tryptone, 5 g/L yeast extract, 5 g/L NaCl) solid medium or in ½ LB broth with shaking at 225 RPM. The five D-series *S. maltophilia* strains were acquired from the Canadian *Burkholderia cepacia* complex Research and Referral Repository (Vancouver, BC) and an additionally 22 numbered strains were gifted from the Provincial Laboratory for Public Health – North (Microbiology), Alberta Health Services. Strains ATCC13637 and SMDP92 were gifted by Dr. Jorge Giron and strain VLJ1 was received from the Center for Innovative Phage Applications and Therapeutics (IPATH; UCSD, USA). *X. campestris* XC114 (HER1103) and phage HXX (HER103) were obtained from the Félix d'Hérelle Reference Center for Bacterial Viruses, along with a *X. oryzae* (thy H; HER1154) strain. *X. translucens* pv. *translucens* ATCC19319 and *X. axonopodis* pv. *vasculorum* FB570 were obtained from the Summerland Research Centre in British Columbia for extended host range analysis. Additional work with *S. maltophilia* as well as *Xanthomonas* and *P. aeruginosa* strains was conducted in full strength LB at 30°C. *Escherichia coli* strains were grown at 37°C in full LB, unless otherwise noted. Media was

supplemented with antibiotics at the following final concentration when necessary for selection or plasmid maintenance ($\mu\text{g per mL}$): chloramphenicol (Cm), 35 for *S. maltophilia* D1585, D1571 and *E. coli* DH5 α ; gentamicin (Gm), 10 for *E. coli* and 35 for *P. aeruginosa*; tetracycline (Tc), 10 for *E. coli*, 100 for *S. maltophilia* D1585, and 60 for D1571.

Seven *S. maltophilia* phages having Siphoviridae morphologies, DLP1, DLP2, DLP3, DLP4, DLP5, AXL3 (Chapter 4), and AXL1 (Chapter 5), and one Myoviridae phage, DLP6, used in this work were previously isolated from soil samples in our lab and characterized [11,114,115,177–179]. Phage propagation was performed on strain D1585 for phages DLP1, DLP2, DLP4, AXL1, and AXL3, or strain D1571 for phages DLP3, DLP5, and DLP6 using soft agar overlays as previously described [11,229], or liquid infections. Briefly, 150 μL of overnight culture and 150 μL of phage lysate were incubated for 30 min at 30°C with shaking at 225 RPM before adding 15 mL LB broth and 1.5 mL modified suspension medium (SM) (50 mM Tris–HCl [pH 7.5], 100 mM NaCl, 10 mM MgSO_4) and incubating overnight under the same conditions. 200 μL of chloroform was added the following day and incubated on a platform rocker at room temperature for 30 min. Following centrifugation, the supernatant was collected, filter sterilized using a Millex-HA 0.45 μm syringe-driven filter unit (Millipore, Billerica, MA) and stored at 4 °C. Phage stocks were standardized to 10^{10} or 10^{11} PFU/mL on their propagation host and serially diluted as required. Phage HXX was propagated by soft agar overlay using *X. campestris* XC114.

Table 3-1: Bacterial strains and plasmids used in this study.

Bacterial Strain	Genotype or Description	Source
<i>S. maltophilia</i> D1585	Wildtype, host strain for phage propagation	CBCCR ^{RR} *
D1585 $\Delta pilA1$	Clean deletion of <i>pilA1</i> in D1585	[160]
D1585 $\Delta smfI$	Clean deletion of <i>smfI</i> in D1585	This study
D1585 $\Delta pilA1\Delta smfI$	Clean deletion of <i>pilA1</i> and <i>smfI</i> in D1585	This study
D1585 $\Delta pilT$	Clean deletion of <i>pilT</i> in D1585	This study/[178]
<i>S. maltophilia</i> D1571	Wildtype, host strain for phage propagation	CBCCR ^{RR} *
D1571 <i>pilQ</i> ⁻	D1571 DLP5-resistant mutant #24	This study
D1571 $\Delta pilA1$	Clean deletion of <i>pilA1</i> in D1571	This study

D1571::DLP3	Lysogen D1571; carrying DLP3 as a prophage	[178]
<i>S. maltophilia</i> 280	Wildtype, host strain for phage	PLPHN/AHS**
280 $\Delta pilA1$	Clean deletion of <i>pilA1</i> in 280	[160]
<i>S. maltophilia</i> ATCC13637	Wildtype, virulent in <i>G. mellonella</i>	[49]
<i>S. maltophilia</i> ATCC13637 $\Delta pilA1 \Delta pilA2 \Delta smf1$	Clean deletion of <i>pilA1</i> , <i>pilA2</i> , and <i>smf1</i> in ATCC13637	This study
PA01 <i>pilA</i> ⁻	PW8621; <i>lacZ-hah</i> transposon insertion in <i>pilA</i>	[219]
<i>E. coli</i> S17-1	Conjugative donor strain	[222]
<i>E. coli</i> DH5 α	Host for plasmid cloning	[223]
Plasmids		
pBBR1MCS	Broad-host range cloning vector, Cm ^R	[226]
pD1585 <i>pilA1</i>	pBBR1MCS carrying D1585 <i>pilA</i> , Cm ^R	[160]
pD1585 <i>pilT</i>	pBBR1MCS carrying D1585 <i>pilT</i> , Cm ^R	This study/[178]
pD1571 <i>pilQ</i>	pBBR1MCS carrying D1571 <i>pilQ</i> , Cm ^R	This study
pD1571 <i>pilA1</i>	pBBR1MCS carrying D1571 <i>pilA1</i> , Cm ^R	This study
pUCP22	Broad-host range cloning vector, Gm ^R	[227]
pUCP(D1585 <i>pilA1</i>)	pUCP22 carrying D1585 <i>pilA</i> , Gm ^R	[160]
pEX18Tc	Tc ^R , <i>oriT</i> , <i>sacB</i> , gene replacement vector	[228]
pD1585 $\Delta pilT$	pEX18Tc, 2 kb $\Delta pilT$ D1585 region	This study/[178]
pD1585 $\Delta smf1$	pEX18Tc, 2 kb $\Delta smf1$ D1585 region	This study
pATCC13637 $\Delta pilA1$	pEX18Tc, 2 kb $\Delta pilA1$ ATCC13637 region	This study
pATCC13637 $\Delta pilA2$	pEX18Tc, 2 kb $\Delta pilA2$ ATCC13637 region	This study
pATCC13637 $\Delta smf1$	pEX18Tc, 2 kb $\Delta smf1$ ATCC13637 region	This study
pD1571 $\Delta pilA1$	pEX18Tc, 2 kb $\Delta pilA1$ D1571 region	This study

* Canadian *Burkholderia cepacia* complex Research Referral Repository

** Provincial Laboratory for Public Health - North, Alberta Health Services.

Host range analysis

Host range analysis was conducted on a panel of 30 phenotypically distinct clinical *S. maltophilia* isolates, 21 *P. aeruginosa* isolates and four *Xanthomonas* strains. Soft agar overlays

containing 100 μ L of overnight culture mixed with 3 mL of 0.7% ½ LB top agar were spotted with 5 μ L of serially diluted phage lysate and scored for clearing and/or plaque formation after incubation at 30°C for 24 h and 48 h. Efficiency of plating (EOP) was calculated as the ratio of the number of plaques on a given strain to the titre on the isolation and propagation host. Where plaques were not detected, the lowest dilution with evidence of phage activity was considered for EOP. Predicted phage production was scored based on EOPs greater than 0.5 (high), between 0.1 and 0.5 (medium) or 0.1 to 0.001 (low) [260].

Phage plaquing assays

Phage plaquing ability was determined by spotting on bacterial soft agar overlays as previously described [160]. Briefly, 100 μ L of overnight culture was mixed with 3 mL of 0.7% ½ LB top agar, overlaid onto LB agar with or without antibiotics and allowed to solidify at room temperature for 30 min. Phage lysates were standardized to 10^{10} or 10^{11} PFU/mL on *S. maltophilia* D1571 for DLP3, DLP5, and DLP6, *X. campestris* XC114 for HXX, or strain D1585 for the remaining phages, and tenfold serially diluted in SM. 5 μ L of each dilution was spotted on the prepared plates in triplicate and incubated upright for 18 h at 30°C before imaging. Each experiment was repeated in biological triplicate.

Mutant construction

A *pilT* or *smfI* clean deletion mutant of *S. maltophilia* D1585 and a *pilAI* clean deletion mutant of *S. maltophilia* D1571 were constructed using overlap-extension PCR and allele exchange as previously described [160] using primers listed in Table 3-2. Briefly, regions upstream and downstream of the *pilT* gene in D1585 were PCR amplified using Phusion High-Fidelity DNA Polymerase (New England Biolabs) with primer pairs D1585*pilT*UpF-*HindIII* and D1585*pilT*UpR-OE for the upstream region, and D1585*pilT*DnF-OE and D1585*pilT*DnR-*XbaI* for the downstream region. Similarly, for the *smfI* gene, primer pairs D1585*smfI*UpF-*XbaI* and D1585*smfI*UpR-OE for the upstream region, and D1585*smfI*DnF-OE and D1585*smfI*DnR-*KpnI* for the downstream region were used. For deletion of the *pilAI* gene in D1571, primer pairs D1571*pilAI*DnF-*XbaI* and D1571*pilAI*DnR-OE for the downstream region, and D1571*pilAI*UpF-OE and D1571*pilAI*UpR-*KpnI* for the upstream region were used. Overlap regions are italicized and restriction enzyme recognition sites are bolded. Following overlap-

extension PCR, the deletion cassettes were ligated into pEX18Tc and the plasmids, pD1585 $\Delta pilT$, pD1585 $\Delta smfI$ and pD1571 $\Delta pilAI$, were transformed into *E. coli* S17-1 for bacterial mating with D1585 and D1571, respectively. Single crossover transconjugants were selected on LB agar containing 100 μ g/mL Tc for D1585 and 60 μ g/mL Tc for D1571 and merodiploid status was confirmed by colony PCR with *pilT* specific primers D1585*pilTF* and D1585*pilTR*, *smfI* specific primers D1585*smfIF* and D1585*smfIR*, or *pilAI* specific primers D1571*pilAIF-HindIII* and D1571*pilAIR-XbaI*. Positive merodiploids were grown in LB broth and plated on LB with 10 % sucrose to select for double crossover $\Delta pilT$, $\Delta smfI$ or $\Delta pilAI$ mutants that were confirmed by colony PCR as above. The D1585 $\Delta pilAI \Delta smfI$ double mutant was constructed using suicide vector pD1585 $\Delta smfI$ in the single D1585 $\Delta pilAI$ background. For complementation, the D1585 *pilT* gene was cloned into pBBR1MCS using *pilTF* and *pilTR* primers with tails for *HindIII* and *XbaI* restriction enzymes (Thermo Fisher) to create pD1585*pilT* and the D1571 *pilAI* gene was cloned into pBBR1MCS using the above primers to create pD1571*pilAI*.

Construction of the ATCC13637 $\Delta pilAI \Delta pilA2 \Delta smfI$ triple mutant was completed using the process above with the appropriate primers found in Table 3-2 resulting in the creation of three suicide vectors, pATCC13637 $\Delta pilAI$, pATCC13637 $\Delta pilA2$, and pATCC13637 $\Delta smfI$, for the deletion of *pilAI*, *pilA2*, and *smfI*, respectively. These plasmids were introduced into ATCC13637 by bacterial mating and selected on LB agar containing 60 μ g/mL Tc, and mutants isolated using the process described above. ATCC13637 $\Delta pilAI$ was created first followed by introduction of the $\Delta pilA2$ mutation and finally the $\Delta smfI$ mutation.

Table 3-2: Primers used in this study.

Primer name	Sequence (5' – 3')*
D1585 <i>pilT</i> UpF- <i>HindIII</i>	GGGCAAGCTTCAGTACCTGCGGCTTCACTG
D1585 <i>pilT</i> UpR-OE	CTCGAACAGGCGCTTGGACGCTTTGTTCTTTACGG
D1585 <i>pilT</i> DnF-OE	AAGAACAAGCGTCCAAGCGCCTGTTCGAGTAAGG
D1585 <i>pilT</i> DnR- <i>XbaI</i>	GGGCTCTAGACTTCAGCTTGTGGATCTCGC
D1571 <i>pilAI</i> DnF- <i>XbaI</i>	TTGCTCTAGAAAGGTGGACACGTCGAACAG

D1571 <i>pilA</i> ΔDnR-OE	GGGGATGTACCAATGTAATTCAGCTGTACTAAGAG
D1571 <i>pilA</i> ΔUpF-OE	AGTACAGCTGAATTACATTGGTACATCCCCAAGAT
D1571 <i>pilA</i> ΔUpR- <i>KpnI</i>	TTCAG GTACCA AGCTCTTGAACACGTCCTC
D1585 <i>pil</i> ΔTF	GTTCCGTTGAATCAGGAGGC
D1585 <i>pil</i> ΔTR	GAGGGCATGTACCAGGAAAC
D1571 <i>pilA</i> ΔF- <i>HindIII</i>	TCGTA AGCTTC GCTGAACTCAACCACCAC
D1571 <i>pilA</i> ΔR- <i>XbaI</i>	TCGTT CTAGAC CGACCGGGATTTGTACTCC
D1585 <i>smfI</i> ΔUpF- <i>XbaI</i>	CCGCT CTAGAC GCACCTGACCAATGATCTG
D1585 <i>smfI</i> ΔUpR-OE	GCGATCAGTTGTAGACGGCAATGAGGTTGATCTTG
D1585 <i>smfI</i> ΔDnF-OE	TCAACCTCATTGCCGTCTACA ACTGATCG CAGTCG
D1585 <i>smfI</i> ΔDnR- <i>KpnI</i>	GCATGGTACCGAAGCTGGAATTGAACTGGG
D1585 <i>smfI</i> ΔF	CTCCTTGCTTCCTCCTCTAC
D1585 <i>smfI</i> ΔR	CATCGGAAGTACTACGCTCG
ATCC13637 <i>smfI</i> ΔUpF- <i>KpnI</i>	TAGTGGTACCGTAAACACGTCGGCTTACAG
ATCC13637 <i>smfI</i> ΔUpR-OE	CTACGATCAGTTGTACTTGTGCATT CGCTTTTACC
ATCC13637 <i>smfI</i> ΔDnF-OE	AAGCGAATGCACAAGTACA ACTGATCG TAGCCGTA
ATCC13637 <i>smfI</i> ΔDnR- <i>XbaI</i>	ATTAT CTAGA AGGCGGATGGTGTGTTCCAC
ATCC13637 <i>pilA</i> ΔUpF- <i>BamHI</i>	CTAGGGATCCAAGCTCTTGAACACGTCCTC
ATCC13637 <i>pilA</i> ΔUpR-OE	GGTACCAGTGCAGCCGTTCTTCATTGGTACATCCC
ATCC13637 <i>pilA</i> ΔDnF-OE	GTACCAATGAAGAACGGCTGCACTGGTACCTAATA
ATCC13637 <i>pilA</i> ΔDnR- <i>HindIII</i>	GTAGA AGCTTA AGTGGACACGTCGAACAGC
ATCC13637 <i>pilA2</i> ΔUpF- <i>HindIII</i>	ATTTA AGCTT GGTCCCCTCCCAGACAAACG
ATCC13637 <i>pilA2</i> ΔUpR-OE	GAAGTGTGATCAGCACTTCTGCGTGTT CATGACTC
ATCC13637 <i>pilA2</i> ΔDnF-OE	ATGAACACGCAGAAGTGCTGATCACACTT CAGCGC
ATCC13637 <i>pilA2</i> ΔDnR- <i>XbaI</i>	GTGGT CTAGA AGCTGTGCCATCACCTTCAG

*Bold regions indicate restriction enzyme cut site. Overlap regions are italicized

Transmission electron microscopy (TEM)

S. maltophilia D1585 $\Delta pilT$ bacterial cells were prepared for electron microscopy as follows. Cells grown on ½ LB agarose plates overnight at 30°C were collected and washed in 1 × phosphate-buffered saline (PBS), pH 7.2, and fixed at room temperature in EM fixative (2.5% glutaraldehyde, 2% paraformaldehyde, 0.1 M phosphate buffer, pH 7.2) for 15 min. The fixed cells were pelleted and resuspended in 1 × PBS. 5 µL of this sample was incubated on a copper grid for 30 sec and stained with 2% phosphotungstic acid (PTA) for 10 sec. Transmission electron micrographs were captured using a Philips/FEI Morgagni transmission electron microscope with charge-coupled device camera at 80 kV (University of Alberta Department of Biological Sciences Advanced Microscopy Facility).

For visualization of phage DLP6 on *S. maltophilia* D1571, cells were prepared as described above and phage lysate was prepared by soft agar overlay using ½ LB agarose in place of ½ LB agar, producing a 10¹¹ PFU/mL stock. Bacterial cells were mixed in a 1:2 ratio with DLP6 and incubated on ice for 50 min. 10 µL of this mixture was incubated on a copper grid for 3 min, stained with 2% PTA for 10 sec and imaged as above.

Phage resistant mutant isolation and genome sequencing

Spontaneous *S. maltophilia* D1571 mutants resistant against phages DLP5 and DLP6 were isolated following infection with each respective phage at high titre. For phage DLP5, soft agar overlays with high titre phage lysate were conducted to produce completely cleared plates with resistant colonies growing following overnight incubation at 30°C. LB broth was added to the overlay and collected into a microcentrifuge tube and centrifuged at 5,000 × g for 5 min. The supernatant was discarded, and 1 mL fresh LB was added to resuspend the cell pellet, followed by centrifugation. This wash step was repeated three times in total to remove contaminating phage before plating for single colonies on LB agar. For phage DLP6, liquid phage infections were used to isolate resistant mutants due to lack of phage infection on solid media at high titre [177]. Briefly, 100 µL D1571 overnight culture and 100 µL 10¹¹ PFU/mL DLP6 lysate was incubated at 30°C for 30 min with shaking before adding 1 mL SM and 10 mL LB broth and incubating overnight at 30°C and 225 RPM. The following day an aliquot was removed, serially diluted, and plated for single colonies. Surviving colonies from both phage treatments were grown in LB and screened for phage resistance by spotting phage lysate on small overlays made

using 50 µL overnight culture and 500 µL 0.7% top agar or by running 20 µL phage lysate across an LB agar plate and cross-streaking individual colonies with toothpicks. PCR of resistant colonies with DLP5 primers (3F 5'-GCCGCCAATGTAGATCCGTA-3'; 3R 5'-GATTCTGGTAGCTCTCCGGC-3') were used to screen for resistant mutants that were non-lysogens, and DLP6 primers (101,772F 5'-TGCAAGTACCAAGTGCAGCT-3'; 101,772R 5'-CTCCCTCAACTCGCCCTTAC-3') confirmed that resistance was not due to pseudolysogeny.

Genomic DNA of wildtype D1571, four DLP5 resistant mutants and three DLP6 resistant mutants was isolated following standard procedures [261]. Briefly, bacterial cells suspended in TE buffer were treated with SDS and proteinase K for 1 h at 37°C. 5M NaCl and 10% CTAB in 0.7M NaCl was added to the solution, mixed thoroughly, and incubated for 10 min at 55°C. An equal volume of 24:1 chloroform:isoamyl alcohol was added, inverted rapidly and centrifuged at 13,000 rpm for 5 min. The aqueous layer was retained and mixed with an equal volume of 1:1 phenol:chloroform and centrifuged again. DNA from the upper aqueous layer was precipitated with isopropanol and resuspended in sterile milliQ water.

Sequencing was performed at the Microbial Genome Sequencing Center (MiGS; Pittsburgh, PA, USA). Sample libraries were prepared using the Illumina DNA Prep kit and IDT 10bp UDI indices, and sequenced on an Illumina NextSeq 2000, producing 2x 151bp reads. Demultiplexing, quality control and adapter trimming was performed with bcl-convert (v3.9.3) [1]. All genome samples produced greater than 4 million reads with at least 91% bp greater than Q30.

Twitching motility

Twitching motility assays were used as an indirect measurement of type IV pili function. A single bacterial colony was suspended in 100 µL LB broth and stab inoculated with a toothpick through a 3 mm thick LB agar layer (1% agar) containing 0.3% porcine mucin to the bottom of the petri dish and incubated with humidity at 37°C for 24 h. Twitching motility zones between the agar and petri dish interface were visualized by gently removing the agar and staining each plate with 1% (w/v) crystal violet for 30 min followed by rinsing excess stain away with water. Stained twitching zone areas were measured using ImageJ software (NIH, Bethesda, MD, USA) [239]. Each strain was tested in biological and technical triplicate and average twitching area was calculated from the nine twitching zones.

Bioinformatics

Genome assembly, annotation and SNP analysis was completed using tools within the Galaxy webserver at usegalaxy.org [262]. Reads were assembled using Shovill (<https://github.com/tseemann/shovill>) and resulting contigs were annotated using Prokka [263]. Identification of single nucleotide polymorphisms (SNPs) between DLP5 and DLP6 resistant mutant sequencing reads compared to wildtype D1571 contigs was completed by snippy (<https://github.com/tseemann/snippy>). Visualization of the D1571 annotated genome was done using Geneious Prime v2022.0.1 [230]. Mutated gene products identified by snippy were analyzed using BLASTp limited to Bacteria (taxid:2) on the NCBI non-redundant protein sequence database (update date: 2022/04/11) [264] and conserved domain searches were performed using CD-Search against the CDD v3.19-58235 PSSMs database and default options [265].

Pilin gene clusters were identified using Geneious v2022.0.1 [230] and BLASTp analysis using PilA as a query against *P. aeruginosa* PA01 (accession: NZ_CP053028) and the phytopathogen *Xylella fastidiosa* Temecula1 (accession: NC_004556). The sequence and annotations between *pilR* and *pilD* were manually extracted from each genome and analyzed by clinker v0.0.23 [266].

Complementation of D1571 *pilQ*

The *pilQ* gene was PCR amplified from D1571 genomic DNA with Phusion High-Fidelity DNA Polymerase (New England Biolabs) using primer pair *pilQF-HindIII* (TTTTAAGCTTCGTGTGGAGCTGATCGAACT) and *pilQR-XbaI* (TTGTTCTAGAGGCATCAAGAACGGCTGAAC). The resulting product was digested with *HindIII* and *XbaI* Fast Digest restriction endonucleases (Thermo Scientific) and ligated using T4 DNA ligase (NEB) into pBBR1MCS for expression in D1571 *pilQ* DLP5 resistant mutant #24. The pD1571*pilQ* construct was subcloned into electrocompetent *E. coli* DH5α before transforming *S. maltophilia* D1571 *pilQ* electrocompetent cells prepared as previously described [160]. Sequence verification of the cloned gene identified a c.1220G>A (p.Gly407Asp) point mutation, however this did not affect complementation of twitching motility or phage infection.

Galleria mellonella killing and phage rescue assays

G. mellonella infections were performed as previously described, with modifications [267,268]. Single colony triplicate overnight cultures of wildtype ATCC13637, ATCC13637 $\Delta pilA1\Delta pilA2\Delta smf1$, wildtype D1571 and the DLP3 lysogen, D1571::DLP3, were grown aerobically at 37°C in LB for 19 h corresponding to approximately 2×10^{10} CFU/mL. Overnight cultures of wildtype D1585 and 280 and their corresponding mutants were grown at 30°C in LB for 18 h corresponding to approximately 5×10^9 CFU/mL. Cultures were standardized by OD₆₀₀, washed once in $1 \times$ PBS (pH 7.4) and serially diluted tenfold in PBS. *G. mellonella* larvae were bred in-house at 30°C using artificial food (wheat germ: 264 g, brewer's yeast: 132 g, beeswax: 210 g, glycerol: 132 g, honey: 132 g, water: 66 g) and larvae weighing approximately 250 mg were selected for experiments. Each experiment consisted of ten larvae per group and 5 μ L aliquots of bacterial culture were injected into the rear left proleg of each larva using a 250 μ L Hamilton syringe fitted with a repeating dispenser. Sterile PBS injected larvae were used as negative controls and showed 100 % survival for the duration of all experiments. Colony counts on LB agar were used to determine the CFUs injected. Following injection, larvae were placed in a static incubator in the dark at 37°C and scored for death every 24 h until 72- or 120-hours post-infection (hpi). Larvae were considered dead when they did not respond to touch with movement.

For DLP3 phage rescue trials, wildtype D1571 culture was prepared as described above and an inoculum of approximately 8×10^6 CFU/larvae was chosen. DLP3 lysate was used at 8.9×10^{10} PFU/mL. Larvae were injected with 10 μ L of DLP3 lysate dilutions to give MOIs of approximately 100 and 50 into the rear right proleg at 1.5 hpi with D1571. Aliquots of 5 μ L PBS and 10 μ L SM were used in place of bacteria and phage, respectively, for negative controls. Each worm was therefore injected with 15 μ L total volume. Larvae were incubated and scored for survival as above. Results from three separate trials were combined and survival at each timepoint was plotted using the Kaplan-Meier method with error bars for standard error using GraphPad Prism 8. Statistical analysis of survival differences was completed using the Log-rank (Mantel-Cox) test.

Lemna minor virulence assay

Four *Xanthomonas* species were tested for virulence using the *L. minor* (duckweed) plant infection model [269]. Sterile plants were grown in Schenk-Hildebrandt medium supplemented with 1% w/v sucrose (SHS) under a light dark cycle of 18/6 h to promote asexual reproduction. Virulence assays were conducted in 96-well microplates as previously described [269]. Briefly, single plants having 2-3 fronds were transferred to wells containing 180 μ L SHS. Outer wells were not used and were filled with 200 μ L of sterile milliQ to avoid edge evaporation. Overnight cultures of four *Xanthomonas* strains were grown in LB at 30°C for 18 h and 1 mL was washed with and resuspended in SHS. 20 μ L of cell suspension was inoculated into the first column of wells and serially diluted across the plate to produce inoculums of approximately 10^9 to 10^1 CFU per well for each strain. Infection plates were wrapped in cellophane to reduce evaporation and incubated at 30°C in the dark. Plant survivors were determined by green pigmentation at 72 hpi. A single trial was completed consisting of 3 technical replicates.

Results and Discussion

Phage *S. maltophilia* host ranges

Beyond phages DLP1 and DLP2 discussed in Chapter 2, the Dennis lab has isolated and characterized six additional bacteriophages against *S. maltophilia*; DLP3 [178], DLP4 [114], DLP5 [179], DLP6 [177], AXL1 [168] (Chapter 5), and AXL3 [115] (Chapter 4). The host ranges of these phage were examined after their isolation from the environment prior to 2014 for the DLP_ phages and in 2018 for the AXL_ phages, however due to repeated passaging in the laboratory over time and increase in phage lysate titres, the host ranges have shifted in the current phage lysate populations used in this thesis compared to those initially described. Table 3-3 summarizes the current host ranges of the eight *S. maltophilia* phages against 30 *S. maltophilia* clinical isolates and 26 *P. aeruginosa* hosts. These strains were further examined for productive phage infection by calculating the phage efficiency of plating (EOP) from plaque formation in serial dilutions of phage lysate compared to the isolation host strain, D1585 or D1571 [260]. Values greater than 0.5 indicate a highly productive infection, EOP between 0.1 and 0.5 suggest a medium productive infection and values between 0.001 and 0.1 indicate low phage production. Plaques were observed on some phage-bacterium combinations at low

dilutions producing an EOP less than 0.001, suggesting there is little to no phage production on these hosts. Where there is evidence of bacterial cell lysis, but plaque formation did not occur, we consider this a non-productive phage infection likely due to lysis from without [270].

We attribute many of these changes in host range to the repeated propagation of phages on their main hosts, D1585 or D1571, and hypothesize that propagation on a single host has selected for phages optimized to that host over time, resulting in the differences observed. Changes in susceptibility or resistance of a host to a given phage compared to the originally published susceptibility are shaded grey and include a reduction in host ranges for DLP1, DLP2, DLP3, and DLP4, and dramatically increased host ranges for DLP5 and DLP6 (Table 3-3). Although these changes appear significant, the EOP for the majority of these host changes are very low and infection did not likely produce progeny virions at high titre. Serial passaging of phages on strains with low EOP may train them to infect more efficiently [271].

Table 3-3: Host range analysis of *S. maltophilia* phages on clinical *S. maltophilia* and *P. aeruginosa* isolates.

<i>S. maltophilia</i>	Bacteriophage EOP ^{a,b}							
strain	DLP1	DLP2	DLP3	DLP4	DLP5	DLP6	AXL1	AXL3
101	-	-	+	+++	++	0.085	0.0013	-
102	-	-	++++	++	0.125	++	++	-
103	-	-	2.7x10 ⁻⁵	0.3	++	+++	1.9x10 ⁻⁶	-
152	-	-	-	-	-	++	-	-
155	-	-	-	-	-	+++++	-	-
174	-	-	+	-	+++	++	-	-
176	-	-	++	-	++++	+++	-	-
213	+	-	+	-	++	+++++	0.64	0.32
214	-	-	+	-	-	++	-	-
217	-	-	-	-	-	++	-	-
218	+	-	-	-	-	++	-	-
219	-	-	++	++	+++	-	0.0013	-
230	-	-	+++++	-	++++	+++	-	-
236	-	-	-	-	-	-	-	-
242	-	-	1.1x10 ⁻⁴	-	-	+	-	-

249	-	-	-	-	-	-	-	-
278	-	-	-	-	-	+	-	-
280	++	+++++	++	+++	++++	++	0.0033	+
282	-	-	-	1.4	+	+	1.4x10 ⁻⁵	-
287	-	-	-	+	++	++++	+	-
446	-	-	-	-	-	+++	-	-
667	-	-	+	+++	++	+++	0.0016	-
D1585	1.0	1.0	++	1.0	5.8x10 ⁻⁴	-	1.0	1.0
D1571	-	-	1.0	-	1.0	1.0	-	-
D1614	-	-	-	-	0.175	++	-	-
D1576	-	-	+++	++++	+++++	++	7.6x10 ⁻⁷	+
D1568	-	-	-	0.08	-	-	0.79	2.7x10 ⁻⁵
ATCC 13637	-	-	-	-	-	+++	1.2x10 ⁻⁷	-
SMDP92	-	-	0.43	-	0.15	++++	7.6x10 ⁻⁸	-
VLJ1	-	-	-	-	++++	++++	-	-

P. aeruginosa

strain ^c

PA01	+++	-	-	-	-	-	-	-
HER1004	-	+++	-	-	-	-	-	-
14,715	-	1.1x10 ⁻⁵	-	-	-	-	-	-
Utah3	++	+	-	-	-	-	-	-
ENV009 ^a	5.7x10 ⁻⁷	-	-	-	-	-	-	-

^a Where plaque formation was not observed, phages were scored as having lytic activity on a given strain at a 10⁻⁴ dilution (+++++), a 10⁻³ dilution (++++), a 10⁻² dilution (+++), a 10⁻¹ dilution (++) , undiluted lysate (+), or no infection (-). Phage stocks used had concentrations of 10¹¹ PFU/mL for DLP2 and AXL1 or 10¹⁰ PFU/mL for remaining stocks on their main propagation host having an EOP of **1.0**

^b Shading indicates changes in susceptibility of host to given phage compared to the originally described host range

^c Only *P. aeruginosa* strains positive for phage infection are listed.

Type IV pili receptor identification

Compared to the type-IV pili phages DLP1 and DLP2, the additional *S. maltophilia* phages have more extensive host ranges within *S. maltophilia*, however none can infect *P. aeruginosa* (Table 3-3). Despite these vast differences, all but DLP6 share *S. maltophilia* strain D1585 as a host. We therefore assessed phage plaquing ability by spot assay on the previously constructed D1585 $\Delta pilA1$ mutant lacking the major pilin subunit [160]. Remarkably, DLP3, DLP4, AXL1, and AXL3 showed similar results to DLP1 and DLP2; mutants lacking a type IV pilus are resistant to infection by these phages as evidenced by a lack of plaque formation or clearing of the bacterial lawn compared to infection of wildtype cells (Figure 3-1A). Subsequent genetic complementation of the *pilA1* mutant with the endogenous *pilA1* gene restores phage infection to wildtype levels, whereas transformation with an empty pBBR1MCS vector did not restore phage infection and no change in bacterial growth in each phage spot was observed.

The type IV pilus is a surface exposed virulence factor found on many bacterial pathogens that is used for adhering to biotic and abiotic surfaces, contributes to the formation of biofilms, and is the sole protein structure responsible for a form of surface translocation known as twitching motility [134,272]. Through extension and retraction of the pilus, which is controlled by intracellular ATPases PilB and PilT respectively, combined with adherence to a surface, a bacterium may travel across that surface via twitching motility. Deletion of either ATPase-encoding gene results in a non-functional type IV pilus [240]. In *S. maltophilia* D1585, deletion of *pilT* encoding the retraction ATPase required for depolymerization of the pilus results in hyperpilated, non-motile cells having numerous non-functional pili projecting from the cell surface in bundles (Figure 3-2). In addition to loss of twitching motility, deletion of *pilT* in D1585 also prevents infection by DLP3, DLP4, AXL1 and AXL3 (Figure 3-1A), as well as DLP1 and DLP2 (Figure 3-3). This strain grows poorly in liquid, as observed in the speckled overlay lawn, however this phenotype, as well as susceptibility to the phages, is restored by complementation with the *pilT* gene (Figures 3-1A, 3-3).

Although a common virulence factor with highly conserved machinery, type IV pili major pilin proteins are highly variable between species and even strains, allowing for the evasion of host immune responses [133] and phage resistance [253]. Despite this variability, the type IV pilus assembly machinery is highly conserved and allows the expression of exogenous pilins and assembly of functional heterogenous pili [160,243]. To further assess phage

recognition of the type IV pilus, the D1585 *pilA1* gene was expressed in a *S. maltophilia* host strain, D1571, that is not susceptible to DLP1, DLP2, DLP4, AXL1 or AXL3, and phage infection was examined. Remarkably, expression of the exogenous D1585 *pilA1* gene allows phage infection; plaque formation occurs at 10^6 PFU/mL for AXL1 whereas for phages AXL3 and DLP4 (Figure 3-1B) or DLP1 and DLP2 (Figure 3-3), complete lysis of the bacterial lawn occurs at 10^{10} PFU/mL and partial infection is observed at 10^9 PFU/mL. No evidence of phage infection appears in the D1571 empty vector control. Although infection efficiency is low, repeat passaging of AXL3 on D1571 expressing the D1585 *pilA1* gene produces lysate with a titre of 10^{10} PFU/mL and forms plaques at a 10^{-7} dilution after three infection cycles. This was not observed on the D1571 wildtype strain, indicating that the D1585 pilin is sufficient for infection and phage replication. Additionally, cross-genera expression of the D1585 *pilA1* gene in *P. aeruginosa* PA01 to complement a *pilA*⁻ mutant permits binding of AXL1, DLP4, and AXL3 virions and cell lysis as compared to the empty vector control, albeit at low efficiency. This is reminiscent of *S. maltophilia* DLP2, a phage capable of cross-taxonomic order infection, that is only capable of infecting strain PA01 with the expression of the D1585 pilin (Figure 2-1) [160]. Phage DLP3 could not infect PA01 *pilA*⁻ expressing the D1585 pilin (data not shown).

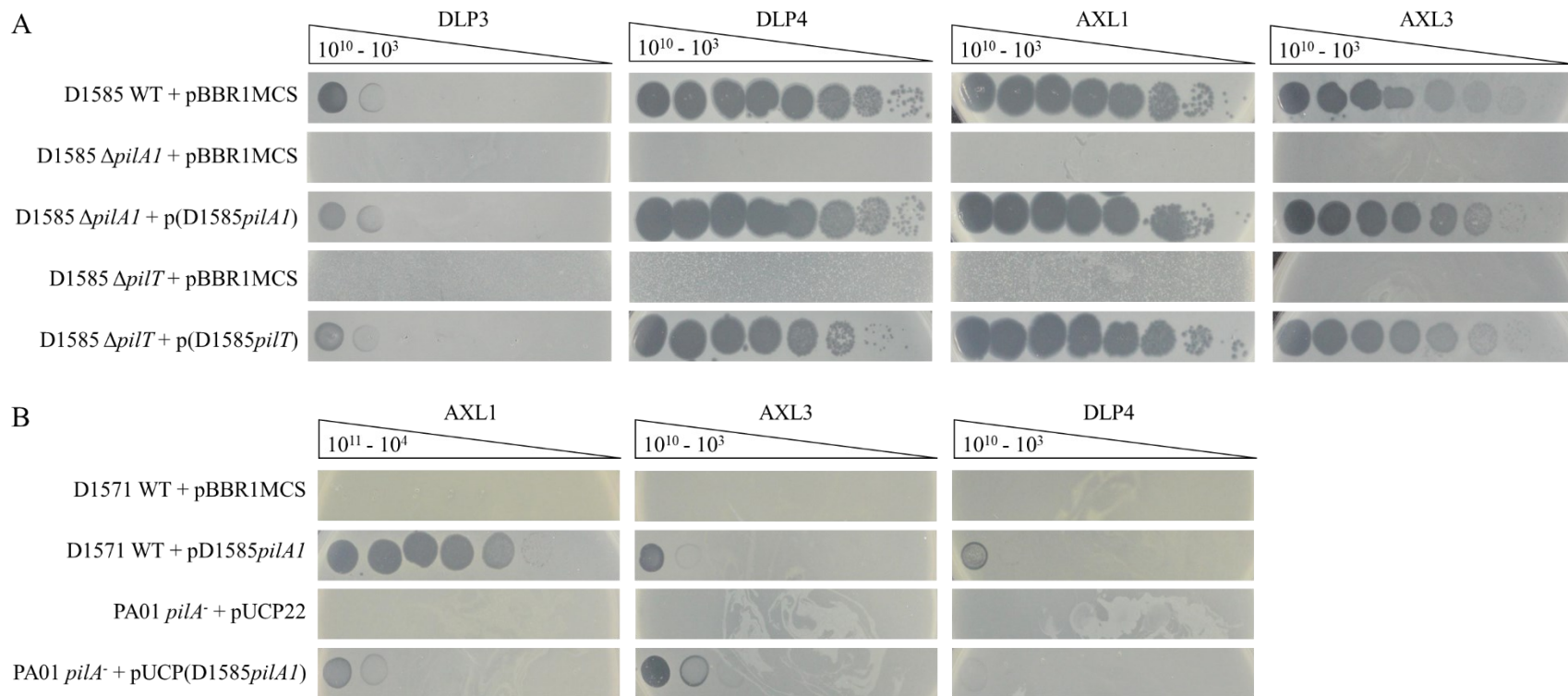


Figure 3-1: *S. maltophilia* bacteriophages require functional type IV pili for infection. (A) Wildtype (WT) *S. maltophilia* strain D1585 is susceptible to DLP3, DLP4, AXL1 and AXL3. Deletion of the major pilin subunit encoded by *pilA1*, or the retraction ATPase encoded by *pilT*, abolishes infection by these phages. Complementation restores phage infection to wildtype levels. (B) Exogenous expression of the D1585 *pilA1* gene in phage-resistant hosts, *S. maltophilia* D1571 and *P. aeruginosa* PA01, permits infection by AXL3, AXL1 and DLP4 at low levels.

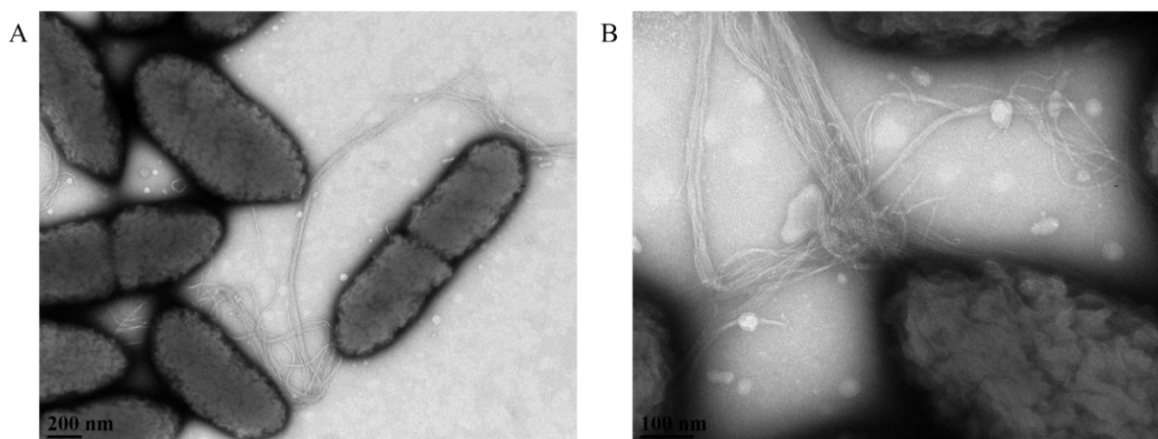


Figure 3-2: Deletion of *pilT* in *S. maltophilia* D1585 produces hyperpiliated cells.

Electron micrographs show numerous pili projecting from the pole of *S. maltophilia* D1585 $\Delta pilT$ cells and bundling together. Cells were stained with 2% phosphotungstic acid and visualized at (A) 36,000-fold and (B) 110,000-fold magnification by transmission electron microscopy.

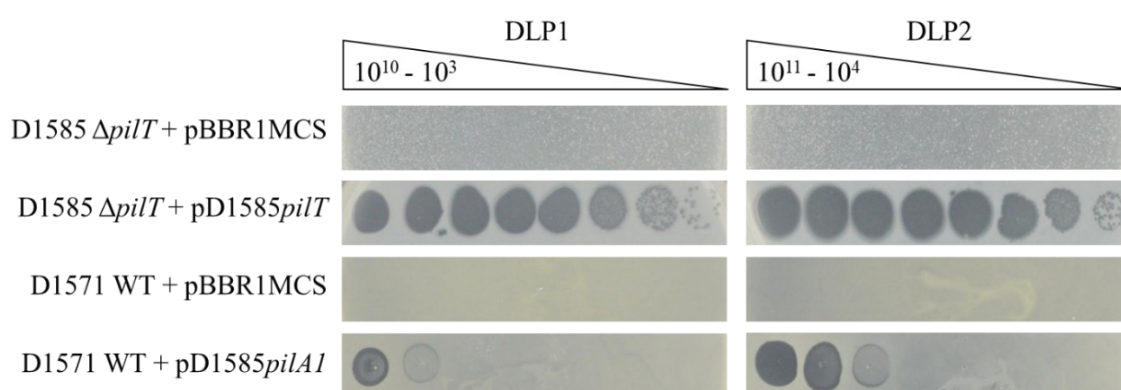


Figure 3-3: DLP1 and DLP2 bacteriophages require a functional type IV pilus for infection. Deletion of the retraction ATPase encoded by *pilT* in D1585 abolishes infection by DLP1 and DLP2. Complementation restores phage infection to wildtype levels. Exogenous expression of the D1585 *pilA1* gene in a phage-resistant host, *S. maltophilia* D1571, permits infection by these phages at low levels.

These results identify the type IV pilus as a cell surface receptor for four additional *S. maltophilia* phages and provide evidence that all six pili phages require a functional pilus

capable of retraction to reach the cell surface for successful host infection. All six phages were isolated from soil [11,114,160,178]. It is possible that the competitive advantage of type IV pili to aid in the colonization of plants [6,273] has selected for the use of these structures as phage receptors in soil microbes. It is unknown if the type IV pilus is a favoured receptor of *S. maltophilia* phages isolated from other environmental sources, such as water and sewage, as the receptors for these phages have not been examined [172–175,180,196–199]. However, the T4-like virulent phage Smp14 isolated from sewage has been observed by TEM to bind to the poles of *S. maltophilia* cells [171] where type IV pili are normally expressed. How the phages inject their genomes once they reach the cell surface with the help of cell-mediated pilus retraction is still unclear. For filamentous phages that bind the tips of a variety of pilus structures and rely on pilus retraction for infection, this process has been examined in more detail. Research shows that the bound end of the virion penetrates the periplasm, likely through the pilus porin, and the distal pIII protein interacts with the periplasmic C-terminal domain of the inner membrane protein TolA as a coreceptor [191,274]. This interaction is thought to induce TolA to bring the outer and inner membranes closer together and allow the phage contact with the inner membrane to transfer DNA from the phage particle into the cytoplasm [275]. To my knowledge, no research has been conducted on tailed, type IV pili-binding dsDNA phages interacting with cell membrane proteins to allow genome injection to the cytoplasm. As type IV pili are also important for the colonization of medical devices and patients, phages that use pili as receptors are good candidates for an anti-virulence phage therapy strategy; should bacteria become resistant to phages through modification or loss of the type IV pili receptor, this mutation provides phage resistance at the cost of lowered virulence and reduced fitness compared to non-resistant cells [160,259].

Analysis of the DLP5 phage receptor

Phage DLP5 is closely related to phage DLP3, both members of the genus *Delephquintavirus* [178,179], however initial research on these phages suggested a narrow

host range for DLP5 (Danielle Peters, PhD thesis) [179], that did not include susceptibility of wildtype D1585 or 280 for which I had *pilA1* knockouts. We hypothesized that minor differences in the genomes of these two phages likely explains the significant differences observed in phage host range due to the binding of different receptors. At the time, the *pilA1* gene was undetectable in the incompletely assembled D1571 genome, which prevented construction of pili mutants in this background. To examine the differences in host range and identify the DLP5 receptor, I sought to create a plasposon mutant library in *S. maltophilia* D1571, a common host for DLP5, DLP6 and the pili-specific phage DLP3, that would be screened for loss of phage infection to identify genes encoding receptors for these phages using DLP3 as a control. Unfortunately, the plasposon mutagenesis system originally designed for use in *Burkholderia cepacia* complex bacteria [276] did not function in *S. maltophilia* and creation of a mutant library was unsuccessful (research conducted by summer/499 undergraduate research student, Marta Ruest, under my supervision).

As an alternative approach, I screened *S. maltophilia* D1571 survivors of DLP5 infection for colonies that had accumulated spontaneous mutations to provide resistance to DLP5 rather than obtaining superinfection immunity from lysogenization. Four phage resistant mutants along with wildtype D1571 were whole genome sequenced to identify mutations compared to the wildtype strain that confer phage resistance. Assembly and analysis of the reads for single nucleotide polymorphisms (SNPs) against wildtype D1571 revealed numerous point mutations present in intergenic regions, as well as mutations in genes coding for a putative oxidoreductase YciK, and hypothetical protein D1571_02321 in all four mutants. The most notable and promising hit that was present only in mutant #24 was a single base pair deletion resulting in a frameshift and premature stop codon in the type IV pilus biogenesis *pilQ* gene. This mutation results in translation of a truncated protein 494 amino acids in length compared to the wildtype protein that is 655 amino acids long, likely abolishing function. Additionally, mutant #20 carries a two base pair insertion leading to a frameshift and premature stop codon in *pilZ* that encodes a small cytosolic protein identified to interact with the ATPase PilB and c-di-GMP receptor FimX to regulate

type IV pilus biogenesis [134,277]. This results in truncation of the 118 amino acid length PilZ protein to 52 amino acids in length. The two additional sequenced mutants did not have mutations in genes associated with type IV pilus assembly or other surface structures that would affect phage infection. However, all four mutants were negative for twitching motility compared to the wildtype D1571 that has an average twitching zone of 236 ± 143 mm² in the presence of 0.3% mucin, indicating that type IV pilus function is interrupted in all four mutants and affecting DLP5 cell binding. Screening of DLP3 against these mutants revealed no phage infection, confirming that DLP5 also uses the type IV pilus for host recognition and infection.

PilQ assembles into a dodecameric outer membrane secretin that is required for polymerization of pilins through the outer membrane during type IV pilus biogenesis [134]. To confirm that this is the sole mutation responsible for resistance to DLP5 infection in mutant #24 (*pilQ*⁻), the wildtype *pilQ* gene was cloned into pBBR1MCS and electroporated into the mutant. As shown in Figure 3-4, expression of *pilQ* in mutant #24 restores infection by both DLP5 and DLP3 compared to the empty vector control having no effect on phage infection. Infection by phage DLP6 is unaffected by the presence or absence of *pilQ* (Figure 3-4B). The restoration of phage infection upon complementation with *pilQ* rules out the other mutations present in mutant #24 as being involved with phage infection. These additional mutations discovered in each of the mutants are likely spontaneous mutations unrelated to phage resistance that arose due to the passaging of cells over multiple days during the phage infection and screening process, compared to a single day's growth from freezer stock for the wildtype.

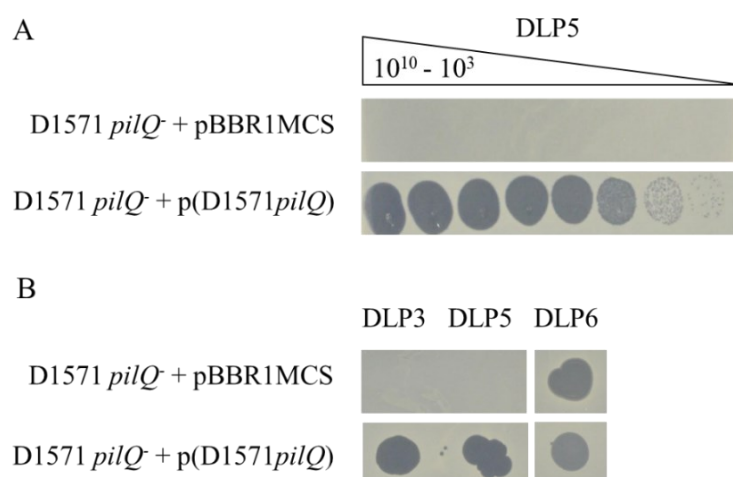


Figure 3-4: Truncation of PilQ in D1571 provides resistance to DLP5 and DLP3. (A)

S. maltophilia D1571 mutant #24 has a non-functional PilQ protein (*pilQ*⁻), resulting in loss of infection by phage DLP5, and phage infection is restored upon complementation. (B) Similar to DLP5, type IV pili-binding phage DLP3 is unable to infect mutant #24 (*pilQ*⁻) unless PilQ function is restored by genetic complementation. Phage DLP6 infection is unaffected by the loss of PilQ.

With additional D1571 genome sequencing data, I identified and deleted the *pilA1* gene in D1571, producing a non-motile mutant that is resistant to DLP5 and DLP3 infection, but sensitive to DLP6. Genetic complementation restored infection to wildtype levels for both DLP3 and DLP5 (Figure 3-5). DLP6 infection of D1571 is unaffected by loss of *pilA1*. Further testing showed that DLP5 was also unable to infect the D1585 Δ *pilA1* and Δ *pilT* mutants described above, and as expected, infection was restored upon complementation with the respective genes (Figure 3-6). Like DLP3, DLP5 was unable to infect *P. aeruginosa* PA01 *pilA*⁻ expressing the D1585 *pilA1* gene (data not shown) and cross-genera complementation with the D1571 *pilA1* gene was not examined. Based on the genetic relatedness of DLP3 and DLP5 it is not surprising that DLP5 also uses the type IV pilus as its receptor. Remarkably, DLP5 can be propagated to incredibly high titre of 10¹² PFU/mL on D1571 via simple soft agar overlay propagation, producing phage-rich lysate that is visibly turbid after removal of bacterial cells by filter sterilization.

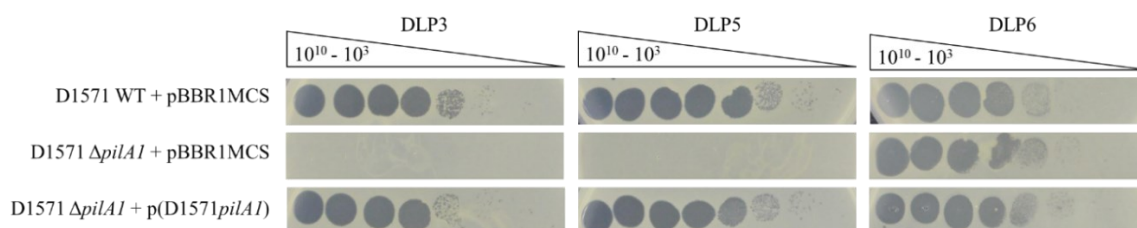


Figure 3-5: *S. maltophilia* phages DLP3 and DLP5 require a type IV pilus for infection. Wildtype *S. maltophilia* strain D1571 is susceptible to DLP3, DLP5 and DLP6. Deletion of the major pilin subunit encoded by *pilA1* provides resistance to infection by phages DLP3 and DLP5, but not DLP6. Genetic complementation restores phage infection to wildtype levels. Images are representative of three biological replicates, each with three technical replicates.

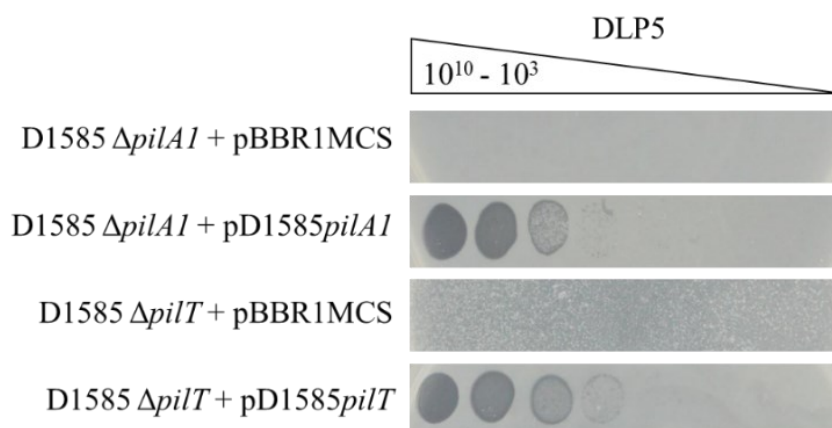


Figure 3-6: DLP5 requires cell-mediated pilus retraction for successful infection. Loss of surface pili in a D1585 $\Delta pilA1$ mutant, or loss of pili retraction in a $\Delta pilT$ mutant, result in resistance to infection by phage DLP5. Complementation with the respective genes restores phage infection.

***Xanthomonas* spp. phage susceptibility**

The genetic similarity of some *S. maltophilia* phages to *Xanthomonas* phages, discussed more in Chapter 5 and Peters et al. (2019) [114], and the similarity in type IV pilus genetic organization between these bacteria [272], led to the investigation of cross-genus infection in these phages, as observed for phages DLP1 and DLP2 and their ability to

infect *P. aeruginosa* [11]. Four strains of different *Xanthomonas* species were obtained and screened for susceptibility to our panel of eight *S. maltophilia* phages, including *Xanthomonas* phage HXX as a control. Remarkably, all our phages were capable of infecting at least one species of *Xanthomonas*, with DLP4 and AXL1 producing plaques on *X. axonopodis* pv. *vasulorum* FB570 (Table 3-4). Other *S. maltophilia* phages Smp131 [176] and ϕ SMA5 [170] were also screened for infection against a broad range of bacterial genera, including *Xanthomonas* spp. and *P. aeruginosa*, however no cross-genera infection was observed.

Table 3-4: Efficiency of plating (EOP) of *S. maltophilia* phages on *Xanthomonas* spp.

<i>Xanthomonas</i> strain	Phage EOP ^a								
	DLP1	DLP2	DLP3	DLP4	DLP5	DLP6	AXL1	AXL3	HXX
<i>X. campestris</i> XC114	-	-	++	-	++++	++	-	-	1.0
<i>X. oryzae</i>	-	-	+++	-	++++	++	-	-	0.87
<i>X. translucens</i> pv. <i>translucens</i> ATCC19319	+	-	-	-	-	-	-	+	++
<i>X. axonopodis</i> pv. <i>vasculorum</i> FB570	-	++	+++	0.04 ^b	+++++	++++	0.03 ^b	+++++	++

^a Where plaque formation was not observed, phages were scored as having lytic activity on a given strain at a 10⁻⁴ dilution (+++++), a 10⁻³ dilution (++++), a 10⁻² dilution (+++), a 10⁻¹ dilution (++), undiluted lysate (+), or no infection (-). Phage stocks used had concentrations of 10¹¹ PFU/mL for DLP2, AXL1 and HXX or 10¹⁰ PFU/mL for remaining stocks on their main propagation host having an EOP of 1.0

^b EOP calculated as compared to infection on main *S. maltophilia* host strain, D1585

The *Xanthomonas* phage HXX used as a control in the above host range was obtained from the Félix d'Hérelle Reference Center for Bacterial Viruses. Originally

isolated and characterized in 1981 from soil at a Hawaiian cabbage farm with a history of black rot disease for use in detecting and phage-typing *X. campestris* strains [278], the genome of this phage is not available in the NCBI database. Genome sequencing and BLASTn analysis revealed HXX is closely related to other *S. maltophilia* phages, and host range analysis identified 18 out of 30 *S. maltophilia* strains as susceptible to infection by HXX in addition to the four *Xanthomonas* spp. listed above. These features are discussed in further detail in Appendix One. To my knowledge, no *Xanthomonas* phages have previously been screened for their ability to infect *S. maltophilia* [279]. Because the HXX host range included *S. maltophilia* D1585, I examined the ability of this phage to infect $\Delta pilA1$ and $\Delta pilT$ mutants. Unexpectedly, loss of a functional pilus in these mutants prevented HXX infection, as was observed for the *S. maltophilia* phages described above, and infection was restored upon genetic complementation (Figure 3-7). Additionally, evidence of lysis was observed in HXX spotted on *P. aeruginosa* PA01 *pilA*⁻ expressing the D1585 *pilA1* gene. The type IV pilus has been described as a receptor for *Xanthomonas* phage Φ Xacm4-11 [280], as well as the Siphoviridae phages Sano and Salvo and Podoviridae phages Prado and Paz that infect *Xanthomonas* and *Xylella fastidiosa* [281]. A combination of these four phages has been used commercially for the successful treatment of Pierce's Disease of grapevines caused by *Xylella fastidiosa* subsp. *fastidiosa* [282]. Although the type IV pilus has not been well studied in *S. maltophilia* to date, in recent years researchers have examined the role of this dynamic structure in *Xanthomonas* spp. for the colonization of plants and disease, with varying effects on bacterial virulence observed in pili mutants between species [272].

The identification of *S. maltophilia* phages that infect phytopathogenic *Xanthomonas* spp. suggests that these phages have potential as biocontrol agents for agricultural diseases. The four *Xanthomonas* strains were subsequently tested for virulence in a *Lemna minor* plant infection model established in our lab [269] for the ability to cause disease, and possibly be rescued by phages. Unfortunately, these strains are not virulent in this plant model, with individual plants surviving even in the presence of 10⁹ CFU (Figure

3-8). Although the *Xanthomonas* genus collectively infects a wide range of crops and plant species, individual *Xanthomonas* species and pathovars are incredibly host-specific, often only having pathogenic interactions with plants from a single botanical family [283]. Of the strains tested, *X. campestris* pv. *campestris* infects plants of the *Brassicaceae* family [283], *X. axonopodis* pv. *vasculorum* FB570, recently proposed to belong to *X. euvesicatoria* pv. *euvesicatoria*, was isolated from diseased sugarcane [284], *X. translucens* pv. *translucens* is the causal agent of a bacterial wilt on *Hordeum vulgare* (barley) [285], and *X. oryzae* causes bacterial leaf blight in rice and grasses [279]. Because of the specificity of these phytopathogens, alternate plant models of infection will be required to test the utility of HXX and *S. maltophilia* phages for biocontrol. It is important to note that the broad host range of these phages may have environmental implications for biocontrol; use of phages to target *Xanthomonas* spp. in the treatment of agricultural disease can have detrimental impacts on crop yield or efficacy due to the removal of non-target potentially beneficial bacteria [286], such as those in the *Stenotrophomonas* genus [6].

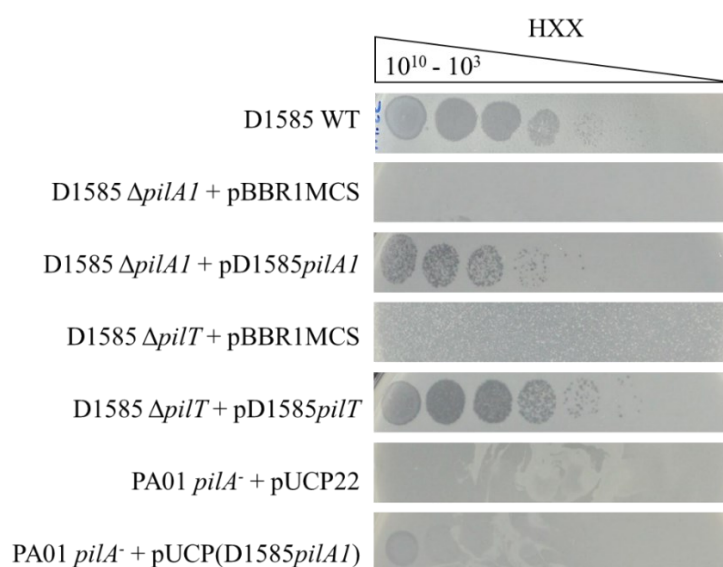


Figure 3-7: *Xanthomonas* phage HXX uses the type IV pilus as its receptor. Phage HXX can infect *S. maltophilia* strain D1585, forming plaques at 10^5 PFU/mL. Infection is abolished in $\Delta pilA1$ and $\Delta pilT$ mutants lacking the major pilin subunit or retraction ATPase, respectively. Complementation of with the wildtype genes restores HXX infection

to wildtype levels. Expression of the exogenous D1585 *pilA1* gene in a *P. aeruginosa* PA01 *pilA*⁻ background results in cell lysis at high phage titre not observed in the empty vector control.

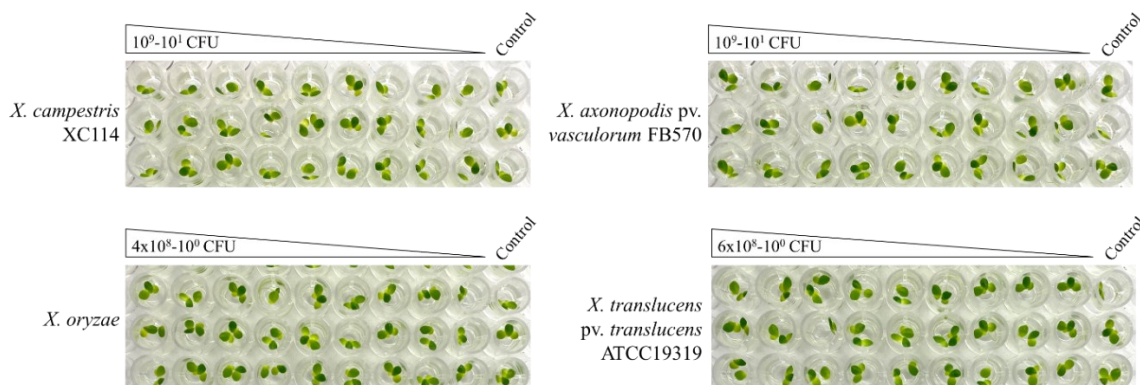


Figure 3-8: Virulence of *Xanthomonas* spp. in *Lemna minor*. Individual *L. minor* plants were infected with four species of *Xanthomonas* ranging from 10^9 CFU per well to approximately 4 CFU per well and incubated at 30°C. After 72 hpi, no effect on plant health was observed in the presence of any strain. Results represent a single biological replicate.

S. maltophilia* type IV pili as virulence factors and phage rescue in *G. mellonella

Unlike the well-characterized *P. aeruginosa* type IV pili system that encodes a single major pilin protein, *S. maltophilia* encodes two major pilin homologs in tandem, *pilA1* and *pilA2*, similar to many *Xanthomonas* species within the *Xanthomonadaceae* family [272]. This is true of strains D1585 and D1571 described above, as well as strains 280 and ATCC13637 used in the present study. These strains encode two major pilin genes directly upstream of *pilB*, which encodes the assembly ATPase, and clustered within genes encoding the platform protein, PilC, prepilin peptidase, PilD, and two-component system regulatory proteins PilS and PilR (Figure 3-9). This organization is present in other *Stenotrophomonas* and *Xanthomonas* species, however the function of these duplicated major pilins compared to the canonical system is unknown [272]. In the above D1585 and D1571 *pilA1* mutants, we deleted the *pilA1* paralog leaving *pilA2* intact directly

downstream. Deletion of the single gene abolishes infection by all seven phages and pili function as indicated via loss of twitching motility [160]. These results suggest that the major pilin PilA1 is required for expression of functional pili in *S. maltophilia* while the role of PilA2 is unknown. The presence of two neighboring *pilA* genes with a pairwise identity of 51.1% across the length of the protein in D1585 suggests that *S. maltophilia* may be capable of antigenic variation of its type IV pilus to evade host immune systems and alter pili function, as observed in *Neisseria* species [133]. Because deletion of *pilA1* was sufficient to disrupt phage infection we did not explore mutagenesis of *pilA2* further in relation to phage binding, however its role in virulence is intriguing and requires further experimentation.

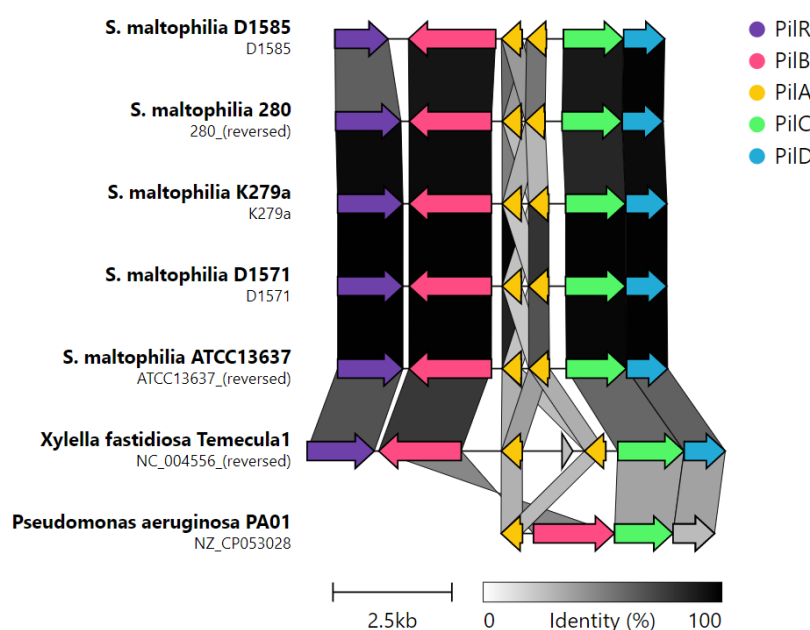


Figure 3-9: *S. maltophilia* type IV pilin gene cluster compared to related phytopathogen *Xylella fastidiosa* and pathogen *P. aeruginosa*. Type IV pilin gene clusters present between the conserved *pilR/B* and *pilC/D* were analyzed using clinker [266]. Substantial sequence variation exists between pilins. Arrows represent coding sequences coloured to indicate homologous groups and are linked by grey regions, with shading representing percentage amino acid identity.

The recognition and use of a bacterial virulence factor, such as the type IV pilus, as a phage receptor is a desirable property for the use of phages in therapy. In an “anti-virulence” or phage-steering therapeutic strategy, phage resistant bacterial mutants that arise due to loss of their surface receptor are likely to have reduced virulence in their host. To test if this principle can be applied to type IV pili-binding phages of *S. maltophilia*, we examined changes in percent survival of *Galleria mellonella* larvae infected with pili mutants compared to their wildtype counterparts in a number of *S. maltophilia* strains. *G. mellonella* have been used as a non-mammalian eukaryotic model for assessing the virulence of many bacterial pathogens, including *S. maltophilia* [287–289]. Injection of *G. mellonella* larvae with wildtype *S. maltophilia* 280 showed 100% lethality at 10^6 and 10^7 CFU per larva by 48 or 72 hours post infection, respectively, in a single infection trial (Figure 3-10). No significant change in killing was observed for a single $\Delta pilA1$ knockout mutant at the same inoculums.

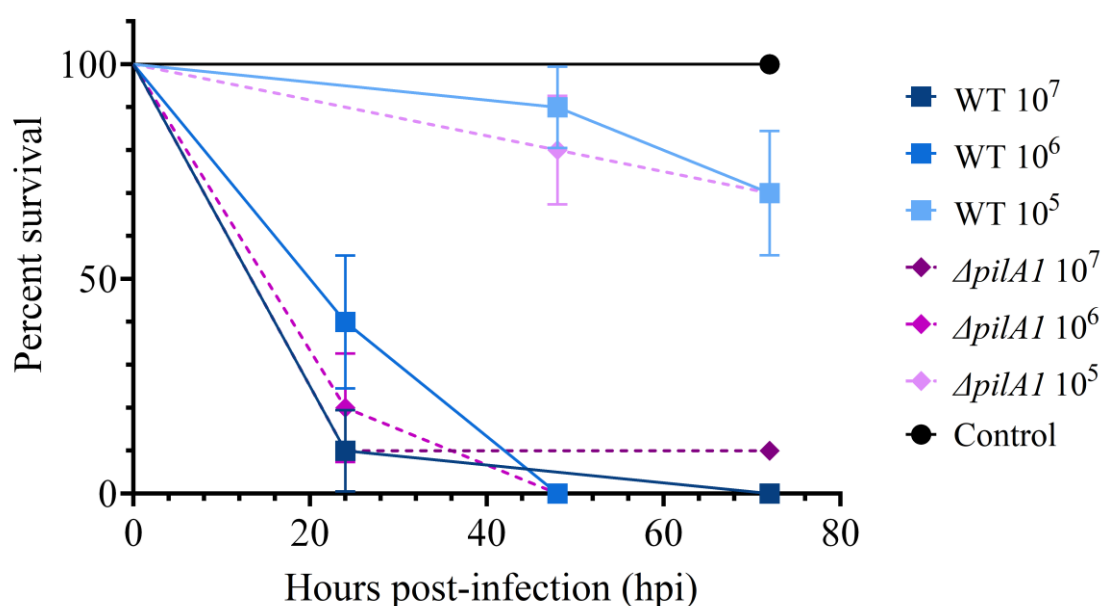


Figure 3-10: Role of the type IV pilus in virulence of *S. maltophilia* strain 280 in *G. mellonella*. Survival of *G. mellonella* larvae over 72 h following infection with *S. maltophilia* 280 wildtype or $\Delta pilA1$ mutant at varying CFU. Larvae infected with pili mutants showed no significant difference in survival at any of the three CFU tested compared to larvae injected with the same inoculum of wildtype 280 (log-rank test). Sterile

PBS was used in place of bacterial injections for the control. Ten larvae were injected per group and results from a single trial are plotted using the Kaplan-Meier method with standard error bars.

Using strain D1585, we observe an LD₅₀ of 10⁶ CFU per larva at 48 hpi, with no significant changes to larvae survival with loss of *pilA1* (Figure 3-11). In addition to type IV pili, *S. maltophilia* express the type 1 fimbriae SMF-1 that function in surface adhesion, haemagglutination and biofilm formation [53]. Similar to loss of type IV pili however, we saw no change in percent survival of larvae infected with a $\Delta smf1$ mutant. Although the double mutant lacking both type IV pili and fimbriae showed slightly higher survival across the time course of the experiment, this was not statistically significant (Figure 3-11).

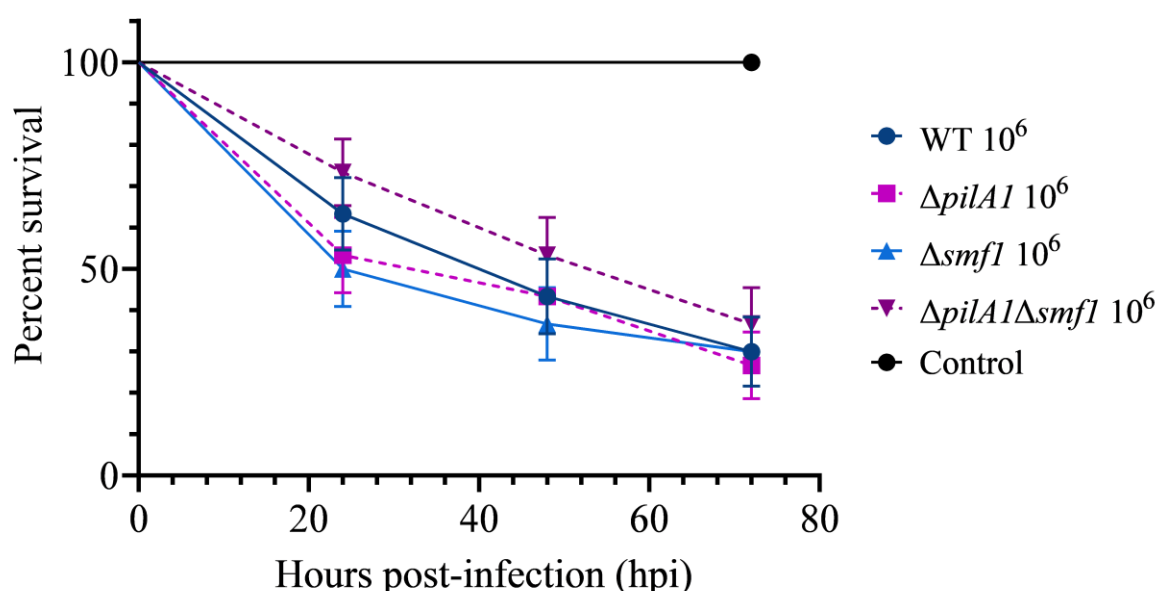


Figure 3-11: Role of type IV pili or fimbriae in virulence of *S. maltophilia* strain D1585 in *G. mellonella*. Survival of *G. mellonella* larvae over 72 h following infection with *S. maltophilia* D1585 wildtype or $\Delta pilA1$ and $\Delta smf1$ single or double mutants lacking type IV pili and/or SMF-1 fimbriae, respectively, at 10⁶ CFU. Larvae infected with mutants lacking pili and/or fimbriae surface structures showed no significant difference in survival compared to larvae injected with the same inoculum of wildtype D1585 (log-rank test). Sterile PBS was used in place of bacterial injections for the control. Ten larvae were

injected per group and results were obtained from three separate trials and plotted using the Kaplan-Meier method with standard error bars.

The final strain tested in *G. mellonella* for virulence was ATCC13637 that was used in the study first characterizing SMF-1 fimbriae in *S. maltophilia* [53]. Because differences in survival between wildtype and single mutants were not observed for D1585 and 280, I tested a triple mutant lacking both *pilA1* and *pilA2* pilin genes and *smf1* for reduced virulence compared to wildtype. This strain was less virulent in *G. mellonella* than the previous two strains, requiring greater than 1.5×10^8 CFU per larva to reach an LD₉₀ by 120 hpi (Figure 3-12). Infection with the triple mutant at the same inoculum resulted in significantly lower mortality, with an average of 55% of the larvae surviving to 120 hpi ($P < 0.01$) (Figure 3-12). These results suggest that pili and/or fimbriae structures play a role in *S. maltophilia* virulence in vivo, however the contribution of these structures varies between clinical isolates. A different infection model or assays investigating adherence to tissue culture and abiotic surface and the formation of biofilms may provide a more informative perspective on the importance of type IV pili in virulence for these strains.

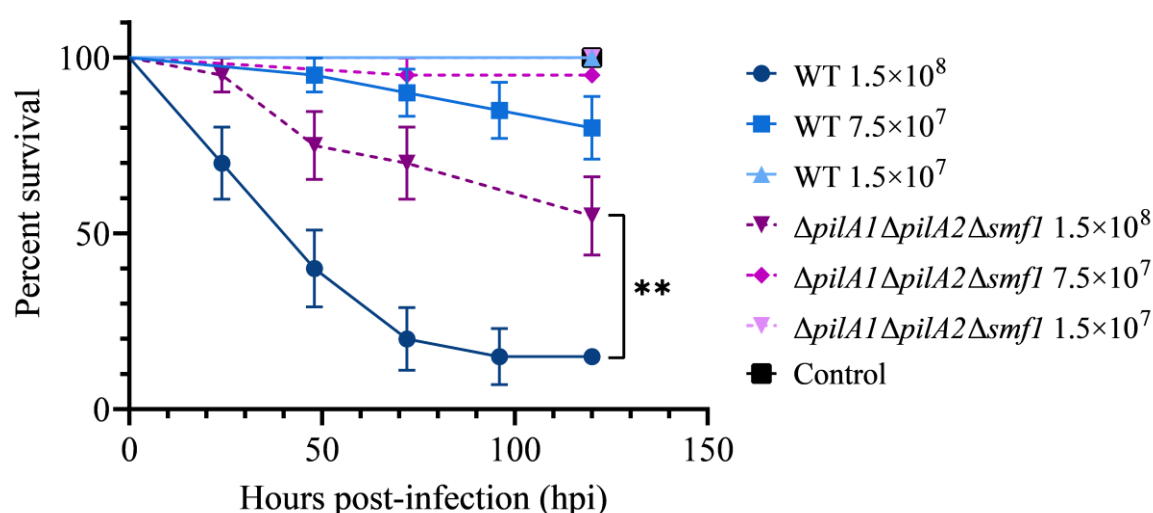


Figure 3-12: Role of type IV pili and fimbriae in virulence of *S. maltophilia* strain ATCC13637 in *G. mellonella*. Survival of *G. mellonella* larvae over 120 h following infection with *S. maltophilia* ATCC13637 wildtype or $\Delta pilA1 \Delta pilA2 \Delta smf1$ triple mutants

lacking type IV pili and SMF-1 fimbriae at varying CFU. Larvae infected with mutants lacking pili and fimbriae surface structures showed significantly reduced mortality at 1.5×10^8 CFU than larvae injected with the same inoculum of wildtype ATCC13637 (**, $P < 0.01$; log-rank test). Sterile PBS was used in place of bacterial injections for the control. Ten larvae were injected per group and results were obtained from two separate trials and plotted using the Kaplan-Meier method with standard error bars.

Although the differences in virulence of mutants lacking type IV pili and their wildtype counterparts may be too subtle to observe in *G. mellonella*, this model is well established to study the efficacy of novel antimicrobial compounds and phages [157,290,291]. I therefore examined the ability of the broad host range, type IV pili-binding phage DLP3 to rescue *G. mellonella* from infection with strain D1571. Because this phage is temperate and differing growth characteristics were observed between the D1571::DLP3 lysogen and the wildtype strain [178], I first examined if the increased growth rate of the lysogen observed in vitro affected the virulence of strain D1571 in vivo using the *G. mellonella* larvae infection model. Injection of *G. mellonella* larvae with *S. maltophilia* D1571 results in dose-dependent killing, with the lethal dose for this strain greater than 10^7 CFU per larva (Figure 3-13A). Coinciding with the faster growth rate observed in vitro, the D1571::DLP3 lysogen was more virulent than the wildtype D1571 strain, resulting in significantly lower survival for *G. mellonella* larvae injected with 10^7 ($P < 0.01$) or 10^6 ($P < 0.001$) CFU over 120 h (Figure 3-13A). This increased virulence may be due to the faster growth rate of D1571::DLP3, however CFU were not recovered from the larvae following infection.

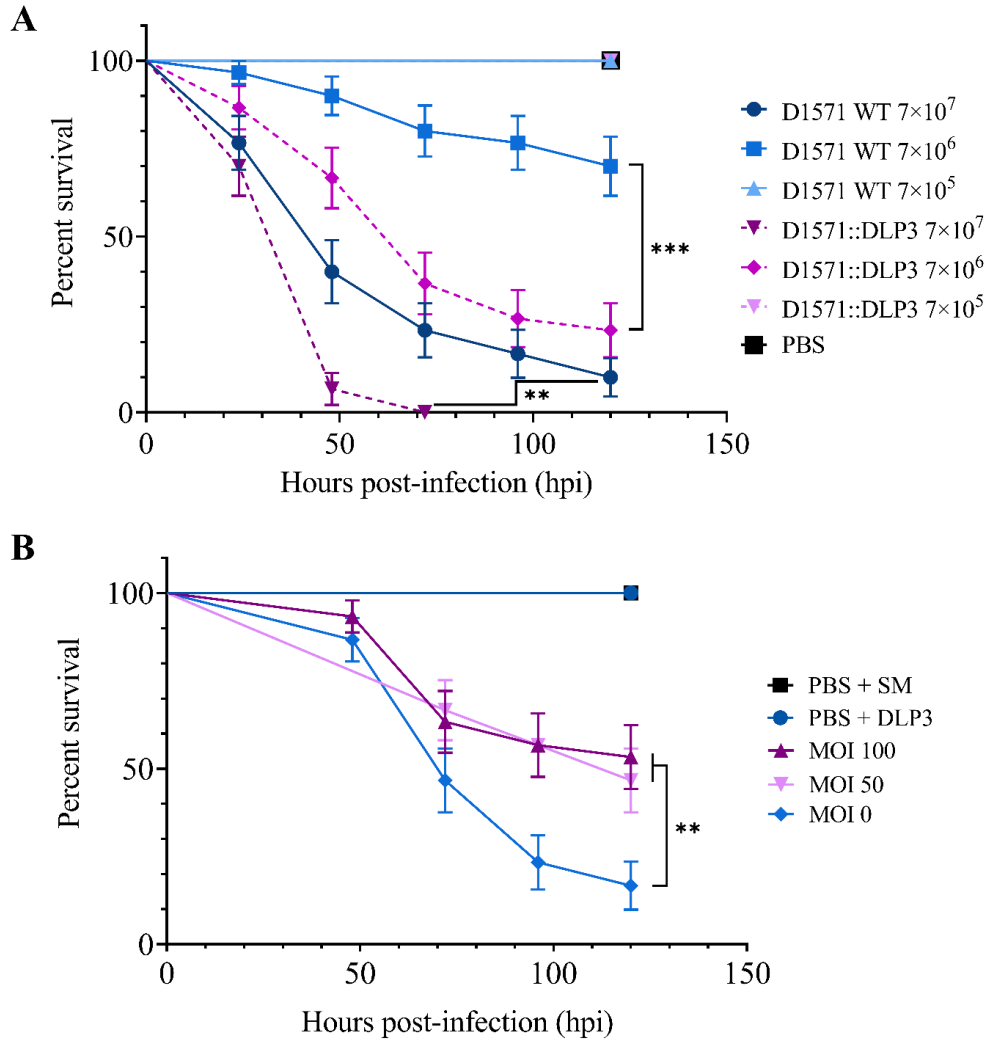


Figure 3-13: Effect of DLP3 on the virulence of D1571 in *G. mellonella*. (A) Survival of *G. mellonella* larvae over 120 h following infection with *S. maltophilia* D1571 wildtype or D1571::DLP3 lysogen at varying CFU. Larvae infected with D1571::DLP3 showed significantly lower survival at 10^7 (**, $P < 0.01$) and 10^6 (***, $P < 0.001$) CFU than larvae injected with the same inoculum of D1571 (log-rank test). (B) Survival of *G. mellonella* larvae injected with 8×10^8 CFU of D1571 over 120 h treated with DLP3 at an MOI of 100 (8.9×10^8 PFU), 50 (4.5×10^8 PFU) or 0 at 1.5 h post-infection. For controls, sterile PBS and SM were used in place of bacteria and phage injections, respectively. A significant difference in survival was observed between untreated larvae (MOI 0) and either phage treatment (**, $P < 0.01$; log-rank test). Ten larvae were injected per group and results were obtained from three separate trials and plotted using the Kaplan-Meier method with standard error bars.

Despite the DLP3 lysogen showing increased virulence in vivo, we sought to determine if DLP3 could rescue *G. mellonella* from wildtype D1571 infection. An inoculum of approximately 10^6 CFU per larva was chosen to allow for phage rescue at a multiplicity of infection of at least 100, as DLP3 does not propagate higher than 10^{10} PFU/mL. Larvae were injected with DLP3 lysate at 1.5 h post-infection with D1571 and survival monitored over 120 h. Compared to treatment with SM buffer, significantly more larvae survived when given phage at a MOI of 50 or 100 (Figure 3-13B, $P < 0.01$), with an average survival at 120 h of 53% or 47% for worms treated at an MOI of 100 or 50, respectively, compared to 17% survival of untreated larvae. Attempts to concentrate DLP3 to a titre greater than 10^{12} PFU/mL without causing melanization of larvae following phage injection were unsuccessful, however, we expect that treatment at a higher MOI would increase the survival of infected larvae. Increased survival may also occur with repeated phage injections over the course of the experiment, however, this was not tested. Overall, this preliminary investigation using *G. mellonella* indicates the potential of DLP3 as therapeutic for the treatment of *S. maltophilia* infections.

Investigation of the DLP6 receptor

Given the strong evidence for a non-pili receptor for DLP6 (Figures 3-4, 3-5) and broad host range of this phage, which includes *Xanthomonas* spp., identification of the receptor for this virulent phage is beneficial for its use therapeutically. I sought to identify the DLP6 receptor using a similar approach to that used for DLP5, however isolation of DLP6 resistant D1571 colonies proved difficult; due to lack of infection on solid media at high titre [177], surviving colonies were obtained from liquid infections and screened for DLP6 resistance. Over 300 colonies were tested with only three colonies retaining resistance to DLP6 after passaging twice on LB. These mutants are resistant to DLP6 but remain sensitive to infection by type IV pili phages HXX, DLP3, and DLP5 (Figure 3-14).

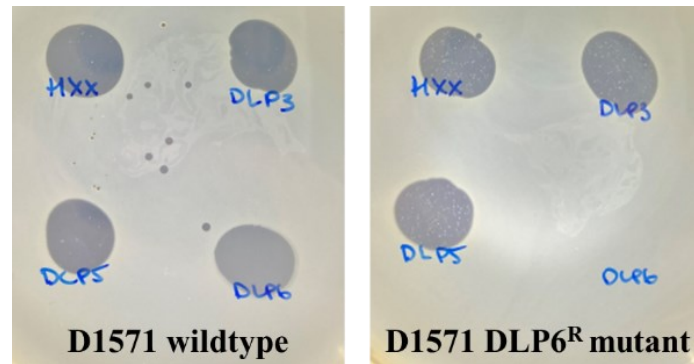


Figure 3-14: Phage susceptibility of *S. maltophilia* D1571 DLP6 resistant mutant.

Wildtype D1571 (left) is susceptible to HXX, DLP3, DLP5, and DLP6. A representative spontaneous mutant (right) that is resistant to phage DLP6 (bottom right quadrant) remains susceptible to infection by the other phages.

Whole genome sequencing of the three DLP6 resistant mutants revealed numerous point mutations in both intergenic and coding sequences, similar to those observed in the DLP5 resistant mutants. One detrimental change present in all three mutants was a nonsense point mutation resulting in a truncated putative glycosyltransferase (Figure 3-15A). This gene is located downstream of the *rmlBACD* operon and upstream of the *xanAB* operon (*spgM/manCI*), genes that are all involved in LPS biosynthesis [47,48] (Table 3-5), suggesting a role for this gene product in the synthesis of LPS on the cell surface. A conserved domain search identified a glycosyltransferase family A (GT-A) superfamily domain (c111394; E-value 3.58e-18) at the N-terminus of the D1571 protein from amino acids 5 to 171. The Ser239* nonsense mutation present in the three DLP6 resistant mutants results in loss of 74 amino acids at the C-terminal end of the protein. Whether this region is essential for proper protein folding or enzyme activity requires further study. Changes in LPS sugar moieties present on the cell surface due to loss of function mutations in glycosyltransferases are possible mechanisms for phage resistance in other bacteria [130] and warrants further investigation in the case of DLP6.

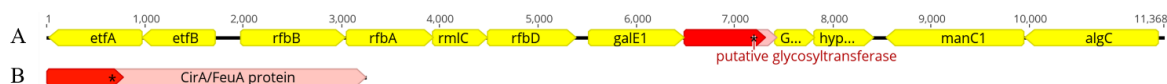


Figure 3-15: *S. maltophilia* D1571 gene mutations in DLP6 resistant isolates. (A) Three D1571 DLP6 resistant mutants contain a c.716C>A (p.Ser239*) nonsense mutation in a gene encoding a putative glycosyltransferase (red) that produces a truncated protein lacking 74 amino acids at its C-terminus. This gene is directly downstream from the lipopolysaccharide/exopolysaccharide-coupled biosynthetic genes *rfbBACD* (*rmlBACD*). (B) Two of the three mutants also contain a c.673C>T (p.Gln225*) nonsense mutation in a gene encoding a CirA/FeuA outer membrane protein, producing a substantially truncated protein missing 857 amino acids. Red ORFs indicate the truncated protein while pink shows the full-length wildtype ORF. Numbers above indicate base pair length. Image created with Geneious Prime v2022.0.1 [230].

Table 3-5: Gene clusters surrounding the putative glycosyltransferase mutated in DLP6 resistant *S. maltophilia* D1571 isolates.

Gene	Length (bp)	Direction	Product
<i>ugd</i>	1167	forward	UDP-glucose 6-dehydrogenase
<i>etfA</i>	942	reverse	Electron transfer flavoprotein subunit alpha
<i>etfB</i>	747	reverse	Electron transfer flavoprotein subunit beta
<i>rfbB/rmlB</i>	1056	forward	dTDP-glucose 4,6-dehydratase
<i>rfbA/rmlA</i>	888	forward	Glucose-1-phosphate thymidyltransferase
<i>rmlC/rfbC</i>	558	forward	dTDP-4-dehydroxamnose 3,5-epimerase
<i>rfbD/rmlD</i>	906	forward	dTDP-4-dehydroxamnose reductase
<i>galE1</i>	969	forward	UDP-glucose 4-epimerase
putative glycosyltransferase	939	forward	putative glycosyltransferase
GtrA family protein	399	forward	GtrA family protein
hypothetical protein	600	forward	hypothetical protein
<i>manC1/xanB</i>	1404	reverse	Mannose-1-phosphate guanylyltransferase 1
<i>algC/spgM/xanA</i>	1347	reverse	Phosphomannomutase/phosphoglucomutase

In addition to the glycosyltransferase mutation, two of the three DLP6 resistant mutants also had a nonsense mutation in a TonB-dependent receptor resulting in truncation of the 1081 amino acid protein to 224 amino acids in length (Figure 3-15B). A conserved domain search identified a carboxypeptidase regulatory-like domain (pfam13620, E-value 9.38e-20) at the N-terminus of this protein (31-112 aa) as well as a CirA super family domain (cl34327, E-value 1.96e-08) from amino acids 115 to 626. In *E. coli*, CirA allows the uptake of catecholate siderophores and is also the major receptor for colicin Ia, a lethal bacteriocin that penetrates and kills susceptible cells following interaction with the TonB-dependent transporter [292]. Although other iron-transport proteins are well characterized as phage receptors, such as FhuA, the surface receptor for phages T1 and T5 [130,293], a phage has not yet been identified to use CirA specifically.

In most Gram-negative bacteria, iron homeostasis is regulated by the ferric uptake regulator protein (Fur) that uses ferrous iron as a cofactor to repress transcription of iron uptake systems and siderophores [43,294]. Many TonB-dependent receptors in *S. maltophilia* have been predicted to contain Fur-boxes bioinformatically, however no experimental confirmation of Fur binding and regulation has been conducted in *S. maltophilia* to date [43,295]. I identified a predicted promoter for *cirA* in D1571 132 bp upstream of the start codon and compared the sequence in this region with the 19 bp long consensus Fur-box motif predicted for *S. maltophilia* K279a *in silico* [295]. This identified a tentative Fur-box sequence (Figure 3-16), suggesting *cirA* expression may be regulated by Fur. Upregulation of *cirA* expression due to Fur de-repression under low-iron conditions, such as those found in the lungs of patients with cystic fibrosis, would provide increased numbers of receptors for infection by phage DLP6, making this a promising phage-host interaction for future study. Additionally, the discovery of iron ions present in the tail proteins of phages, including the gp37 tail fiber protein of *E. coli* phage T4, led to the “Ferrojan Horse Hypothesis” that suggests phages are important iron-binding ligands and may compete with siderophore-bound iron to gain access to the cell surface, acting like a Trojan horse where the phage gift of iron leads to cell lysis [296]. As DLP6 is a T4-like

phage, the role of iron in phage infection efficiency in our system warrants further investigation.

-35
-10
 CGGTGCCGTTTG **TCGCACAACC** GTCACATTG ATGGCGTAGCGT TGTTAATCT AGTGTTAACCGTTG
 TGGCTGCCTTCAGCCAAGCGGTAGGGAACCCAGATAAATCTCCGACCAGCCACCCGCAGGGC
 TGTTTGGATGCGCTTTTTTCCGCCATCGCCAACTCGCATCGAGGCTACCGAAAA**ATG**

Figure 3-16: Putative Fur-box and promoter sequence upstream of D1571 *cirA* gene.

The DNA sequence upstream of the *cirA* start codon (in bold) was analyzed for promoter -10 and -35 regions using BPROM (Softberry, Inc.) and the nearby sequence was compared to the 19 bp long putative Fur-box consensus sequence in *S. maltophilia* K279a [295] to identify a putative Fur-box sequence (highlighted yellow and underlined).

Iron-uptake proteins are also the targets of β -lactam ceftazidime and catechol-conjugated antibiotics, such as cefiderocol [297]. Studies in *E. coli* and *P. aeruginosa* show little change in resistance to cefiderocol in single *cirA* mutants [297], however in *Klebsiella pneumoniae*, a *cirA* mutant obtained by serial passaging in increasing concentrations of cefiderocol had significantly higher resistance to the antibiotic, but at the cost of reduced fitness in competition assays [298]. Further study is needed to determine the effect of phage-induced selective pressure for loss of CirA function on limiting the competitiveness and antibiotic susceptibility of these mutants in low iron environments.

Transmission electron microscopy was used to visualize DLP6 interaction with *S. maltophilia* host strain D1571, however clear evidence of phage adsorption was not observed after allowing the phage/bacteria mixture to incubate for 50 min. Figure 3-17 shows representative images of phages surrounding cells but not interacting with pili or flagella structures or the cell surface where LPS would be abundant. In one instance, a single phage was observed bound to the surface of a cell (Figure 3-17B). Compared with LPS-binding phage E79 on *P. aeruginosa* that readily coats the cell surface [158] (personal observations), the lack of DLP6 adherence to D1571 supports its use of a proteinaceous receptor that is less abundant on the cell surface than LPS. Additionally, to distinguish

between LPS or proteinaceous structure as a phage cell surface receptor, adsorption assays with or without the pre-treatment of host cells using periodate or proteinase K may be used. Periodate degrades surface exposed carbohydrates, such as LPS, while proteinase K degrades proteins on the cell surface [299]. Changes in the adsorption of phages to cells treated with either condition provides evidence for the use of LPS or surface proteins as its receptor. Unfortunately, initial attempts to determine the adsorption of either DLP6 or DLP5 on untreated *S. maltophilia* D1571 were unsuccessful, and no evidence of phage adsorption was observed following 30 min of incubation. Due to time constraints, this assay was not pursued further, however personal communications with other lab members indicate that LPS-binding phages that infect *Burkholderia cepacia* complex bacteria adsorb readily, producing near 100% adsorption under the same conditions tested with DLP6. Conducting this experiment in iron-limiting media where CirA should be upregulated may produce detectable adsorption.

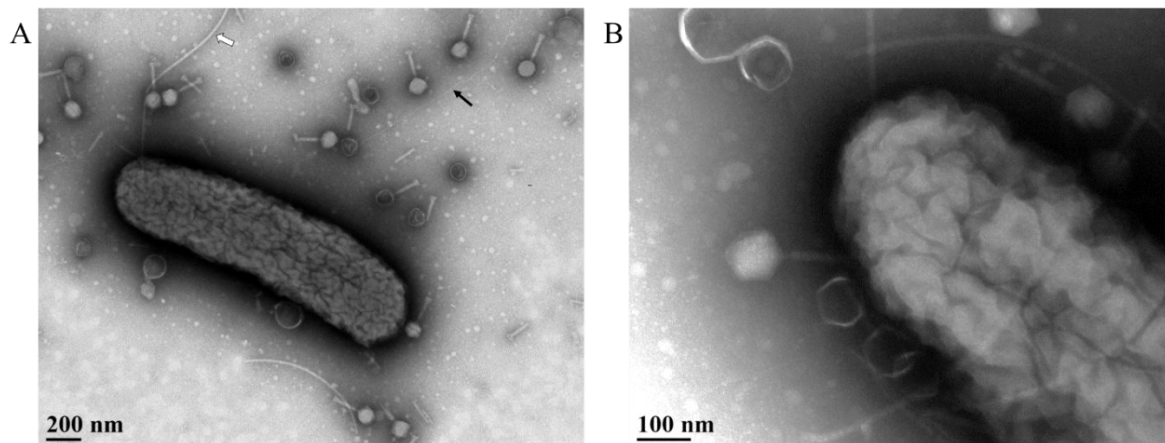


Figure 3-17: Transmission electron micrographs of *S. maltophilia* D1571 in the presence of phage DLP6. Fixed D1571 cells were incubated with DLP6 phages for 50 min before staining with 2% phosphotungstic acid and visualizing by electron microscopy. (A) An individual D1571 cell with both a flagellum (white arrow) and pilus (black arrow) in the presence of numerous DLP6 phages shows no phage interaction with these structures or the cell surface. (B) A single DLP6 virion appears to bind the cell surface. Images were taken at (A) 36,000-fold and (B) 110,000-fold magnification.

Conclusions

This study identifies the type IV pilus as the cell surface receptor for five additional *S. maltophilia* phages isolated from soil, in addition to the previously characterized DLP1 and DLP2 phages described in Chapter 2. These phages have broad host ranges that are distinct from one another and can infect *Xanthomonas* spp. Construction and complementation of numerous bacterial mutants provide evidence that these phages interact directly with the PilA major pilin subunit and require a functional pilus capable of retraction for host infection. The popularity of the type IV pilus as a receptor for *S. maltophilia* phages suggests that this is an important structure for bacterial survival and/or competition in the rhizosphere. I have shown that loss of pili and fimbriae reduces *S. maltophilia* virulence in a *G. mellonella* infection model. As phage resistant pili mutants readily emerge following phage exposure in vitro, the loss of virulence of pili mutants is promising for use of these phages in an anti-virulence phage therapy strategy. Investigation of DLP6 resistant mutants also implicate a TonB-dependent iron uptake protein, CirA, as a novel phage receptor for future study.

Acknowledgements

I would like to thank Arlene Oatway from the University of Alberta Department of Biological Sciences Advanced Microscopy Facility for her assistance and endless patience with transmission electron microscopy, as well as the staff at the Molecular Biology Service Unit. I would also like to thank Dr. Andrew Keddie for supplying the *G. mellonella* larvae used to establish our lab colony and Dr. Brent Weber for providing information and advice on breeding *G. mellonella*, as well as my fellow lab members for helping me with the moth stage of breeding. I am also grateful to Marta Ruest for her valiant efforts at creating a plasmid mutant library and Brittany Supina for her assistance with *Xanthomonas* phage HXX and use of her phage lysate. I was supported by a CGS-D award from NSERC and an AIGSS award from Alberta Innovates, as well as numerous individual awards from the Department of Biological Sciences during this research.

CHAPTER 4 - Isolation and characterization of the novel bacteriophage AXL3 against *Stenotrophomonas maltophilia*

A version of this chapter has been published as:

McCutcheon JG, Lin A, Dennis JJ. 2020. Isolation and characterization of the novel bacteriophage AXL3 against *Stenotrophomonas maltophilia*. *Int. J. Mol. Sci.* 21:6338. doi.org/10.3390/ijms21176338. IF: 5.923.

Objectives

Of the seven *Stenotrophomonas maltophilia* phages that I have determined to bind the type IV pilus, phage AXL3 was yet uncharacterized. The objectives of this study were therefore to analyze the physical and genomic characteristics of this phage and determine its suitability as a candidate for phage therapy against the emerging multidrug resistant nosocomial pathogen, *S. maltophilia*.

Materials and Methods

Bacterial strains and growth conditions

30 phenotypically distinct *S. maltophilia* strains were used for host range analysis. Five *S. maltophilia* strains were acquired from the Canadian *Burkholderia cepacia* complex Research and Referral Repository (CBCCRRR; Vancouver, BC), with strain D1585 used for isolation of phages from soil samples. An additional 22 *S. maltophilia* strains were gifted from the Provincial Laboratory for Public Health – North (Microbiology), Alberta Health Services, and strains ATCC13637 and SMDP92 were gifted from Dr. Jorge Girón at the University of Virginia School of Medicine. All strains were grown aerobically overnight at 30 °C on half-strength Lennox (½ LB; 10 g/L tryptone, 5 g/L yeast extract, 5 g/L NaCl) solid medium or in ½ LB broth with shaking at 225 RPM. Media was supplemented with 35 µg/mL chloramphenicol (Cm) antibiotic for plasmid maintenance when necessary.

Phage isolation, propagation, and host range

Undergraduate student Andrea Lin isolated AXL3 from soil she collected in the Patrick Seymour Alpine Garden at the University of Alberta Botanic Gardens in Spruce Grove, Alberta, Canada using strain D1585 and a previously described extraction protocol [11]. Briefly, soil was incubated overnight with shaking at 30 °C in ½ LB broth, modified suspension medium (SM) (50 mM Tris–HCl [pH 7.5], 100 mM NaCl, 10 mM MgSO₄), and

S. maltophilia D1585 liquid overnight culture. Solids were pelleted by centrifugation and the supernatant was filter sterilized using a Millex-HA 0.45 μ M syringe-driven filter unit (Millipore, Billerica, MA, USA) before using in a soft agar overlay with strain D1585. After overnight incubation, a single plaque was isolated using a sterile Pasteur pipette and suspended in 500 μ L of SM with 20 μ L chloroform to generate an AXL3 stock.

Propagation of AXL3 was performed using soft agar overlays as previously described [11,229]. Briefly, 100 μ L of D1585 overnight culture was incubated with 100 μ L of phage for 20 min, mixed with 3 mL of 0.7% $\frac{1}{2}$ LB top agar, and overlaid onto $\frac{1}{2}$ LB solid media. Plates were incubated at 30 °C overnight and those with confluent lysis were used to make high titre stocks by overlaying with 3 mL of SM, collecting the top agar and incubating with 20 μ L chloroform per plate for 30 min at room temperature on a platform rocker. The supernatant was collected and filter sterilized as above and stored at 4 °C. The phage stock titre was determined using serial dilutions of phage stock into SM, followed by the soft agar overlay technique on strain D1585. Plaques were backlit and viewed under the magnifying glass of a New Brunswick Scientific colony counter (model C110) and plaque size was measured using digital calipers manufactured by Tresna (Guilin, China) and reported as the average from 10 plaques \pm standard deviation.

Host range analysis was performed using a panel of 30 clinical *S. maltophilia* and 26 *Pseudomonas aeruginosa* strains. Soft agar overlays containing 100 μ L liquid culture solidified at room temperature were spotted with 5 μ L of a 10^{10} pfu/mL AXL3 stock at multiple dilutions and assayed for clearing and/or plaque formation after incubation at 30°C for 24 h and 48 h. To assess phage replication in strains with low efficiency of plating, AXL3 was passaged on these strains using the soft agar overlays with 100 μ L of a 10^{-1} diluted overnight culture and 300 μ L AXL3 phage stock. Dilutions of the passaged lysates were spotted on overlays containing the strain of interest as described above to assess changes in efficiency of plating.

Transmission electron microscopy

For transmission electron microscopy, phage stocks were prepared as above with the following modifications; ½ LB agarose plates and ½ LB soft agarose were used for overlays and a 0.22 µm filter was used for syringe-driven filtration. To visualize phages, a carbon-coated copper grid was incubated with 10 µL of phage lysate for 2 min and stained with 4% uranyl acetate for 30 s. Transmission electron micrographs were captured using a Philips/FEI Morgagni transmission electron microscope with charge-coupled device camera at 80 kV (University of Alberta Department of Biological Sciences Advanced Microscopy Facility). The average capsid and tail dimensions ± standard deviation was calculated using Microsoft Excel based on measurements from 10 individual virions taken using ImageJ software (NIH, Bethesda, MD, USA) [239].

Determining phage lifecycle

Soft agar overlay plates showing confluent lysis of D1585 by AXL3 were used to obtain phage resistant colonies for analysis. Briefly, 2 mL ½ LB broth was added to the plates and rocked at room temperature for 10 min. The broth was collected into microcentrifuge tubes and centrifuged at 5,000× g for 5 min. The supernatant was discarded and 1 mL of fresh ½ LB was added to resuspend the pellet, followed by centrifugation. This wash step was repeated three times in total to remove contaminating phage. After the final centrifugation step and removal of the supernatant, the pellet was used to streak for isolation on ½ LB agar and incubated at 30 °C for 36 h. Single colony isolates were selected for further study and tested for superinfection resistance using overnight cultures of every isolate in a top agar overlay lawn spotted with 5 µL AXL3 phage. After 16 h incubation at 30 °C, the plates were examined and isolates without plaques or clearing in the phage spot were analyzed by colony PCR with TopTaq DNA Polymerase (Qiagen, Inc., Germantown, MD, USA) following manufacturer protocols using primers specific to AXL3 gDNA (F 5'-GTCAACGAGGAATCCAAGCC-3'; R 5'-CGAAGTGGTTGATCTGCTCG-3').

One-step phage growth curve

One-step analysis of phage growth on *S. maltophilia* D1585 was conducted to determine the burst size and latent period of AXL3 as previously described, with modifications [300]. Overnight liquid cultures of D1585 were subcultured and grown to an OD₆₀₀ of 0.2 in full-strength LB at 30°C. AXL3 lysate was added at an MOI of ~3 and allowed to adsorb for 5 min at room temperature, followed by incubation at 30°C with aeration at 225 RPM. Samples were taken at 30 min intervals and immediately serially diluted in SM. Phage titres were determined by spotting 5 µL of each dilution on soft agar overlays containing D1585 culture. Plaques were enumerated following overnight incubation at 30°C. Resulting data from four replicates were analyzed using GraphPad Prism 8 (GraphPad Software Inc., San Diego, CA, United States) with data points representing the average from four biological replicates. Burst size was calculated as $(P - x)/(I - x)$, where P is the maximum number of phages after lysis, I is the number of phages initially added to the culture, and x is unadsorbed phage.

Growth reduction assay

To analyze the killing effect of AXL3 phage in liquid culture, growth reduction assays were conducted. Three D1585 overnight liquid cultures were subcultured in LB broth and grown at 30°C to an OD₆₀₀ of 0.2, corresponding to 4.0×10^8 CFU/mL. 100 µL of each culture was added to wells of a 96 well plate containing 100 µL of AXL3 phage lysate at multiple concentrations to give MOIs of approximately 10, 1, 0.1, and 0.01, or LB broth as a control, resulting in biological triplicate with three replicates each. The plate was incubated at 30°C with continuous orbital shaking at 237 cpm in an Epoch 2 microplate spectrophotometer (Bio Tek Instruments, Inc., VT, USA), with the OD₆₀₀ measured every 30 min for 48 h. Data from three biological replicates was analyzed using GraphPad Prism 9 (GraphPad Software Inc., San Diego, CA, US).

Phage plaquing assays

AXL3 plaquing ability was determined by spotting on bacterial soft agar overlays, as previously described [160]. Briefly, 100 μ L of overnight culture was mixed with 3 mL of 0.7% $\frac{1}{2}$ LB top agar, overlaid onto $\frac{1}{2}$ LB agar with or without 35 μ g/mL Cm and allowed to dry at room temperature for 30 min. AXL3 phage stock was standardized to 10^{10} PFU/mL on *S. maltophilia* D1585 and tenfold serially diluted in SM to 10^3 PFU/mL. 5 μ L of each dilution was spotted onto the prepared plates and incubated at 30 °C for 18 h. Efficiency of plating on each strain was repeated in biological and technical triplicate.

Phage DNA isolation, RFLP analysis, and sequencing

AXL3 genomic DNA (gDNA) was isolated from bacteriophage lysate by phenol/chloroform extraction and ethanol precipitation. A 1 mL aliquot of high titre filter sterilized phage lysate was nuclease treated with 1 μ L of 10 mg/mL DNase I (Thermo Scientific, Waltham, MA), 10 μ L 100 \times DNase I buffer (1 M Tris-HCl, 0.25 M MgCl₂, 10 mM CaCl₂), and 0.6 μ L of 10 mg/mL RNase A (Thermo Scientific) and incubated at 37°C for 1 h to degrade contaminating bacterial nucleic acids. Following incubation, 40 μ L of 0.5 M EDTA was added to inactivate DNase I and 2.5 μ L of 25 mg/mL Proteinase K (Applied Biosystems, Carlsbad, CA) and 50 μ L 10% SDS was added and incubated at 55°C for 1 h to release phage DNA. The treated lysate was split into two 1.5 mL microcentrifuge tubes and mixed with an equal volume of a 1:1 phenol:chloroform mixture followed by centrifugation at 17,900 \times g for 5 min. The aqueous layers were transferred to new tubes and phenol:chloroform extracted twice more followed by a single chloroform wash to remove residual phenol. Phage gDNA was precipitated from each aqueous layer by the addition of 1 mL ice-cold 95% EtOH and 50 μ L 3M sodium acetate and incubated on ice for 30 min followed by centrifugation at 17,900 \times g for 10 min. The pellet was washed with 1 mL ice-cold 70% EtOH and the supernatant was removed following centrifugation. The gDNA pellet was air dried and dissolved in 50 μ L sterile milli-Q water overnight. A

NanoDrop ND-1000 spectrophotometer (Thermo Scientific, Waltham, MA) was used to determine purity and concentration of phage gDNA.

Restriction fragment length polymorphism (RFLP) analysis was used with 32 FastDigest (Thermo Scientific) restriction enzymes (*AccI*, *MspI*, *HpaII*, *HhaI*, *Bsh1236I*, *MauBI*, *PdmI*, *HaeIII*, *NheI*, *Acil*, *Eam1105I*, *SmaI*, *XbaI*, *BamHI*, *KpnI*, *ApaI*, *SacI*, *EcoRI*, *HindIII*, *Sall*, *PstI*, *ClaI*, *XhoI*, *NotI*, *StuI*, *BglII*, *AvrII*, *PvuI*, *MscI*, *StyI*, *TasI*, *TruII*) and five High-Fidelity (New England Biolabs) restriction enzymes (*BsaAI*, *PspXI*, *EcoOI09I*, *BsaI*, *AlwNI*). Restriction digest reactions were set up using 1 µL of enzyme, 2 µL of restriction buffer, 1 µg of AXL3 DNA and topped up to 20 µL with sterile milliQ water. Reactions were incubated at 37°C for 30 min and separated on a 0.8% (wt/vol) agarose gel in 1× TAE (pH 8.0).

Sequencing of AXL3 was performed at The Applied Genomics Core at the University of Alberta. A DNA genomic library was constructed using a Nextera XT library prep kit followed by paired-end sequencing on a MiSeq (Illumina, San Diego, CA) platform using a MiSeq v3 reagent kit.

Bioinformatic analysis

Quality control analysis was completed using FastQC v0.11.9 [301] and the 1,308,137 paired-end reads were processed using Trimmomatic v.0.38 [302] and the following requirements; removal of Nextera adapter sequences, quality trimming using a four-base sliding window that cuts when the average quality per base drops below 15, removal of the first 20 bases from each read and a minimum read length of 50 bp. 83.74% of both read pairs survived these trimming parameters. SPAdes v.3.12.0 [303] was used to assemble a 47,544 bp contig with 1,998,763 reads mapping to the contig to give a mean coverage of 7516 reads with no gaps or ambiguous sites. The assembly was confirmed with PCR using 13 primer pairs randomly spaced throughout the genome and Sanger sequencing of the PCR products. A primer pair (EndF 5'-CTTGGGTTACAGTGGTGAGC-3'; EndR 5'-AAGGGTGACATCGAGCAGTA-3') flanking the ends of the contig produced a product

with an additional base upon sequencing when compared to the assembled contig, suggesting a complete genome of 47,545 bp in length.

Predicted protein-coding genes were identified using the GLIMMER plugin [304] for Geneious using the Bacteria and Archaea setting, as well as GeneMarkS for phage [305] and Prodigal [306] and annotations to the contig were made using Geneious Prime v2020.0.4 [230]. BLASTn was used to gain information on relatives based on genomic data and putative protein functions were assigned using BLASTp limited to Viruses (taxid:10239), or Bacteria (taxid:2) when Viruses produced no significant hits, on the NCBI non-redundant protein sequence and nucleotide collection databases (update date: 2020/05/19) [264]. Results with E-values greater than 1.00×10^{-3} were not recorded and the coding sequences were annotated as hypothetical. Conserved domain searches were performed using CD-Search against the CDD v3.18—55,570 PSSMs database and default options [265] to aid in functional annotation. Lysis protein analysis was performed using TMHMM [307] for transmembrane region identification and LipoP 1.0 [308] for the prediction of lipoproteins. tRNAscan-SE software with the general tRNA model [309] and Aragorn v1.2.36 [310] were used to identify potential tRNA genes. Protein alignments were accomplished using MUSCLE [231].

vConTACT2 (v0.9.16) [311] was used for taxonomic classification against the National Center for Biotechnology Information (NCBI) Prokaryotic Viral RefSeq94-Merged database using Diamond for protein-protein similarity, MCL for protein cluster generation and ClusterONE for viral cluster generation. The resulting network was visualized in Cytoscape (v3.8.0) [312] using an edge-weighted spring-embedded model, which places the genomes sharing more protein clusters closer together.

Results and Discussion

Isolation, morphology, and host range

Bacteriophage AXL3 (vB_SmaS-AXL_3) was isolated using clinical *S. maltophilia* strain D1585 from soil collected at the Patrick Seymour Alpine Garden at the University of Alberta Botanic Gardens by undergraduate student Andrea Lin. *S. maltophilia* phages have previously been isolated from soil and rhizosphere samples [11,114,177–179]. This phage forms small plaques 0.78 ± 0.12 mm in diameter with clear borders after 16 h incubation on its main host, D1585.

Transmission electron microscopy (TEM) classifies AXL3 as a Siphoviridae phage having a B1 morphotype [313] based on the long, noncontractile tail averaging 145.3 ± 5.4 nm in length and isometric head with an average capsid length and width of 64.3 ± 3.2 nm and 63.3 ± 4.3 nm, respectively (Figure 4-1). No tail fibers were observed in the TEM images.



Figure 4-1: Transmission electron micrograph of AXL3. High titer lysate was stained with 4% uranyl acetate on a copper grid and viewed at 110,000 \times magnification with a transmission electron microscope. Measurements of 10 phage particles have an average capsid length and width of 64 nm and 63 nm, and tail length of 145 nm.

Host range analysis using a panel of 30 phenotypically distinct *S. maltophilia* clinical isolates reveals a narrow tropism, with AXL3 capable of infecting only 5 strains, D1585, 213, 280, D1576, and D1568, and propagating to a high titre of 10^{10} PFU/mL on strain D1585 (Table 4-1, 3-2). Although the original AXL3 lysate that was propagated on strain D1585 did not infect strains 280 and D1576 at high efficiency, successive passaging of AXL3 on these strains produced lysates with higher efficiencies of plating, forming plaques on 280 when diluted to 10^{-5} and clearing on D1576 when diluted to 10^{-2} , indicating that AXL3 successfully replicates in these hosts. Extended host range analysis using a panel of 26 *Pseudomonas aeruginosa* strains did not yield successful infections, unlike the broad host range *S. maltophilia* phages DLP1 and DLP2 [11]. Analysis of AXL3-resistant D1585 and 213 single colony isolates by PCR with internal AXL3-specific primers produced a low number of isolates positive for AXL3 gDNA. These isolates were PCR-negative after passaging twice, indicating that AXL3 cannot stably lysogenize its host, however pseudolysogeny may be possible.

Table 4-1: *S. maltophilia* clinical strains susceptible to AXL3.

<i>S. maltophilia</i> strain	Efficiency of plating (EOP)*
213	0.32
280	+
D1585 ^a	1.0
D1576 ^a	+
D1568 ^a	2.7×10^{-5}

* Where plaque formation was not observed, AXL3 was scored as having lytic activity on a given strain with undiluted lysate (+), or no infection (not shown).

^a Isolates from the Canadian *Burkholderia cepacia* complex Research Referral Repository.

To analyze infection dynamics of AXL3, a one-step growth curve on strain D1585 was conducted. At a multiplicity of infection (MOI) of three, AXL3 exhibits a long productive cycle having a latent period of approximately 2.5 h and a burst size of

approximately 38 virions per cell at 6.5 h (Figure 4-2A). Inhibition of bacterial growth in liquid culture by AXL3 was effective at an MOI of 10, preventing bacterial growth until a resistant population arises at approximately 20 h (Figure 4-2B). This growth reduction is delayed with decreasing MOI, with AXL3 having little effect on bacterial growth at an MOI of 0.01. As discussed in Chapter 3, AXL3 binds to the type IV pilus as its host cell surface receptor and requires cell-mediated retraction to bring the bound phage particle to the cell surface for successful infection.

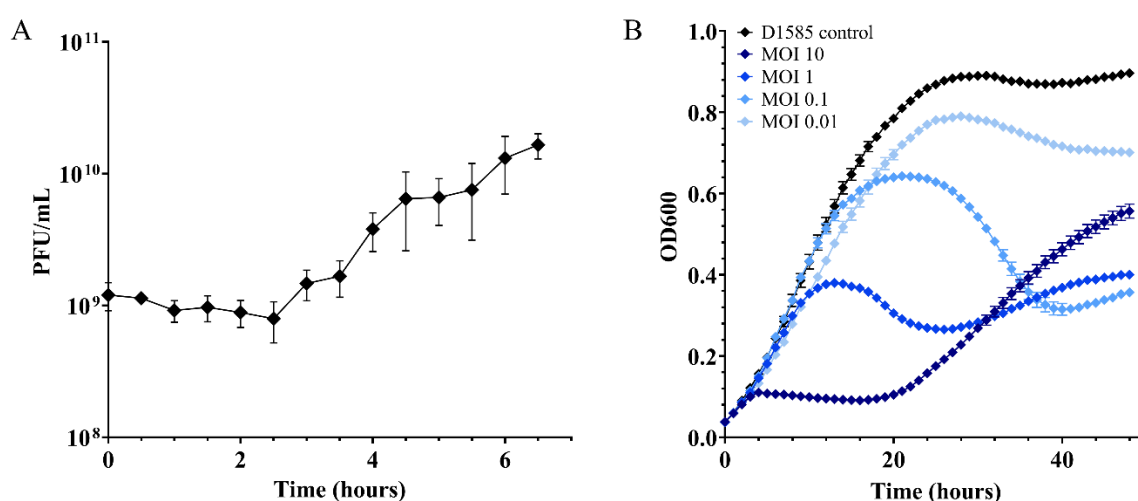


Figure 4-2: Infection dynamics of AXL3 on *S. maltophilia* strain D1585. (A)

Subcultured D1585 was grown to an OD₆₀₀ of 0.2 in LB at 30°C and AXL3 lysate was added at an MOI of ~3. Samples were taken at 30 min intervals and serially dilutions were spotted on soft agar overlays containing D1585 and plaques enumerated following overnight incubation at 30°C. The average from four replicates is shown and error bars represent standard error of the mean (SEM). (B) Liquid bacterial growth reduction curves were conducted at multiple MOIs over 48 h at 30°C. Data from three biological replicates are plotted as mean \pm SEM. Where error bars are smaller than the size of the symbol, they are not visible.

Genomic characterization

The AXL3 genome is 47,545 bp in length (Figure 4-3) with a GC content of 63.3%, which is slightly lower than the D1585 host GC content of approximately 67%. Interestingly, BLASTn analysis of AXL3 shows limited identity to other phages in the NCBI database, exhibiting a maximum identity of 67.65% with the Siphoviridae *P. aeruginosa* phage JG012 over 4% of the AXL3 genome at the time of publishing. This region of identity aligns the AXL3 region containing genes AXL3_12 and AXL3_13 with JG012 major tail structural proteins encoded by genes 13 and 14. BLASTn analysis of the AXL3 genome against *Stenotrophomonas* sp. (taxid:40323) produced no significant results with greater than 2% query coverage, indicating that remnants of this phage are not present as prophage elements in any *Stenotrophomonas* species sequenced and further supports the virulent nature of this phage.

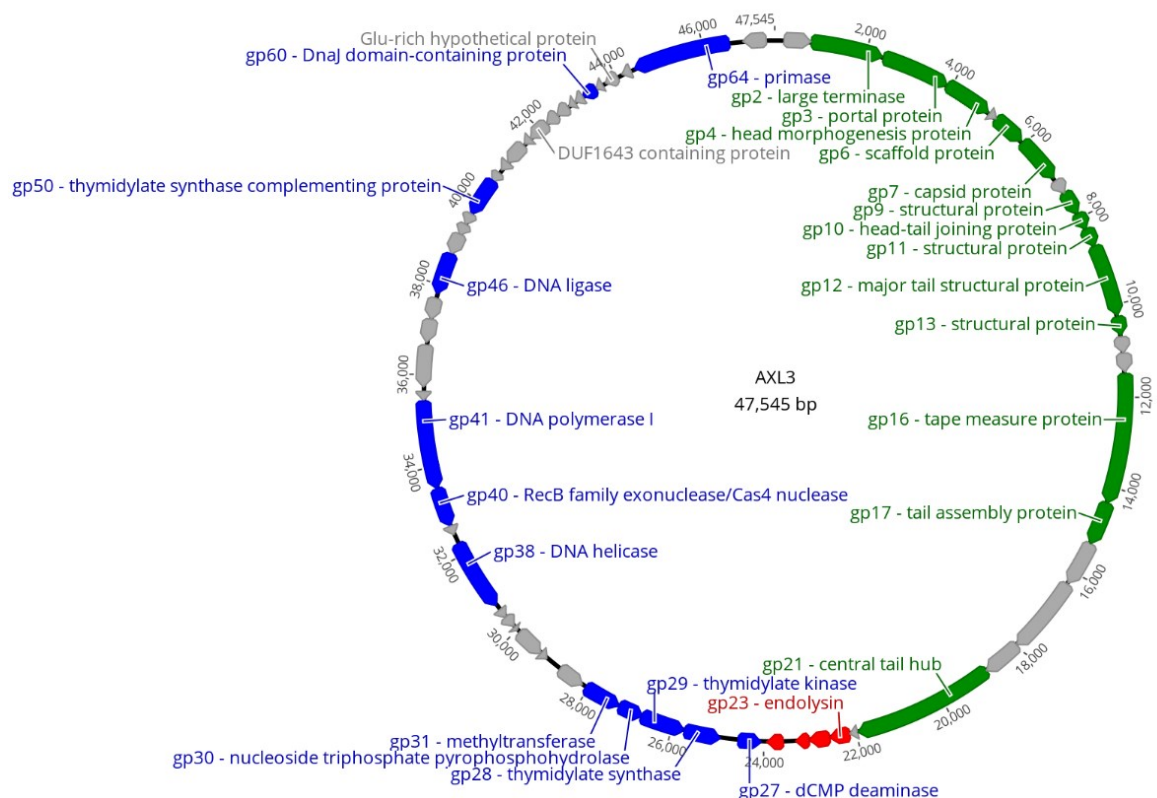


Figure 4-3: Circularized genomic map of AXL3. Scale (in bp) is shown on the outer periphery. Assigned putative functions for each of the 65 predicted open reading frames are as follows: lysis (red), DNA replication and repair (blue), virion morphogenesis (green),

hypothetical (grey). No tRNA or lysogeny genes were identified. AXL3 has a GC content of 63.3%. Image created using Geneious Prime [230].

Restriction fragment length polymorphism (RFLP) analysis of purified AXL3 gDNA using 37 restriction endonucleases with recognition sequences present in the genome showed successful digestion with only two enzymes, *TasI* and *TruII* (Figure 4-4). These enzymes contain only A/T bases in their recognition sequences, suggesting that the AXL3 genome is modified or contains atypical bases to protect it against host restriction-modification systems. Although the specific modifications are unknown, the 35 enzymes tested that could not digest the DNA contain G/C bases in their recognition sites, suggesting that these nucleotides may be altered in AXL3 gDNA to resist digestion. Phage genome resistance to restriction digestion is common and has been documented in other *S. maltophilia* phages to varying degrees [170,172,177–179], with phage DLP4 gDNA resistant to a similar panel of enzymes as AXL3 [114].

AXL3 is predicted to encode 65 putative protein-coding genes (Table 4-2, Figure 4-3), producing a coding density of approximately 94%. The majority of start codons are ATG (56 of 65), with fewer GTG (8) present, and only gp14 using TTG. Most stop codons are TGA (43 of 65), with the remaining mainly TAA (20) and only two, gp27 and gp628, using TAG. No tRNA genes were identified. Functional predictions for the 65 putative proteins by BLASTp analysis produced significant matches for 43 proteins, with conserved domains identified in 22 of the proteins. Of the 43 proteins with hits, only 26 were given putative functions. The remaining 22 proteins did not have any sequence identity to proteins in the NCBI database and were annotated as hypothetical (Table 4-2). Although these hypothetical proteins are distributed throughout the AXL3 genome, a clear modular organization is evident, consisting of genes involved in DNA repair and replication (blue) on the negative strand and genes required for virion morphogenesis (green) and lysis (red) on the positive strand (Figure 4-3). The genome sequence of AXL3 with putative annotations has been deposited in Genbank with the accession number MT536174.

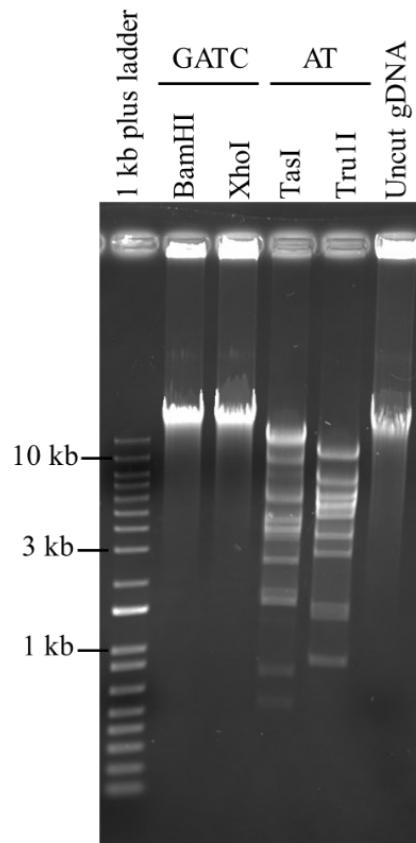


Figure 4-4: Restriction digests of AXL3 gDNA show evidence of base modification.

Agarose gel electrophoresis of AXL3 gDNA following incubation with *BamHI* and *XhoI* enzymes containing GATC bases in their recognition sites compared with *TasI* and *TruII* enzymes containing only AT bases in their recognition sites.

The International Committee on Taxonomy of Viruses recommends a cut off of 70% nucleotide identity across the length of the genome for phage genera [314]. Based on the absence of nucleotide identity with known phages, we propose that AXL3 belongs to a new genus of phages, *Axeltriavirus*, named after this phage. Given the mosaic nature of phage genomes and high degree of horizontal gene transfer between phages [315], we analyzed taxonomic relationships using vConTACT2 (v0.9.16), a network-based tool that uses phage genome protein content for viral classification and accurate clustering of phages at the genus level [311]. Analysis against the Prokaryotic Viral RefSeq94-Merged database classifies AXL3 as an outlier genome, meaning it is weakly connected with a cluster of sequences based on shared genes but lacks statistical significance to be included with the

cluster. Visualization of the network shows that AXL3 shares similarities to 24 phage genomes that belong to three viral clusters or are also outliers (Figure 4-5). Further sampling of the virosphere is needed to strengthen the connection of AXL3 with existing taxonomy and identify additional genus members.

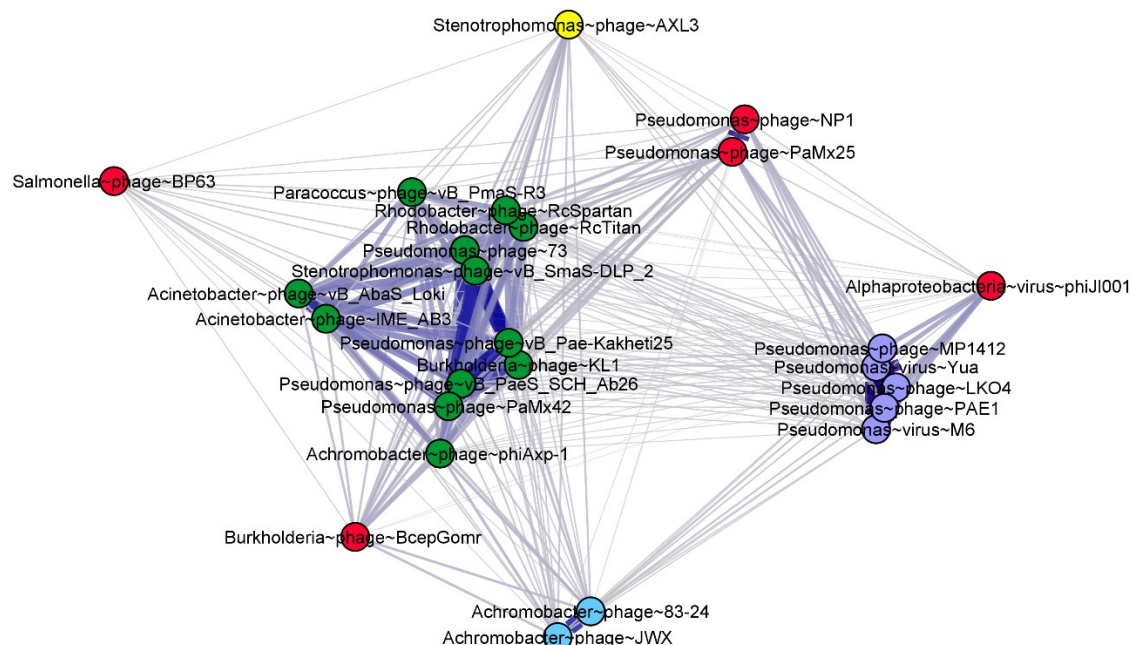


Figure 4-5: Network representation of AXL3 phylogeny. Analysis with vConTACT2 [36] identifies AXL3 as an outlier genome weakly connected to three phage clusters. This network comprises 24 out of 2,617 National Center for Biotechnology Information (NCBI) RefSeq phage genomes with connections to the AXL3 genome (yellow), each represented by a node (circles). Each colour 3 represents a viral cluster, with red and yellow indicating outliers. An edge (line) represents a connection between two nodes (genomes) based on the number of shared protein clusters, with darker and thicker edges indicating increased significance. Visualization of the network was performed using Cytoscape [71].

Table 4-2: Genome annotations for AXL3 obtained from BLASTp and CD-Search data. Results below 1.00×10^{-3} were not recorded and the function was annotated as hypothetical.

CDS	Coding Region	Strand	Length (AA)	Putative Function	Hit	Species	Cov. (%)	E-Value	Identity (%)	Accession
1	204-806	+	200	hypothetical protein	hypothetical protein	<i>Burkholderia</i> sp. SRS-W-2-2016	40	3.0×10^{-4}	35.56	WP_143752284.1
2	806-2368	+	520	large terminase	terminase large subunit	<i>Microcystic</i> phage Me-ZS1	95	0	59.96	AZF88145.1
3	2379-3887	+	502	portal protein	putative portal protein	Prokaryotic dsDNA virus sp.	97	2.0×10^{-141}	47.7	QDP56576.1
4	3891-4952	+	353	head morphogenesis protein	hypothetical protein	uncultured <i>Caudovirales</i> phage	98	1.0×10^{-91}	44.17	ASN68636.1
5	4998-5156	+	52	hypothetical protein	-					
6	5177-5911	+	244	scaffold protein	scaffold protein	<i>Pseudomonas</i> phage vB_PaeS_SCH_Ab26	99	6.0×10^{-41}	41.3	YP_009044344.1
7	5946-6962	+	338	capsid protein	capsid protein	<i>Salmonella</i> phage PMBT28	98	8.0×10^{-124}	51.46	AUZ95497.1
8	7041-7340	+	99	hypothetical protein	-					
9	7347-7871	+	174	structural protein	structural protein	<i>Achromobacter</i> phage vB_Ade_ART	99	1.0×10^{-32}	45.56	AYD82587.1
10	7876-8259	+	127	head-tail joining protein	hypothetical protein	<i>Pseudomonas</i> phage PaSz-4	100	4.0×10^{-14}	32.56	QAX99460.1
11	8256-8687	+	143	structural protein	putative structural protein	<i>Pseudomonas</i> phage PAE1	94	3.0×10^{-33}	41.55	YP_009215709.1

12	8692-10245	+	517	major tail structural protein	major tail structural protein	Pseudomonas phage NP1	98	0	65.36	YP_009285827.1
13	10272-10691	+	139	structural protein	putative structural protein	Pseudomonas phage NP1	100	4.0×10^{-56}	57.55	YP_009285828.1
14	10712-11071	+	119	hypothetical protein	hypothetical protein	<i>Pseudomonas</i> phage LKO4	73	9.0×10^{-27}	54.02	YP_009601866.1
15	11068-11496	+	142	hypothetical protein	hypothetical protein	Bordetella phage FP1	98	2.0×10^{-37}	50	YP_009794086.1
16	11501-14341	+	946	tape measure protein	hypothetical protein	Pseudomonas virus M6	98	0	47.08	YP_001294539.1
17	14352-15296	+	314	tail assembly protein	tail assembly protein	<i>Xylella</i> phage Salvo	99	6.0×10^{-133}	58.72	YP_009639180.1
18	15296-16279	+	327	hypothetical protein	hypothetical protein	<i>Stenotrophomonas</i> phage vB_SmaS-DLP_1	98	1.0×10^{-72}	42.04	AKI28800.1
19	16282-18018	+	578	hypothetical protein	hypothetical protein	<i>Pseudomonas</i> phage vB_PaeS_C1	91	2.0×10^{-115}	36.84	AVJ48097.1
20	18015-18854	+	279	hypothetical protein	hypothetical protein	<i>Burkholderia</i> phage vB_BceS_KL1	99	3.0×10^{-80}	45.68	YP_006560776.1
21	18858-21968	+	1036	central tail hub	tail protein	<i>Burkholderia</i> phage vB_BceS_KL1	77	0	46.73	YP_006560777.1
22	21965-22138	+	57	hypothetical protein	-					
23	22135-22584	+	149	endolysin	endolysin	<i>Xanthomonas</i> phage Xp15	98	2.0×10^{-53}	53.9	YP_239293.1
24	22590-23021	+	143	hypothetical protein	-					

25	23018-23323	+	101	hypothetical protein	hypothetical protein	Sinobacteraceae bacterium	92	1.0×10^{-9}	40	TXH02718.1
26	23579-23941	+	120	hypothetical protein	-					
27	24050-24571	-	173	dCMP deaminase	dCMP deaminase	uncultured Mediterranean phage uvMED	91	6.0×10^{-43}	47.17	YP_009778145.1
28	24942-25751	-	269	thymidylate synthase	thymidylate synthase	<i>Pelagibacter</i> phage HTVC200P	87	6.0×10^{-65}	44.49	AXH71582.1
29	25732-26715	-	327	thymidylate kinase	thymidylate kinase	Caudovirales sp. ctOwN3	93	3.0×10^{-33}	33.98	QGH72154.1
30	26696-27250	-	184	nucleoside triphosphate pyrophosphohydrolase	NTP-Ppase	Caudovirales sp. ctOwN3	69	5.0×10^{-32}	46.21	QGH72159.1
31	27260-28084	-	274	methyltransferase	methyltransferase domain-containing protein	Nitrospira cf. moscoviensis SBR1015	94	5.0×10^{-133}	73.08	WP_087475488.1
32	28162-28761	-	199	hypothetical protein	hypothetical protein	Nitrospira cf. moscoviensis SBR1015	74	3.0×10^{-26}	44.13	WP_087475489.1
33	29100-29273	-	57	hypothetical protein	-					
34	29273-29920	-	215	hypothetical protein	-					
35	29997-30089	-	30	hypothetical protein	-					
36	30100-30375	-	91	hypothetical protein	hypothetical protein	<i>Xanthomonas</i> phage Xoo-sp2	93	4.0×10^{-20}	48.24	ANT45253.1
37	30379-30588	-	69	hypothetical protein	-					
38	30700-32256	-	518	DNA helicase	hypothetical protein	Prokaryotic dsDNA virus sp.	91	4.0×10^{-123}	44.49	QDP55885.1

39	32463-32690	-	75	hypothetical protein	-					
40	32678-33532	-	284	RecB family exonuclease/Cas4	putative RecB family exonuclease	<i>Campylobacter</i> phage vB_CjeM_Los1	84	1.0×10^{-10}	27.31	YP_009597155.1
41	33532-35457	-	641	DNA polymerase I	DNA polymerase A	<i>Vibrio</i> phage VpKK5	71	1.0×10^{-29}	27.62	YP_009126593.1
42	35454-35672	-	72	hypothetical protein	hypothetical protein	Sandarakinorhabdus limnophila	72	4.0×10^{-5}	46.15	WP_022681046.1
43	35750-36652	-	300	hypothetical protein	hypothetical protein	<i>Pseudomonas</i> phage KPP25	72	4.0×10^{-12}	24.55	YP_009030602.1
44	36720-37232	-	170	hypothetical protein	hypothetical protein	Nitrospira cf. moscoviensis SBR1015	76	9.0×10^{-35}	52.31	WP_087475496.1
45	37232-37702	-	156	hypothetical protein	-					
46	37789-38694	-	301	DNA ligase	DNA ligase	<i>Xanthomonas</i> phage Xoo-sp2	99	3.0×10^{-81}	45	ANT45243.1
47	38691-39158	-	155	hypothetical protein	hypothetical protein	<i>Microcystic</i> phage Me- ZS1	92	1.0×10^{-25}	40.28	AZF88158.1
48	39155-39403	-	82	hypothetical protein	hypothetical protein	<i>Cupriavidus</i> sp. UYMSc13B	100	3.0×10^{-9}	37.35	RWA55322.1
49	39405-39674	-	89	hypothetical protein	-					
50	39667-40515	-	282	thymidylate synthase complementing protein	thimidilate synthase	<i>Caulobacter</i> phage Seuss	98	3.0×10^{-66}	43.77	YP_009785564.1
51	40505-40747	-	80	hypothetical protein	-					
52	40816-41031	-	71	hypothetical protein	-					
53	41028-41546	-	172	hypothetical protein	hypothetical protein	<i>Mycobacterium</i> phage OkiRoe	56	4.0×10^{-9}	36.61	YP_009043654.1

54	41548-41745	-	65	hypothetical protein	-					
55	41742-42221	-	159	DUF1643 containing protein	hypothetical protein	Pseudomonas phage Epa33	95	2.0×10^{-47}	53.85	QIQ65784.1
56	42218-42520	-	100	hypothetical protein	hypothetical protein	<i>Xylella</i> phage Sano	99	3.0×10^{-16}	42.16	YP_009639092.1
57	42517-42801	-	94	hypothetical protein	-					
58	42830-42973	-	47	hypothetical protein	-					
59	42970-43182	-	70	hypothetical protein	-					
60	43179-43514	-	111	DnaJ domain-containing protein	DnaJ domain-containing protein	Pseudoalteromonas sp. FUC4	53	2.0×10^{-5}	38.33	WP_149594670.1
61	43511-43693	-	60	hypothetical protein	-					
62	43756-44055	-	99	Glu-rich hypothetical protein	-					
63	44148-44369	-	73	hypothetical protein	-					
64	44463-46577	-	704	Primase	putative primase	Stenotrophomonas phage S1	33	4.0×10^{-28}	32.91	YP_002321451.1
65	46876-47385	-	169	hypothetical protein	-					

DNA replication and repair module

AXL3 encodes at least 12 genes related to DNA replication, repair and the generation and processing of nucleotides within the region AXL3_27 to AXL3_65 (Table 4-2, Figure 4-3). Within this co-directionally oriented gene cluster, gene products that could be assigned putative enzymatic functions by homology include dCMP deaminase (gp27), thymidylate synthase (gp28), thymidylate kinase (gp29), nucleoside triphosphate pyrophosphohydrolase (gp30), methyltransferase (gp31), DNA helicase (gp38), RecB family exonuclease (gp40), DNA polymerase I (gp41), DNA ligase (gp46), thymidylate synthase complementing protein (gp50), DnaJ molecular chaperone (gp60) and primase (gp64). An interesting hypothetical protein within this module is gp62, a glutamic acid-rich protein with 36 glutamic acid residues out of 99 in the protein, including a 27 glutamic acid repeat at its C-terminus. While polyamino acid repeats appear to be rare in prokaryotes and viruses [316], in eukaryotes, many proteins containing aspartic acid and glutamic acid-rich repeats are related to DNA/RNA functions [317].

A cluster of genes within this module encode enzymes involved in the thymidylate synthesis pathway, functioning to create dTDP from dCMP precursor. AXL3 encodes a putative deoxycytidylate (dCMP) deaminase (gp27) that processes dCMP to produce deoxyuridine monophosphate (dUMP) [318]. This product is the nucleotide substrate for thymidylate synthase, gp28, which catalyzes the conversion of dUMP into deoxythymidine monophosphate (dTMP) by means of reductive methylation using the cofactor 5,10-methylenetetrahydrofolate ($\text{CH}_2\text{H}_4\text{folate}$) [319]. Interestingly, AXL3 also encodes a putative thymidylate synthase complementing protein (gp50) that is typically found in organisms that lack a thymidylate synthase and complements its activity to convert dUMP into dTMP using FAD as an additional cofactor with $\text{CH}_2\text{H}_4\text{folate}$ [320]. The dTMP product can be further processed by the AXL3 encoded thymidylate kinase (gp29) into dTDP on its way to being used in DNA synthesis. The identification of some proteins known to be involved in nucleotide biosynthesis and the restriction-resistant nature of the AXL3 gDNA suggest that the large number of hypothetical proteins in this module may be

involved in the synthesis and incorporation of altered nucleotides, however further study is needed.

Of the 39 genes in this area, 11 gene products share high sequence identity with bacteria of the *Nitrospira* genus when BLASTp searches are limited to Bacteria (taxid:2) (Table 4-3). These Gram-negative, nitrite-oxidizing bacteria are widespread in the environment, found in both aquatic and terrestrial habitats, and play a key role in nitrogen cycling [321]. Specifically, ten proteins have top hits to the *Nitrospira* cf. *moscoviensis* strain SBR1015, including gp27 to gp31 described above. However, no AXL3 phage morphogenesis or lysis proteins had BLASTp hits to bacteria in this genus. The clustering of these genes, the significant sequence identity, and the location of these genes amongst non-prophage genes on the *Nitrospira* genome contigs, suggest that these AXL3 genes are of bacterial origin.

Of particular interest in this module is the identification of a Cas4 conserved domain in gp40 (Table 4-4). Cas4 proteins are DNA nucleases with 5'-3' exonuclease activity shown to create recombinogenic ends for spacer acquisition in host CRISPR arrays to generate host immunity to invading DNA, including viruses and plasmids [322,323]. Phylogenetic analyses have identified *cas4* genes in many mobile genetic elements lacking CRISPR-Cas systems, including archaeal viruses and phages, suggesting the involvement of Cas4 nucleases in anti-defense functions [324]. In *Campylobacter jejuni* phages specifically, phage-encoded Cas4-like proteins have been identified and experimentally determined to be capable of incorporating host-derived spacers into the CRISPR array of their host bacterium during infection to evade host immunity [323]. BLASTp analysis reveals that AXL3 gp40 is conserved with these *Campylobacter* phage-encoded Cas4 proteins, suggesting a similar function of spacer acquisition in AXL3, however CRISPR-Cas immunity has not yet been characterized in *S. maltophilia* [113,114]. It is possible that phage-encoded Cas4-like proteins may play an uncharacterized role in defense against host restriction-modification systems; the *Campylobacter* phages encoding Cas4 nuclease homologs are also predicted to contain modified guanosine nucleotides that provide

Table 4-3: AXL3 proteins with *Nitrospira* sp. as the top BLASTp hit when search is limited to Bacteria (taxid:2).

gp	Putative function	Hit	Species	Coverage (%)	E-value	Identity (%)	Accession
27	dCMP deaminase	dCMP deaminase family protein	<i>Nitrospira cf. moscoviensis</i> SBR1015	98	3.0×10^{-66}	59.65	WP_087475484.1
28	thymidylate synthase	hypothetical protein	<i>Nitrospira cf. moscoviensis</i> SBR1015	83	3.0×10^{-83}	54.82	WP_140393856.1
29	thymidylate kinase	hypothetical protein	<i>Nitrospira</i> sp. SG-bin2	96	2.0×10^{-61}	41.93	OQW33949.1
30	nucleoside triphosphate pyrophosphohydrolase	hypothetical protein	<i>Nitrospira cf. moscoviensis</i> SBR1015	73	2.0×10^{-38}	52.17	WP_087475487.1
31	methyltransferase	methyltransferase domain- containing protein	<i>Nitrospira cf. moscoviensis</i> SBR1015	94	5.0×10^{-133}	73.08	WP_087475488.1
32	hypothetical protein	hypothetical protein	<i>Nitrospira cf. moscoviensis</i> SBR1015	74	3.0×10^{-26}	44.13	WP_087475489.1
38	DNA helicase	DEAD/DEAH box helicase	<i>Nitrospira cf. moscoviensis</i> SBR1015	93	0	57.91	WP_087475490.1
41	DNA polymerase I	hypothetical protein	<i>Nitrospira cf. moscoviensis</i> SBR1015	95	0	50.57	WP_087475493.1
43	hypothetical protein	hypothetical protein	<i>Nitrospira cf. moscoviensis</i> SBR1015	92	6.0×10^{-91}	52.63	WP_087475495.1
44	hypothetical protein	hypothetical protein	<i>Nitrospira cf. moscoviensis</i> SBR1015	76	9.0×10^{-35}	52.31	WP_087475496.1
64	primase	DUF3854 domain-containing protein	<i>Nitrospira cf. moscoviensis</i> SBR1015	97	0	50.66	WP_087475499.1

resistance to gDNA digestion with restriction enzymes [325], as observed in AXL3. A Cas4-like nuclease has also been identified in close proximity to deoxyarchaeosine (dG+) synthesis genes in the restriction-resistant genome of *E. coli* phage 9g, suggesting a possible role for Cas4 in a restriction system of unmodified DNA, or degradation of host DNA for nucleotide recycling [326]. Further characterization of these phage-encoded Cas4 proteins will likely reveal uncharacterized defense and anti-defense systems.

Virion Morphogenesis Module

The virion morphogenesis module of AXL3 consists of 22 genes (AXL3_1 to AXL3_22) oriented on the positive strand, the gene products for 13 of which were assigned functions based on BLASTp sequence identity (Table 4-2, Figure 4-3). Proteins involved in capsid assembly and packaging include the large terminase protein (gp2), portal protein (gp3), head morphogenesis protein (gp4), scaffold protein (gp6), and capsid protein (gp7). Eight proteins were identified as structural proteins involved in tail morphogenesis and phage assembly including three putative virion structural proteins (gp9, gp11, and gp13), a head-tail joining protein (gp10), a major tail protein (gp12), tape measure protein (gp16), tail assembly protein (gp17) and central tail hub protein (gp21). These proteins have sequence identity with phages specific to numerous bacterial species, including *P. aeruginosa*, *S. maltophilia*, and *Burkholderia cenocepacia*. This module follows the typical gene architecture for Siphoviridae morphogenesis modules; the capsid assembly genes are located upstream of the tail assembly genes that are organized starting with genes encoding the major tail proteins [327]. The tape measure protein generally corresponds to the length of the phage tail in Siphoviridae phages and is therefore the largest gene, however in AXL3 this gene is second in length to the gene encoding the central tail hub.

A conserved domain search revealed two domains of interest in the central tail hub protein, gp21, of AXL3 (Table 4-4). The pfam13550 Phage-tail_3 domain present in gp21 has been found in the tail proteins of other *S. maltophilia* phages experimentally confirmed to use the type IV pilus as a cell surface receptor [11,114,160,178]. We previously

described the prediction that tail fibreless phages with baseplate proteins containing the Phage-tail_3 domain are capable of using the type IV pilus as a primary receptor [160], and the identification of this domain in the AXL3 central tail hub and functional analysis of the type IV pilus as the AXL3 receptor supports this hypothesis. Additionally, a Laminin G domain is present in gp21. Peters et al. [178] identified this domain in the tail proteins of two *Delepliquintavirus* phages against *S. maltophilia* and predicted that they may play role in host specificity due to their variation in protein sequence, showing high pairwise identity at the C-terminus and low percent identity at the N-terminus; as presented in Chapter 3, both phages bind the type IV pilus as their receptor. This pattern of sequence variation is also observed in the tail fiber proteins for type IV pili-binding *Xylella* phages, Salvo and Sano [281]. Further experimental investigation into the function of gp21 in AXL3 as a receptor binding protein is currently underway to determine whether this protein plays a role in host recognition and is discussed in Chapter 6.

Lysis module

The lysis module directly follows the virion morphogenesis module in the AXL3 genome and consists of four genes (AXL3_23 to AXL3_26) (Table 4-2, Figure 4-3). The first gene in this module encodes a predicted endolysin, gp23, and has a conserved L-alanyl-D-glutamate peptidase domain identified by CD-Search (Table 4-4). This domain is found in other bacteriophage endolysins, including *Escherichia coli* T5 phage endolysin and the endolysins of *Listeria monocytogenes* phages A118 and A500, Ply118 and Ply500, respectively [328,329]. These cell wall lytic enzymes cleave between the L-alanine and D-glutamate residues of the peptidoglycan wall to cause cell lysis late in phage infection.

The genes downstream of the AXL3 endolysin are annotated as hypotheticals based on lack of sequence identity to known proteins in the NCBI database. Analysis of the gene products with TMHMM revealed the predicted presence of four transmembrane domains in gp24 and three transmembrane domains in gp25, suggesting potential functions as holin or i-spanin proteins [192]. Canonical holin proteins reside in the cytoplasmic membrane and

Table 4-4: The conserved domains found in the 65 gene products of AXL3.

Gp	Hit Type	PSSM-ID	Interval	E-Value	Accession	Short Name	Superfamily
2	Superfamily	392065	31-274	1.96×10^{-3}	cl29365	Terminase_6 superfamily	-
3	Specific	372539	261-406	6.28×10^{-34}	pfam13264	DUF4055	cl16196
4	Superfamily	385666	186-261	3.11×10^{-12}	cl10072	Phage_Mu_F superfamily	-
4	Superfamily	225244	30-263	2.65×10^{-5}	cl26983	COG2369 superfamily	-
6	Superfamily	374274	41-106	2.85×10^{-3}	cl25765	G_path_suppress superfamily	-
7	Superfamily	391678	156-250	9.22×10^{-3}	cl27082	Phage_capsid superfamily	-
11	Superfamily	372633	16-94	1.13×10^{-4}	cl16304	DUF4128 superfamily	-
16	Specific	131723	128-202	7.49×10^{-19}	TIGR02675	tap_meas_nterm	cl31236
16	Specific	227606	114-682	4.31×10^{-13}	COG5281	COG5281	cl34971
20	Superfamily	378160	211-271	7.98×10^{-11}	cl10710	Phage_BR0599 superfamily	-
21	Specific	379255	278-448	2.40×10^{-13}	pfam13550	Phage-tail_3	cl38419
21	Superfamily	389952	874-1024	9.63×10^{-4}	cl22861	LamG superfamily	-
23	Specific	350620	9-147	4.62×10^{-29}	cd14845	L-Ala-D-Glu_peptidase_like	cl38918
27	Superfamily	381914	6-159	1.31×10^{-36}	cl00269	cytidine_deaminase-like superfamily	-
28	Superfamily	388507	30-219	1.84×10^{-31}	cl19097	TS_Pyrimidine_HMase superfamily	-
30	Specific	212137	34-122	1.32×10^{-21}	cd11530	NTP-Ppase_DR2231_like	cl16941
31	Superfamily	225139	52-192	1.16×10^{-10}	cl34437	Cfa superfamily	-
38	Specific	223627	7-509	7.90×10^{-32}	COG0553	HepA	cl33945
38	Superfamily	391939	38-266	2.73×10^{-64}	cl28899	DEAD-like_helicase_N superfamily	-

40	Superfamily	378929	33-271	1.75×10^{-13}	cl00641	Cas4_I-A_I-B_I-C_I-D_II-B superfamily	-
41	Superfamily	223820	73-630	1.20×10^{-40}	cl34031	PolA	-
46	Specific	185707	5-188	2.94×10^{-38}	cd07896	Adenylation_kDNA_ligase_like	cl12015
46	Specific	153443	190-296	4.19×10^{-13}	cd08041	OBF_kDNA_ligase_like	cl08424
50	Superfamily	391735	26-169	1.67×10^{-12}	cl27413	Thy1 superfamily	-
55	Specific	377919	17-145	4.55×10^{-57}	pfam07799	DUF1643	cl01787
60	Superfamily	389798	74-110	1.31×10^{-04}	cl21539	DnaJ_zf superfamily	-
60	Superfamily	383015	14-64	1.99×10^{-03}	cl02542	DnaJ superfamily	-
64	Superfamily	382163	142-252	1.19×10^{-14}	cl00718	TOPRIM superfamily	-

upon triggering, create pores in the membrane to release phage endolysin into the periplasm to degrade the cell wall peptidoglycan. For complete cell lysis, disruption of the outer membrane is required by the spanin complex that consists of two proteins localized to the inner membrane and outer membranes [192]. No transmembrane domains were predicted in gp26, however analysis with Lipop 1.0 predicted gp26 to be a lipoprotein signal peptide with a predicted signal peptidase II cleavage site between amino acids 17 and 18. This suggests that gp26 acts as an o-spanin, anchored in the outer membrane and spanning the periplasm to reach the cytoplasmic membrane i-spanin protein [192].

Conclusions

These results characterize a novel virulent phage that is active against the multidrug resistant bacterial pathogen *S. maltophilia*. Genomic characterization of AXL3 reveals a 47,545 bp genome that is resistant to digestion with restriction enzymes containing G/C bases in their recognition sequences and predicted to encode 65 proteins, many of which have hypothetical functions. Phage AXL3 encodes numerous nucleotide processing enzymes and a putative Cas4 nuclease that may function to provide defense against host anti-phage defenses, however further experimentation is required. This phage is capable of infecting a narrow range of *S. maltophilia* hosts using the type IV pilus, an important virulence factor used for biofilm formation, adherence, and twitching motility [240]. No lysogeny genes were identified in our bioinformatic analyses and lysogens in strains D1585 or 213 could not be isolated, indicating that AXL3 is a virulent phage. Further investigation of the receptor binding proteins for *S. maltophilia* type IV pili binding phages with different host ranges may allow for genetic engineering of AXL3 to broaden its host range and increase its value as an “anti-virulence” candidate for phage therapy.

Acknowledgments

I would like to thank Arlene Oatway from the University of Alberta Department of Biological Sciences Advanced Microscopy Facility for her assistance with TEM. We are grateful to Dr. James Zlosnik and the CBCCR and LeeAnn Turnbull of the Provincial Laboratory for Public Health -North, Alberta Health Services for *S. maltophilia* clinical isolates, as well as Dr. Jorge Girón for gifting strains SMDP92 and ATCC13637. I was kindly supported by a CGS-D award from NSERC and an AIGSS award from Alberta Innovates during this research project.

CHAPTER 5 - Characterization of *Stenotrophomonas maltophilia* phage AXL1 as a member of the genus *Pamexvirus* encoding resistance to trimethoprim-sulfamethoxazole

A version of this chapter has been published as:

McCutcheon JG, Lin A, Dennis JJ. 2022. Characterization of *Stenotrophomonas maltophilia* phage AXL1 as a member of the genus *Pamexvirus* encoding resistance to trimethoprim-sulfamethoxazole. *Sci Rep.* 12:10299. doi:10.1038/s41598-022-14025-z. IF: 5.516

Objectives

AXL1 is the final *Stenotrophomonas maltophilia* phage I have identified to bind the type IV pilus as a receptor for infection. The evaluation of phages for their possible use in phage therapy requires extensive physical and genomic characterization. To this aim, the objectives of this chapter are to further characterize the physical attributes of this phage and assess its genetic safety for use as a phage therapy candidate.

Materials and Methods

Bacterial strains and growth conditions

The bacterial strains and plasmids used in this study are listed in Tables 5-1 and 5-2. 30 phenotypically distinct *S. maltophilia* strains were used for host range analysis. *S. maltophilia* strain D1585 was used for phage isolation and as the primary host for propagation. All strains were grown overnight at 30°C on Lennox (LB; 10 g/L tryptone, 5 g/L yeast extract, 5 g/L NaCl) solid medium or in LB broth with shaking at 225 RPM. Media was supplemented with 35 µg/mL chloramphenicol (Cm) antibiotic for plasmid maintenance in *E. coli* and *S. maltophilia* D1585, D1571 and ATCC13637, 75 µg/mL Cm for *S. maltophilia* 280 and SMDP92, or 35 µg/mL gentamicin (Gm) for *P. aeruginosa* when necessary.

Table 5-1: Strains and plasmids used in this study.

Bacterial Strain	Genotype or Description	Source
<i>S. maltophilia</i> D1585	Wildtype, AXL1 ^S	CBCCR ^R
<i>S. maltophilia</i> D1571	Wildtype, AXL1 ^R	CBCCR ^R
<i>S. maltophilia</i> 280	Wildtype, AXL1 ^S	PLPHN/AHS ^{**}
<i>S. maltophilia</i> SMDP92	Wildtype, AXL1 ^S	[49]
<i>S. maltophilia</i> ATCC13637	Wildtype, AXL1 ^S	[49]
<i>E. coli</i> DH5α	Host for plasmid cloning	[223]
Plasmids		
pBBR1MCS	Broad-host range cloning vector, Cm ^R	[226]

pAXL1 <i>dhfr</i>	pBBR1MCS carrying AXL1 <i>dhfr</i> , Cm ^R	This study
-------------------	--	------------

* Canadian *Burkholderia cepacia* complex Research Referral Repository

** Provincial Laboratory for Public Health – North (Microbiology), Alberta Health Services

Phage isolation, propagation and host range analysis

Undergraduate student Andrea Lin isolated phage AXL1 from empty planter soil she collected in Edmonton, Alberta, Canada using *S. maltophilia* strain D1585 and a previously described enrichment protocol [11]. Briefly, soil was enriched for phage by overnight incubation at 30°C and shaking at 225 RPM with *S. maltophilia* D1585 liquid overnight culture and additional LB broth and modified suspension medium (SM) (50 mM Tris–HCl [pH 7.5], 100 mM NaCl, 10 mM MgSO₄). Solids were pelleted by centrifugation and the supernatant was filter sterilized using a Millex-HA 0.45 µm syringe-driven filter unit (Millipore, Billerica, MA, USA). After overnight incubation of soft agar overlays with *S. maltophilia* D1585, a single plaque was picked into 500 µL of SM with 20 µL chloroform to generate an AXL1 stock.

High titre working stocks of AXL1 were propagated using soft agar overlays as previously described [115,229] or liquid infections. Briefly, 150 µL of D1585 overnight culture and 150 µL of phage were incubated for 30 min at 30°C with shaking at 225 RPM before adding 15 mL LB broth and 1.5 mL SM and incubating overnight under the same conditions. 200 µL of chloroform was added the following day and incubated on a platform rocker at room temperature for 30 min. Following centrifugation, the supernatant was collected, filter sterilized as above and stored at 4 °C. Phage titre was determined by soft agar overlays on D1585. Plaques were backlit and viewed under the magnifying glass of a New Brunswick Scientific colony counter (model C110) and plaque size was measured using digital calipers manufactured by Tresna (Guilin, China) and reported as the average from 10 plaques ± standard deviation.

Host range analysis was conducted on a panel of 30 phenotypically distinct clinical *S. maltophilia* isolates that vary in phage susceptibility profiles [11,114,115,177–179] and colony morphology, 21 *P. aeruginosa* isolates and four *Xanthomonas* strains. Soft agar overlays containing 100 µL of overnight culture mixed with 3 mL of 0.7% 1/2 LB top agar were spotted with 5 µL of a 10¹¹ pfu/mL AXL1 stock at multiple dilutions and scored for clearing and/or plaque formation after incubation at 30 °C for 24 h and 48 h. Efficiency of plating (EOP) was calculated as the ratio of the number of plaques on a given strain to the titre on the isolation host,

D1585. Where plaques were not detected, the lowest dilution with evidence of phage activity was considered for EOP. Predicted phage production was scored based on EOPs greater than 0.5 (high) or 0.001 (low) [260]. The same procedure was conducted for AXL1 efficiency of plating on host mutants for receptor analysis, with antibiotics added to the bottom and top agar as required for plasmid maintenance.

Temperature stability of AXL1 virions was determined after incubation of 100 μ L of a 10^7 PFU/mL lysate at various temperatures (-20°C, 22°C (room temperature), 30°C, 35°C, 37°C, 42°C, 50°C, 60°C, 80°C, 90°C) for 1 h. The treated lysate was serially diluted and 5 μ L of each dilution was spotted on soft agar overlays containing 100 μ L of overnight D1585 culture. Plaques were counted after overnight incubation at 30°C and reported as the average phage titre from three biological replicates with error bars showing standard deviation.

Transmission electron microscopy

For electron microscopy, phages were purified by cesium chloride density gradient ultracentrifugation and dialysis. CsCl was dissolved in high titre 10^{11} pfu/mL AXL1 lysate to 1.45 g/mL followed by ultracentrifugation at 35,000 RPM in a 50.2 Ti rotor for 20 h at 4 °C. The phage band was extracted using an 18 G needle into 12 kDa molecular weight cutoff dialysis tubing and dialyzed at 4 °C in 1.5 L SM for 4 days, with the SM buffer changed every 24 h. To visualize phages, 10 μ L purified phage lysate was loaded onto a carbon-coated copper grid for 2 min and stained with 4% uranyl acetate for 20 s. Transmission electron micrographs were captured using a Philips/FEI Morgagni transmission electron microscope with charge-coupled device camera at 80 kV (University of Alberta Department of Biological Sciences Advanced Microscopy Facility). The average capsid and tail dimensions \pm standard deviation was calculated using Microsoft Excel based on measurements from 10 individual virions taken using ImageJ software (NIH, Bethesda, MD, USA) [239].

One-step growth curve

To determine burst size and latent period of AXL1, one-step phage growth analysis of AXL1 on *S. maltophilia* D1585 was conducted as previously described [115,300], with modifications. Overnight liquid cultures of D1585 were subcultured in LB broth and grown to an OD₆₀₀ of 0.2 at 30°C. AXL1 lysate was added at an MOI of ~1 and allowed to adsorb for 5 min

at room temperature followed by incubation at 30°C with aeration at 225 RPM for 6 h. Samples were taken in triplicate at 30 min intervals and serially diluted in SM for spotting on soft agar overlays containing D1585. Plaques were counted after overnight incubation at 30°C. Resulting data from four biological replicates was analyzed using GraphPad Prism 9 (GraphPad Software Inc., San Diego, CA, US).

Growth reduction assay and phage lifestyle analysis

To analyze the killing effect of AXL1 phage in liquid culture, growth reduction assays were conducted. Three D1585 overnight liquid cultures were subcultured in LB broth and grown at 30°C to an OD₆₀₀ of 0.2, corresponding to 4.0×10^8 CFU/mL. 100 µL of each culture was added to wells of a 96 well plate containing 100 µL of AXL1 phage lysate at multiple concentrations to give MOIs of approximately 30, 6, 0.6, and 0.06, or LB broth as a control, resulting in biological triplicate with three replicates each. The plate was incubated at 30°C with continuous orbital shaking at 237 cpm in an Epoch 2 microplate spectrophotometer (Bio Tek Instruments, Inc., VT, USA), with the OD₆₀₀ measured every 30 min for 48 h. Data from three biological replicates was analyzed using GraphPad Prism 9 (GraphPad Software Inc., San Diego, CA, US).

To investigate AXL1 lifestyle, the isolation of lysogens was attempted from both confluent lysis plate infections and liquid infections as described above at 30°C and 37°C. Surviving bacterial cells were washed three times to remove contaminating phage and plated for single colonies. Individual colonies were tested for superinfection resistance by spotting with phage lysate and resistant colonies were analyzed by colony PCR with AllTaq DNA polymerase (Qiagen, Inc., Germantown, MD, USA) following manufacturer protocols using primers specific to AXL1 gDNA (F 5'-GACTACGACGCCTTCTCCGC-3'; R 5'-TTTGCCTGCCTCGACGCCAG-3').

Twitching motility

As an indirect measurement of type IV pili function, twitching motility assays were conducted as previously described [160]. Single colonies were suspended in 100 µL LB and stab inoculated through a 3 mm thick LB 1% agar layer containing 0.3% porcine mucin to the bottom of the petri plate and incubated with humidity at 30°C or 37°C for 48 h. Twitching zones stained

with crystal violet were imaged and measurements using ImageJ software (NIH, Bethesda, MD, USA) [239] are reported as average twitching area \pm standard deviation from nine twitching zones representing results in biological triplicate for each strain.

Phage DNA isolation, RFLP analysis and genome sequencing

AXL1 genomic DNA (gDNA) was isolated by phenol/chloroform extraction and ethanol precipitation as previously described [115]. Following incubation with proteinase K, gDNA from a nuclease-treated high titre phage lysate was isolated with three phenol:chloroform extractions and a single chloroform wash. Phage DNA was ethanol precipitated and dissolved in sterile milli-Q water. A NanoDrop ND-1000 spectrophotometer (Thermo Scientific, Waltham, MA) was used to determine the purity and concentration of phage gDNA.

Restriction fragment length polymorphism (RFLP) analysis was conducted using 31 FastDigest (Thermo Scientific) restriction enzymes: AccI, AseI, MspI, HpaII, HhaI, Bsh1236I, MauBI, PdmI, HaeIII, NheI, AciI, Eam1105I, SmaI, XbaI, BamHI, KpnI, ApaI, SacI, HindIII, Sall, PstI, ClaI, XhoI, NotI, StuI, BglII, AvrII, MscI, StyI, TasI, and TruI. Digests were set up in 20 μ L volumes using 1 μ L of enzyme, 2 μ L of restriction buffer and 1 μ g of AXL1 gDNA. Reactions were incubated at 37°C for 1 h, separated on a 0.8% (wt/vol) agarose gel in 1 \times TAE (pH 8.0) and DNA visualized with ethidium bromide post-staining.

Sequencing of AXL1 was performed at The Applied Genomics Core at the University of Alberta. A DNA genomic library was constructed using a Nextera XT library prep kit followed by paired-end sequencing on a MiSeq (Illumina, San Diego, CA) platform using a MiSeq v3 reagent kit.

Bioinformatic analysis

Quality control analysis was completed using FastQC v0.11.9 [301] and the 1,266,570 paired-end reads were processed using Trimmomatic v0.38 [302], with 80.07% of both read pairs surviving. SPAdes v3.11.1 [303] was used to assemble a 64,089 bp contig with 2,023,812 reads mapping to the contig to give a mean coverage of 5,850 reads. Regions of low coverage, random sites, and ends of the contig were confirmed with PCR using seven primer pairs followed by Sanger sequencing of the PCR products to confirm the complete genome of 63,962 bp in length due to a duplication of 127 bp between AXL1_67 and AXL1_68 at the assembly ends.

Exploration of this region as direct terminal repeats did not produce confirmatory results. In the absence of data supporting physical genomic termini, the genome start site was determined by convention and placed upstream of the small terminase, similar to related phage genomes PaMx28 (accession: NC_028931) and PaMx74 (accession: NC_028809) [330].

Predicted protein coding genes were identified using the GLIMMER plugin [304] for Geneious using the Bacteria and Archaea setting, as well as GeneMarkS for phage [331] and Prodigal [306]. Annotations to the contig and visualization of the genome was done using Geneious Prime v2022.0.1 [230]. BLASTn was used to identify relatives based on genomic data and putative protein functions were assigned using BLASTp limited to Viruses (taxid:10239) on the NCBI non-redundant protein sequence and nucleotide collection databases (update date: 2021/11/04) [264]. Conserved domain searches were performed using CD-Search against the CDD v3.19-58235 PSSMs database and default options [265] to support functional annotation. TMHMM [307] and LipoP 1.0 [308] were used to identify transmembrane regions and predict lipoproteins, respectively, in putative lysis proteins. tRNAscan-SE software with the general tRNA model [309] and Aragorn v1.2.36 [310] were used to identify potential tRNA genes. Rho-independent transcription terminator sequences were identified using ARNold [332] and 13 putative intergenic terminators with ΔG values less than -10 kcal/mol were included. Phage promoters were identified using the PhagePromoter tool in the CPT Galaxy webserver [333]. Protein alignments were accomplished using MUSCLE [231]. Protein structural and functional predictions were conducted using I-TASSER [334], COACH [335] and COFACTOR [336].

Genomic comparison of phages in the *Pamexvirus* genus was conducted using Clinker v0.0.23 [266] on phage genomes that were first oriented to have the same start site as AXL1 upstream of the small terminase protein. Only links with 30-100% identity are shown.

Proteomic analysis of virion-associated proteins

Phage particles were purified for proteomic analysis by CsCl density gradient ultracentrifugation as described above. The equivalent of $\sim 2 \times 10^9$ PFU was boiled for 5 min in Laemmli sample buffer and loaded into a single lane of an SDS-PAGE gel with 5% stacking and 10% resolving sections and run at 80V for 2 h followed by Coomassie R-250 staining. Whole lane in gel trypsin digestion and protein identification was conducted by the Alberta Proteomics and Mass Spectrometry (APM) facility at the University of Alberta as previously described

[178], with modifications. The lane was cut into four equal gel sections and following processing, proteins were trypsin digested (6 ng/ μ L) at 37°C overnight. Tryptic peptides were extracted from the gel and fractions containing tryptic peptides were resolved and ionized using nanoflow high-performance liquid chromatography (HPLC) (Easy-nLC 1000; Thermo Scientific) coupled to a Q Exactive Orbitrap mass spectrometer (Thermo Scientific). A PepMap RSLC C18 EASY-Spray column (Thermo Scientific) with a 75- μ m inner diameter (100 Å, 3 μ m pore size) was used for nanoflow chromatography and electrospray ionization. Peptide mixtures were injected onto the column at a flow rate of 3,000 nL/min and resolved at 350 nL/min using 60-min step gradients of 4% to 37% (vol/vol) aqueous ACN with 0.2% (vol/vol) formic acid. The mass spectrometer was operated in data-dependent acquisition mode, recording high-accuracy and high-resolution Orbitrap survey spectra using external mass calibration, with a resolution of 35,000 and m/z range of 400 to 2,000. The 12 most intensely multiply charged ions were sequentially fragmented by HCD fragmentation and their spectra were collected at a resolution of 17,500. After two fragmentations, all precursors selected for dissociation were dynamically excluded for 30 s. Data were processed using Proteome Discoverer 1.4 (Thermo Scientific) and all AXL1 and *S. maltophilia* D1585 proteins were searched using SEQUEST (Thermo Scientific).

Antibacterial susceptibility checkerboard assays

The AXL1 *dhfr* gene was amplified from phage genomic DNA using Phusion high-fidelity DNA polymerase (New England Biolabs) with GC buffer and 3% DMSO according to manufacturer protocols and using primer pair AXL1gp63F (TTCTAAAGCTTTACCCATCACCTACATTGCG) and AXL1gp63R (TTATTCTAGAGAGCTCACCAGGTTCTCGAC). Restriction enzyme recognition sites are underlined. The resulting product was purified by gel extraction using the QIAquick gel extraction kit (Qiagen, Inc., Germantown, MD, USA), digested with *HindIII* and *XbaI* Fast Digest restriction endonucleases (Thermo Scientific) and ligated into the similarly digested vector pBBR1MCS using T4 DNA ligase (New England Biolabs), producing the construct pAXL1*dhfr*. This plasmid was transformed into electrocompetent *E. coli* DH5 α and verified by Sanger sequencing before transforming *S. maltophilia* strains by electroporation as previously described [160].

Overnight cultures of *S. maltophilia* strains carrying pBBR1MCS or pAXL1*dhfr* were grown in LB with chloramphenicol for 18 h at 30°C before subculturing 1:100 in Mueller Hinton (MH) broth and growing to an OD₆₀₀ corresponding to 10⁸ CFU/mL. 190 µL of each subculture was added to 96-well plates, followed by 5 µL each of serially diluted sulfamethoxazole (Sigma-Aldrich) and trimethoprim (MP Biomedicals), with DMSO added in place of either antibiotic as a solvent growth control. One lane contained MH and DMSO to serve as a negative control. Plates were incubated at 30°C with shaking at 225 RPM for 20-24 h and OD₆₀₀ was measured using a Wallac 1420 VICTOR2 multilabel counter (PerkinElmer, Waltham, MA). Data from three biological replicates was analysed using GraphPad Prism 9 (GraphPad Software Inc., San Diego, CA, US), with blank values subtracted from the absorbance and data normalized to the no antibiotic, solvent control well.

Results

AXL1 phage physical characteristics

Bacteriophage AXL1 (vB_SmaS-AXL_1) was isolated from potting soil following enrichment with the clinical *S. maltophilia* strain D1585 by undergraduate student Andrea Lin. AXL1 produces two sizes of clear plaques with diffuse borders averaging 1.67 ± 0.17 mm and 0.73 ± 0.12 mm in diameter after overnight incubation on its isolation host, D1585 (Figure 5-1). This plaque polymorphism is persistent upon picking and propagating individual plaques of each size, a phenotype that has been observed in *S. maltophilia* phage IME13 [173]. The use of chloroform during phage propagation to high titre indicates AXL1 is stable in the presence of this organic compound. Transmission electron microscopy (TEM) permits classification of AXL1 as a Siphoviridae phage of the B2 morphotype [313] having an icosahedral elongated capsid 81.0 ± 4.7 nm long and 53.2 ± 3.7 nm wide and a long, non-contractile tail averaging 150.3 ± 4.2 nm in length with a unique baseplate structure present at the distal tail region (Figure 5-1).

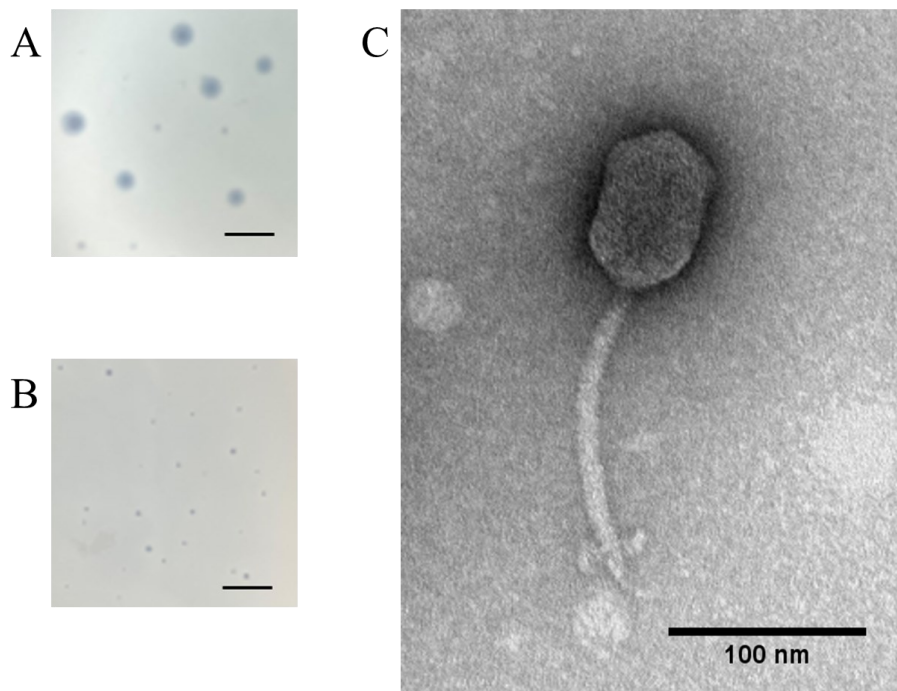


Figure 5-1: AXL1 phage morphology. AXL1 plated on (A) D1585 or (B) 213 show different plaque morphologies. Bar equals 5 mm. (C) Transmission electron micrograph of an AXL1 virion shows a Siphoviridae morphology. High titre CsCl purified lysate was stained with 4% uranyl acetate on a copper grid and viewed at 110,000 \times magnification with a transmission electron microscope.

Host range analysis on 30 distinct *S. maltophilia* clinical isolates revealed a moderate tropism, with AXL1 showing evidence of bacterial cell lysis as clearing of the bacterial lawn on 14 strains when spotted at a high titre of 10^{11} PFU/mL. (Tables 5-2, 3-2). These strains were further examined for productive phage infection by calculating the AXL1 efficiency of plating (EOP) from plaque formation in serial dilutions of phage lysate compared to the isolation host strain, D1585 [260]. Only two additional hosts produced high levels of phage production having EOPs greater than 0.5, while four strains could be classified as having low phage production with EOPs greater than 0.001 (Table 5-2). Although plaques formed on five of the remaining strains, this occurred at low dilutions, suggesting little to no phage production on these hosts. No plaque formation was observed on strains 102 and 287 in the dilution series beyond clearing of the bacterial lawn at high titre. Serial passaging of AXL1 on strains with low EOP may train this phage to infect more efficiently [271]. Of note, AXL1 produced plaques that were significantly

smaller in diameter than observed on D1585 on all hosts except D1568, with plaque sizes averaging 0.296 ± 0.047 mm on strain 213 (Figure 5-1B); plaques did not increase in size with longer incubation up to 48 h. For ease of plaque enumeration and because strain D1568 is more difficult to grow, strain D1585 was used for all further experiments.

Table 5-2: *S. maltophilia* clinical isolates susceptible to AXL1.

<i>S. maltophilia</i> strain	EOP ^a	AXL1 Productivity ^b
101	0.0013	Low
102	++	
103	1.9×10^{-6}	
213	0.64	High
219	0.0013	Low
280	0.0033	Low
282	1.43×10^{-5}	Low
287	+	
667	0.0016	
D1585 ^c	1.0	High
D1576 ^c	7.57×10^{-7}	High
D1568 ^c	0.79	
ATCC 13637	1.24×10^{-7}	
SMDP92	7.57×10^{-8}	

^a Where plaque formation was not observed, strains were scored as ++, clearing at 10^{-2} dilution; +, clearing at 10^{-1} dilution; -, no infection (not shown)

^b AXL1 predicted productivity is scored as high when EOP is > 0.5 and low when > 0.001

^c Isolates are from the Canadian *Burkholderia cepacia* complex Research Referral Repository

To analyze infection dynamics of AXL1, a one-step growth curve was conducted. Similar to previously characterized *S. maltophilia* phage AXL3 [115], AXL1 exhibits a long productive cycle having a latent period of approximately 1.5 h and burst size of 58 virions per cell after 5.5 h (Figure 5-2A). Inhibition of bacterial growth in liquid culture by AXL1 produced varying levels of growth reduction with changing multiplicities of infection (MOI). At an MOI of 30, bacterial growth began decreasing at 3.5 h (Figure 5-2B). This growth reduction was delayed with decreasing MOI, with all phage groups showing resistant outgrowths by 20 h. The higher MOIs tested produce greater levels of resistant growth than lower MOIs, likely due to earlier depletion of sensitive bacterial cells by AXL1 and growth of resistant cells without competition

for nutrients. Unexpectedly, AXL1 was ineffective at growth inhibition in liquid culture when the same experiment was conducted at 37°C and unlike *S. maltophilia* phage DLP3 [178], in vivo rescue of *Galleria mellonella* larvae infected with *S. maltophilia* D1585 was not successful at this temperature (data not shown). Assessment of phage activity on solid media at 37°C revealed a decreased EOP of 0.002 relative to plaquing ability on D1585 at 30°C set as an EOP of 1.0 (Table 5-2). Additional type IV pili-binding phages DLP1 and DLP2 [160] do not exhibit weaker infection at 37°C on strain D1585 (data not shown). This drop in infection efficiency is not due to temperature instability of AXL1 phage particles, as virions remained active after incubation for 1 h at temperatures ranging from -20°C to 50°C (Figure 5-3).

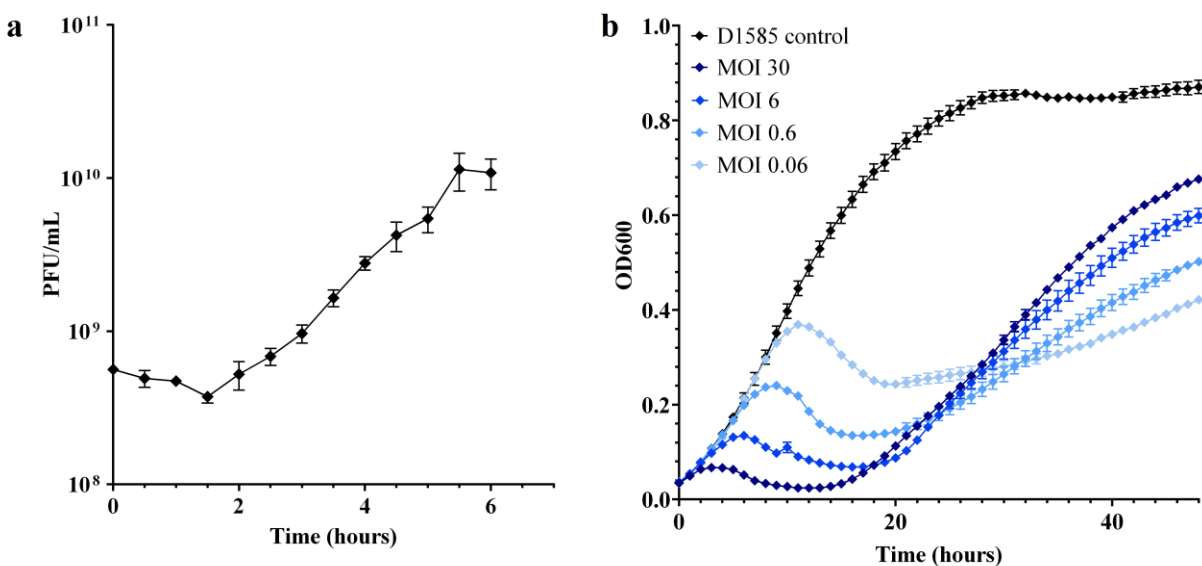


Figure 5-2: Infection dynamics of AXL1 on *S. maltophilia* strain D1585. (A) A one step growth curve of AXL1 at an MOI of 1 shows a latent period of 1.5 h and burst size of approximately 58 virions per cell. (B) Liquid bacterial growth reduction curves were conducted at multiple MOIs over 48 h at 30°C. Data from three biological replicates are plotted as mean \pm SEM. Where error bars are smaller than the size of the symbol, they are not visible.

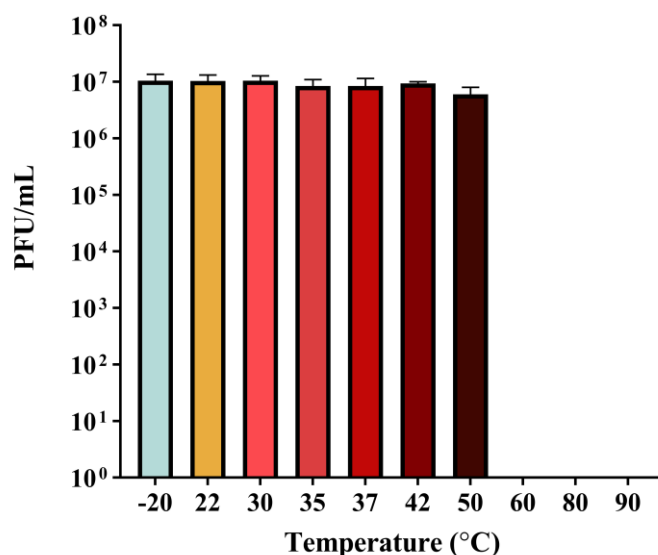


Figure 5-3: Temperature stability of AXL1 virions. AXL1 phage lysate diluted to 10⁷ PFU/mL was incubated at temperatures ranging from -20°C to 90°C for 1 h, followed by serial dilution and calculation of titre by spot assay on *S. maltophilia* D1585 after overnight incubation at 30°C. Bars represent mean titres from three replicates and error bars show standard deviation.

As discussed in Chapter 3, AXL1 binds to the type IV pilus as its host cell surface receptor and requires cell-mediated retraction to bring the bound phage particle to the cell surface for successful infection. Although AXL1 was unable to infect at high efficiency at 37°C and this was not due to temperature instability of the phage particles, decreased host receptor expression was also not involved. The area of the twitching motility zone of host strain D1585 did not change under different temperature conditions. Interestingly, in one *S. maltophilia* strain 213, twitching motility did increase to produce a zone of 122.2 ± 18.4 mm² at 37°C, up from 64.7 ± 12.1 mm² in diameter at 30°C.

Genomic characterization

The AXL1 genome assembled into a single contig 63,692 bp in length (Figure 5-4) with a GC content of 67.3% that is similar to the host *S. maltophilia* GC content. BLASTn analysis of AXL1 showed high relatedness to phages in the genus *Pamexvirus*, most closely aligning to *Xanthomonas* phage Bosa [337] with 91.01% identity over 97% of the genome. Among this genus, in order of percent identity to AXL1, are *Xanthomonas* phage Xp12 [338],

Stenotrophomonas phage DLP4 [114], *Xanthomonas* phage Xoo-sp2 [339], and the *Pseudomonas* phages AAT-1 [340], PaMx28, and PaMx74 [330]. Despite shared nucleotide sequence identity with three *P. aeruginosa* phages and previous observation of cross-taxonomic order infectivity of *S. maltophilia* phages DLP1 and DLP2 [11], AXL1 was incapable of infecting 21 *P. aeruginosa* strains tested. To the contrary, examination of AXL1 infectivity of strains of four *Xanthomonas* species revealed infection of *X. axonopodis* pv. *vasculorum* FB570 at an EOP of 0.03 as compared to infection of *S. maltophilia* D1585. No phage lysis was observed on the *X. oryzae* host strain of related phage Xp12 or *X. translucens* pv. *translucens* ATCC 19319 and *X. campestris* ATCC 33440.

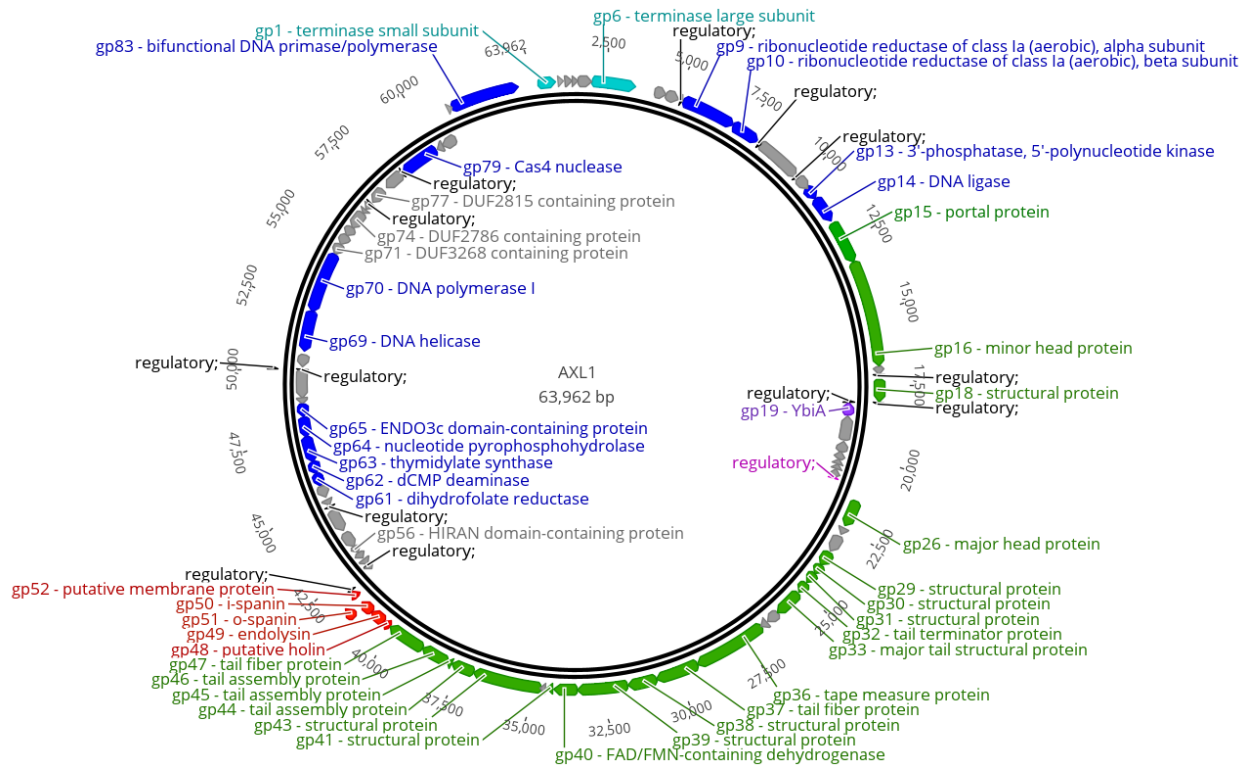


Figure 5-4: Circularized genomic map of AXL1. The scale (in bp) is shown on the outer periphery. Assigned putative functions for each of the 83 predicted open reading frames are classified as follows: lysis (red), DNA replication and repair (blue), DNA packaging (teal), virion morphogenesis (green), hypothetical (grey), moron (purple). Regulatory elements are promoters (pink) and terminators (black). No tRNA genes were identified. AXL1 has a GC content of 67.3%. Image created using Geneious Prime [230].

Comparative genomic analysis of AXL1 with the seven members of the *Pamexvirus* genus shows high relatedness to *Xanthomonas* phages Bosa and Xp12, as well as the *Stenotrophomonas* phage DLP4, whereas *Xanthomonas* phage Xoo-sp2 shares a high percent identity with only half of the morphogenesis proteins (Figure 5-5). The three *Pseudomonas* phages show greater amino acid sequence identity with each other than with the *Stenotrophomonas* and *Xanthomonas* phages. This comparison supports the classification of AXL1 as the eighth member of the *Pamexvirus* genus.

Restriction fragment length polymorphism (RFLP) analysis of the AXL1 genome using 31 restriction enzymes with recognition sequences present in the genome revealed digestion by only five enzymes: *AseI*, *Eam1105I*, *KpnI*, *TasI*, and *TruII* (Figure 5-6). A similar result has been observed for *Xanthomonas* phage Xp12, known to contain 5-methylcytosine in place of all cytosines in its genome [338]; as *AseI*, *TasI*, and *TruII* contain only A/T bases in their recognition sequences, digestion is not impaired by this base modification. Compared to the expected digestion patterns, *Eam1105I* and *KpnI* partially digest the AXL1 genome. For the *Pamexvirus* phages with RFLP analysis, resistance to digestion with some restriction enzymes was also observed for DLP4[114] and PaMx28 and PaMx74 [330].

AXL1 is predicted to encode 83 open reading frames (ORFs) (Figure 5-4, Table 5-3) producing a coding density of approximately 93%. The majority of start codons are ATG (71 out of 83), with fewer GTG and TTG start codons present in 10 and two ORFs, respectively. The stop codon TGA is found in 58 ORFs, with TAA second most abundant in 20 ORFs, and TAG in only five. No standard tRNA genes were detected. Functional predictions based on BLASTp analysis produced significant hits for all 83 putative proteins, however putative functions beyond hypothetical could be assigned for only 37 proteins. The majority of top hits were to *Stenotrophomonas* phage DLP4, having 30 unique hits, and *Xanthomonas* phage Bosa, having 17, with an additional 28 proteins identical between the two phages as noted by the asterisks in Table 5-3. Seven of the remaining proteins shared the highest percent identity with *Xanthomonas* phage Xp12 and only gp5 hit to *Xanthomonas* phage Xoo-sp2. The assigned functions of these proteins place them in distinct modules consisting of those related to DNA replication and repair (blue) or DNA packaging (teal) on the positive and negative strands, virion morphogenesis (green) and lysis (red) on the positive strand, and a small operon of unknown function (purple) on the negative strand containing a gene encoding a YbiA homolog (Figure 5-4).

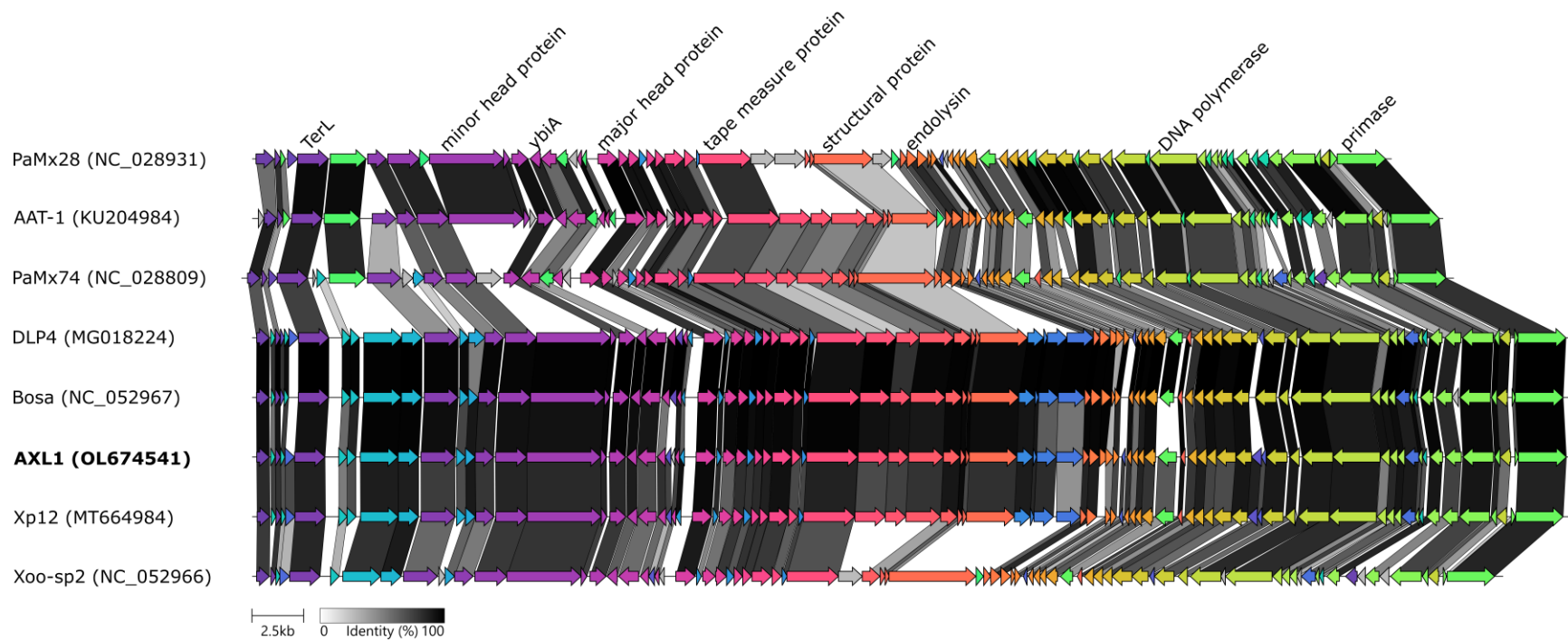


Figure 5-5: Comparative genome alignment of AXL1 and phages of the *Pamexvirus* genus. A linear representation of AXL1 (bold) and seven related phage genomes shows high amino acid sequence identity following analysis with clinker [266]. Arrows represent phage coding sequences coloured to indicate homologous groups and are linked by grey regions, with shading representing percentage amino acid identity. Genome accession numbers are in parentheses for each phage

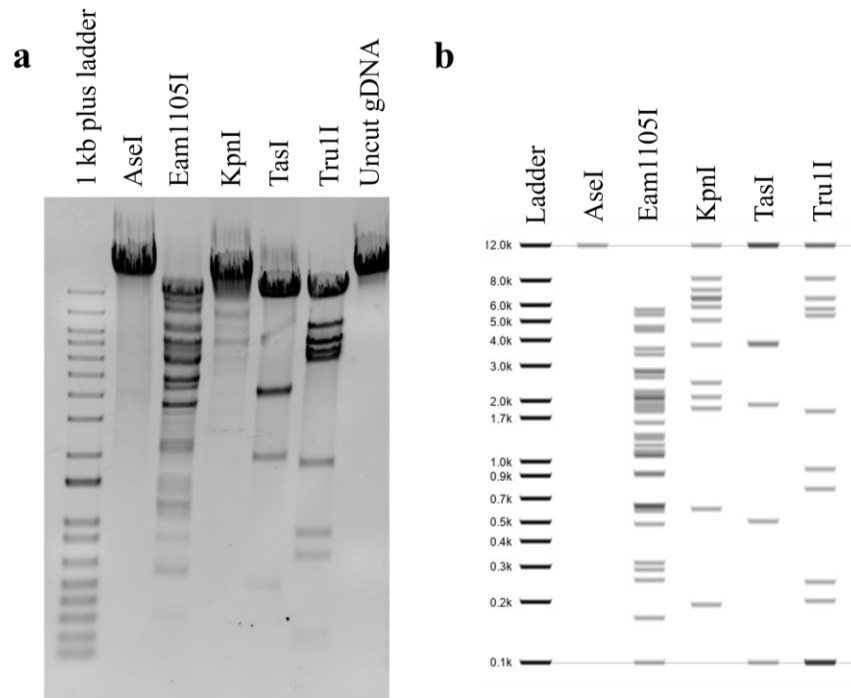


Figure 5-6: Restriction digests of AXL1 gDNA. (A) Agarose gel electrophoresis of AXL1 gDNA following incubation with *AseI*, *TasI*, and *TruII* containing only AT bases in their recognition sites, and *Eam1105I* and *KpnI*. Only one *AseI* cut site is present in the AXL1 genome, resulting in linearization of the genome. (B) A virtual gel created with Geneious [230] shows the expected cleavage pattern of the AXL1 genome in the absence of DNA modification.

The genome sequence of AXL1 with putative annotations has been deposited in Genbank under the accession number OL674541.

DNA replication, repair, and packaging module

There are at least 14 genes encoded in two bi-directional gene clusters in the AXL1 genome involved in DNA replication, processing of nucleotides, and genome packaging (Figure 5-4, Table 5-3). Gene products that could be assigned putative enzymatic functions within the positive stranded region AXL1_1 to AXL1_14 include terminase small subunit (gp1), terminase large subunit (gp6, TerL), ribonucleotide reductase of class 1a (aerobic) alpha (gp9) and beta (gp10) subunits, 3'-phosphatase/5'-polynucleotide kinase (gp13), and DNA ligase (gp14), as well as bifunctional DNA primase/polymerase (gp83). The class 1a ribonucleotide reductase

(RNR) complex composed of gp9 and gp10 contributes to DNA synthesis by catalyzing the reduction of ribonucleosides (NDPs) into their corresponding deoxyribonucleosides (dNDPs) [341].

On the negative strand within AXL1_53 to AXL1_81, putative functional annotations include dihydrofolate reductase (gp61), dCMP deaminase (gp62), thymidylate synthase (gp63), nucleotide pyrophosphohydrolase (gp64), DNA helicase (gp69), DNA polymerase I (gp70), and Cas4 nuclease (gp79). All of these proteins also have conserved domains associated with their assigned functions, except for the small and large terminase subunits (Table 5-4). Similar to *Stenotrophomonas* phages DLP4 and AXL3 are the enzymes involved in the thymidylate synthesis pathway, gp62 and gp63, that function to convert deoxycytidylate (dCMP) into deoxyuridine monophosphate (dUMP), and dUMP into deoxythymidine monophosphate (dTMP), respectively [318,319]. The reductive methylation of dUMP into dTMP relies on the cofactor 5,10-methylenetetrahydrofolate that is converted into dihydrofolate in the process. This cofactor can be regenerated by the function of dihydrofolate reductase, gp61 in AXL1, that reduces dihydrofolate into tetrahydrofolate, which is subsequently processed by serine hydroxymethyltransferase, not encoded by AXL1, into the cofactor for use by thymidylate synthase [342].

Two additional proteins of interest are gp56 that contains a HIRAN domain predicted to bind DNA, helping to resolve stalled replication forks or recognize regions of DNA damage [343], and gp65, a protein found only in the related *Xanthomonas* phage Xp12, containing an ENDO3c domain with an intact minor groove reading motif and helix-hairpin-helix signature motif. This domain is found in endonuclease III enzymes that act in the site-specific repair of DNA damage. However, conserved domain search [265] results showed the absence of the canonical substrate binding pocket and active site motifs, and COFACTOR [336] and COACH [335] analysis based on I-TASSER [334] structural prediction produced an aspartate at position 141 as the putative catalytic site with a confidence score of only 0.33 based on structural similarity with the *Escherichia coli* endonuclease III. Additionally, hypothetical proteins gp71, gp74, and gp77 contain conserved domains of unknown function.

Table 5-3: Genome annotations for AXL1 obtained from BLASTp and CD-search data.

CDS	Coding region	Strand	Length (AA)	Putative function	Hit	Species	Cov. (%)	E-value	Identity (%)	Accession
1	221-838	+	205	terminase small subunit	hypothetical protein	<i>Xanthomonas</i> phage Bosa	100	6.00E-147	96.1	YP_009997078.1
2	901-1119	+	72	hypothetical protein	hypothetical protein	<i>Stenotrophomonas</i> phage DLP4	100	1.00E-34	77.78	ATS92261.1
3	1129-1371	+	80	hypothetical protein	hypothetical protein	<i>Xanthomonas</i> phage Xoo-sp2	100	2.00E-43	80	YP_009996934.1
4	1373-1588	+	71	hypothetical protein	hypothetical protein	<i>Stenotrophomonas</i> phage DLP4	98	3.00E-39	88.57	ATS92262.1
5	1592-2053	+	153	hypothetical protein	RNA pseudouridine synthase	<i>Stenotrophomonas</i> phage DLP4	100	5.00E-86	79.22	ATS92231.1
6	2053-3525	+	490	terminase large subunit	phage terminase, large subunit	<i>Xanthomonas</i> phage Bosa*	100	0.00E+00	94.08	YP_009997003.1 ATS92199.1
7	4189-4590	+	133	hypothetical protein	hypothetical protein	<i>Stenotrophomonas</i> phage DLP4	100	2.00E-63	67.16	ATS92238.1
8	4587-5021	+	144	hypothetical protein	hypothetical protein	<i>Xanthomonas</i> phage Bosa	100	5.00E-80	88.89	YP_009997005.1
9	5231-7051	+	606	ribonucleotide reductase of class Ia (aerobic), alpha subunit	ribonucleotide reductase of class Ia (aerobic), alpha subunit	<i>Xanthomonas</i> phage Bosa	100	0.00E+00	98.68	YP_009997006.1

10	7059-8051	+	330	ribonucleotide reductase of class Ia (aerobic), beta subunit	ribonucleotide reductase of class Ia (aerobic), beta subunit	<i>Xanthomonas</i> phage Bosa*	100	0.00E+00	99.09	YP_009997007.1 ATS92204.1
11	8162-9802	+	546	hypothetical protein	phage protein	<i>Xanthomonas</i> phage Bosa	100	0.00E+00	95.43	YP_009997008.1
12	9872-10327	+	151	hypothetical protein	hypothetical protein	<i>Stenotrophomonas</i> phage DLP4	88	5.00E-76	86.57	ATS92236.1
13	10320-10790	+	156	3'-phosphatase, 5'-polynucleotide kinase	3'-phosphatase, 5'-polynucleotide kinase, phage-associated	<i>Xanthomonas</i> phage Bosa	98	8.00E-106	94.16	YP_009997010.1
14	10790-11683	+	297	DNA ligase	DNA ligase	<i>Stenotrophomonas</i> phage DLP4	100	0.00E+00	91.28	ATS92210.1
15	11769-13280	+	503	portal protein	portal protein	<i>Stenotrophomonas</i> phage DLP4	100	0.00E+00	96.25	ATS92196.1
16	13280-16858	+	1192	minor head protein	phage protein	<i>Xanthomonas</i> phage Bosa	100	0.00E+00	94.04	YP_009997013.1
17	16860-17132	+	90	hypothetical protein	hypothetical protein	<i>Xanthomonas</i> phage Bosa	100	1.00E-56	97.78	YP_009997014.1
18	17276-18061	+	261	structural protein	phage protein	<i>Xanthomonas</i> phage Bosa*	100	0.00E+00	98.85	YP_009997015.1 ATS92213.1
19	18111-18596	-	161	YbiA	uncharacterized protein COG3236	<i>Xanthomonas</i> phage Bosa*	100	2.00E-113	96.89	YP_009997016.1 ATS92227.1

20	18635-19525	-	296	hypothetical protein	hypothetical protein	<i>Xanthomonas</i> phage Bosa*	100	0.00E+00	92.38	YP_009997017.1 ATS92209.1
21	19591-19980	-	129	hypothetical protein	hypothetical protein	<i>Xanthomonas</i> phage Xp12	99	1.00E-74	86.15	QNN97174.1
22	19980-20252	-	90	hypothetical protein	hypothetical protein	<i>Xanthomonas</i> phage Xp12	95	8.00E-46	82.56	QNN97175.1
23	20263-20448	-	61	hypothetical protein	hypothetical protein	<i>Xanthomonas</i> phage Bosa*	78	3.00E-12	54.17	YP_009997019.1 ATS92245.1
24	20448-20660	-	70	hypothetical protein	hypothetical protein	<i>Xanthomonas</i> phage Bosa*	100	2.00E-43	91.43	YP_009997020.1 ATS92263.1
25	20668-20907	-	79	hypothetical protein	hypothetical protein	<i>Stenotrophomonas</i> phage DLP4	100	1.00E-52	98.73	ATS92254.1
26	21470-22402	+	310	major head protein	hypothetical protein	<i>Xanthomonas</i> phage Bosa*	100	0.00E+00	99.03	YP_009997022.1 ATS92208.1
27	22470-22703	+	77	hypothetical protein	hypothetical protein	<i>Xanthomonas</i> phage Bosa*	100	6.00E-36	93.51	YP_009997023.1 ATS92256.1
28	22770-23381	+	203	hypothetical protein	phage protein	<i>Xanthomonas</i> phage Bosa*	100	9.00E-145	97.54	YP_009997024.1 ATS92221.1
29	23403-23927	+	174	structural protein	putative virion structural protein	<i>Stenotrophomonas</i> phage DLP4	100	4.00E-124	100	ATS92224.1
30	23929-24297	+	122	structural protein	JK_22P	<i>Xanthomonas</i> phage Bosa*	100	2.00E-80	96.72	YP_009997026.1 ATS92243.1
31	24299-24691	+	130	structural protein	phage protein	<i>Xanthomonas</i> phage Bosa*	100	8.00E-91	99.23	YP_009997027.1 ATS92239.1

32	24704- 25126	+	140	tail terminator protein	hypothetical protein	<i>Xanthomonas</i> phage Bosa	100	4.00E -99	97.86	YP_009997028.1
33	25149- 26090	+	313	major tail structural protein	phage protein	<i>Xanthomonas</i> phage Bosa*	100	0.00E +00	98.08	YP_009997029.1 ATS92207.1
34	26093- 26542	+	149	hypothetical protein	hypothetical protein	<i>Xanthomonas</i> phage Bosa*	89	1.00E -89	96.27	YP_009997030.1 ATS92234.1
35	26581- 26826	+	81	hypothetical protein	hypothetical protein	<i>Xanthomonas</i> phage Bosa*	100	1.00E -51	98.77	YP_009997031.1 ATS92252.1
36	26807- 29287	+	826	tape measure protein	phage tail length tape-measure protein 1	<i>Xanthomonas</i> phage Bosa	100	0.00E +00	98.67	YP_009997032.1
37	29303- 30757	+	484	tail fiber protein	tail fiber protein	<i>Stenotrophomonas</i> phage DLP4	100	0.00E +00	94.83	ATS92200.1
38	30763- 31743	+	326	structural protein	phage protein	<i>Xanthomonas</i> phage Bosa	100	0.00E +00	93.27	YP_009997034.1
39	31745- 33427	+	560	structural protein	putative virion structural protein	<i>Stenotrophomonas</i> phage DLP4	100	0.00E +00	92.68	ATS92194.1
40	33427- 34239	+	270	FAD/FMN-containing dehydrogenase	putative FAD/FMN- containing dehydrogenase	<i>Stenotrophomonas</i> phage DLP4	100	0.00E +00	98.52	ATS92211.1
41	34252- 34485	+	77	structural protein	putative virion structural protein	<i>Stenotrophomonas</i> phage DLP4	100	1.00E -49	100	ATS92255.1
42	34509- 34685	+	58	hypothetical protein	hypothetical protein	<i>Stenotrophomonas</i> phage DLP4	100	2.00E -35	100	ATS92264.1

43	34672-36987	+	771	structural protein	putative virion structural protein	<i>Stenotrophomonas</i> phage DLP4	100	0.00E+00	97.92	ATS92192.1
44	36987-37766	+	259	tail assembly protein	tail assembly protein	<i>Stenotrophomonas</i> phage DLP4	100	3.00E-170	93.44	ATS92214.1
45	37770-37934	+	54	tail assembly protein	hypothetical protein	<i>Xanthomonas</i> phage Bosa*	100	2.00E-20	94.44	YP_009997041.1 ATS92269.1
46	37945-38889	+	314	tail assembly protein	hypothetical protein	<i>Xanthomonas</i> phage Xp12	100	0.00E+00	85.99	QNN97198.1
47	38892-40181	+	429	tail fiber protein	tail fiber protein	<i>Stenotrophomonas</i> phage DLP4	99	0.00E+00	62.88	ATS92201.1
48	40181-40483	+	100	putative holin	hypothetical protein	<i>Xanthomonas</i> phage Bosa*	99	1.00E-67	100	YP_009997044.1 ATS92246.1
49	40480-40974	+	164	endolysin	phage endolysin	<i>Xanthomonas</i> phage Bosa	100	4.00E-115	98.17	YP_009997045.1
50	40985-41461	+	158	i-spanin	i-spanin	<i>Stenotrophomonas</i> phage DLP4	100	2.00E-108	100	ATS92228.1
51	41274-41645	+	124	o-spanin	o-spanin	<i>Stenotrophomonas</i> phage DLP4	100	1.00E-64	93.55	ATS92242.1
52	41642-41917	+	91	putative membrane protein	phage protein	<i>Xanthomonas</i> phage Bosa*	100	1.00E-55	90.11	YP_009997048.1 ATS92249.1
53	42049-42225	-	58	hypothetical protein	hypothetical protein	<i>Stenotrophomonas</i> phage DLP4	100	9.00E-29	87.93	ATS92267.1
54	42293-42523	-	76	hypothetical protein	hypothetical protein	<i>Xanthomonas</i> phage Bosa*	100	4.00E-48	96.05	YP_009997049.1 ATS92257.1

55	42550-42840	-	96	hypothetical protein	hypothetical protein	<i>Xanthomonas</i> phage Xp12	100	8.00E-35	65.62	QNN97206.1
56	42824-43129	-	101	HIRAN domain-containing protein	HIRAN domain-containing protein	<i>Stenotrophomonas</i> phage DLP4	100	2.00E-65	92.08	ATS92247.1
57	43129-43686	-	185	hypothetical protein	hypothetical protein	<i>Xanthomonas</i> phage Bosa*	100	1.00E-110	95.68	YP_009997052.1 ATS92222.1
58	43809-44696	-	295	hypothetical protein	hypothetical protein	<i>Xanthomonas</i> phage Xp12	99	2.00E-154	73.31	QNN97209.1
59	44895-45119	-	74	hypothetical protein	hypothetical protein	<i>Xanthomonas</i> phage Bosa*	100	1.00E-47	100	YP_009997054.1 ATS92260.1
60	45242-45688	-	148	hypothetical protein	hypothetical protein	<i>Stenotrophomonas</i> phage DLP4	100	4.00E-100	96.62	ATS92232.1
61	45673-46161	-	162	dihydrofolate reductase	hypothetical protein	<i>Xanthomonas</i> phage Xp12	100	6.00E-105	90.74	QNN97212.1
62	46146-46622	-	158	dCMP deaminase	dCMP deaminase	<i>Xanthomonas</i> phage Bosa*	100	4.00E-110	95.57	YP_009997057.1 ATS92229.1
63	46622-47563	-	313	thymidylate synthase	thymidylate synthase	<i>Stenotrophomonas</i> phage DLP4	100	0.00E+00	94.57	ATS92206.1
64	47560-48333	-	257	nucleotide pyrophosphohydrolase	hydrolase (HAD superfamily)	<i>Xanthomonas</i> phage Bosa*	100	0.00E+00	95.72	YP_009997059.1 ATS92216.1
65	48326-48808	-	160	ENDO3c containing protein	hypothetical protein	<i>Xanthomonas</i> phage Xp12	100	9.00E-100	90	QNN97216.1
66	48805-49035	-	76	hypothetical protein	hypothetical protein	<i>Stenotrophomonas</i> phage DLP4	100	8.00E-42	89.47	ATS92258.1

67	49038-50057	-	339	hypothetical protein	hypothetical protein	<i>Xanthomonas</i> phage Bosa*	100	0.00E+00	97.05	YP_009997060.1 ATS92203.1
68	50172-50636	-	154	hypothetical protein	hypothetical protein	<i>Stenotrophomonas</i> phage DLP4	100	2.00E-95	96.1	ATS92230.1
69	50784-52262	-	492	DNA helicase	DNA helicase, phage-associated	<i>Xanthomonas</i> phage Bosa*	100	0.00E+00	97.97	YP_009997062.1 ATS92197.1
70	52259-54544	-	761	DNA polymerase I	DNA polymerase	<i>Stenotrophomonas</i> phage DLP4	99	0.00E+00	95.9	ATS92189.1
71	54570-55010	-	146	DUF3268 containing protein	phage protein	<i>Xanthomonas</i> phage Bosa	100	1.00E-94	95.21	YP_009997064.1
72	55007-55396	-	129	hypothetical protein	hypothetical protein	<i>Xanthomonas</i> phage Bosa*	100	1.00E-84	95.35	YP_009997065.1 ATS92240.1
73	55393-55737	-	114	hypothetical protein	hypothetical protein	<i>Xanthomonas</i> phage Bosa*	100	6.00E-76	96.49	YP_009997066.1 ATS92244.1
74	55734-56417	-	227	DUF2786 containing protein	hypothetical protein	<i>Stenotrophomonas</i> phage DLP4	100	4.00E-147	91.63	ATS92217.1
75	56407-56589	-	60	hypothetical protein	hypothetical protein	<i>Stenotrophomonas</i> phage DLP4	100	6.00E-36	98.33	ATS92265.1
76	56604-56798	-	64	hypothetical protein	hypothetical protein	<i>Xanthomonas</i> phage Bosa	100	3.00E-31	87.5	YP_009997069.1
77	56952-57569	-	205	DUF2815 containing protein	phage protein	<i>Xanthomonas</i> phage Bosa	100	9.00E-145	98.05	YP_009997070.1
78	57702-58481	-	259	hypothetical protein	hypothetical protein	<i>Stenotrophomonas</i> phage DLP4	100	0.00E+00	96.14	ATS92215.1

79	58553-60031	-	492	Cas4 nuclease	phage protein	<i>Xanthomonas</i> phage Bosa	100	0.00E+00	97.56	YP_009997073.1
80	60081-60344	-	87	hypothetical protein	hypothetical protein	<i>Xanthomonas</i> phage Bosa*	100	1.00E-56	97.7	YP_009997074.1 ATS92251.1
81	60341-60862	-	173	hypothetical protein	hypothetical protein	<i>Xanthomonas</i> phage Bosa	100	3.00E-78	81.71	YP_009997075.1
82	61064-61237	+	57	hypothetical protein	hypothetical protein	<i>Stenotrophomonas</i> phage DLP4	91	2.00E-27	96.15	ATS92268.1
83	61234-63555	+	773	bifunctional DNA primase/polymerase	bifunctional DNA primase/polymerase	<i>Xanthomonas</i> phage Bosa	100	0	99.48	YP_009997077.1

* Identical protein sequence between *Xanthomonas* phage Bosa and *Stenotrophomonas* phage DLP4. Both accession numbers reported.

Table 5-4: The conserved domains found in 83 AXL1 proteins.

Gp	Hit type	PSSM-ID	Interval	E-Value	Accession	Short name	Superfamily
9	superfamily	236378	4-605	0	cl35765	PRK09102 superfamily	-
10	specific	236591	17-329	4.85E-107	PRK09614	nrdF	cl00264
13	superfamily	419670	4-156	6.11E-26	cl21460	HAD_like superfamily	-
14	superfamily	416404	5-183	2.73E-30	cl12015	Adenylation_DNA_ligase_like superfamily	-
14	superfamily	415534	225-292	1.34E-12	cl08424	OBF_DNA_ligase_family superfamily	-
15	specific	404196	260-395	1.15E-41	pfam13264	DUF4055	cl16196

16	superfamily	415838	145-259	2.33E-18	cl10072	Phage_Mu_F superfamily	-
16	superfamily	412198	1027-1190	2.82E-15	cl00173	VIP2 superfamily	-
19	specific	271319	8-155	4.75E-68	cd15457	NADAR	cl21532
26	superfamily	421447	62-201	0.00225904	cl27082	Phage_capsid superfamily	-
32	superfamily	404444	9-133	7.52E-16	cl16303	DUF4128 superfamily	-
33	specific	408676	4-255	1.12E-47	pfam18906	Phage_tube_2	cl40912
36	superfamily	375164	367-648	8.84E-10	cl38662	DUF5401 superfamily	-
36	superfamily	226450	21-272	2.92E-07	cl34696	HI1514 superfamily	-
37	superfamily	419973	83-178	0.00598795	cl23730	F5_F8_type_C superfamily	-
40	specific	401340	189-259	1.80E-20	pfam09356	Phage_BR0599	cl110710
40	superfamily	274038	18-269	1.02E-15	cl37077	phg_TIGR02218 superfamily	-
43	superfamily	404441	223-392	1.98E-09	cl38419	Phage-tail_3 superfamily	-
44	superfamily	421990	13-51	7.48E-06	cl31489	Mtd_N superfamily	-
47	specific	398814	192-242	2.16E-06	pfam05345	He_PIG	cl40844
49	specific	350620	9-159	1.48E-23	cd14845	L-Ala-D-Glu_peptidase_like	cl38918
56	specific	400928	5-85	9.59E-14	pfam08797	HIRAN	cl07418
61	superfamily	418440	6-123	1.74E-16	cl17279	DHFR superfamily	-
62	superfamily	412274	13-121	4.33E-32	cl00269	cytidine_deaminase-like superfamily	-
63	specific	238211	25-259	1.04E-44	cd00351	TS_Pyrimidine_HMase	cl19097
64	superfamily	418386	24-136	2.42E-25	cl16941	NTP-PPase superfamily	-

65	superfamily	419995	36-123	3.60E-10	cl23768	ENDO3c superfamily	-
69	specific	350180	332-448	6.84E-19	cd18793	SF2_C_SNF	cl38915
69	specific	223627	32-475	1.24E-15	COG0553	HepA	cl33945
70	superfamily	413410	316-760	8.02E-86	cl02626	DNA_pol_A superfamily	-
71	superfamily	403009	19-133	2.75E-25	cl13172	DUF3268 superfamily	-
74	specific	402523	8-46	1.96E-05	pfam10979	DUF2786	cl12553
77	specific	402534	11-187	2.17E-49	pfam10991	DUF2815	cl29140
79	superfamily	412491	1-470	8.62E-46	cl00641	Cas4_I-A_I-B_I-C_I-D_II-B superfamily	-
83	specific	401258	14-178	1.83E-25	pfam09250	Prim-Pol	cl01287
83	specific	400859	209-275	2.08E-10	pfam08707	PriCT_2	cl07361

Structural proteins within the virion morphogenesis module

The virion morphogenesis module includes 26 genes spanning AXL1_15 to AXL1_47 on the positive strand, however this module is interrupted by an operon containing six genes, AXL1_19 to AXL1_25, in the reverse orientation that is described below. The gene products for 20 of the 26 genes could be assigned function based on BLASTp comparisons (Figure 5-4, Table 5-3). Proteins involved in capsid assembly and packaging include portal protein (gp15), minor head protein (gp16), and major head protein (gp26). 17 proteins identified as structural proteins in phage assembly and tail morphogenesis include seven virion structural proteins (gp18, gp29-31, gp38, gp39, gp41), tail terminator protein (gp32), major tail structural protein (gp33), tape measure protein (gp36), tail fiber protein (gp37), FAD/FMN-containing dehydrogenase (gp40), central tail hub protein (gp43), three tail assembly proteins (gp44-46), and tail fiber protein (gp47). Proteomic analysis of CsCl-purified AXL1 virions by HPLC-MS confirmed 17 of the above proteins as virion-associated, in addition to the hypothetical protein gp27; below the limit of detection were gp18, gp41, and gp45 (Table 5-5). The most abundant virion protein identified, and the only band evident in SDS-PAGE, is the major head protein, gp26, an estimated 32.5 kDa protein. Interestingly, a single *S. maltophilia* protein, bacterioferritin, was identified in the AXL1 sample by the presence of two peptides after analysis against D1585 proteins (Table 5-5).

In general, the largest gene in Siphoviridae phage genomes encodes the tape measure protein [327], which determines the length of the phage tail. In AXL1 however, this gene is second in length to AXL1_16 encoding the putative minor head protein. A conserved domain search of this protein revealed a Phage_Mu_F domain at the N-terminal end of the protein that is commonly found in head morphogenesis proteins of phages, as well as an unexpected VIP2 domain at the C-terminal end that is found in actin-ADP-ribosylating toxins such as *Clostridium botulinum* C2 toxin and *C. difficile* toxin [344] (Table 5-4). The function of this protein in AXL1 infection is unknown, however polyvalent proteins containing MuF and VIP2 domains have been identified in phages infecting *Microbacterium* [345] and are overrepresented in prophages of Firmicutes in the gut microbiota [346]. In *E. coli* phage T4, the ADP-ribosylating protein Alt is packaged in the phage capsid and injected into the bacterial cell with the phage genome where Alt ADP-ribosylates the host RNA polymerase to commandeer it for transcription of viral genes [347]. A search of the Virulence Factor Database (VFDB) [348] also showed similarity of the C-terminus of AXL1 gp16 with T3SS and T4SS effector proteins with ADP ribosyltransferase

activity. In the *Pamexvirus* phages, only *Pseudomonas* phage PaMx74 lacks this VIP2 domain fused to its minor head protein (Figure 5-5). The enzymatic function of this fusion protein in AXL1 virion morphogenesis or during phage replication to alter phage gene expression is unknown.

Within the tail morphogenesis proteins, numerous proteins of interest stand out as potential receptor binding proteins for virion interaction with the type IV pilus. Located between the tape measure protein and lysis module, gp37 to gp47 comprise the distal tail tip proteins and show amino acid sequence identity to known type IV pili binding phages. Specifically, gp44 shared nearly 100% query coverage with type IV pili binding *S. maltophilia* phages DLP3 [178] and DLP4 [114] and *Xylella* phages Sano and Salvo [281]. A conserved domain search revealed a major tropism determinant N-terminal (Mtd_N) domain (Table 5-4) found in the major tropism determinant (Mtd) protein known to determine receptor binding in *Bordetella* phage BPP-1 [349]. Conserved domain searches also revealed a phage-tail_3 domain in the structural protein gp43; this domain is present in the central tail hub or major baseplate proteins of numerous type IV pili binding phages that infect *Stenotrophomonas*, *Xylella*, and *Pseudomonas* and is hypothesized to play a role in receptor binding [115,160]. Further research is ongoing to determine the function of these putative receptor binding proteins in host recognition.

YbiA operon

The genes AXL1_19 to AXL1_25 encoded on the negative strand that disrupt the virion morphogenesis module are expressed from a promoter 58 bp upstream of AXL1_25 (Figure 5-4). This operon includes seven genes encoding hypothetical proteins with unknown function and a YbiA homolog (AXL1_19) shown to play a role in swarming motility in *E. coli* [350]. A similar protein is present in all members of the *Pamexvirus* genus except PaMx74 (Figure 5-5), and although swarming motility capability has not been confirmed in *S. maltophilia*, including our host strain D1585, the *ybiA* gene from *Stenotrophomonas* phage DLP4 was experimentally determined to complement swarming motility in an *E. coli ybiA* insertional mutant [114]. No change in swarming was observed in *S. maltophilia* D1585 expressing the DLP4 *ybiA* gene [114].

Table 5-5: Virion-associated proteins identified by proteomic analysis of CsCl-purified AXL1 virions.

AXL1 gp	Function	Score	Coverage (%)	Peptides ^a	PSMs	AAs	MW (kDa)	Calculated pI
26	Major head protein	1012.15	74.52	18	703	310	32.5	4.97
36	Tape measure protein	175.11	57.38	41	130	826	89.9	4.97
15	Portal protein	168.38	52.88	21	109	503	55.6	4.65
33	Major tail structural protein	152.18	41.21	14	143	313	33.5	4.96
16	Minor head protein	125.96	47.99	48	117	1192	126.7	9.17
43	Structural protein	91.14	35.15	18	56	771	82.6	5.14
46	Tail assembly protein	88.19	34.71	7	54	314	33.4	7.03
39	Structural protein	72.37	49.82	18	49	560	62.0	5.49
29	Structural protein	70.64	57.47	10	41	174	18.5	6.71
38	Structural protein	49.98	32.52	10	43	326	35.8	6.23
37	Tail fiber protein	42.50	35.12	10	39	484	53.4	5.44
44	Tail assembly protein	14.90	21.24	5	10	259	27.7	4.70
32	Tail terminator protein	12.36	35.00	4	12	140	15.1	6.55
40	FAD/FMN-containing dehydrogenase	6.01	31.85	6	7	270	29.6	7.39
31	Structural protein	5.67	26.92	3	5	130	14.4	10.26
27	Hypothetical protein	4.11	36.36	2	6	77	8.0	5.01
47	Tail fiber protein	4.00	17.72	4	4	429	44.5	5.10
30	Structural protein	1.73	6.56	1	3	122	13.3	4.50
<i>S. maltophilia</i> D1585								
Bfr 2	Bacterioferritin	4.22	14.1	2	2	156	18.1	4.86

^aAll peptides identified are unique

Although originally identified to play a role in swarming motility, recent research describes the NADAR and COG3236 domains found in the structurally related *E. coli* YbiA protein to putatively function in ADP ribose metabolism based on clustering with related genes [351] and was experimentally shown to function as an N-glycosidase in riboflavin biosynthesis [352]. The absence of putative functions or conserved domains in neighbouring genes in this operon limit predictions for the classification of the AXL1 YbiA-like protein, however structural predictions by I-TASSER analysis produced high structural homology to the *E. coli* YbiA protein, with a TM-score of 0.902 and 0.913 coverage. Additionally, catalytic residues identified to be essential for hydrolysis of N-glycosidic bonds [352] are conserved indicating enzymatic function. The function of this operon in phage replication is unknown; in *S. maltophilia*, the *ybiA*-like gene is located between genes encoding a transketolase and acetyl-CoA hydrolase, however in the D1585 host for AXL1, this *ybiA* gene is absent.

Lysis module

Similar to *S. maltophilia* phage DLP4, the AXL1 lysis module contains five genes, AXL1_48 to AXL1_52, directly downstream of the virion morphogenesis module (Figure 5-4). BLASTp results combined with Lipop 1.0 and TMHMM analyses to identify lipoproteins and transmembrane domains, respectively, provide putative functional roles of these proteins in cell lysis. The first gene in this module encodes a putative holin, gp48, based on the presence of two transmembrane domains [353]. The insertion of canonical holin proteins in the cytoplasmic membrane create pores upon activation that allow phage endolysin to enter the periplasm and degrade the peptidoglycan [353]. In AXL1, the endolysin gp49 contains a conserved L-alanyl-D-glutamate peptidase domain identified by CD-Search (Table 5-4) that cleaves between the L-alanine and D-glutamate residues of the peptidoglycan cell wall. For complete cell lysis to occur, phage spanin proteins form a complex to disrupt the outer membrane [192]. In AXL1, the i-spanin, gp50, contains a predicted N-terminal transmembrane domain that anchors the protein in the cytoplasmic membrane where it can span the periplasm to interact with the o-spanin localized in the outer membrane. Encoded by a gene overlapping the i-spanin coding sequence, gp51 putatively functions as the o-spanin based on the presence of a predicted lipoprotein signal peptide II cleavage site located between amino acids 32 and 33. The final gene in this module

encodes a protein with a single transmembrane domain at the N-terminus, however its role in cell lysis is unknown.

Lifestyle analysis

Based on high sequence identity with the temperate *Stenotrophomonas* phage DLP4, we sought to isolate AXL1 lysogens to confirm its temperate lifestyle. Using the primary host strain, D1585, phage resistant colonies were isolated and tested for the presence of viral DNA using AXL1 specific primers. AXL1-positive colonies were isolated on few occasions and did not maintain AXL1 as a stable prophage. Attempts to isolate stable lysogens of strain 213 were also unsuccessful. Due to the low lytic phage production observed at 37°C, we hypothesized that AXL1 may lysogenize more stably at this temperature, as some *Burkholderia* tropical phages have been shown to have temperature-dependent lifestyles [354,355]. However, this was not the case for AXL1. It is possible that AXL1 cannot stably integrate into the host genomes tested under lab conditions in rich media. However, the genome of AXL1, as well as all *Pamexvirus* genomes, lacks any identifiable lysogeny-associated repressor or integrase genes, which is indicative of virulent phages. BLASTn analysis of the AXL1 genome against Gamma proteobacteria (taxid:1236) also produced no significant results with query coverage greater than 3%, suggesting a lack of remnants of AXL1 as prophage elements in bacterial genomes.

AXL1-encoded DHFR contributes to host resistance to trimethoprim

Dihydrofolate reductase is an essential enzyme in folate metabolism required for the synthesis of DNA and bacterial growth and is also the target of the antibiotic trimethoprim in bacteria. Trimethoprim binds to and inhibits the enzymatic activity of dihydrofolate reductase, preventing the conversion of dihydrofolate into tetrahydrofolate, the active form of folic acid that is required for the synthesis of thymidine [356]. We therefore sought to examine the function of the AXL1-encoded dihydrofolate reductase (gp61, DHFR) in providing resistance to trimethoprim in the *S. maltophilia* host. Putative DHFR enzymes are encoded by all eight viruses of the *Pamexvirus* genus, with varying degrees of sequence identity to the AXL1 protein ranging from approximately 91% identity with *Xanthomonas* phage Xp12 to 44% identity with *Pseudomonas* phage PaMx28. Despite the known role of DHFR in antibiotic resistance, the possible contribution of these phage-encoded enzymes to host antimicrobial resistance was only

examined in *S. maltophilia* phage DLP4 where we found a significant increase in bacterial resistance to high concentrations of trimethoprim in a D1585::DLP4 lysogen compared to the wildtype bacterial host, as well as in *E. coli* expressing the DLP4 *dhfr* gene compared to an empty vector control [114]. We conducted a similar experiment to test the function of AXL1 *dhfr* in promoting resistance to trimethoprim in *E. coli* DH5 α ; minimum inhibitory concentration (MIC) assays with *E. coli* carrying the AXL1 *dhfr* gene on a plasmid resulted in a significant increase in growth in the presence of trimethoprim, with the MIC greater than 256 μ g/mL compared to the empty vector control strain having an MIC of less than 1 μ g/mL (Table 5-6). These results indicate that the AXL1 DHFR variant is less vulnerable to inhibition by trimethoprim than the *E. coli* dihydrofolate reductase protein and may play a role in increasing antibiotic resistance in its native bacterial host.

Table 5-6: Minimum inhibitory concentrations (MICs) of trimethoprim (μ g/mL) in *E. coli* DH5 α and *S. maltophilia* clinical isolates expressing AXL1 *dhfr* in the presence of 32 μ g/mL sulfamethoxazole.

Strain	MIC		Fold increase
	+ pBBR1MCS	+ pAXL1 <i>dhfr</i>	
<i>E. coli</i> DH5 α ^a	<1	>256	>256
D1585	512	512	0
D1571	2	128	64
280	128	>512	>4
SMDP92	128	>512	>4
ATCC13637	32	256	8

^a Trimethoprim MIC determined without added sulfamethoxazole

In *S. maltophilia*, resistance to trimethoprim is naturally high due to chromosomally encoded efflux pumps SmeDEF, SmeOP, and SmeYZ, and this resistance is rising worldwide with the spread of trimethoprim insensitive dihydrofolate reductase *dfrA* genes encoded on integrons [100,217]. In a subset of our *S. maltophilia* collection, in the four strains with genome sequencing data, a gene encoding dihydrofolate reductase type III (*dhfrIII*, *dfrA3*) was found directly downstream of *thyA* encoding thymidylate synthase. These *dfrA3* genes contribute to the

high intrinsic resistance to trimethoprim observed in our lab, with all strains tested having an MIC to trimethoprim of 256 µg/mL or greater (Figure 5-7). Because of the intrinsic resistance to trimethoprim observed in clinical *S. maltophilia* samples, the current recommended treatment is a combination of trimethoprim and sulfamethoxazole. Although functionally similar, the AXL1 DHFR protein shares only a maximum of 24.5% identity with the *S. maltophilia* DfrA3 proteins in our strains, and BLASTn analysis reveals no significant hits to genes outside of the *Pamexvirus dhfr* gene, suggesting an unknown origin. To determine the contribution of the AXL1-encoded dihydrofolate reductase to its host's ability to survive in the presence of trimethoprim, we conducted checkerboard assays containing increasing concentrations of trimethoprim and sulfamethoxazole on five *S. maltophilia* strains carrying the AXL1 *dhfr* gene on a plasmid and compared the MICs to their corresponding empty vector controls. Under the conditions tested, only two strains, D1585 and D1571, had detectable MICs to trimethoprim alone; in D1585, the expression of AXL1 *dhfr* increased the MIC of trimethoprim from 256 µg/mL to 512 µg/mL and in D1571, the MIC increased from 512 µg/mL to >512 µg/mL (Figure 5-7).

In all strains examined except D1585, the addition of sulfamethoxazole effectively reduced the concentration of trimethoprim required to inhibit bacterial growth beyond what was required alone, as expected for these synergistic antibiotics [357] (Figure 5-7). Examination of the trimethoprim concentration required to reduce bacterial growth to below 10% of the solvent control in the presence of 32 µg/mL sulfamethoxazole shows a substantial increase in MIC for most strains expressing AXL1 *dhfr*, with fold changes ranging from zero for D1585 to a 64-fold increase for D1571 (Table 5-6). These results support the conclusion that AXL1 encodes a functional dihydrofolate reductase enzyme that is capable of increasing resistance to a clinically relevant antibiotic combination in its native host.

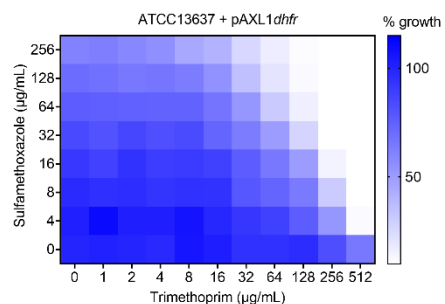
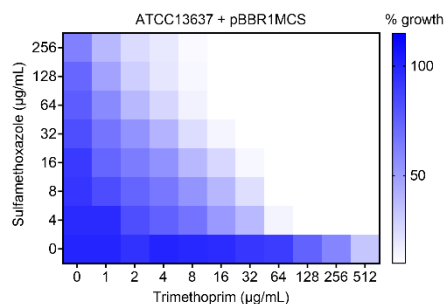
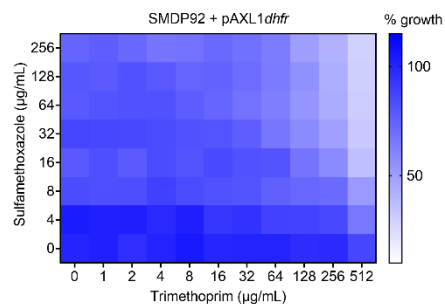
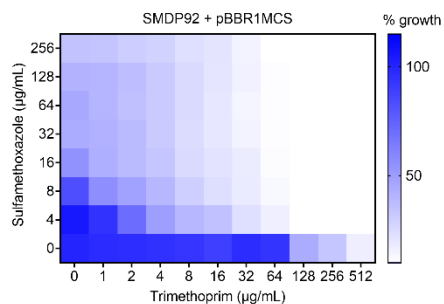
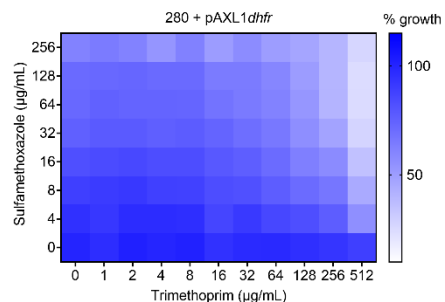
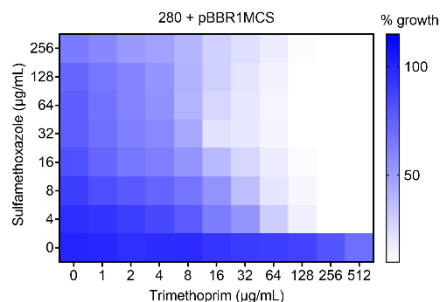
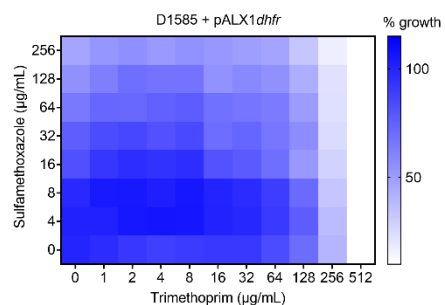
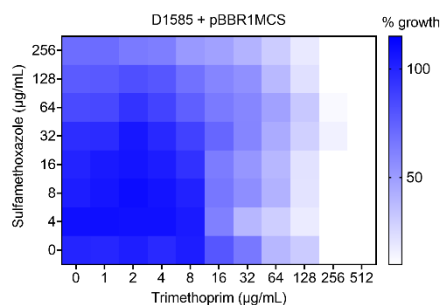
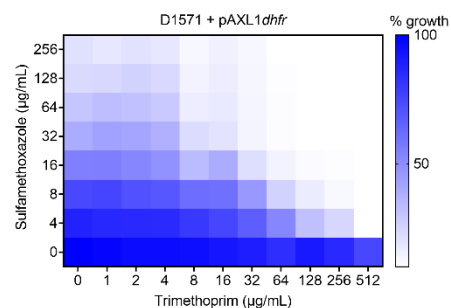
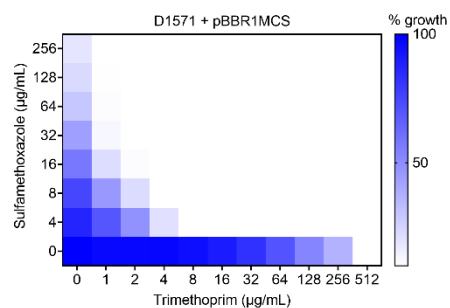


Figure 5-7: AXL1-encoded dihydrofolate reductase functions to increase trimethoprim resistance in *S. maltophilia* in the presence of sulfamethoxazole. Colour intensity represents percent bacterial growth normalized to the solvent treated controls, with growth below 10% shown as white. Strain names are shown above each checkerboard, with pBBR1MCS representing the empty vector control in the left-hand panels and pAXL1*dhfr* representing the AXL1 dihydrofolate reductase gene on the same plasmid in the right-hand panels. Checkerboards were conducted in biological triplicate, with the average of the replicates shown.

Discussion

The genomic and functional characterization of *S. maltophilia* phage AXL1 identifies the eighth member of the genus *Pamexvirus* based on the high degree of sequence identity with the previously characterized *S. maltophilia* phage DLP4 and phages that infect the nosocomial pathogen *P. aeruginosa* and species of agricultural crop pathogens in the genus *Xanthomonas*. Host range analysis indicates that AXL1 infects a moderate range of *S. maltophilia* strains, however high EOP associated with productive phage infection was observed for only half of the isolates (Table 5-2). For strains with apparent non-productive phage infection, 102, 103, 282, 287, D1576, ATCC13637, and SMDP92, these may be observations of abortive infection and/or lysis from without [260,270,358] where AXL1 is not actively replicating within the host but is still capable of binding to the bacterial cell surface and affecting bacterial survival at a high multiplicity of infection (MOI). Bacterial internal phage defense mechanisms that block phage infection, such as restriction/modification systems, may also vary between strains and upregulation of such phage defense mechanisms could account for the reduced plating efficiency of AXL1 observed at 37 °C. However, because previously characterized pili-binding phages do not exhibit this temperature sensitivity when infecting strain D1585, this suggests there is something lacking in the AXL1 genome for intracellular replication at 37°C.

Our results show that this phage binds to the major pilin subunit of host type IV pili and requires cellular-mediated pilus retraction to reach the cell surface for successful infection. *S. maltophilia*, along with many *Xanthomonas* and *Xylella* species within the *Xanthomonadaceae* family [272], encode two neighbouring major pilin genes, whereas type IV pili in other well-studied pathogens encode a single *pilA* gene. The role of *pilA2* in these bacteria is unknown, as deletion of *pilA1* is sufficient to abolish twitching motility [160], as well as phage infection in *S.*

maltophilia, as shown in Chapter 3. The frequent use of the type IV pilus as a receptor for infection of *S. maltophilia* by phages isolated from soil suggests a key role for the pilus for survival in the environment and pathogenesis in humans [217]. Although AXL1 was isolated on *S. maltophilia*, comparable phage production was observed on *X. axonopodis* pv. *vasculorum* strain FB570. Given the similarities in type IV pili architecture and environmental niches of *S. maltophilia* and *Xanthomonas* species [272], this ability to infect across host species would be evolutionarily advantageous for phage proliferation in the environment. Few studies have examined *Xanthomonas* as a potential host for *S. maltophilia* phages; despite genomic similarity of *S. maltophilia* phage Smp131 to prophages of *Xanthomonas* strains, Smp131 was unable to infect any of the 59 *Xanthomonas* strains of seven pathovars tested [176]. Previous research by Lee et al. however identified strong lytic activity of *Xanthomonas oryzae* phage ϕ Xo411 encoded lysozyme against *S. maltophilia* [193]. Although AXL1 was unable to infect any of the 21 *P. aeruginosa* strains tested, the ability to cause cell lysis in PA01 expressing the D1585 *pilA1* gene (Figure 3-1B) suggests that there are no intracellular blocks to infection and with a compatible surface receptor, cross taxonomic order infection may also occur. Comparative genome analysis of AXL1 to phages of the *Pamexvirus* genus shows a high degree of amino acid sequence identity with type IV pili-binding *S. maltophilia* phage DLP4 and the *Xanthomonas* phages Bosa and Xp12; these four phages share nearly identical gene order, including the presence of four homologous tail proteins encoded between a structural protein and the lysis operon that are not present in the other *Pamexvirus* phages (Figure 5-5). Three of these proteins were identified in AXL1 virions by mass spectrometry (Table 5-5). The high relatedness of these tail morphogenesis proteins between known type IV pili phages DLP4 and AXL1 with Bosa and Xp12 (Figure 5-5), specifically with AXL1 gp44 that contains an Mtd_N domain involved in receptor specificity, suggests that these phages may also use the type IV pilus virulence factor as their receptor for host infection.

The AXL1 genome is 63,962 bp in length and encodes 83 ORFs (Figure 5-4). The resistance of the DNA to digestion by restriction enzymes with G/C bases in their recognition sequences suggest that the AXL1 genome is modified or contains atypical bases that protect it from degradation by host restriction-modification systems. Based on the genomic relatedness to *Xanthomonas* phage Xp12 and similar enzyme susceptibilities, AXL1 may also contain 5-methylcytosine bases as described for Xp12 [338], however the percentage of cytosine

replacement and genetic mechanism for this modification is unknown. Within the DNA replication and repair module few genes stand out as candidates involved in DNA modification beyond AXL1_62 and AXL1_63 that encode enzymes involved in the thymidylate synthase pathway; however, AXL1_79 encodes a PD-(D/E)XK Cas4-like nuclease. Putative Cas4 nucleases have been identified in other *S. maltophilia* phages, DLP4 [114] and AXL3 [115], and were functionally characterized in *Campylobacter jejuni* phages to be capable of incorporating host-derived spacers into host CRISPR arrays to ultimately evade host immune defenses [323]. Given the apparent lack of CRISPR-Cas defense systems in *S. maltophilia* however and the restriction enzyme-resistant nature of phage genomes encoding *cas4* genes, we have hypothesized a potential role of phage-encoded Cas4 enzymes in defense against host restriction-modification systems [115,326].

Functional analysis of the 83 proteins encoded by AXL1 revealed an additional gene of interest encoding a dihydrofolate reductase enzyme. During the phage infection cycle, AXL1-encoded dihydrofolate reductase (gp61, DHFR) likely functions in nucleotide biosynthesis, as described above, based on its genomic location and the functions of neighbouring genes. Antibiotic susceptibility assays show that AXL1 encoded DHFR increases bacterial resistance to the antibiotic combination trimethoprim-sulfamethoxazole, the drug of choice for treatment of *S. maltophilia* infections (Table 5-6, Figure 5-7). This effect varies between strains. This may be due to slight sequence variation between endogenous DfrA3 host proteins that provide different levels of protection against trimethoprim, or differential expression of efflux pumps that were not examined between strains.

The presence of a gene encoding antimicrobial resistance to trimethoprim in phages that infect nosocomial pathogens such as *S. maltophilia* and *P. aeruginosa* that are often found in co-microbial infections in patients with cystic fibrosis [38,217] is cause for concern, specifically because the recommended treatment option for *S. maltophilia* infections is trimethoprim-sulfamethoxazole [100]. We have shown that DHFR encoded by *S. maltophilia* phages AXL1 and DLP4 [114] promotes resistance to trimethoprim in their hosts, however the sequence variability between these proteins and other *Pamexvirus* phage-encoded DHFR proteins suggests that additional testing is needed to determine if they are also insensitive to trimethoprim or capable of conferring resistance in their hosts by a gene dosage effect. Although it is commonly understood in the field that phages seldom encode antibiotic resistance genes and play a lesser

role in the spread of antimicrobial resistance through rare generalized transduction events than other mobile genetic elements [359,360], our data indicates this is not the case for phages of the *Pamexvirus* genus. The lack of homology between these DHFR phage proteins and known trimethoprim insensitive DfrA proteins found in bacteria falls below the conservative criteria for identification of antimicrobial resistance when searching against a database [359]. This limited homology to bacterial dihydrofolate reductase enzymes also indicates an unknown origin of this gene. These results suggest revisiting the potential that phages have in contributing to the spread of antimicrobial resistance. The recent increase in sequencing of phage genomes submitted to public databases without corresponding thorough functional characterization may overlook the potential for phage-spread of multidrug resistance in the environment. Overall, we determine that AXL1 is not a good candidate for use in phage therapy, however further study may provide insight into novel phage mechanisms of DNA modification and regulation of phage gene expression.

Acknowledgements

I would like to thank Arlene Oatway from the University of Alberta Department of Biological Sciences Advanced Microscopy Facility for her assistance with TEM and Brent Weber for advice and thoughtful discussion regarding antibiotic susceptibility assays. We also thank James Zlosnik and the Canadian *Burkholderia cepacia* complex Research and Referral Repository (CBCCRRL) and LeeAnn Turnbull of the Provincial Laboratory for Public Health - North, Alberta Health Services for providing *S. maltophilia* clinical isolates, as well as Jorge Girón for gifting strains SMDP92 and ATCC13637. We thank Guus Bakkeren of Agriculture and Agri-Foods Canada for contributing *Xanthomonas* strains from an AAFC strain collection. I was kindly supported by a CGS-D award from NSERC and an AIGSS award from Alberta Innovates during this research.

**CHAPTER 6 - Investigating the host interactions
of type IV pili-binding bacteriophages of
*Stenotrophomonas maltophilia***

Objectives

My discovery that seven of the eight *Stenotrophomonas maltophilia* phages in our collection use the type IV pilus as their receptor, despite vastly different host ranges, suggests that phages may select for the diversification of pilin proteins in *S. maltophilia* through co-evolution. Knowledge of the molecular mechanism behind these phage-pili interactions will inform our ability to harness this selective pressure in an anti-virulence phage therapy strategy. The objective of this chapter is therefore to determine features that are important for host recognition and pili binding, including analysis of type IV pilins in *S. maltophilia* for phage binding sites and comparison of phage putative receptor binding proteins.

Materials and Methods

Bacterial strains, bacteriophages and growth conditions

Bacterial strains and plasmids used in this study are listed in Table 6-1. *S. maltophilia* and *Pseudomonas aeruginosa* strains were grown overnight at 30°C on full-strength Lennox (LB; 10 g/L tryptone, 5 g/L yeast extract, 5 g/L NaCl) solid medium or in LB broth with shaking at 225 RPM unless otherwise indicated. *Escherichia coli* strains were grown at 37°C in full LB, unless otherwise noted. Media was supplemented with antibiotics at the following final concentration when necessary for selection or plasmid maintenance (µg per mL): chloramphenicol (Cm), 35 for *S. maltophilia* D1585, D1571 and *E. coli* DH5α, 75 for *S. maltophilia* D1614 and 214; gentamicin (Gm), 10 for *E. coli* and 35 for *P. aeruginosa*.

Seven *S. maltophilia* phages having Siphoviridae morphologies, DLP1, DLP2, DLP3, DLP4, DLP5, AXL3 (Chapter 4), and AXL1 (Chapter 5), used in this work were previously isolated from soil samples in our lab and characterized [11,114,115,168,177–179]. Phage propagation was performed on strain D1585 for phages DLP1, DLP2, DLP4, AXL1, and AXL3, or strain D1571 for phages DLP3 and DLP5 using soft agar overlays as previously described [11,229], or liquid infections. Briefly, 150 µL of overnight culture and 150 µL of phage lysate were incubated for 30 min at 30°C with shaking at 225 RPM before adding 15 mL LB broth and 1.5 mL modified suspension medium (SM) (50 mM Tris–HCl [pH 7.5], 100 mM NaCl, 10 mM MgSO₄) and incubating overnight under the same conditions. 200 µL of chloroform was added

the following day and incubated on a platform rocker at room temperature for 30 min. Following centrifugation, the supernatant was collected, filter sterilized using a Millex-HA 0.45 µm syringe-driven filter unit (Millipore, Billerica, MA) and stored at 4 °C. Phage stocks were standardized to 10¹⁰ PFU/mL on their propagation host.

Phage plaquing ability on host strains carrying different plasmids was determined by spotting on bacterial soft agar overlays as previously described [160]. Briefly, 100 µL of overnight culture was mixed with 3 mL of 0.7% ½ LB top agar, overlaid onto LB agar with the appropriate antibiotic and allowed to solidify at room temperature for 30 min. Phage lysates were tenfold serially diluted in SM. 5 µL of each dilution or 10 µL of undiluted phages was spotted on the prepared plates in triplicate and incubated upright for 18 h at 30°C before imaging.

Table 6-1: Bacterial strains and plasmids used in this study.

Bacterial Strain	Genotype or Description	Source ^a
<i>S. maltophilia</i> D1585	Wildtype phage host	CBCCR
D1585 $\Delta pilA1$	Clean deletion of <i>pilA1</i> in D1585	[160]
<i>S. maltophilia</i> 280	Wildtype phage host	PLPHN/AHS
280 $\Delta pilA1$	Clean deletion of <i>pilA1</i> in 280	[160]
<i>S. maltophilia</i> D1571	Wildtype phage host	CBCCR
<i>S. maltophilia</i> 213	Wildtype strain	PLPHN/AHS
<i>S. maltophilia</i> D1614	Wildtype; DLP5 susceptible, DLP3 resistant	CBCCR
<i>S. maltophilia</i> 214	Wildtype; DLP3 susceptible, DLP5 resistant	PLPHN/AHS
<i>P. aeruginosa</i> PA01	Wildtype, DLP1 and DLP2b sensitive	[221]
<i>E. coli</i> DH5 α	Host for plasmid cloning	[223]
Plasmids		
pBBR1MCS	Broad-host range cloning vector, Cm ^R	[226]
pD1585 <i>pilA1</i>	pBBR1MCS carrying D1585 <i>pilA</i> , Cm ^R	[160]
p213 <i>pilA</i>	pBBR1MCS carrying 213 <i>pilA</i> , Cm ^R	This study
pWT <i>pilA1</i> (p280 <i>pilA</i>)	pBBR1MCS carrying WT 280 <i>pilA1</i> , Cm ^R	[160]
p Δ 60-80	pWT <i>pilA1</i> with codons for 60-80aa deleted	This study
p Δ 60-65	pWT <i>pilA1</i> with codons for 60-65aa deleted	This study
p Δ 66-73	pWT <i>pilA1</i> with codons for 66-73aa deleted	This study

pΔ72-80	pWTPilA1 with codons for 72-80aa deleted	This study
pΔ80-95	pWTPilA1 with codons for 80-95aa deleted	This study
pΔ80-86	pWTPilA1 with codons for 80-86aa deleted	This study
pΔ87-91	pWTPilA1 with codons for 87-91aa deleted	This study
pΔ91-95	pWTPilA1 with codons for 91-95aa deleted	This study
pΔ96-111	pWTPilA1 with codons for 96-111aa deleted	This study
pΔ96-100	pWTPilA1 with codons for 96-100aa deleted	This study
pΔ101-106	pWTPilA1 with codons for 101-106aa deleted	This study
pΔ107-111	pWTPilA1 with codons for 107-111aa deleted	This study
pDLP5gp24	pBBR1MCS carrying DLP5 <i>gp24</i> , Cm ^R	This study
pDLP5gp28	pBBR1MCS carrying DLP5 <i>gp28</i> , Cm ^R	This study
pDLP3gp24	pBBR1MCS carrying DLP3 <i>gp24</i> , Cm ^R	This study
pDLP3gp28	pBBR1MCS carrying DLP3 <i>gp28</i> , Cm ^R	This study
pDLP2b-23	pBBR1MCS carrying DLP2b <i>gp23</i> , Cm ^R	This study
pDLP2b-26	pBBR1MCS carrying DLP2b <i>gp26</i> , Cm ^R	This study
pUCP22	Broad-host range cloning vector, Gm ^R	[227]
pUCP(DLP2b-23)	pUCP22 carrying DLP2b <i>gp23</i> , Gm ^R	This study
pUCP(DLP2b-26)	pUCP22 carrying DLP2b <i>gp26</i> , Gm ^R	This study

^a CBCCRRL, Canadian *Burkholderia cepacia* complex Research and Referral Repository; PLPHN/AHS, Provincial Laboratory for Public Health - North, Alberta Health Services.

Cloning and modification of *S. maltophilia pilA1* genes

Variants of the 280 *pilA1* gene containing internal deletions were constructed by overlap extension PCR [160] using the primers listed in Table 6-2 and cloned into pBBR1MCS for complementation of the 280 Δ *pilA1* mutant. Briefly, two separate PCRs were performed to amplify DNA fragments 5' and 3' to the desired deletion using p280*pilA* as a template and primer pairs 280*pilAF* with a reverse deletion primer and 280*pilAR* with a forward deletion primer. These products were purified using a QIAquick PCR purification kit (Qiagen, Inc., Germantown, MD, USA), or the QIAquick gel extraction kit when necessary. Overlap extension

PCR was used to join these two fragments as previously described [160] using the primers 280*pilAF* and 280*pilAR*. All PCR products were amplified using TopTaq DNA Polymerase (Qiagen, Inc., Germantown, MD, USA) according to manufacturer protocols. The resulting constructs as listed in Table 2-1 were verified by Sanger sequencing and subcloned into electrocompetent *E. coli* DH5 α before transforming *S. maltophilia* 280 Δ *pilA1* by electroporation.

The wildtype *pilA1* gene was amplified from *S. maltophilia* strain 213 by colony PCR using primer pair Smp*pilAF* and Smp*pilAR* designed for D1585 [160]. The resulting product was purified by gel extraction, digested with *Sal*I and *Hind*III Fast Digest restriction endonucleases (Thermo Scientific) and ligated using T4 DNA ligase (New England Biolabs) into the vector pBBR1MCS, producing the construct p213*pilA1*. This plasmid was subcloned into electrocompetent *E. coli* DH5 α and verified by Sanger sequencing before transforming *S. maltophilia* D1585 Δ *pilA1* by electroporation.

Electrocompetent *S. maltophilia* D1585 and 280 cells were prepared as described by Ye et al. (2014) [237]. Overnight cultures were subcultured and grown to an optical density at 600 nm (OD₆₀₀) of 1.0 in LB at 37°C and placed on ice for 30 min. The chilled cells were harvested by centrifugation for 5 min at 4,000 \times g and 4°C and washed 3 times with ice-cold 10% glycerol (v/v). The cells were resuspended in residual 10% glycerol and stored in 100 μ L aliquots at –80°C prior to use. Electrocompetent *E. coli* DH5 α cells were prepared similarly to *S. maltophilia*, however subcultures were grown to an OD₆₀₀ of 0.5 – 0.7 at 37°C.

Table 6-2: Primers used in this study.

Primer name	Sequence (5' – 3')	Function
280 <i>pilAF</i>	GCAAGTCGACCAGACCG ATCCTGTGCTCTG	Anneals upstream of the 280 <i>pilA</i> gene. <i>Sal</i> I site underlined.
280 <i>pilAR</i>	GACCAAGCTTCCCCTAGT TCGCTTCATGGC	Anneals downstream of the 280 <i>pilA</i> gene. <i>Hind</i> III site underlined.
<i>pilA</i> del60-80F	GATTTCGCTGATTCTTCC GGTGCAGCCTCG	Used with 280 <i>pilAR</i> to amplify 3' segment for Δ 60-80aa in 280 <i>pilA</i> . Overlap section in bold.

pilAdel60-80R	TGCACCGGAAGAATCAG CGAAATCCTTG	Used with 280 <i>pilAF</i> to amplify 5' segment for Δ 60-80aa in 280 <i>pilA</i> . Overlap section in bold.
pilAdel60-65F	GATTTCGCTGATAAGGT TTCGACCCGTTGC	Used with 280 <i>pilAR</i> to amplify 3' segment for Δ 60-65aa in 280 <i>pilA</i> . Overlap section in bold.
pilAdel60-65R	GGTCGAAACCTTATCAG CGAAATCCTTG	Used with 280 <i>pilAF</i> to amplify 5' segment for Δ 60-65aa in 280 <i>pilA</i> . Overlap section in bold.
pilAdel66-73F	GACATCGGTCTGGTCAC CGTGAAGGGCACC	Used with 280 <i>pilAR</i> to amplify 3' segment for Δ 66-73aa in 280 <i>pilA</i> . Overlap section in bold.
pilAdel66-73R	CTTCACGGTGACCAGAC CGATGTCAGCC	Used with 280 <i>pilAF</i> to amplify 5' segment for Δ 66-73aa in 280 <i>pilA</i> . Overlap section in bold.
pilAdel72-80F	TCGACCCGTTGCTCTTCC GGTGCAG	Used with 280 <i>pilAR</i> to amplify 3' segment for Δ 72-80aa in 280 <i>pilA</i> . Overlap section in bold.
pilAdel72-80R	TGCACCGGCAGAGCAAC GGGTCGAAAC	Used with 280 <i>pilAF</i> to amplify 5' segment for Δ 72-80aa in 280 <i>pilA</i> . Overlap section in bold.
pilAdel80-95F	GTGAAGGGCACCCAGGT GAAGGACAAGACC	Used with 280 <i>pilAR</i> to amplify 3' segment for Δ 80-95aa in 280 <i>pilA</i> . Overlap section in bold.
pilAdel80-95R	GTCTTCACCTGGGTGC CCTTCACGGTG	Used with 280 <i>pilAF</i> to amplify 5' segment for Δ 80-95aa in 280 <i>pilA</i> . Overlap section in bold.
pilAdel80-86F	GTGAAGGGCACCATCGC CTGCACCCTT	Used with 280 <i>pilAR</i> to amplify 3' segment for Δ 80-86aa in 280 <i>pilA</i> . Overlap section in bold.
pilAdel80-86R	GGTGCAGGCGATGGTGC CCTTCACGGT	Used with 280 <i>pilAF</i> to amplify 5' segment for Δ 80-86aa in 280 <i>pilA</i> . Overlap section in bold.
pilAdel87-91F	GGTGCAGCCTCGGCTGG TAACTCTCAGGTG	Used with 280 <i>pilAR</i> to amplify 3' segment for Δ 87-91aa in 280 <i>pilA</i> . Overlap section in bold.
pilAdel87-91R	AGAGTTACCAGCCGAGG CTGCACCGGAAGA	Used with 280 <i>pilAF</i> to amplify 5' segment for Δ 87-91aa in 280 <i>pilA</i> . Overlap section in bold.
pilAdel91-95F	ATCGCCTGCACCCAGGT GAAGGACAAGACC	Used with 280 <i>pilAR</i> to amplify 3' segment for Δ 91-95aa in 280 <i>pilA</i> . Overlap section in bold.
pilAdel91-95R	GTCTTCACCTGGGTGC AGGCGATCGAGGC	Used with 280 <i>pilAF</i> to amplify 5' segment for Δ 91-95aa in 280 <i>pilA</i> . Overlap section in bold.

pilAdel96-111F	GCTGGTAACTCTACTTG GACCTGTGCCACG	Used with 280 <i>pilAR</i> to amplify 3' segment for Δ 96-111aa in 280 <i>pilA</i> . Overlap section in bold.
pilAdel96-111R	CACAGGTCCAAGTAGAG TTACCAGCAAG	Used with 280 <i>pilAF</i> to amplify 5' segment for Δ 96-111aa in 280 <i>pilA</i> . Overlap section in bold.
pilAdel96-100F	GCTGGTAACTCTACCAT CACCTGACCCGC	Used with 280 <i>pilAR</i> to amplify 3' segment for Δ 96-100aa in 280 <i>pilA</i> . Overlap section in bold.
pilAdel96-100R	CAGGGTGATGGTAGAGT TACCAGCAAGGG	Used with 280 <i>pilAF</i> to amplify 5' segment for Δ 96-100aa in 280 <i>pilA</i> . Overlap section in bold.
pilAdel101-106F	GTGAAGGACAAGGCCAC TGCTGACGGTACT	Used with 280 <i>pilAR</i> to amplify 3' segment for Δ 101-106aa in 280 <i>pilA</i> . Overlap section in bold.
pilAdel101-106R	GTCAGCAGTGGCCTTGT CCTTCACCTGAG	Used with 280 <i>pilAF</i> to amplify 5' segment for Δ 101-106aa in 280 <i>pilA</i> . Overlap section in bold.
pilAdel107-111F	ACCCTGACCCGCACTTG GACCTGTGCCACG	Used with 280 <i>pilAR</i> to amplify 3' segment for Δ 107-111aa in 280 <i>pilA</i> . Overlap section in bold.
pilAdel107-111R	ACAGGTCCAAGTGCGGG TCAGGGTGATGG	Used with 280 <i>pilAF</i> to amplify 5' segment for Δ 107-111aa in 280 <i>pilA</i> . Overlap section in bold.
Smp <i>pilAF</i>	CCAAGTCGACCCATCC GTGAAATAGCTGCC	Anneals upstream of 213 <i>pilA</i> start codon. <i>Sall</i> site underlined.
Smp <i>pilAR</i>	CGCCAAGCTTACGAGC CGACAAAAGAAAGGC	Anneals downstream of 213 <i>pilA</i> stop codon. <i>HindIII</i> site underlined.
DLP3gp24F	TTTTGTCGACTGGACTTC AGGGATTTTCGCC	Anneals upstream of the DLP3 gene encoding gp24. <i>Sall</i> site underlined.
DLP3gp24R	TCTTAAGCTTCCATCACC GGGTTGATCGAA	Anneals downstream of the DLP3 gene encoding gp24. <i>HindIII</i> site underlined.
DLP3gp28F	TTTTGTCGACGGGTATTT GGGTGCCTCTCC	Anneals upstream of the DLP3 gene encoding gp28. <i>Sall</i> site underlined.
DLP3gp28R	CGGTAAGCTTTGTTCTCA CGACCACCACAC	Anneals downstream of the DLP3 gene encoding gp28. <i>HindIII</i> site underlined.
DLP5gp24F	TTTTGTCGACCGATGGTG GAAGAGGCAAAG	Anneals upstream of the DLP5 gene encoding gp24. <i>Sall</i> site underlined.

DLP5gp24R	TTTT <u>AAGCTT</u> GGTTGACC GAAGCCCAATTG	Anneals downstream of the DLP5 gene encoding gp24. <i>HindIII</i> site underlined.
DLP5gp28F	TTTTGTCGACCGGCCTGC TTTGAAATCTCG	Anneals upstream of the DLP5 gene encoding gp28. <i>SalI</i> site underlined.
DLP5gp28R	TTTT <u>AAGCTT</u> GGAACACC CGAACAAGTTGC	Anneals downstream of the DLP5 gene encoding gp28. <i>HindIII</i> site underlined.
DLP2bgp23F	TTTTGTCGACCGGGCGTT TGTAATGTTGCA	Anneals upstream of the DLP2b gene encoding gp23. <i>SalI</i> site underlined.
DLP2bgp23R	GGGGTCTAGATGTTCCAA TTCTTCCGGCCA	Anneals downstream of the DLP2b gene encoding gp23. <i>XbaI</i> site underlined.
DLP2bgp26F	TTTTGTCGACTTGTTCCGG GCGAATCGAAT	Anneals upstream of the DLP2b gene encoding gp26. <i>SalI</i> site underlined.
DLP2bgp26R	GGGCTCTAGACGAAATGC TGTAAGACTGCG	Anneals downstream of the DLP2b gene encoding gp26. <i>XbaI</i> site underlined.
DLP2bgp31F	CCGCCATATGCAAAACAG CAAAGACGCGAA	Anneals within the start codon of the DLP2b gene encoding gp31.
DLP2bgp31R	ATGACTCGAGGACATTCT TTGCAACCGCTG	Anneals over the stop codon of the DLP2b gene encoding gp31.

Twitching motility

Twitching motility assays were used to determine type IV pili function of *S. maltophilia* 280 $\Delta pilA1$ complemented with mutant *pilA1* alleles. Strains were grown on ½ LB agar supplemented with 75 µg/mL Cm at 30°C for 48 h. A single bacterial colony was suspended in 100 µL LB broth and stab inoculated with a toothpick through a 3 mm thick ½ LB, 1% agar layer containing 0.3% porcine mucin and 75 µg/mL Cm to the bottom of the petri dish and incubated with humidity at 37°C for 24 h. Twitching motility zones between the agar and petri dish interface were visualized by gently removing the agar and staining each plate with 1% (w/v) crystal violet for 30 min followed by rinsing away excess stain with water. Stained twitching zone areas were measured using ImageJ software (NIH, Bethesda, MD, USA) [239]. Each strain was tested in biological and technical triplicate and average twitching area was calculated from the nine twitching zones.

DLP2 training on PA01

S. maltophilia phages DLP2 and DLP4 were repeatedly passaged by soft agar overlay on a non-susceptible host, *P. aeruginosa* PA01, to isolate new variants with broadened host ranges. Briefly, 100 µL of PA01 overnight culture was incubated with 200 µL of a 10¹¹ PFU/mL DLP2 lysate or a 10¹⁰ PFU/mL DLP4 lysate for 20 min before adding 3 mL 0.7% ½ LB top agar and incubating at 30°C overnight. The top agar containing bacteria and phage was collected in 3 mL modified suspension media (SM) (50 mM Tris-HCl pH 7.5, 100 mM NaCl, 10 mM MgSO₄), with 300 µL chloroform added and incubated at room temperature on a platform rocker for 30 min. The cell debris was pelleted by centrifugation and supernatant collected and filter sterilized with a Millex-HA 0.45 µm syringe-driven filter unit (Millipore, Billerica, MA) and stored at 4°C. This process was repeated twice for DLP2 and four times for DLP4.

Phage genomic DNA was isolated by phenol:chloroform extraction as previously described [115] and sequenced at The Applied Genomics Core at the University of Alberta. A DNA genomic library was constructed using a Nextera XT library prep kit followed by paired-end sequencing on a MiSeq (Illumina, San Diego, CA) platform using a MiSeq v3 reagent kit. Quality control analysis was completed using FastQC v0.11.9 [301] and paired-end reads were processed using Trimmomatic v.0.38 [302] before assembling with SPAdes v.3.12.0 [303]. The assembled contig was compared to the wildtype DLP2 genome (accession: NC_029019) using Geneious Prime v2020.0.4 [230] and point mutations were confirmed by PCR and Sanger sequencing with primer pairs DLP2bgp23F and DLP2bgp23R, and DLP2bgp31F and DLP2gp31R (Table 6-2).

Bioinformatics

Protein structural predictions were made using the SWISS-MODEL server (<https://swissmodel.expasy.org>) [361] and figures made using PyMOL Molecular Graphics System, Version 2.1.1. Schrödinger, LLC. Protein alignments were accomplished using MUSCLE [231] or CLC Sequence Viewer 8 (Qiagen, Toronto, ON). Conserved domain and protein homology searches were performed using CD-Search against the CDD v3.19—58,235 PSSMs database and default options [265] and HHpred [362].

S. maltophilia complete genomes were retrieved from Genbank and pilin gene clusters were identified using Geneious v2022.0.1 [230]. The sequence and annotations between *pilR* and

pilD were manually extracted from each genome and analyzed by clinker v0.0.23 [266]. Only links with 30-100% identity are shown.

Phage receptor binding protein swapping

Phage genes were amplified from phage genomic DNA for DLP2b or phage lysate for DLP3 and DLP5 by PCR using primer pairs listed in Table 6-2. DLP3 and DLP5 genes were amplified using Phusion high-fidelity DNA polymerase (New England Biolabs) with GC buffer and 3% DMSO according to manufacturer protocols. DLP2b genes were amplified using Q5 high-fidelity DNA polymerase (New England Biolabs) as directed by the manufacturer. The products were purified using a QIAquick PCR purification kit (Qiagen, Inc., Germantown, MD, USA), digested with Fast Digest restriction endonucleases (Thermo Scientific) and ligated using T4 DNA ligase (NEB) into the vector pBBR1MCS to create the constructs listed in Table 6-1. These plasmids were subcloned into electrocompetent *E. coli* DH5 α and verified by Sanger sequencing before electroporating the *S. maltophilia* strains listed in Table 6-3, with electrocompetent cells prepared as described above. For expression in *P. aeruginosa* PA01, DLP2b gene inserts were digested from pDLP2b-23 and pDLP2b-26 using *KpnI* and *XbaI* Fast Digest restriction endonucleases (Thermo Scientific) and ligated using T4 DNA ligase (NEB) into the vector pUCP22. These plasmids were electroporated into PA01 cells as previously described [160].

Phages were propagated on D1585 or D1571 carrying the appropriate plasmid, as listed in Table 6-3, by soft agar overlay or liquid infection, as described above. This was repeated at least twice for each combination before screening on a non-susceptible host carrying the same plasmid for evidence of phage lysis.

Results and Discussion

Investigation of phage binding sites on PilA1 of the type IV pilus

As described in Chapters 2 and 3, seven of our eight *S. maltophilia* phages use the type IV pilus as their receptor for host recognition and infection. However, the host ranges of these phages are vastly different (Table 3-3), prompting the question of whether specific pilin amino

acid(s) dictate phage binding and host susceptibility. I therefore sought to identify specific regions of the pilus that are bound by different phages to aid in understanding their different host ranges. Type IV pilin subunits have a conserved architecture consisting of a long, hydrophobic N-terminal α -helix that is joined to a hydrophilic C-terminal globular head domain of antiparallel β -sheets, terminating in a hypervariable disulfide-bonded loop (DSL) that is essential for inter-subunit interaction within the assembled pilus [133]. Extensive studies of *P. aeruginosa* and *Neisseria gonorrhoeae* pilus structure by cryo-electron microscopy and crystallography have confirmed that the α -helix mediates assembly of a strong, flexible pilus by forming a hydrophobic helical bundle in the filament core with the globular head domain forming the outer surface [133,363]. Structural prediction of the *S. maltophilia* 280 mature PilA1 that is 131 amino acids in length match this conserved protein structure (Figure 6-1A).

Possible phage binding amino acids were examined by genetic complementation of a clean deletion $\Delta pilA1$ strain using internally truncated *pilA1* genes to preserve the integrity of the conserved N-terminus sequence and C-terminal disulfide-bonded loop that are essential for assembly of a functional pilus. This approach involved deleting nucleotide stretches coding for five amino acids within the predicted surface exposed regions and using these internally truncated genes to complement a $\Delta pilA1$ mutant. These complemented strains would be screened for differential patterns of phage resistance to identify regions important for binding between phages. Because our phages require a functional pilus capable of retraction for successful infection (Chapter 3), twitching motility was used to test if the mutant *pilA1* alleles were able to assemble into a functional pilus prior to testing phage susceptibility. Due to the lack of strong twitching motility in the main host strain, D1585, I chose to conduct this mutagenesis in *S. maltophilia* 280, a strain that is naturally more motile (Chapter 2) [160] and still susceptible to all seven phages. All 12 mutant alleles constructed partially restored twitching motility in a 280 $\Delta pilA1$ background compared to the empty vector control (Figure 6-2B), which exhibits a twitching zone comparable to wildtype (Figure 2-5), however, phage infection was not restored for any of the phages tested, which include DLP1, DLP2, DLP3, DLP4, AXL1, and AXL3. This suggests that the deleted regions affected the pilus structure such that pili function was not impeded, but phage binding regions were either removed or masked by changes in pilin protein folding and subunit interaction causing changes in the pilus surface.

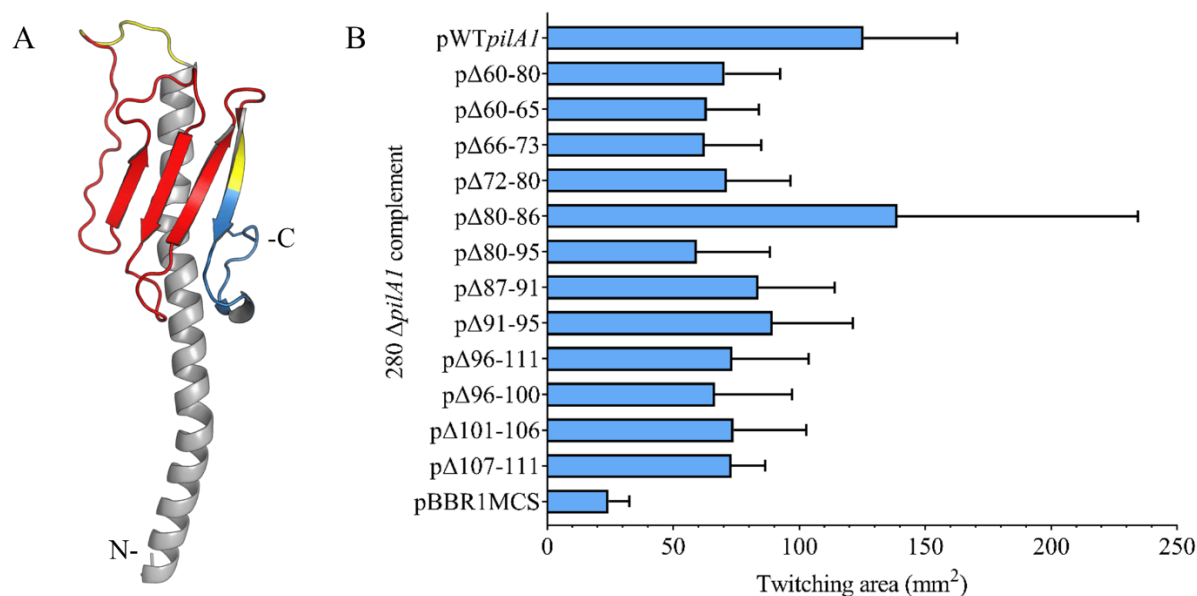


Figure 6-1: Effect of internal *pilA1* truncation on twitching motility in *S. maltophilia* 280.

(A) SWISS-MODEL [361] predicted structure of the mature 280 PilA1 protein. Amino acids 60-111 of the mature protein targeted for mutagenesis are shown in red. Blue represents the C-terminal DSL structure. Structure was visualized in Pymol [364]. (B) Deletion of short internal regions of *pilA1* does not prevent complementation of pili function in a 280 $\Delta pilA1$ mutant, compared to absence of twitching in a vector control, pBBR1MCS. Bars show average area of the twitching zones with standard deviation error bars.

The spiraling assembly of pilins produces prominent grooves and a highly corrugated pilus surface [363]. Based on the above results, *S. maltophilia* phages are likely recognizing surface protein folds of the pilus that are disrupted by internal deletions in *pilA1* rather than interacting with specific amino acid sequences. This hypothesis is also supported by the lack of clear regions of sequence homology shared between pilins that correlate with phage host range. In our collection, four *S. maltophilia* strains have been partially sequenced and an additional two *pilA1* gene sequences from strains 213 and 287 were obtained from Sanger sequencing of PCR products using primers designed against the D1585 *pilA1* gene. Comparison of mature PilA1 amino acid sequences between these six *S. maltophilia* host strains shows substantial sequence variation at the C-terminus, corresponding to the surface exposed region of the assembled pilus that is accessible for phage binding (Figure 6-2). More specifically, comparison of the amino

acid sequences by MUSCLE [231] revealed pilins with 98.55% identity between the main host strain D1585 and 213, a strain that is only infected by AXL1 at a high EOP indicative of productive phage infection and is not susceptible to type IV pili phages DLP2 and DLP4 (Table 3-3). Strains with low efficiencies of plating for infective phages, 280 and 287, have lower percent identity scores with D1585 PilA1 of 61.87% and 66.91%, respectively. The final two strains with sequenced PilA1 are susceptible to only DLP3 and DLP5 for strain D1571 and AXL1 at low EOP for strain ATCC13637, and not unsurprisingly, have pilin percent identity scores with the D1585 PilA1 sequence in the 40s; most of this identity is found in the conserved N-terminal region of the pilin that is required for pilus assembly.

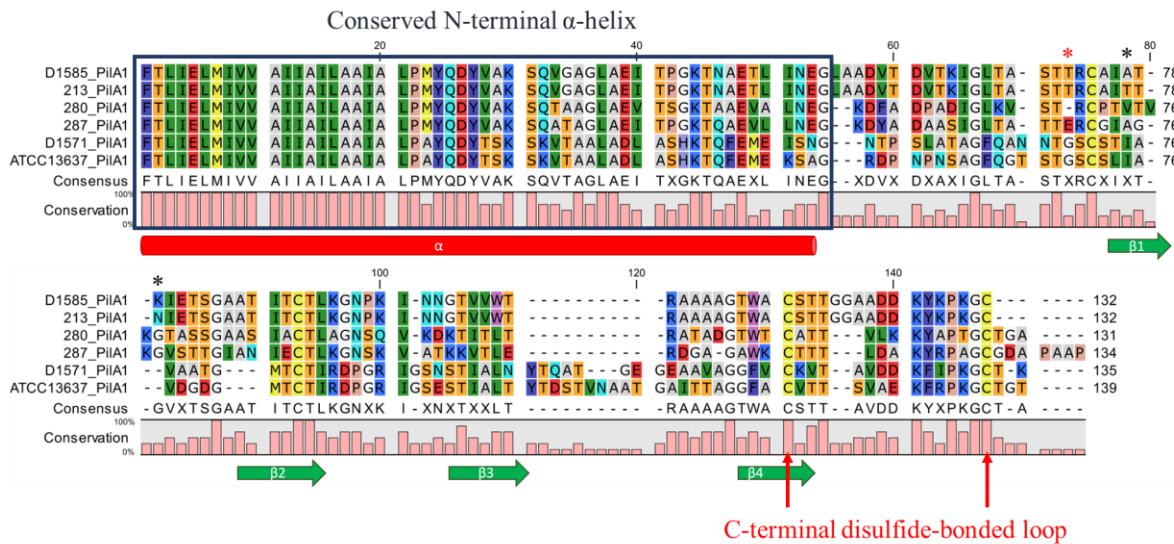


Figure 6-2: *S. maltophilia* pilins exhibit sequence heterogeneity and a conserved structure.

An amino acid sequence alignment of PilA1 mature pilin proteins from six *S. maltophilia* strains. PilA1 sequences are highly conserved at the N-terminus, however homology decreases along the length of the protein sequence towards the C-terminus, which is exposed on the surface of assembled pili. Black asterisks highlight amino acid differences between D1585 and 213 PilA1 sequences, and the red asterisk indicates the point mutation in a D1585 *pilA1* cloned variant. Predicted secondary structure is labeled to produce a pilin structure shown in Figure 6-1A. Sequence alignment was produced in CLC Sequence Viewer 8.0 (Qiagen).

The nearly identical PilA1 proteins of strains 213 and D1585 with significantly different host ranges are intriguing. The major pilins of these strains differ by only two amino acids at positions 77 and 79, identified by black asterisks in Figure 6-2, with strain D1585 having an alanine and lysine and strain 213 having a threonine and asparagine at these positions. These changes lie within the $\alpha\beta$ -loop that connects the N-terminal α -helix to the β -sheet. This loop is a partially surface exposed region that forms one outer edge of the globular head domain and interacts with neighbouring subunits within the pilus [133]. It is highly variable in sequence, length and structure between species [133], and in the *Neisseria gonorrhoeae* GC pilin, this loop is the location of two post-translational modifications [363]. Because DLP2 and DLP4 are unable to infect strain 213 but use D1585 as their main host for propagation, these amino acid differences may represent the phage binding sites or otherwise influence the surface structure of the assembled pilus. As shown in Figure 6-3, complementation of the D1585 $\Delta pilA1$ mutant with the 213 pilin reduces the efficiency of infection for phage DLP3, as well as for phages DLP2 and DLP4 to a lesser extent compared to complementation with the wildtype D1585 *pilA1* gene. Efficiency of plating was not further examined. We hypothesize that these subtle differences in pilin sequence are affecting phage binding, however other factors such as intracellular phage defense mechanisms not examined in this study may also contribute to the differences in phage infection observed. Additionally, complementation of D1585 $\Delta pilA1$ with a D1585 *pilA1* gene carrying a point mutation that results in an amino acid change from threonine to isoleucine at position 72 (red asterisk in Figure 6-2) did not fully restore infection by phages DLP3 and AXL3 to wildtype levels (data not shown). These subtle changes in phage infection efficiency in response to single amino acid changes in the major pilin protein warrant further investigation. Although phage binding of the $\alpha\beta$ -loop has not previously been described, research on the *P. aeruginosa* RNA phage, PP7, identified a single amino acid change, G96S, in the $\beta1$ - $\beta2$ loop of the PA01 pilin that abolished phage infection but retained pili function [137]. Because only the *pilA* gene was obtained from 213 by PCR and not the flanking DNA, it is unknown whether 213 encodes neighbouring accessory genes for post-translational modification of the pilus, as observed in *P. aeruginosa* [253], that block infection by phages DLP2 and DLP4 in the wildtype strain but not in a *S. maltophilia* D1585 genetic background.

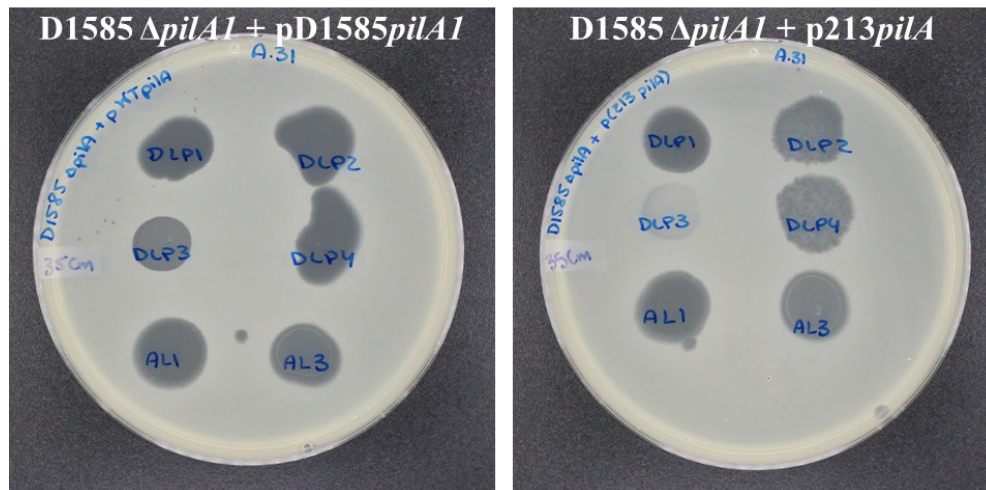


Figure 6-3: Amino acids 77 and 79 affect phage infection in *S. maltophilia* D1585.

Complementation of D1585 $\Delta pilA1$ with the *pilA* gene from 213 (right) that contains two amino acid changes at positions 77 and 79 results in lower phage infection efficiency for DLP3 and to a lesser degree, phages DLP2 and DLP4, compared to complementation with the wildtype D1585 gene (left). AL1 and AL3 correspond to phages AXL1 and AXL3.

To determine if *S. maltophilia* has the genetic potential for pilin modification via glycosylation or other mechanisms, I extracted and compared the pilin gene cluster sequences located between conserved genes *pilD* and *pilR* in our four lab strains and 47 *S. maltophilia* strains with complete genomes found on NCBI. Of these 47 strains, 23 are of clinical origin, 20 are from environmental sources and four are of unknown origin. Including our four lab strains, 31 isolates have a simple pilin gene cluster containing two major pilin genes and no accessory genes (Figure 6-4), with 20 of these being of clinical origin, nine of environmental origin and two of unknown origin. Interestingly, 14 strains carry only a single pilin gene either alone or upstream of protein-coding genes with a range of different putative functions. Few species in the related genus, *Xanthomonas*, also encode only a single *pilA* gene at this locus [272]. Although most strains carry two solitary tandem pilin genes, a subset of strains encode a variety of glycosyltransferases and other post-translational modification proteins downstream of the pilins, indicating that some *S. maltophilia* have modified type IV pili. Surprisingly, all six strains encoding glycosyltransferases downstream of the pilin alleles were of environmental origin, suggesting a benefit to pili modification in the rhizosphere. These strains also have greater pilin

amino acid sequence conservation than those strains without accessory genes where we observe substantial sequence variation between PilA1 and PilA2. In our *S. maltophilia* strain collection, we have several strains that are not susceptible to any of the type IV pili-binding phages. Based on this gene cluster analysis, this could be due to the presence of accessory genes that provide post-translational modification to the pilus to possibly evade phage predation.

Prediction of phage receptor binding proteins

The other determining factor of phage-host interactions are phage receptor binding proteins (RBPs); these proteins mediate the first point of contact with bacterial host cells and this specific interaction dictates a phage's host range. RBPs are found at the base of the phage tail, often as a tail spike protein within the baseplate or tail fibers [315,365]. Based on transmission electron microscopy of phage DLP1 binding to pili protruding from host cells (Figure 2-2), this phage interacts with its receptor using the baseplate structure. Notably, no tail fibers were detected in electron micrographs of any of our type IV pili-binding phages [11,114,115,178,179]. Comparative genomic analysis of the seven *S. maltophilia* phages shows their diversity and reveals very little homology across the length of their genomes, or within the tail morphogenesis modules, specifically (Figure 6-5). Some connections exist between dissimilar phages, including sequence identity between the large terminase proteins (dark purple), DNA ligase (salmon), proteins flanking the central tail tub (light pink), and many hypothetical proteins. Previous bioinformatic analysis of the tail morphogenesis regions of phages DLP1 and DLP2 against those of other type IV pili binding Siphoviridae phages in the literature by past PhD candidate Danielle Peters identified a conserved pfam 13550 phage-tail_3 domain in the central tail hub or major baseplate proteins of these phages, including both *P. aeruginosa* and *Xylella fastidiosa* phages [160]. This suggested to us that these proteins may be required for phage binding to host cell pili.

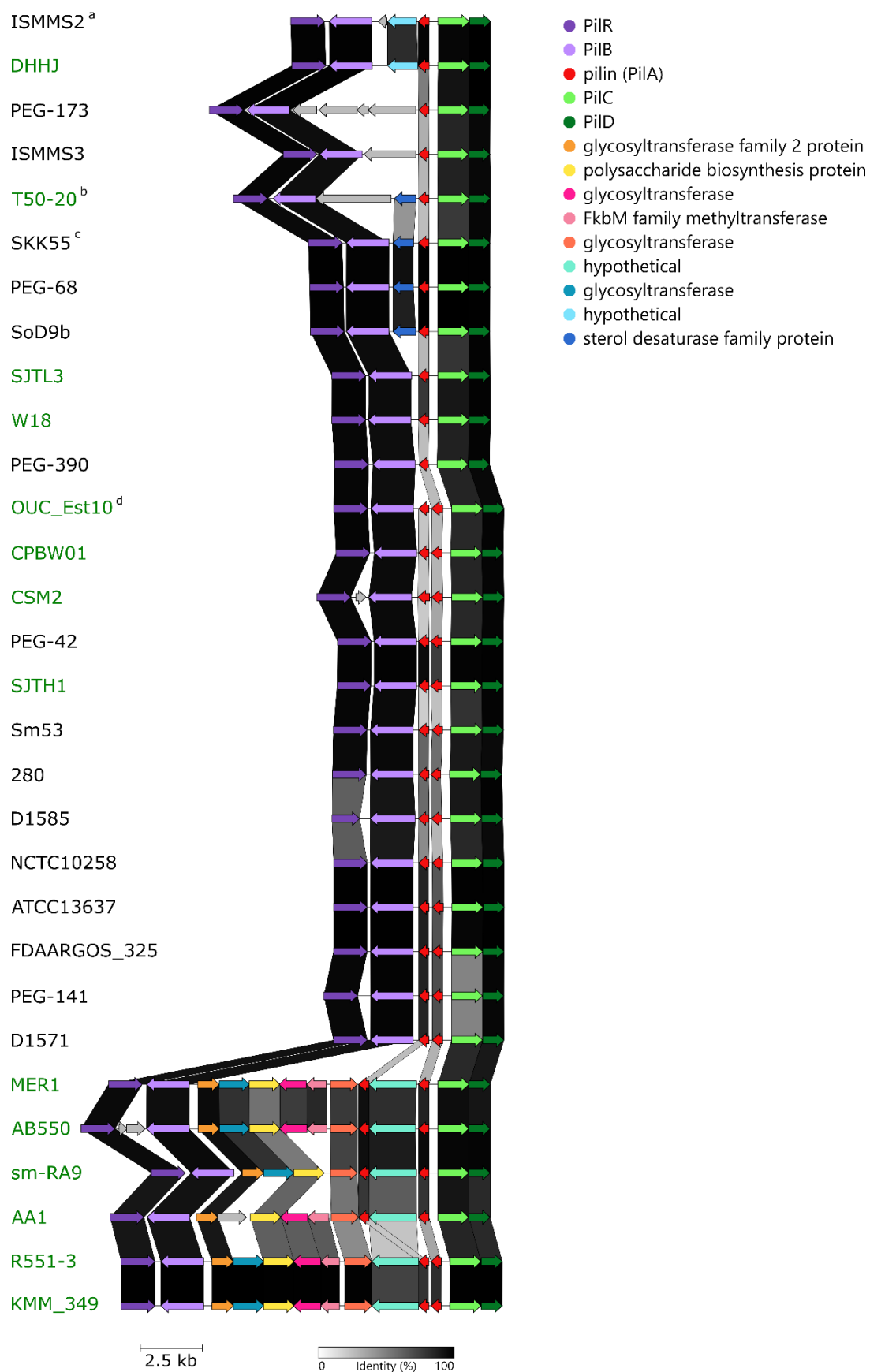


Figure 6-4: *S. maltophilia* type IV pilin gene cluster organization. Type IV pilin gene cluster sequences present between the conserved *pilR/B* and *pilC/D* genes were extracted from four lab strains and 47 *S. maltophilia* strains with complete genomes present in NCBI and analyzed using clinker [266]. Shown is a subset of the types of gene organizations identified. Arrows represent coding sequences coloured to indicate homologous groups as determined by clinker and are linked by grey regions, with shading representing percentage amino acid identity. Only the best links are shown between pilins. Strain names in black are of clinical (c) origin and those in green are environmental (e) isolates. Additional strains with similar organizations not shown are indicated by superscripts: ^a ISMMS2R (c), ^b NCTC13014 (unknown), ^c NCTC10259 (unknown), ^d clinical isolates PEG-305, D457, FDAARGOS_649, NCTC10498, CF13, FDAARGOS_507, K279a, SM_866, FDAARGOS_92, sm454, and NCTC10257; environmental isolates JV3, NEB515, WP1-W18-CRE-01, X28, and U5; unknown origin ICU331 and FDAARGOS_1004.

Further analysis of the additional type IV pili *S. maltophilia* phage virion morphogenesis modules identified major baseplate proteins containing this domain in all five additional phages, as well as in the newly sequenced *Xanthomonas* phage HXX (Appendix 1). The *E. coli* Lambda phage host specificity protein J also carries this domain and is known to play a role in receptor binding, although Lambda phage does not interact with a pilus structure [143]. A MUSCLE [231] alignment of these proteins shows a high degree of variability and clustering into four groups (Figure 6-6), with phages in each group sharing a similar host range, suggesting a possible role in receptor binding.

As discussed in previous chapters, *S. maltophilia* phages DLP1, DLP2, DLP4 and AXL1 share a high percent identity across their genomes to *P. aeruginosa* phages. Despite testing of each phage on our panel of *P. aeruginosa* strains, only DLP1 and DLP2 were discovered to infect a few strains [11] (Table 3-3). Given the genetic potential of these phages to infect across taxonomic orders, we sought to isolate phage variants of DLP2 and DLP4 that can infect the non-susceptible *P. aeruginosa* strain PA01 by repeated passaging of phage lysate in soft agar overlays. This was unsuccessful for DLP4, with no plaques observed after four passages on PA01, however for DLP2, plaques were observed on the second passage and could be propagated to 10¹⁰ PFU/mL on PA01. We named this variant DLP2b. Host range analysis of DLP2b revealed no changes on *S. maltophilia* compared to the original DLP2, however

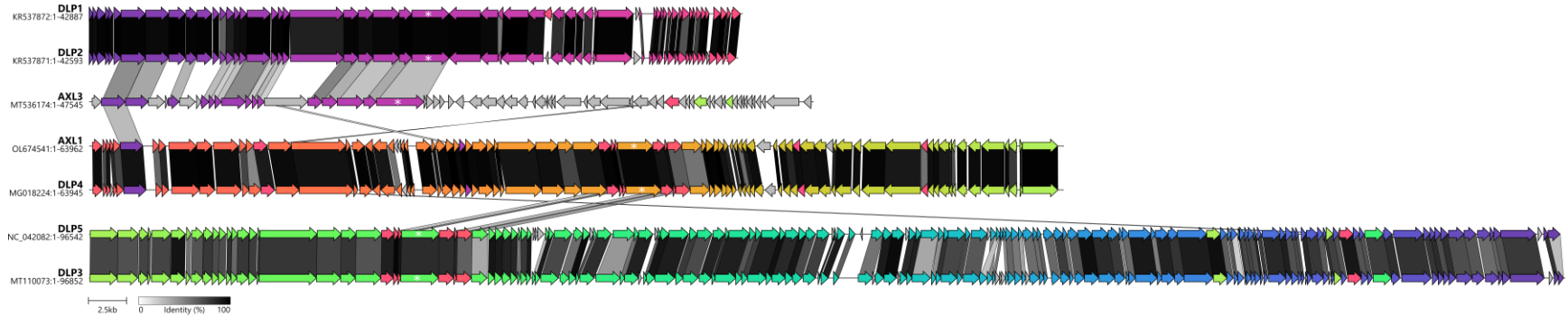


Figure 6-5: Comparative genome alignment of type IV pili-binding *S. maltophilia* phages. A linear representation of the seven Siphoviridae phages experimentally determined to bind the type IV pilus of *S. maltophilia* shows great sequence diversity. Coding sequences are represented by arrows and coloured to reflect homologous groups identified by clinker [266] analysis. Homologous proteins are linked by grey bars shaded to represent percent amino acid identity. Phage accession numbers and genome lengths are provided below each phage name. The protein with a pfam 13550 phage-tail_3 domain in each phage is indicated by a white asterisk.

	AXL3 gp21	DLP1 gp26	DLP2 gp26	DLP4 gp6	AXL1 gp43	DLP3 gp24	DLP5 gp24
AXL3 gp21		36.62%	36.62%	20.28%	20.08%	19.09%	19.58%
DLP1 gp26	36.62%		98.28%	26.44%	26.32%	23.28%	23.88%
DLP2 gp26	36.62%	98.28%		26.44%	26.57%	23.28%	23.88%
DLP4 gp6	20.28%	26.44%	26.44%		97.92%	28.03%	27.91%
AXL1 gp43	20.08%	26.32%	26.57%	97.92%		28.26%	28.26%
DLP3 gp24	19.09%	23.28%	23.28%	28.03%	28.26%		85.71%
DLP5 gp24	19.58%	23.88%	23.88%	27.91%	28.26%	85.71%	

Figure 6-6: Percent identity matrix of type IV pili phage tail proteins containing a phage-tail_3 domain. MUSCLE alignment of phage-tail_3 domain-containing proteins shows variation in percent sequence identity and clustering into four groups. Protein sequence clustering correlates with phage host range. Alignment created in Geneious Prime v2022.0.1.

infectivity on *P. aeruginosa* and *Xanthomonas* spp. was shifted; DLP2b lost the ability to infect *P. aeruginosa* 14,715 and *X. axonopodis* pv. *vasculorum* FB570 but gained the ability to infect *X. translucens* pv. *translucens* ATCC19319. Genome sequencing of DLP2b and comparison to the wildtype DLP2 genome identified single point mutations in genes coding for gp31, a putative RecB exonuclease resulting in a L68F mutation, and gp23, a hypothetical protein located downstream of the tape measure protein, resulting in a D301Y mutation at the C-terminus. No changes in other tail proteins, including the central tail hub protein gp26 predicted to be involved in host specificity, were observed. The mutation in the putative RecB exonuclease at amino acid location 68 of 366 is surprising but may provide some intracellular benefit during phage replication and host cell takeover. More promising is the mutation in gp23, a 321 amino acid length protein and one of five proteins encoded in the tail morphogenesis module downstream of the tape measure protein (Figure 6-7). BLASTp analysis identifies a similar protein in numerous phages with percent identities ranging from approximately 96% to 42%, including hits to known type IV pili binding phages AXL3 and DLP1 and *Xylella* phages Sano and Salvo [281]. Conserved domain and HHpred searches reveal no putative function for gp23, however its genomic location suggests it assembles into the tail base and therefore may function in host receptor binding.

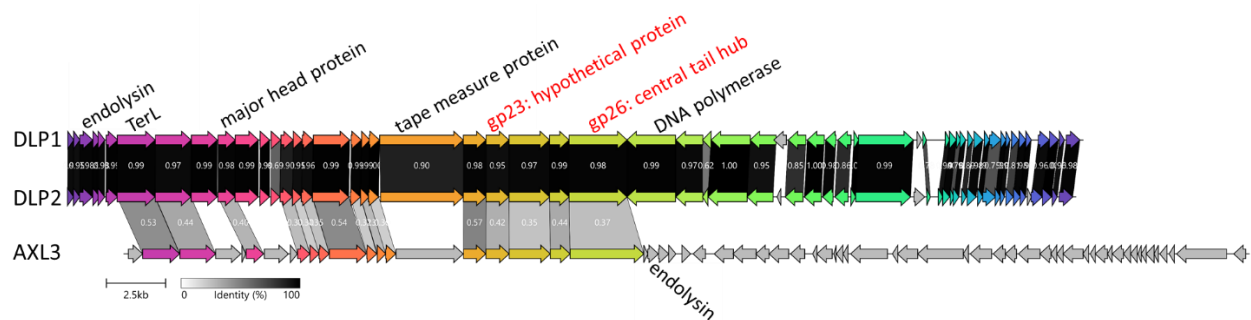


Figure 6-7: Comparative genomic alignment of related phages, DLP1 and DLP2, to AXL3.

AXL3 shares little sequence homology with DLP1 and DLP2 across their genomes, however low percent amino acid identity exists between candidate RBP genes labeled in red. Coding sequences are represented by arrows and coloured to reflect homologous groups identified by clinker [266] analysis. Homologous proteins are linked by grey bars shaded to represent percent amino acid identity.

Examining putative phage RBPs

To explore the possible function of these proteins as RBPs, I initially explored a cell binding assay based on the RBP discovery assay by Simpson et al. (2016) [366]. This modified method involved the expression of putative phage RBPs in *E. coli* BL21(DE3) cells, sonication, and use of cell lysate on a nitrocellulose membrane that is then probed with host *S. maltophilia* cells followed by growth on selective media. Proteins that bind the cell surface should produce a colony after incubation, identifying that protein as a RBP. Unfortunately, this method repeatedly produced background growth and was not effective at distinguishing positive and negative hits.

The above approach was conducted under very artificial circumstances, with protein misfolding and low concentrations likely affecting my results. I therefore turned to a more natural approach involving the expression of putative phage RBP genes in *S. maltophilia* hosts followed by infection with a different phage to produce “chimeric” phage progeny with mixed tail proteins (Figure 6-8). If the exogenous RBP can assemble with the morphogenesis proteins expressed by the infecting phage, we expect the resulting phage lysate will contain particles with either the endogenous or foreign tail protein, or a mixture of both. This lysate can then be tested on host strains that the parent phage is unable to infect but the RBP source phage can infect to determine broadened host susceptibility. Positive infection would indicate that the foreign phage protein functions in receptor binding. This method does not require complicated genetic engineering of phage genomes and allows for simple screening by relying on the host cell expression of phage RBPs.

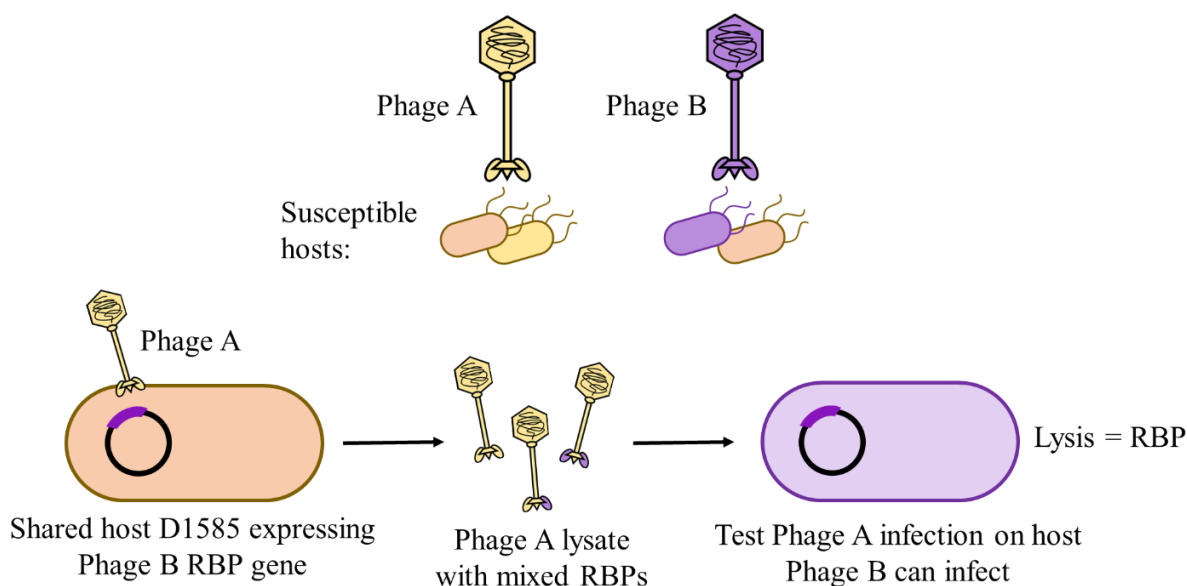


Figure 6-8: Schematic of phage RBP swapping in phage progeny without genetic engineering. Propagation of “Phage A” in *S. maltophilia* D1585 expressing a putative phage RBP from “Phage B” on a plasmid can result in “Phage A” progeny with mixed tail proteins. Screening this “Phage A” chimeric lysate on host strains susceptible to only “Phage B” for cell lysis can confirm the function of putative RBPs.

Given the broad host ranges and genetic relatedness of phages DLP3 and DLP5, I first tested this method using genes from both phages encoding the tail protein gp24 that contains a phage-tail_3 domain. Additionally, the annotated tail protein gp28 shares only 43.8% amino acid identity between these phages, and is related to the tail fiber protein of type IV pilus binding *Xylella* phage Sano, suggesting this may be a protein involved in host specificity [178]. A Laminin G domain involved in laminin binding to cell surface receptors [367] is also present in gp28, as well as in the AXL3 central tail hub protein gp43 that also contains a phage-tail_3 domain. These phages are good candidates for this method, as host range analysis shows that DLP5 infects *S. maltophilia* D1614 but DLP3 does not, while DLP3 partially infects strain 214 and DLP5 does not. Expression of gp24 and gp28 from either phage in the common host strain D1571 for propagation of the opposite phage, followed by screening on the appropriate resistant host did not however produce positive cell lysis (Table 6-3). Positive results were not observed for phages propagated in either liquid or solid media, nor after repeated passaging on D1571 expressing the foreign phage protein. Given the large genome sizes of DLP3 and DLP5, with each phage encoding over a dozen putative tail structural proteins [178], it is likely that a combination of proteins contribute to receptor binding in these phages and these could not be determined through analysis of a single protein in this assay.

To follow up on the mutation identified in the PA01-trained DLP2b isolate and work with more simple phage genomes, I examined the effect of this hypothetical protein, gp23, on wildtype DLP2 as well as the virulent, narrow host range phage AXL3. Phage AXL3 is unrelated to DLP2 but shares some amino acid sequence identity with the tail proteins of DLP2 and DLP1, including gp23 and the central tail hub protein gp26 (Figure 6-7). Expression of the *S. maltophilia* D1585 *pilA1* gene in *P. aeruginosa* PA01 allows infection by DLP2, AXL1, AXL3, and DLP4 (Figures 2-1, 3-1B), suggesting there are no intracellular blocks to phage infection. Swapping phage RBPs in the same way pilins were swapped may also allow infection. Using the

same method as described above, I examined the effect of gp23 from DLP2b on the ability of DLP2 and AXL3 to infect PA01. Phage lysate propagated on D1585 expressing the DLP2b *gp23* gene from a plasmid produced zones of clearing when spotted on *P. aeruginosa* PA01, indicating that this protein assembles into progeny phages of both DLP2 and AXL3, named DLP2-23 and AXL3-23 respectively, and provides expanded host infectivity on PA01 (Table 6-3, Figure 6-9). Clearing occurred regardless of whether PA01 was also expressing the DLP2b *gp23* gene, however the effect was stronger when the gene was present. Oddly, expression of DLP2 *gp26* in D1585 as a host for AXL3 propagation to produce AXL3-26 lysate also allows infection of PA01 despite wildtype DLP2 being unable to infect PA01 (Figure 6-9B). There are 14 amino acid differences between gp26 of DLP1, a phage that can infect PA01, and the DLP2 gp26; this protein may assemble differently in AXL3 than DLP2 to allow infection of PA01. Alternatively, the process of phage propagation in the presence of chloramphenicol for plasmid maintenance may also have an effect. Further experimentation is required to clarify the role of gp23 and gp26 in host binding in phages DLP1 and DLP2. However, the results obtain show promise for the use of this method with additional phage protein combinations and hint at the potential of genetic engineering of AXL3 to infect *P. aeruginosa*.

Table 6-3: Summary of putative phage RBPs tested for broadened host infectivity in new phages.

Phage	Putative phage RBP	Susceptible host for propagation	Resistant host for screening	Infection?
DLP3	DLP5 gp24	D1571 + pDLP5gp24	D1614 + pDLP5gp24	No
DLP3	DLP5 gp28	D1571 + pDLP5gp28	D1614 + pDLP5gp28	No
DLP5	DLP3 gp24	D1571 + pDLP3gp24	214 + pDLP3gp24	No
DLP5	DLP3 gp28	D1571 + pDLP3gp28	214 + pDLP3gp28	No
DLP2	DLP2b gp23	D1585 + pDLP2b-23	PA01 + pUCP(DLP2b-23)	Yes
AXL3	DLP2b gp23	D1585 + pDLP2b-23	PA01 + pUCP(DLP2b-23)	Yes
AXL3	DLP2b gp26	D1585 + pDLP2b-26	PA01 + pUCP(DLP2b-26)	Yes

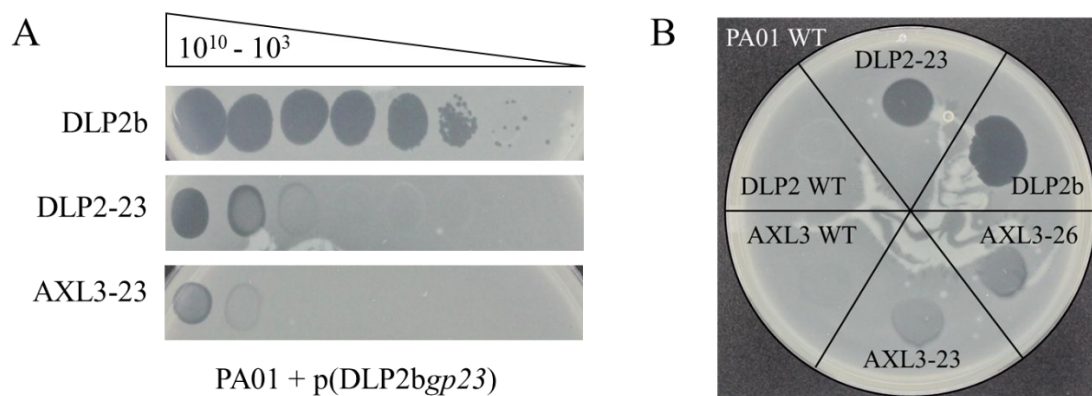


Figure 6-9: Effect of exogenous putative RBPs in progeny phage on host susceptibility.

Propagation of DLP2 or AXL3 in the presence of host-expressed gp23 or gp26 from DLP2b affects their ability to infect *P. aeruginosa* PA01. (A) Serial dilutions of DLP2b and DLP2-23 or AXL3-23 phage progeny propagated in the presence of host-expressed gp23 from DLP2b were spotted on PA01 expressing the same gene. DLP2-23 and AXL3-23 produce zones of clearing at 10^9 and 10^{10} PFU/mL, respectively. (B) Wildtype PA01 is not susceptible to wildtype DLP2 or AXL3, whereas phage progeny with chimeric tail proteins from DLP2b show evidence of cell lysis.

Conclusions

Phage recognition of host cells for infection relies on specific interactions between phage receptor binding proteins (RBPs) and the correct cell surface receptor. In our panel of *S. maltophilia* phages that bind the type IV pilus, I have identified the α - β loop of the major pilin subunit as a potentially important structural region for phage binding. Bioinformatic analysis of pilin gene clusters in *S. maltophilia* isolates from different sources suggests that this bacterium has the potential for post-translational modification of its pilus based on the presence of pilin accessory genes. However, the manifestation of these modifications on the extracellular assembled pili and their prevalence in clinical *S. maltophilia* isolates remains unexplored. Comparison of the tail morphogenesis modules of these phages reveal little sequence similarity, however conserved protein domains hint at putative RBPs. Additionally, point mutations in a *Pseudomonas* trained DLP2 variant support the identity of gp23 as a RBP in this phage. Definitive identification of the RBPs for these phages will provide molecular mechanisms for

differences in host ranges, as well as have implications for genetic engineering towards broadened phage host ranges. I propose that AXL3 is a candidate for this future work.

Acknowledgements

I would like to thank Dr. Dominic Sauvageau for suggestion of the phage RBP screening method, as well as the staff at the Molecular Biology Service Unit for the hundreds of Sanger sequencing samples I submitted. I am also grateful for the support of both my committee and colleagues in the Dennis lab and Raivio lab for support and discussion during the rollercoaster of experiments in this project. I was supported by a CGS-D award from NSERC and an AIGSS award from Alberta Innovates, as well as numerous individual awards from the Department of Biological Sciences during this research.

CHAPTER 7 - Conclusions and future directions

A portion of this chapter was published as:

McCutcheon JG, Dennis JJ. 2021. The potential of phage therapy against the emerging opportunistic pathogen *Stenotrophomonas maltophilia*. *Viruses*. 13:1057. doi.org/10.3390/v13061057. Impact factor (IF): 5.048

Summary

The isolation and characterization of bacteriophages for the treatment of infections caused by multidrug resistant *Stenotrophomonas maltophilia* is imperative to combat this increasingly prevalent nosocomial pathogen. This increase in infection prevalence is largely due to the numerous virulence factors and antimicrobial resistance genes encoded by this bacterium. Phage therapy is a promising alternative therapeutic option that is gaining traction in North America, in part due to the creation of phage therapy centers for personalized medicine in the USA. Research on *S. maltophilia* phages to date has focused on the isolation and in vitro characterization of novel phages from the environment, often including genomic characterization, particularly in recent years. Genome sequencing alone suggests that a large proportion of *S. maltophilia* phages are virulent due to a lack of identifiable genes associated a temperate replication cycle, as well as limited identification of moron genes encoding virulence factors or antimicrobial resistance. Despite this potential, a large knowledge gap exists in *S. maltophilia* phage research; this is the identification of phage receptors and characterization of phage-host interactions.

The research presented in this thesis addresses the lack of information on phage interactions with *S. maltophilia* hosts. Chapters 2 and 3 identify the type IV pilus as the receptor for seven unique Siphoviridae phages, with each phage reliant on host-mediated pilus retraction to reach the cell surface for successful infection. This is the first description of host cell surface receptors for *S. maltophilia* phages, and despite the heterogeneity of type IV pilins, some of these phages are capable of infecting *P. aeruginosa* and *Xanthomonas* spp. as well. Chapter 3 additionally identifies a novel iron-uptake protein, CirA, as a putative receptor for the Myoviridae phage DLP6, along with potential involvement of the LPS. We further address the limited in vivo phage therapy studies conducted against this bacterium by showing the effective phage rescue of *S. maltophilia* infected *G. mellonella* larvae using the broad host range phage DLP3.

Genomic and functional characterizations of two novel type IV pili phages, AXL3 and AXL1, are presented in Chapters 4 and 5 to assess their safety for therapeutic use. Data collected suggests that AXL3 is a virulent phage of a new phage genus that we have proposed as *Axeltriavirus* due to a lack of sequence identity across the length of its genome to known phages. AXL3 has a narrow host range within the panel of *S. maltophilia* strains tested and a genome of

47.5 kb in size and is therefore a suitable candidate for genetic engineering to broaden its host range for therapeutic application. AXL1, however, is unsuitable for therapeutic use due to encoding a functional dihydrofolate reductase enzyme, similar to DLP4, that increases resistance to the frontline recommended antibiotic combination trimethoprim-sulfamethoxazole, when expressed in host cells. This gene is also encoded by other members of the *Pamexvirus* phage genus however was not characterized for its contribution to host antimicrobial resistance in these phages.

In Chapter 6, the interaction between *S. maltophilia* phages and the type IV pilus was further explored to enlighten how and why diverse phages favour a single receptor in this bacterial species. We identify the $\alpha\beta$ -loop of the pilin protein as a putative site for phage interaction and hypothesize that pilin accessory genes leading to post-translational modifications of the pilus could contribute to phage resistance. However, these accessory genes are more abundant in *S. maltophilia* strains from environmental sources than clinical isolates. We also present preliminary data implicating two tail proteins in DLP2 as putative receptor binding proteins capable of broadening the host range of unrelated phage, AXL3.

Future Directions

DLP6 receptor confirmation

We have characterized the type IV pilus as a predominant receptor for *S. maltophilia* siphoviruses, however receptors for phages of other morphologies that infect this bacterium have not been determined. My preliminary data from whole genome sequencing of spontaneous mutants that are resistant to infection by DLP6 implicates the TonB-dependent iron-uptake outer membrane protein, CirA, as a receptor for this phage in two mutants. Follow up research should genetically complementation of these mutants and challenge with DLP6 phage with an expectation of restored phage infection to confirm this receptor. If required, a clean deletion mutant may be constructed for subsequent experiments. Additionally, phages that bind outer membrane proteins, including the iron-uptake protein FhuA, often initially interact reversibly with cell surface lipopolysaccharide (LPS) before finding their proteinaceous receptor for irreversible binding and genome injection [130]. Because a mutation in a gene encoding a

putative glycosyltransferase within the LPS biosynthesis gene cluster was also identified, the role of LPS as a primary receptor for reversible DLP6 phage binding should be assessed by genetic complementation of this mutation. As well, analysis of the LPS profiles of these mutants may be compared to the wildtype strain to identify changes in O-antigen or core LPS. In *S. maltophilia*, LPS plays an important role in colonization and virulence in a host, with *spgM* LPS mutants deficient in biofilm formation [48] and completely avirulent and unable to colonize rat lungs [47]. Loss of function of this glycosyltransferase may therefore have implications in host virulence due to changes in surface LPS.

The discovery of an iron-uptake protein as a putative novel phage receptor is exciting for its potential to add to our proposed anti-virulence strategy for phage therapy treatment of *S. maltophilia* infections. Under iron starvation conditions, such as those in the human body where free iron is sequestered, the expression of iron-acquisition systems in bacteria that are regulated by Fur, including siderophores and iron-uptake proteins, are induced [295]. This would provide numerous phage receptors on the cell surface during bacterial infection. Should CirA be confirmed as the DLP6 receptor, additional experiments using reporter assays to characterize the expression of this protein under normal and iron-depleted conditions can be conducted to determine if CirA is regulated by environmental iron. Additionally, assessing phage adsorption under these conditions will inform how changes in receptor expression potentiates DLP6 efficacy in iron-depleted environments. Studies in *K. pneumoniae* have also shown that *cirA* mutants had significantly higher resistance to a catechol-conjugated antibiotic cefiderocol, but at the cost of reduced fitness in competition assays [298]. In *S. maltophilia*, in vitro growth curves and competition assays between *cirA* DLP6-resistant mutants and wildtype cells in media with varying iron concentrations can determine if a growth defect or fitness cost is associated with phage-induced selective pressure for loss of CirA function.

Role of type IV pili in *S. maltophilia* virulence

The apparent favouring of the type IV pilus as a receptor for *S. maltophilia* phages suggests that this structure plays an important role in bacterial survival and likely virulence, as observed in other pathogens. Therefore, the use of phages that target the pilus are ideal candidates for anti-virulence therapeutics; should phage resistance arise due to modification or loss of the pilus, these mutants will have obtained phage resistance at the cost of lowered

virulence and fitness in a host. Although this thesis further characterizes numerous *S. maltophilia* phages as candidates for therapy, for their effective use in an anti-virulence strategy we must also understand the role of the type IV pilus as a *S. maltophilia* virulence factor and whether it mimics virulence functions observed in the well studied pathogen, *P. aeruginosa*. This avenue was not pursued further than the preliminary *G. mellonella* virulence assays presented in Chapter 3 as biofilm assays, cell adherence assays and further antigenicity tests between *S. maltophilia* wildtype and mutant strains I constructed were planned with a collaborator that unfortunately did not occur due to disruptions to their research lab during the pandemic. These assays would help clarify the role of type IV pili in *S. maltophilia* virulence and inform the validity of our anti-virulence phage therapy strategy using type IV pili binding phages.

Additional features of *S. maltophilia* type IV pili beyond its association with virulence are intriguing for future study. Because phages DLP3 and DLP5 have much broader host ranges than the other type IV pili *S. maltophilia* phages, I hypothesized that they can recognize type IV pili with post-translational modifications, as has been described for *P. aeruginosa* phages able to bind glycosylated pili [253]. Pili modifications have not yet been described in *S. maltophilia*; however, it is clear from the gene cluster analysis presented in Figure 6-4 that some strains encode pilin accessory genes, although this appears to be more prevalent in strains from environmental sources rather than clinical isolates. Analysis of the pilin gene clusters in our panel of clinical *S. maltophilia* isolates by PCR using primers that bind within the highly conserved flanking genes, *pilB* and *pilC*, followed by Sanger sequencing would provide valuable insight to this theory. This approach was used by Kus et al. in 2004 to analyze *pilA* alleles in nearly 300 *P. aeruginosa* isolates and ultimately classify the *P. aeruginosa* type IV pilins into five distinct phylogenetic groups [242]. The identification of pilin accessory genes in our panel of strains may inform resistance to different pili-binding phages. The role of these accessory genes in pilin modification can be examined by the separation of sheared surface pili from strains with accessory genes using SDS-PAGE; pilins with post-translational modifications migrate more slowly than their predicted molecular mass [242], indicating the presence of modifications.

The presence of two major pilin genes encoded in tandem in bacteria of the *Xanthomonadaceae* family [272] is also highly intriguing. Additional experiments are required to understand the role of *pilA2* in *S. maltophilia* pili assembly and the evolution of this gene duplication. In regard to phage infection, a single Δ *pilA2* mutant was constructed only in strain

ATCC 13637 that is susceptible to phage DLP6 and the type IV pili phage AXL1. Spotting of these phages on $\Delta pilA2$ revealed that both can still infect this mutant compared to loss of AXL1 infection on the $\Delta pilA1$ mutant (Figure 7-1). Analysis of twitching motility was not conducted in this mutant but based on the ability of AXL1 to still form plaques on the $\Delta pilA2$ mutant, it is likely that pili function is not affected to a large degree in that absence of PilA2. Additionally, because deletion of *pilA1* abolishes phage infection and twitching motility even though *pilA2* is intact, this suggests that only *pilA1* is the major pilin required for assembly of a functional pilus. No cross-complementation between the *pilA* alleles was completed in the constructed mutants; it is unknown if overexpression of *pilA2* in the $\Delta pilA1$ mutant may complement the phenotypes, as all *pilA2* genes identified in our strains appear to be intact and able to form properly folded pilins.




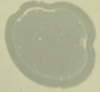


	AXL1	DLP6
ATCC 13637 WT		
ATCC 13637 $\Delta pilA1$		
ATCC 13637 $\Delta pilA2$		

Figure 7-1: Deletion of *pilA2* does not affect phage infection. Phage AXL1 forms plaques on *S. maltophilia* ATCC 13637 at 10^{10} PFU/mL. Deletion of *pilA1* abolishes plaque formation by AXL1, but deletion of *pilA2* does not. Phage DLP6 infection is not affected by deletion of either *pilA* gene.

Also not examined in this thesis is the gene expression profiles of the two pilins in *S. maltophilia*, therefore we do not know at this time whether both pilins are expressed simultaneously. The short intergenic space between *pilA1* and *pilA2* suggests that these pilins are expressed as an operon, similar to the three tandem flagellin *fliC* genes recently identified [52]. Analysis with BPROM (Softberry, Inc.) predicted promoter -10 and -35 sequences approximately 150 bp upstream of the *pilA1* gene start codon in *S. maltophilia* strains D1585,

D1571 and 280 but no promoter sequence was identified in the 105 bp intergenic region upstream of *pilA2*. Additionally, analysis of the sequences flanking the *pilA* genes with ARNold [332] identified Rho-independent transcription terminator sequences downstream of the *pilA1* stop codon in all three strains. Together, this suggests that only *pilA1* is expressed while *pilA2* is not. In the ATCC 13637 strain tested above however, no transcription terminator sequence was detected downstream of *pilA1*, and predicted promoters were present upstream of both alleles. Further examination of the expression of these genes in each strain by RT-PCR and use of a *xylE* or *lux* reporter assay with sequences upstream of each pilin gene will confirm the operon status of these genes and whether *pilA2* is expressed. Additional analysis of sheared surface pili by mass spectrometry will also inform the composition of the wildtype pilus if *pilA2* is expressed.

Phage engineering: expanding phage host range by RBP swapping

To improve the suitability of wild phages as candidates for phage therapy, methods for genetic modification of phage genomes are being explored. Due to the heterogeneity of *S. maltophilia* isolates, treatment of infections will require diverse cocktails of phages and combination therapy with antibiotics or other phage-derived antimicrobials. Genetic modification of lytic phages can overcome limitations and successfully expand phage host range, reduce toxicity and immunogenicity, and improve activity against biofilms or in combination with antibiotics [126,368,369]. A suite of genetic tools is available for the genetic modification of phages. Homologous recombination although common, is labour intensive and time consuming, while more efficient techniques such as bacteriophage recombineering of electroporated DNA (BRED) are limited to specific species, namely mycobacteriophages [369]. Most recently this technique was used to engineer a lytic derivative of a phage targeting *Mycobacterium abscessus* through deletion of its lytic repressor gene; this phage variant was subsequently used in combination with two other phages to treat a patient with cystic fibrosis following bilateral lung transplantation in the United Kingdom who was suffering from an antibiotic resistant infection [370]. This was the first use of engineered phages in human therapy and spearheads the acceptance of genetically engineering phages for human treatment.

A potential pitfall of homologous recombination is that although it is a rapidly occurring process, it does not take place efficiently in the limited time the cell has before phage-induced lysis and therefore requires extensive screening to identify the desired mutant. To circumvent the

toxicity of phage gene products within their bacterial host, phage genome assembly from synthetic DNA fragments containing the desired genetic changes is an alternate approach for more flexible engineering [59]. Widely applicable is Gibson assembly, the construction of synthetic phage genomes from PCR amplified fragments, a technique used by Mageeney et al. to construct their lytic prophage variants [371]. Yeast-based assembly of synthetic phages from PCR fragments has also proved efficient for modification of phage genomes [369]. Recently, Pires et al. used yeast recombineering to construct a minimal phage lacking numerous genes encoding hypothetical proteins that made up to 48% of its original genome with no deleterious effects on phage antibacterial efficacy [372]. Removal of genes encoding hypothetical proteins with unknown function creates room in the phage genome for replacement with genes encoding additional receptor binding proteins or enzymes to aid in host range expansion and cell lysis while remaining within the genome packaging capacity of the phage. However, care must be taken to ensure that hypothetical proteins chosen for removal do not negatively affect phage fitness. Additionally, phage hypothetical proteins encoded by early genes significantly affect host metabolism during phage infection and may have bactericidal effects upon overexpression, demonstrating an untapped source of inspiration for novel antimicrobial molecules with specific narrow spectrum bacterial targets [373,374].

Based on observations of an extended host range for AXL3 propagated in the presence of DLP2b tail proteins, AXL3 may be a suitable phage for genetic engineering specifically to swap receptor binding proteins and broaden its host range. As AXL3 is a virulent phage and will not be stably maintained within a cell during genetic manipulation, the application of synthetic biology and yeast recombineering is promising. In this method, long-range PCR can be used to amplify the entirety of the AXL3 viral genome, minus the gene replacement region, into 10 kb fragments using primers that add >30 bp homology to each adjacent fragment, with the first and last fragments containing ends homologous to a yeast artificial chromosome (YAC). Our desired DLP2b RBP gene(s) can be amplified with ends homologous to the AXL3 insertion site. Upon co-electroporation of these fragments and a linearized YAC into yeast cells, the highly efficient homologous recombination system in yeast joins each fragment to the adjacent one by gap repair, yielding a fully synthetic phage genome containing the desired RBP gene exchange in a replicative yeast plasmid. This phage DNA can then be extracted from the yeast and the phage rebooted by electroporation into the *S. maltophilia* host cells to restart viral replication, with

recombinant phage isolated from plaques. In this method, no screening is required against wildtype phage, and gene replacement options are limited only by PCR. Synthetic phage genomes have been successfully rebooted in numerous bacterial hosts, including *E. coli* and *P. aeruginosa* [58-60], but is not yet described for *S. maltophilia*. Ultimately, virulent AXL3 genome modification will produce broad-host-range phage particles adapted to adhere to and infect both *S. maltophilia* and *P. aeruginosa* strains that can be tested in phage cocktails in vitro for synergistic activity and in vivo for therapeutic effectiveness.

Alternatively, genome engineering of virulent phages has also been possible using CRISPR-Cas9, with studies showing effective gene replacement and deletion in lytic phages of *Streptococcus thermophilus* [375] and *Lactococcus lactis* [376]. Recently, the FDA approved a clinical trial (NCT04191148) sponsored by Locus Bioscience to treat urinary tract infections with their genetically engineering crPhage cocktail, containing CRISPR Cas3-enhanced phages targeting *E. coli* and will be the first controlled clinical trial for recombinant bacteriophage therapy, paving the way for future studies. Although CRISPR-Cas9 gene editing is effective, it largely relies on a native system in the bacterial host and phage escape mutants readily appear. New research has instead investigated the RNA-targeting Cas13a enzyme as an effective counter-selection tool to isolate rare recombinant phages in a mixed population following homologous recombination, with great success in *P. aeruginosa* and *E. coli* virulent phages [377,378]. The seemingly universal effectiveness against phages, even those with modified genomes that are often resistant to DNA-targeting CRISPR systems, and highly efficient counter-selection predicts that this technique will effectively enrich any viable edit in a phage genome whose host can express the Cas13a enzyme [378].

Although regulatory agencies and clinicians generally balk at the inclusion of temperate phages, properties such as the large burst size of *S. maltophilia* phage S4 and broad host range of DLP3 make these phages desirable for therapeutic applications. Recent advances in sequencing technologies and synthetic biology provides new opportunities to explore the use of modified versions of these phages for therapy by eliminating less favourable features or enhancing bacterial killing in different conditions and effectively improve the safety and efficacy of temperate phages [368]. The predicted abundance of prophages in *S. maltophilia* genomes (Figure 1-3), and bacterial genomes in general, described in Chapter 1 makes finding and isolating temperate phages easier than virulent phages. Recently, a technique was described by

Mageeney et al. [371] to mine bacterial genomes related to a target strain of interest for prophage elements that can be isolated and engineered to become lytic through the deletion of the integrase gene. The researchers show proof of concept using five prophages isolated from a single *P. aeruginosa* strain that they engineered for nonlysogeny and were effective against *P. aeruginosa* PA01 in both liquid and *G. mellonella* infection trials. This research sets the precedence to create a platform for on-demand production of therapeutic phages from closely related bacterial strains.

Though the potential application of these techniques to phage therapy has been shown in other species, genetic engineering of *S. maltophilia* phages has yet to be described. Due to the trend of DNA modification observed in *S. maltophilia* phages as the inability of numerous restriction endonucleases to digest DNA (Table 1-1), targeted genetic manipulation techniques may prove difficult. For this reason, alternative methods may be explored for the modification of *S. maltophilia* phages without the need for direct molecular manipulation. Directed evolution approaches harness principles of the natural arms race between phage and bacteria that has occurred in nature for over three billion years [379]. In the “Appelmans protocol,” spontaneous mutation and recombination occurs among a cocktail of phages grown together on a range of susceptible and resistant bacterial strains over several generations resulting in phages with expanded host ranges, created without the addition of new exogenous genetic information [379]. Chemically accelerated viral evolution (CAVE) is another approach to rapidly enhance desired phage characteristics through iterative cycling of chemical mutagenesis and phage selection [380]. Proof of principle was demonstrated using *E. coli* and *Salmonella enterica* phages evolved to possess improved thermal tolerance and stability over 30 rounds of mutagenesis and selection. The authors suggest that a variety of selection criteria may be employed using this platform to develop phages with increased therapeutic potential.

Perspectives on *S. maltophilia* phage therapy

S. maltophilia are good candidates for the application of phage therapy. These bacteria exhibit resistance to a broad range of antimicrobial treatments [217]. Additionally, the significant genetic and phenotypic heterogeneity within this species enables their rapid adaptation under changing selective pressures, with high mutation frequencies observed in clinical isolates [3,5,10,13,16,18]. These features hinder the effectiveness of current antibiotic treatment options in the long term. Fortunately, phages target and kill their bacterial hosts using different

mechanisms than antibiotics, making them effective therapeutics for antibiotic resistant bacteria. However, our research group has identified genes encoding antimicrobial resistance in *S. maltophilia* phages (ie. *dhfr*) and documented the lysogenic conversion by *S. maltophilia* phages, emphasizing the need for complete genomic characterization followed by experimental validation for phage therapy candidates against this bacterium. The development of a recombineering method for *S. maltophilia* phages using one of the methods described above would be extremely beneficial not only for the possibilities of genetic engineering to remove unwanted harmful genes, but to also refine the putative annotations and large proportion of hypothetical proteins encoded in these phages.

Another promising feature of *S. maltophilia* for a target of phage therapy is that to date, no phage defence systems have been characterized in *S. maltophilia*, including CRISPR (clustered regularly interspaced short palindromic repeat) systems that provide adaptive phage immunity in numerous bacterial pathogens. A staggering number of novel defence systems have been identified through bioinformatic analyses however in recent years, with the latest discoveries in two preprints from separate groups that each identify 21 novel systems [381,382]. The use of PADLOC v1.4.0 (Prokaryotic Antiviral Defence LOCator; updated April 25, 2022) [383] to detect phage defence systems in D1571, D1585 and 280 strains in our collection confirmed a lack of CRISPR systems, however a few common defence systems were identified in all strains, with each strain encoding between four and eight defence loci. These include putative restriction-modification systems, darTG [384] and AbiE [385] toxin-antitoxin systems, and novel Zorya type III [383], Gabija, and Wadjet systems [386]. Future research may explore whether these gene clusters are functional for defence against phage in these strains. Understanding the mechanisms of phage defence in *S. maltophilia* beyond mutations in cell surface receptors is beneficial to stave off complications in phage therapy applications; as well, this research may lead to the identification of phage countermeasures to overcome host defences, as observed with phage-encoded anti-CRISPR proteins [387]. Although CRISPR immunity may not present a challenge for the application of phages therapy against *S. maltophilia*, these novel systems require further exploration.

Beyond modification of *S. maltophilia* phages for therapy, reports of in vivo studies to determine the therapeutic potential of these phages are limited. Apart from rescue of *S. maltophilia* infected *G. mellonella* larvae by temperate phage DLP3 (Chapter 3) [178] and

murine rescue by phage SM1 [175], the in vivo behaviour and therapeutic potential of *S. maltophilia* phages is largely unknown. Testing the behaviour of individual phages and combinations in animal models is essential to determine their initial efficacy for therapy, as some phages that exhibit strong therapeutic potential in vitro are ineffective or unstable during in vivo trials [290]. The pharmacokinetics and effectiveness of phages following aerosolization, intravenous injection, or topical applications that mimic treatment of *S. maltophilia* lung, bloodstream and wound infections must also be explored.

Another area of phage research lacking for *S. maltophilia* specifically is the role of prophages in the virulence of *S. maltophilia*, as well as their effect on superinfection resistance. As shown in Figure 1-3, prophages are abundant in *S. maltophilia* genomes with no correlation of prophage abundance in strains of clinical origin compared to environmental origin. Early research into *S. maltophilia* phages examined prophages in the characterization of S1 [172] and Smp131 [176], two temperate phages isolated by induction from *S. maltophilia* strains, and most recently the transposable phage Φ SHP3 [182]. However, no research on native prophages in *S. maltophilia* has been conducted since the early 2010s. The effect of prophage-encoded metabolic genes on host metabolism, or protection from subsequent infection by other phages has been documented in other nosocomial pathogens, such as *P. aeruginosa*; pili-binding temperate phages encode inhibitors of type IV pilus function, ultimately preventing superinfection by other pili-binding phages during lysogeny, in the case of the Tip protein encoded by D3112 [166], and additionally can inhibit host quorum sensing in the case of Aqs1 encoded by phage DMS3 [388]. Based on the work presented in this thesis, the type IV pilus is a very prominent receptor for *S. maltophilia* phages. Similar systems may be encoded by prophages of *S. maltophilia* phages and can have significant impact on the application of phage therapy in patients.

In our panel of strains, we have numerous hosts that are not susceptible to any of our type IV pili phages, including strains 152, 155, 217, 278, and 446, as well as two strains, 236 and 249, that are resistant to all our phages (Table 3-3). Whether this resistance is due to variable pilin sequences or post-translational modifications that are not compatible with phage RBPs, as described above, or possibly intracellular phage defenses encoded by the bacterium or resident prophages is worthy knowledge to inform future phage resistance of clinical isolates. Analysis of the D1585, 280 and D1571 contigs for prophages using PHASTER [111,112] revealed few intact sequences in D1585 and D1571, but none in strain 280. Interestingly, our D1585 main host strain

for the propagation of five type IV pili phages appears to be prophage free when induced; unpublished research conducted by previous PhD candidate Danielle Peters involved treating different *S. maltophilia* strains with mitomycin C to induce any prophages, followed by concentration by ultracentrifugation and visualization by TEM. She observed no phage-like particles in the concentrated supernatant from induction of strain D1585, however phage particles resembling tailed dsDNA phages and filamentous phages were abundant in lysate from strain D1571. Strain D1614 lysate contained obvious *Inoviridae* particles and strain 280 contained many filaments that could represent phages. The apparent absence of functional prophages in D1585 may contribute to the sensitivity of this strain to phages but is also a promising feature for D1585 as a manufacturing strain for GMP production of *S. maltophilia* phages for therapy, as no contaminating phages will be induced from phage production.

As discussed throughout this thesis, there is a lack of receptor knowledge for *S. maltophilia* phages isolated by other groups. As all of our phages have been isolated from soil samples, it is unknown if the type IV pilus is a common receptor for Siphoviridae phages isolated from other sources or if *S. maltophilia* podoviruses also use the type IV pilus, as observed for *Xylella* phages Prado and Paz [281] and *P. aeruginosa* phages MPK7 [258], F116 [255], and Φ KMV [389]. Through personal observations and in vitro bacterial kill curves using pili phages specifically (Figures 4-2, 5-2), resistant mutants arise easily, however phage resistant mutants for the non-pili binding phage DLP6 do not. The discovery of new receptors for *S. maltophilia* phages beyond the type IV pilus would be beneficial in the construction of effective phage combinations to limit the emergence of a resistant bacterial population. However, we have not explored the efficacy of a phage cocktail using only type IV pili-binding phages.

A final discovery from this thesis is the ability of *S. maltophilia* and *Xanthomonas* phages to cross infect these bacterial species. It is possible that an overlap in the environmental niche allows for, and possibly selects for, phages with broad host ranges [144]. The numerous *Xanthomonas* phages characterized for agricultural phage therapy [279] may therefore be an untapped source of diverse phages for the treatment of *S. maltophilia* infections. We have shown that DLP6 can infect *Xanthomonas*, indicating that this cross-genera infection is not limited to type IV pili phages. Although this finding is exciting, it also has implications for agricultural applications of phage therapy to treat plant diseases caused by *Xanthomonas* and *Xylella* species. Commercial phage products exist for the treatment of Pierce's Disease in grapevines, caused by

Xylella fastidiosa; this product contains a mixture of phages that use the type IV pilus as their receptor and also infect *Xanthomonas* spp. [281,282]. To our knowledge, these phages have not been tested against *Stenotrophomonas* spp.; as a prominent environmental bacterial genus shown to have beneficial roles in promoting plant growth [6], the excessive application of these phages may negatively affect the microbial environment of the soil. Adding excessive amounts of these *Xanthomonas* phages to the soil for treatment of plant disease may also create selective pressure in environmental strains of *S. maltophilia*, causing an increase in phage resistance that could cross over to clinical settings. These findings emphasize how a complete understanding of phage host range is imperative prior to releasing phages in an agricultural setting. In this example, broad host range phages may not be ideal in certain applications.

Significance

With the prevalence of multidrug resistant *S. maltophilia* infections rising worldwide, particularly in the cystic fibrosis community, research into the mechanisms underlying disease progression and resistance to antimicrobials is essential. The frontline recommended antimicrobial drug of choice against *S. maltophilia* infections is trimethoprim-sulfamethoxazole, however, resistance to this antibiotic is on the rise globally due to the spread of *sul* and *dfrA* genes [100]. With pharmaceutical companies largely abandoning the development of novel antibiotics due to a lack of return on investment [390,391], alternative therapeutics must be investigated to combat these multidrug resistant *S. maltophilia* infections.

Bacteriophages with the proper characterization represent a promising alternative treatment option for antimicrobial resistant bacterial infections. The isolation of 57 unique dsDNA phages against *S. maltophilia* in the last 15 years, at least twelve of which are experimentally confirmed to be virulent, demonstrates the ease of isolation and shows promise for the future application of phage therapy against this pathogen. The research presented in this thesis expands our knowledge of phage-host interactions in *S. maltophilia* by identifying the type IV pilus as a common receptor for phages infecting this species. This knowledge will be beneficial in the design of therapeutic phage cocktails. Further in vivo research into the efficacy of these phages individually and in multi-phage cocktails or in combination with other antimicrobials will spearhead the clinical use of *S. maltophilia* phage therapy.

Appendix – Genomic characterization of *Xanthomonas* phage HXX

Contributions:

Special thanks to MSc student Brittany Supina for conducting the initial propagation of phage HXX in different media to create the phage lysate that was used in host range analysis, along with initial observations of plaque morphology. Additional thanks to Brittany and 298 undergraduate student Caroline MacDonald for initial screening of HXX on *S. maltophilia* hosts.

Objectives

Xanthomonas phage HXX was obtained from the Félix d'Hérelle Reference Center for Bacterial Viruses at the Université Laval. This phage was originally isolated from soil at a cabbage farm in Honolulu, Hawaii in 1981 using *Xanthomonas campestris* XC114 as an isolation host strain [278]. As shown in Chapter 3, I discovered that phage HXX is also capable of infecting a broad range of *Stenotrophomonas maltophilia* clinical isolates. Despite its isolation in the early 1980s, phage HXX has not been described in the literature since and the genome sequence is not available. To further characterize this phage and understand its relationship to *Xanthomonas* or *Stenotrophomonas* phages, the goal of this chapter is the complete genomic analysis of our HXX phage lysate, which we have named HXX_Dennis to account for genetic drift over the last 40 years.

Materials and Methods

Bacterial strains, growth conditions and phage propagation

X. campestris XC114 (HER1103) (ATCC33440) and phage HXX (HER103) were obtained from the Félix d'Hérelle Reference Center for Bacterial Viruses, along with a *X. oryzae* (thy H; HER1154) strain. *X. translucens* pv. *translucens* ATCC19319 and *X. axonopodis* pv. *vasculorum* FB570 were obtained from the Summerland Research Centre in British Columbia for extended host range analysis. Bacteria were grown at 30°C on full LB solid media for 24 or 48 h until single colonies appeared, or in LB broth with shaking at 225 RPM for 18 h.

Phage HXX was propagated to high titre on *X. campestris* XC114 using soft agar overlays as previously described [115,229]. Briefly, 100 µL of XC114 overnight culture and 100 µL of a 10⁻² dilution of HXX stock was incubated for 20 min, mixed with 3 mL of 0.7% ½ LB top agar and overlaid onto plates of LB solid media and incubated at 30°C overnight. Plates with confluent lysis were overlaid with 3 mL of modified suspension medium (SM) (50 mM Tris-HCl pH 7.5, 100 mM NaCl, 10 mM MgSO₄) and the top agar was collected and incubated for 2 h at room temperature on a platform rocker with 20 µL of chloroform per plate. Solids were pelleted by centrifugation and the supernatant was filter sterilized using a Millex-HA 0.45 µm syringe-driven filter unit (Millipore, Billerica, MA) and stored at 4°C. The titre of the phage stock was

obtained by serial dilutions in SM and spotting on XC114 overlays. Host range analysis on *S. maltophilia* clinical isolates were conducted similarly.

HXX DNA isolation and genome sequencing

HXX genomic DNA (gDNA) was isolated by phenol/chloroform extraction and ethanol precipitation as previously described [115]. Following incubation with proteinase K, gDNA from a nuclease-treated high titre phage lysate was isolated with three phenol:chloroform extractions and a single chloroform wash. Phage DNA was ethanol precipitated and dissolved in sterile milli-Q water. A NanoDrop ND-1000 spectrophotometer (Thermo Scientific, Waltham, MA) was used to determine the purity and concentration of phage gDNA. A second round of ethanol precipitation was conducted on pooled samples to improve the DNA purity and the concentration and quality was confirmed by running an aliquot on a 1% agarose gel.

Sequencing of HXX was performed at the Microbial Genome Sequencing Center (MiGS; Pittsburgh, PA, USA). Sample libraries were prepared using the Illumina DNA Prep kit and IDT 10bp UDI indices, and sequenced on an Illumina NextSeq 2000, producing 2x151bp reads. Demultiplexing, quality control and adapter trimming was performed with bcl-convert (v3.9.3). 2,289,428 total reads were produced with 89.7% bp greater than Q30.

Bioinformatics

Quality control analysis was completed using FastQC v0.11.9 [301]. SPAdes v3.11.1 [303] was used to assemble a 44,700 bp contig with 2,242,808 reads mapping to the contig to give a mean coverage of 7,526 reads. No regions of low coverage were detected and the ends of the contig were confirmed with PCR using primers HHX endF 5'-CGG TAA TCC CAT CCT GTA CGG-3' and HXX endR 5'-CCA TCG TAT CGG AAG CCC AG-3' followed by Sanger sequencing of the product. This identified a 77 bp duplication in the assembly, resulting in a 44,623 bp genome after its removal. The genome start site was determined by convention and placed upstream of the gene encoding the terminase large subunit, similar to related phage genome Suso (accession MZ326866).

Predicted protein coding genes were identified using the GLIMMER3 plugin [304] for Geneious using the Bacteria and Archaea setting, min gene length of 50 bp and max overlap of

75 bp, as well as GeneMarkS for phage [331] and Prodigal [306]. Annotations to the contig and visualization of the genome was done using Geneious Prime v2022.0.1 [230]. BLASTn was used to identify relatives based on genomic data and putative protein functions were assigned using BLASTp limited to Viruses (taxid:10239) on the NCBI non-redundant protein sequence and nucleotide collection databases (update date: 2022/05/16) [264]. Conserved domain searches were performed using CD-Search against the CDD v3.19 – 58235 PSSMs database and default options [265] to support functional annotation. TMHMM [307] and LipoP 1.0 [308] were used to identify transmembrane regions and predict lipoproteins, respectively, in putative lysis proteins. tRNAscan-SE software with the general tRNA model [309] and Aragorn v1.2.36 [310] were used to identify potential tRNA genes. Rho-independent transcription terminator sequences were identified using ARNold [332] and 7 putative terminators with ΔG values less than -10 kcal/mol were included.

Results and Discussion

HXX_Dennis host range

As described in Liew and Alvarez (1981), phage HXX has a Siphoviridae morphology and at the time of isolation, a narrow host range capable of infecting only one out of the nine *X. campestris* strains tested [278]. Using our HXX_Dennis lysate, we found that this phage can infect three additional *Xanthomonas* species (Table 3-4). Furthermore, analysis of phage infectivity across our panel of 30 phenotypically distinct *S. maltophilia* strains revealed positive infection on 18 strains at a range of efficiencies (Table A-1). Surprisingly, HXX_Dennis replicates more efficiently on *S. maltophilia* strain 101 than on its propagation host, *X. campestris* XC114. Additionally, a variation in plaque size was observed on different hosts, as observed for phage AXL1. HXX_Dennis infection of *P. aeruginosa* strains was not tested.

Genomic characterization

The HXX_Dennis genome is 44,623 bp in length with a GC content of 67.4% and is predicted to encode 70 proteins (Figure A-1, Table A-2). BLASTn analysis shows high relatedness to only two *S. maltophilia* phages, Suso [213] with approximately 96% sequence

Table A-1: Host range analysis of *Xanthomonas* phage HXX_Dennis on clinical *S. maltophilia* isolates.

<i>S. maltophilia</i> strain	HXX_Dennis EOP ^a
101	1.22
102	++
103	+
152	-
155	-
174	0.21
176	-
213	++
214	++
217	-
218	-
219	+++
230	2.52x10 ⁻⁵
236	-
242	-
249	-
278	++
280	++
282	-
287	0.088
446	-
667	0.10
D1585	0.0014
D1571	0.59
D1614	-
D1576	0.62
D1568	-
ATCC 13637	2.6x10 ⁻⁸
SMDP92	+
VLJ1	++

^a Where plaque formation was not observed, phages were scored as having lytic activity on a given strain at a 10⁻² dilution (+++), a 10⁻¹ dilution (++), undiluted lysate (+), or no infection (-). The phage stock used had a concentrations of 10¹¹ PFU/mL on *X. campestris* XC114 (EOP 1.0)

identity over 99% of the genome, and SM171 (accession: MZ611865) having 95.4% identity with 98% genome coverage. The next closest relatives share less than 3% identity with HXX_Dennis and include *P. aeruginosa* phages. Functional predictions for the 70 putative proteins by BLASTp analysis produced significant matches for 69 proteins, with 21 sequences

hitting to phage SM171 and the remaining proteins matching to phage Suso (Table A-2). Only 27 proteins could be assigned putative function based on BLASTp hits or the presence of conserved domains (Table A-3). These include genes encoding a terminase large subunit (teal) involved in DNA packaging and 14 proteins required for virion morphogenesis (green), including a T₆C slippery sequence resulting in the expression of two tape measure chaperone proteins, gp28 and gp29, from a single start codon via a translational frameshift. An additional five genes encode proteins predicted to be involved in cell lysis (red) and seven gene encode proteins involved in DNA replication and repair (blue). Interestingly, Gp70 contains a ParB_N_Srx superfamily domain, suggesting a potential partitioning system that allows the maintenance of the HXX_Dennis genome as a phagemid during a temperate replication cycle. Further research can confirm this via isolation of lysogens in *X. campestris* XC114 and *S. maltophilia* strains. The genome sequence of HXX_Dennis with putative annotations has been deposited in Genbank with the accession number ON711490.

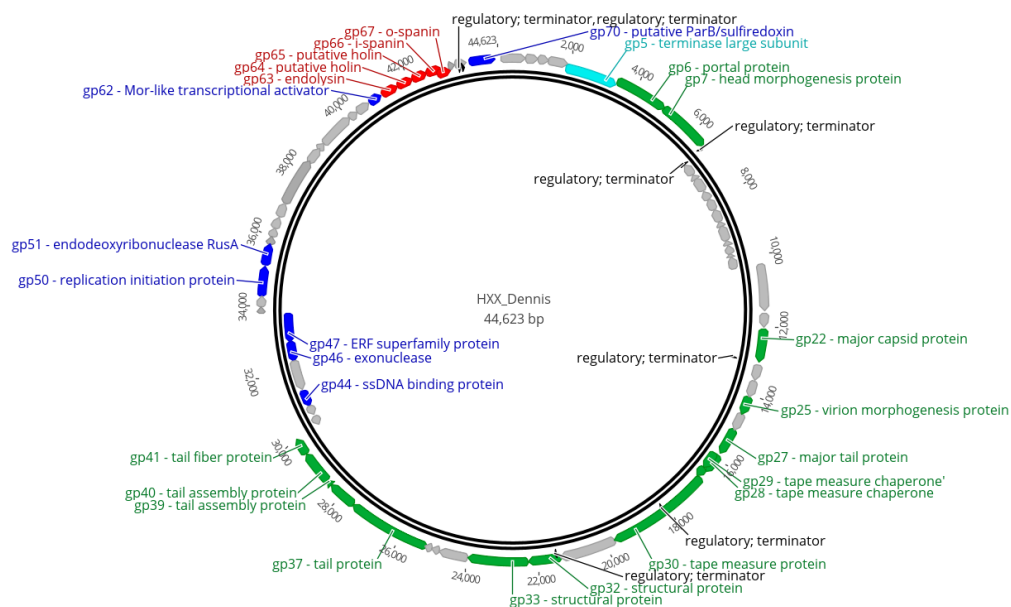


Figure A-1: Circularized genomic map of HXX_Dennis. The scale (in bp) is shown on the outer periphery. Assigned putative functions for each of the 70 predicted open reading frames are classified as follows: lysis (red), DNA replication and repair (blue), DNA packaging (teal), virion morphogenesis (green), hypothetical (grey). Regulatory elements are terminators (black). No tRNA genes were identified. HXX_Dennis has a GC content of 67.4%. Image created using Geneious Prime [230].

Table A-2: Genome annotations for HXX_Dennis obtained from BLASTp and CD-search data.

CDS	Coding region	Strand	Length (AA)	Putative function	Hit	Species	Cov. (%)	E value	ID (%)	Accession
1	52-753	+	233	hypothetical protein	FtsK-like DNA translocase	Stenotrophomonas phage Suso	100	3.00E-163	97.42	QZI85804 .1
2	758-1105	+	115	hypothetical protein	hypothetical protein	Stenotrophomonas phage Suso	100	6.00E-53	68.85	QZI85805 .1
3	1110-1409	+	99	hypothetical protein	hypothetical protein	Stenotrophomonas phage SM171	100	4.00E-61	95.96	QYW063 89.1
4	1411-1968	+	185	hypothetical protein	hypothetical protein	Stenotrophomonas phage SM171	100	3.00E-132	100	QYW063 90.1
5	1929-3452	+	507	terminase large subunit	terminase large subunit	Stenotrophomonas phage Suso	100	0.00E+0	99.8	QZI85808 .1
6	3455-4972	+	505	portal protein	portal protein	Stenotrophomonas phage Suso	100	0.00E+0	100	QZI85809 .1
7	4969-6489	+	506	head morphogenesis protein	capsid morphogenesis protein	Stenotrophomonas phage Suso	100	0.00E+0	100	QZI85810 .1
8	6981-6580	-	133	hypothetical protein	hypothetical protein CPT_Suso_008	Stenotrophomonas phage Suso	100	7.00E-94	100	QZI85811 .1
9	7121-6875	-	48	hypothetical protein	hypothetical protein CPT_Suso_009	Stenotrophomonas phage Suso	100	3.00E-25	100	QZI85812 .1
10	7582-7118	-	154	hypothetical protein	hypothetical protein CPT_Suso_010	Stenotrophomonas phage Suso	100	5.00E-107	100	QZI85813 .1
11	7893-7591	-	100	hypothetical protein	hypothetical protein CPT_Suso_011	Stenotrophomonas phage Suso	100	3.00E-66	100	QZI85814 .1
12	8252-7890	-	120	hypothetical protein	putative membrane protein	Stenotrophomonas phage Suso	100	2.00E-80	100	QZI85815 .1
13	8678-8256	-	140	hypothetical protein	hypothetical protein CPT_Suso_013	Stenotrophomonas phage Suso	100	3.00E-100	100	QZI85816 .1
14	8829-8665	-	54	hypothetical protein	hypothetical protein CPT_Suso_014	Stenotrophomonas phage Suso	100	3.00E-30	98.15	QZI85817 .1
15	9302-8826	-	158	hypothetical protein	hypothetical protein CPT_Suso_015	Stenotrophomonas phage Suso	100	5.00E-111	100	QZI85818 .1
16	9478-9299	-	59	hypothetical protein	putative membrane protein	Stenotrophomonas phage Suso	100	5.00E-34	100	QZI85819 .1
17	9741-9484	-	85	hypothetical protein	hypothetical protein CPT_Suso_017	Stenotrophomonas phage Suso	100	8.00E-54	100	QZI85820 .1

18	9854-9741	-	37	hypothetical protein	-	-	-	-	-	-
19	10243-9851	-	130	hypothetical protein	hypothetical protein CPT Suso_018	Stenotrophomonas phage Suso	64	2.00E-55	100	QZI85821 .1
20	10253-11581	+	442	hypothetical protein	putative membrane protein	Stenotrophomonas phage Suso	100	0.00E+0 0	100	QZI85822 .1
21	11643-12026	+	127	hypothetical protein	hypothetical protein CPT Suso_020	Stenotrophomonas phage Suso	100	3.00E-81	99.21	QZI85823 .1
22	12086-13015	+	309	major capsid protein	major capsid protein	Stenotrophomonas phage Suso	100	0.00E+0 0	100	QZI85824 .1
23	13102-13548	+	148	hypothetical protein	hypothetical protein CPT Suso_022	Stenotrophomonas phage Suso	100	1.00E-95	97.97	QZI85825 .1
24	13574-14044	+	156	hypothetical protein	hypothetical protein CPT Suso_023	Stenotrophomonas phage Suso	100	2.00E-109	99.36	QZI85826 .1
25	14037-14582	+	181	virion morphogenesis protein	virion morphogenesis family protein	Stenotrophomonas phage SM171	100	2.00E-125	98.9	QYW064 08.1
26	14579-15058	+	159	hypothetical protein	hypothetical protein CPT Suso_025	Stenotrophomonas phage Suso	100	9.00E-110	100	QZI85828 .1
27	15071-15835	+	254	major tail protein	major tail protein	Stenotrophomonas phage SM171	100	0.00E+0 0	99.61	QYW064 10.1
28	15929-16507	+	192	tape measure chaperone	tape measure chaperone	Stenotrophomonas phage Suso	100	2.00E-136	100	QZI85830 .1
29	15929-16734	+	269	tape measure chaperone'	tape measure chaperone	Stenotrophomonas phage Suso	100	0	100	QZI85831 .1
30	16731-19757	+	1008	tape measure protein	tail tape measure protein	Stenotrophomonas phage SM171	100	0.00E+0 0	98.61	QYW064 12.1
31	19761-21335	+	524	hypothetical protein	structural protein	Stenotrophomonas phage SM171	94	0.00E+0 0	99.19	QYW063 54.1
32	21342-22286	+	314	structural protein	structural protein	Stenotrophomonas phage SM171	100	0.00E+0 0	98.73	QYW063 55.1
33	22289-23989	+	566	structural protein	structural protein	Stenotrophomonas phage SM171	100	0.00E+0 0	98.23	QYW063 56.1
34	23979-24803	+	274	hypothetical protein	tail assembly protein	Stenotrophomonas phage SM171	100	0.00E+0 0	93.8	QYW063 57.1
35	24812-25045	+	77	hypothetical protein	tail assembly protein	Stenotrophomonas phage SM171	100	2.00E-48	98.7	QYW063 58.1
36	25042-25251	+	69	hypothetical protein	tail assembly protein	Stenotrophomonas phage SM171	100	6.00E-40	92.75	QYW063 59.1

37	25241-27604	+	787	tail protein	minor tail protein	Stenotrophomonas phage Suso	100	0.00E+00	96.57	QZI85839.1
38	27597-28424	+	275	tail fiber protein	tail fiber protein	Stenotrophomonas phage SM171	100	0.00E+00	97.82	QYW06361.1
39	28421-28588	+	55	tail assembly protein	hypothetical protein CPT_Suso_038	Stenotrophomonas phage Suso	100	2.00E-30	100	QZI85841.1
40	28596-29558	+	320	tail assembly protein	tail assembly protein	Stenotrophomonas phage SM171	100	0.00E+00	92.81	QYW06362.1
41	29558-30052	+	164	tail fiber protein	tail fiber protein	Stenotrophomonas phage SM171	100	1.00E-116	100	QYW06363.1
42	30378-30070	-	102	hypothetical protein	hypothetical protein	Stenotrophomonas phage SM171	100	7.00E-62	98.04	QYW06364.1
43	30738-30424	-	104	hypothetical protein	hypothetical protein	Stenotrophomonas phage SM171	100	8.00E-71	100	QYW06365.1
44	31253-30747	-	168	ssDNA -binding protein	DNA-binding protein	Stenotrophomonas phage SM171	100	7.00E-120	100	QYW06366.1
45	32240-31308	-	310	hypothetical protein	hypothetical protein CPT_Suso_044	Stenotrophomonas phage Suso	100	0.00E+00	99.68	QZI85847.1
46	32866-32237	-	209	exonuclease	exonuclease	Stenotrophomonas phage SM171	100	4.00E-153	100	QYW06368.1
47	33771-32869	-	300	ERF superfamily protein	ERF superfamily protein	Stenotrophomonas phage SM171	100	0.00E+00	100	QYW06369.1
48	33770-33964	+	64	hypothetical protein	hypothetical protein CPT_Suso_047	Stenotrophomonas phage Suso	100	1.00E-40	100	QZI85850.1
49	33961-34266	+	101	hypothetical protein	hypothetical protein	Stenotrophomonas phage SM171	100	3.00E-69	100	QYW06370.1
50	34263-35129	+	288	replication initiation protein	DnaD-like primosome initiator	Stenotrophomonas phage Suso	100	0.00E+00	100	QZI85852.1
51	35150-35752	+	200	endodeoxyribonuclease RusA	RusA-like resolvase/endonuclease	Stenotrophomonas phage Suso	100	2.00E-148	100	QZI85853.1
52	35749-35970	+	73	hypothetical protein	hypothetical protein	Stenotrophomonas phage SM171	100	2.00E-45	100	QYW06373.1
53	35960-36217	+	85	hypothetical protein	hypothetical protein CPT_Suso_052	Stenotrophomonas phage Suso	100	5.00E-57	100	QZI85855.1
54	36207-36542	+	111	hypothetical protein	hypothetical protein CPT_Suso_053	Stenotrophomonas phage Suso	100	4.00E-77	100	QZI85856.1
55	36572-36988	+	138	hypothetical protein	hypothetical protein CPT_Suso_54	Stenotrophomonas phage Suso	100	2.00E-93	100	QZI85857.1

56	36981-38357	+	458	hypothetical protein	hypothetical protein CPT_Suso_055	Stenotrophomonas phage Suso	100	0.00E+00	99.56	QZI85858
57	38354-38797	+	147	hypothetical protein	hypothetical protein CPT_Suso_056	Stenotrophomonas phage Suso	100	3.00E-105	99.32	QZI85859
58	38787-39008	+	73	hypothetical protein	hypothetical protein CPT_Suso_057	Stenotrophomonas phage Suso	100	2.00E-45	100	QZI85860
59	39005-40030	+	341	hypothetical protein	hypothetical protein CPT_Suso_058	Stenotrophomonas phage Suso	100	0.00E+00	99.71	QZI85861
60	40027-40296	+	89	hypothetical protein	hypothetical protein CPT_Suso_059	Stenotrophomonas phage Suso	100	7.00E-59	100	QZI85862
61	40293-40718	+	141	hypothetical protein	hypothetical protein CPT_Suso_060	Stenotrophomonas phage Suso	100	4.00E-102	100	QZI85863
62	40737-41114	+	125	Mor-like transcriptional activator	Mor-like transcriptional activator	Stenotrophomonas phage Suso	100	4.00E-85	100	QZI85864
63	41138-41647	+	169	endolysin	endolysin L-alanoyl-D-glutamate peptidase	Stenotrophomonas phage Suso	100	4.00E-120	100	QZI85865
64	41647-42123	+	158	putative holin	holin/antiholin class IV	Stenotrophomonas phage Suso	100	7.00E-109	100	QZI85866
65	42120-42548	+	142	putative holin	holin/antiholin class I	Stenotrophomonas phage Suso	100	1.00E-93	96.48	QZI85867
66	42545-42991	+	148	i-spanin	i-spanin	Stenotrophomonas phage Suso	100	3.00E-96	99.32	QZI85868
67	42825-43214	+	129	o-spanin	o-spanin	Stenotrophomonas phage Suso	100	4.00E-88	99.22	QZI85869
68	43189-43368	+	59	hypothetical protein	hypothetical protein CPT_Suso_067	Stenotrophomonas phage Suso	100	3.00E-33	98.31	QZI85870
69	43393-43722	+	109	hypothetical protein	hypothetical protein CPT_Suso_068	Stenotrophomonas phage Suso	100	4.00E-68	93.1	QZI85871
70	43798-44547	+	249	putative ParB/sulfiredoxin	DNA methylase	Stenotrophomonas phage Suso	100	1.00E-179	99.6	QZI85872

Table A-3: The conserved domains found in 70 HXX_Dennis proteins.

Gp	Hit type	PSSM-ID	From	E-Value	Accession	Short name	Superfamily
4	superfamily	413393	27-87	0.000233	cl02600	HTH_MerR-SF superfamily	-
5	superfamily	413239	293-443	1.33E-33	cl02216	Terminase_6C superfamily	-
6	superfamily	418688	57-500	2.25E-60	cl19863	DUF935 superfamily	-
7	superfamily	225244	21-213	9.134E-25	cl26983	COG2369 superfamily	
24	specific	399783	3-107	5.33E-22	pfam07030	DUF1320	cl01818
25	superfamily	413185	5-154	4.942E-13	cl02089	Phage_tail_S superfamily	
30	specific	131723	163-242	1.18E-13	TIGR02675	tape_meas_nterm	cl31236
30	superfamily	227606	151-905	3.94E-09	cl34971	COG5281 superfamily	-
34	superfamily	274038	23-270	1.32E-20	cl37077	phg_TIGR02218 superfamily	-
37	superfamily	404441	236-410	2.32E-08	cl38419	Phage-tail_3 superfamily	-
38	superfamily	421990	13-46	5.99E-05	cl31489	Mtd_N superfamily	-
38	specific	396114	106-161	0.0028469	pfam01391	Collagen	cl22949
41	superfamily	407331	104-147	1.00E-07	cl25441	SdrD_B superfamily	-
44	specific	181549	1-168	2.72E-88	PRK08763	PRK08763	cl09930
45	superfamily	406371	109-141	0.0007283	cl25546	Casc1_N superfamily	-
45	superfamily	173502	47-139	0.0008828	cl31758	PTZ00266 superfamily	-
47	superfamily	398211	21-147	9.23E-13	cl04500	ERF superfamily	-
50	superfamily	421991	158-224	8.84E-11	cl32029	DnaT superfamily	-

51	specific	399102	16-141	1.09E-30	pfam05866	RusA	cl01885
54	specific	404502	36-94	6.61E-18	pfam13619	KTSC	cl16325
60	specific	396104	26-77	0.0004619	pfam01381	HTH_3	cl22854
62	superfamily	413289	36-117	0.0049606	cl02360	Mor superfamily	
63	specific	350620	18-164	7.55E-20	cd14845	L-Ala-D-Glu_peptidase_like	cl38918
70	superfamily	421688	29-101	1.04E-09	cl28891	ParB_N_Srx superfamily	-

Bibliography

1. O'Neill, J. Tackling drug-resistant infections globally: Final report and recommendations. *Rev. Antimicrob. Resist.* **2016**, 1–84, doi:10.1016/j.jpha.2015.11.005.
2. Academies, C. of C. *When antibiotics fail: the expert panel on the potential socio-economic impacts of antimicrobial resistance in Canada*; Ottawa (ON), 2019; ISBN 9781926522753.
3. Brooke, J.S. *Stenotrophomonas maltophilia*: An emerging global opportunistic pathogen. *Clin. Microbiol. Rev.* **2012**, 25, 2–41, doi:10.1128/CMR.00019-11.
4. Huang, T.P.; Lee Wong, A.C. Extracellular fatty acids facilitate flagella-independent translocation by *Stenotrophomonas maltophilia*. *Res. Microbiol.* **2007**, 158, 702–711, doi:10.1016/j.resmic.2007.09.002.
5. Pompilio, A.; Pomponio, S.; Crocetta, V.; Gherardi, G.; Verginelli, F.; Fiscarelli, E.; Dicuonzo, G.; Savini, V.; D'Antonio, D.; Di Bonaventura, G. Phenotypic and genotypic characterization of *Stenotrophomonas maltophilia* isolates from patients with cystic fibrosis: Genome diversity, biofilm formation, and virulence. *BMC Microbiol.* **2011**, 11, 159, doi:10.1186/1471-2180-11-159.
6. Ryan, R.P.; Monchy, S.; Cardinale, M.; Taghavi, S.; Crossman, L.; Avison, M.B.; Berg, G.; van der Lelie, D.; Dow, J.M. The versatility and adaptation of bacteria from the genus *Stenotrophomonas*. *Nat. Rev. Microbiol.* **2009**, 7, 514–525, doi:10.1038/nrmicro2163.
7. Hugh, R.; Ryschenkow, E. *Pseudomonas maltophilia*, an *Alcaligenes*-like species. *J. Gen. Microbiol.* **1961**, 26, 123–132, doi:10.1099/00221287-26-1-123.
8. Swings, J.; De Vos, P.; Van den Mooter, M.; De Ley, J. Transfer of *Pseudomonas maltophilia* Hugh 1981 to the genus *Xanthomonas* as *Xanthomonas maltophilia* (Hugh 1981) comb. nov. *Int. J. Syst. Bacteriol.* **1983**, 33, 409–413, doi:10.1099/00207713-33-2-409.
9. Palleroni, N.J.; Bradbury, J.F. *Stenotrophomonas*, a new bacterial genus for *Xanthomonas maltophilia* (Hugh 1980) Swings et al. 1983. *Int. J. Syst. Bacteriol.* **1993**, 43, 606–609, doi:10.1099/00207713-43-3-606.
10. Svensson-Stadler, L.A.; Mihaylova, S.A.; Moore, E.R.B. *Stenotrophomonas* interspecies

- differentiation and identification by *gyrB* sequence analysis. *FEMS Microbiol. Lett.* **2012**, 327, 15–24, doi:10.1111/j.1574-6968.2011.02452.x.
11. Peters, D.L.; Lynch, K.H.; Stothard, P.; Dennis, J.J. The isolation and characterization of two *Stenotrophomonas maltophilia* bacteriophages capable of cross-taxonomic order infectivity. *BMC Genomics* **2015**, 16, 664, doi:10.1186/s12864-015-1848-y.
 12. Berg, G.; Roskot, N.; Smalla, K. Genotypic and phenotypic relationships between clinical and environmental isolates of *Stenotrophomonas maltophilia*. *J. Clin. Microbiol.* **1999**, 37, 3594–3600, doi:10.1128/jcm.37.11.3594-3600.1999.
 13. Berg, G.; Martinez, J.L. Friends or foes: can we make a distinction between beneficial and harmful strains of the *Stenotrophomonas maltophilia* complex? *Front. Microbiol.* **2015**, 6, 241, doi:10.3389/fmicb.2015.00241.
 14. Pages, D.; Rose, J.; Conrod, S.; Cuine, S.; Carrier, P.; Heulin, T.; Achouak, W. Heavy metal tolerance in *Stenotrophomonas maltophilia*. *PLoS One* **2008**, 3, 1539, doi:10.1371/journal.pone.0001539.
 15. Mukherjee, P.; Roy, P. Genomic potential of *Stenotrophomonas maltophilia* in bioremediation with an assessment of its multifaceted role in our environment. *Front. Microbiol.* **2016**, 7, 967, doi:10.3389/fmicb.2016.00967.
 16. Pompilio, A.; Crocetta, V.; Ghosh, D.; Chakrabarti, M.; Gherardi, G.; Vitali, L.A.; Fiscarelli, E.; Di Bonaventura, G. *Stenotrophomonas maltophilia* phenotypic and genotypic diversity during a 10-year colonization in the lungs of a cystic fibrosis patient. *Front. Microbiol.* **2016**, 7, 1551, doi:10.3389/fmicb.2016.01551.
 17. Valdezate, S.; Vindel, A.; Martín-Dávila, P.; Del Saz, B.S.; Baquero, F.; Cantón, R. High genetic diversity among *Stenotrophomonas maltophilia* strains despite their originating at a single hospital. *J. Clin. Microbiol.* **2004**, 42, 693–699, doi:10.1128/JCM.42.2.693-699.2003.
 18. Turrientes, M.C.; Baquero, M.R.; Sánchez, M.B.; Valdezate, S.; Escudero, E.; Berg, G.; Cantón, R.; Baquero, F.; Galán, J.C.; Martínez, J.L. Polymorphic mutation frequencies of clinical and environmental *Stenotrophomonas maltophilia* populations. *Appl. Environ. Microbiol.* **2010**, 76, 1746–1758, doi:10.1128/AEM.02817-09.
 19. Chang, Y.T.; Lin, C.Y.; Chen, Y.H.; Hsueh, P.R. Update on infections caused by

- Stenotrophomonas maltophilia* with particular attention to resistance mechanisms and therapeutic options. *Front. Microbiol.* **2015**, *6*, 893, doi:10.3389/fmicb.2015.00893.
20. Canadian Antimicrobial Resistance Alliance CANWARD Pathogens 2018 Available online: <http://www.can-r.com/study.php?study=canw2018&year=2018> (accessed on Apr 26, 2021).
 21. Gröschel, M.I.; Meehan, C.J.; Barilar, I.; Diricks, M.; Gonzaga, A.; Steglich, M.; Conchillo-Solé, O.; Scherer, I.C.; Mamat, U.; Luz, C.F.; et al. The phylogenetic landscape and nosocomial spread of the multidrug-resistant opportunist *Stenotrophomonas maltophilia*. *Nat. Commun.* **2020**, *11*, 28, doi:10.1038/s41467-020-15123-0.
 22. World Health Organization Public health importance of antimicrobial resistance Available online: https://www.who.int/drugresistance/AMR_Importance/en/ (accessed on Apr 26, 2021).
 23. Rello, J.; Kalwaje Eshwara, V.; Lagunes, L.; Alves, J.; Wunderink, R.G.; Conway-Morris, A.; Rojas, J.N.; Alp, E.; Zhang, Z. A global priority list of the TOP TEn resistant Microorganisms (TOTEM) study at intensive care: a prioritization exercise based on multi-criteria decision analysis. *Eur. J. Clin. Microbiol. Infect. Dis.* **2019**, *38*, 319–323, doi:10.1007/s10096-018-3428-y.
 24. Al-Anazi, K.A.; Al-Jasser, A.M. Infections caused by *Stenotrophomonas maltophilia* in recipients of hematopoietic stem cell transplantation. *Front. Oncol.* **2014**, *4*, 232, doi:10.3389/fonc.2014.00232.
 25. Silbaq, F.S. Viable ultramicrocells in drinking water. *J. Appl. Microbiol.* **2009**, *106*, 106–117, doi:10.1111/j.1365-2672.2008.03981.x.
 26. Chung, H.S.; Kim, K.; Hong, S.S.; Hong, S.G.; Lee, K.; Chong, Y. The *sul1* gene in *Stenotrophomonas maltophilia* with high-level resistance to trimethoprim/sulfamethoxazole. *Ann. Lab. Med.* **2015**, *35*, 246–249, doi:10.3343/alm.2015.35.2.246.
 27. Charoenlap, N.; Jiramonai, L.; Chittrakanwong, J.; Tunsakul, N.; Mongkolsuk, S.; Vattanaviboon, P. Inactivation of *ahpC* renders *Stenotrophomonas maltophilia* resistant to the disinfectant hydrogen peroxide. *Antonie van Leeuwenhoek, Int. J. Gen. Mol. Microbiol.* **2019**, *112*, 809–814, doi:10.1007/s10482-018-1203-9.

28. Cystic Fibrosis Foundation 2019 Patient Registry Annual Data Report Available online: <https://www.cff.org/About-Us/Reports-and-Financials/2019-Annual-Report/> (accessed on Apr 27, 2021).
29. Hatziagorou, E.; Orenti, A.; Drevinek, P.; Kashirskaya, N.; Mei-Zahav, M.; De Boeck, K.; Pflieger, A.; Sciensano, M.T.; Lammertyn, E.; Macek, M.; et al. Changing epidemiology of the respiratory bacteriology of patients with cystic fibrosis—data from the European cystic fibrosis society patient registry. *J. Cyst. Fibros.* **2020**, *19*, 376–383, doi:10.1016/j.jcf.2019.08.006.
30. Cystic Fibrosis Canada The Canadian Cystic Fibrosis Registry: 2019 Annual Data Report Available online: <https://www.cysticfibrosis.ca/our-programs/cf-registry> (accessed on Apr 27, 2021).
31. Hansen, C.R. *Stenotrophomonas maltophilia*: To be or not to be a cystic fibrosis pathogen. *Curr. Opin. Pulm. Med.* **2012**, *18*, 628–631, doi:10.1097/MCP.0b013e328358d4f8.
32. Berdah, L.; Taytard, J.; Leyronnas, S.; Clement, A.; Boelle, P.Y.; Corvol, H. *Stenotrophomonas maltophilia*: A marker of lung disease severity. *Pediatr. Pulmonol.* **2018**, *53*, 426–430, doi:10.1002/ppul.23943.
33. Waters, V.; Atenafu, E.G.; Lu, A.; Yau, Y.; Tullis, E.; Ratjen, F. Chronic *Stenotrophomonas maltophilia* infection and mortality or lung transplantation in cystic fibrosis patients. *J. Cyst. Fibros.* **2013**, *12*, 482–486, doi:10.1016/j.jcf.2012.12.006.
34. Talmaciu, I.; Varlotta, L.; Mortensen, J.; Schidlow, D. V. Risk factors for emergence of *Stenotrophomonas maltophilia* in cystic fibrosis. *Pediatr. Pulmonol.* **2000**, *30*, 10–15, doi:10.1002/1099-0496(200007)30:1<10::AID-PPUL3>3.0.CO;2-Q.
35. Waters, V.J.; Gómez, M.I.; Soong, G.; Amin, S.; Ernst, R.K.; Prince, A. Immunostimulatory properties of the emerging pathogen *Stenotrophomonas maltophilia*. *Infect. Immun.* **2007**, *75*, 1698–1703, doi:10.1128/IAI.01469-06.
36. McDaniel, M.S.; Schoeb, T.; Swords, W.E. Cooperativity between *Stenotrophomonas maltophilia* and *Pseudomonas aeruginosa* during polymicrobial airway infections. *Infect. Immun.* **2020**, *88*, doi:10.1128/IAI.00855-19.
37. Kataoka, D.; Fujiwara, H.; Kawakami, T.; Tanaka, Y.; Tanimoto, A.; Ikawa, S.; Tanaka, Y. The indirect pathogenicity of *Stenotrophomonas maltophilia*. *Int. J. Antimicrob. Agents*

- 2003**, 22, 601–606, doi:10.1016/S0924-8579(03)00244-9.
38. Yin, C.; Yang, W.; Meng, J.; Lv, Y.; Wang, J.; Huang, B. Co-infection of *Pseudomonas aeruginosa* and *Stenotrophomonas maltophilia* in hospitalised pneumonia patients has a synergic and significant impact on clinical outcomes. *Eur. J. Clin. Microbiol. Infect. Dis.* **2017**, 36, 2231–2235, doi:10.1007/s10096-017-3050-4.
 39. Ryan, R.P.; Fouhy, Y.; Garcia, B.F.; Watt, S.A.; Niehaus, K.; Yang, L.; Tolker-Nielsen, T.; Dow, J.M. Interspecies signalling via the *Stenotrophomonas maltophilia* diffusible signal factor influences biofilm formation and polymyxin tolerance in *Pseudomonas aeruginosa*. *Mol. Microbiol.* **2008**, 68, 75–86, doi:10.1111/j.1365-2958.2008.06132.x.
 40. Martínez, P.; Huedo, P.; Martinez-Servat, S.; Planell, R.; Ferrer-Navarro, M.; Daura, X.; Yero, D.; Gibert, I. *Stenotrophomonas maltophilia* responds to exogenous AHL signals through the LuxR solo SmoR (Smlt1839). *Front. Cell. Infect. Microbiol.* **2015**, 5, 41, doi:10.3389/fcimb.2015.00041.
 41. Trifonova, A.; Strateva, T. *Stenotrophomonas maltophilia* – a low-grade pathogen with numerous virulence factors. *Infect. Dis. (Auckl).* **2019**, 51, 168–178, doi:10.1080/23744235.2018.1531145.
 42. García, C.A.; Alcaraz, E.S.; Franco, M.A.; De Rossi, B.N.P. Iron is a signal for *Stenotrophomonas maltophilia* biofilm formation, oxidative stress response, OMPs expression, and virulence. *Front. Microbiol.* **2015**, 6, 926, doi:10.3389/fmicb.2015.00926.
 43. Kalidasan, V.; Joseph, N.; Kumar, S.; Awang Hamat, R.; Neela, V.K. Iron and virulence in *Stenotrophomonas maltophilia*: all we know so far. *Front. Cell. Infect. Microbiol.* **2018**, 8, 401, doi:10.3389/fcimb.2018.00401.
 44. Crossman, L.C.; Gould, V.C.; Dow, J.M.; Vernikos, G.S.; Okazaki, A.; Sebahia, M.; Saunders, D.; Arrowsmith, C.; Carver, T.; Peters, N.; et al. The complete genome, comparative and functional analysis of *Stenotrophomonas maltophilia* reveals an organism heavily shielded by drug resistance determinants. *Genome Biol.* **2008**, 9, doi:10.1186/gb-2008-9-4-r74.
 45. Ferrer-Navarro, M.; Planell, R.; Yero, D.; Mongiardini, E.; Torrent, G.; Huedo, P.; Martínez, P.; Roher, N.; Mackenzie, S.; Gibert, I.; et al. Abundance of the quorum-sensing factor Ax21 in four strains of *Stenotrophomonas maltophilia* correlates with mortality rate

- in a new zebrafish model of infection. *PLoS One* **2013**, *8*, 67207, doi:10.1371/journal.pone.0067207.
46. Winn, A.M.; Wilkinson, S.G. Structures of the O4 and O18 antigens of *Stenotrophomonas maltophilia*: A case of enantiomeric repeating units. *Carbohydr. Res.* **2001**, *330*, 215–221, doi:10.1016/S0008-6215(00)00287-1.
 47. McKay, G.A.; Woods, D.E.; MacDonald, K.L.; Poole, K. Role of phosphoglucomutase of *Stenotrophomonas maltophilia* in lipopolysaccharide biosynthesis, virulence, and antibiotic resistance. *Infect. Immun.* **2003**, *71*, 3068–3075, doi:10.1128/IAI.71.6.3068-3075.2003.
 48. Huang, T.P.; Somers, E.B.; Wong, A.C.L. Differential biofilm formation and motility associated with lipopolysaccharide/exopolysaccharide-coupled biosynthetic genes in *Stenotrophomonas maltophilia*. *J. Bacteriol.* **2006**, *188*, 3116–3120, doi:10.1128/JB.188.8.3116-3120.2006.
 49. De Oliveira-Garcia, D.; Dall’Agnol, M.; Rosales, M.; Azzuz, A.C.G.S.; Martinez, M.B.; Girón, J.A. Characterization of flagella produced by clinical strains of *Stenotrophomonas maltophilia*. *Emerg. Infect. Dis.* **2002**, *8*, 918–923, doi:10.3201/eid0809.010535.
 50. Zgair, A.K.; Chhibber, S. Adhesion of *Stenotrophomonas maltophilia* to mouse tracheal mucus is mediated through flagella. *J. Med. Microbiol.* **2011**, *60*, 1032–1037, doi:10.1099/jmm.0.026377-0.
 51. Pompilio, A.; Crocetta, V.; Confalone, P.; Nicoletti, M.; Petrucca, A.; Guarnieri, S.; Fiscarelli, E.; Savini, V.; Piccolomini, R.; Di Bonaventura, G. Adhesion to and biofilm formation on IB3-1 bronchial cells by *Stenotrophomonas maltophilia* isolates from cystic fibrosis patients. *BMC Microbiol.* **2010**, *10*, doi:10.1186/1471-2180-10-102.
 52. Wu, C.-M.; Huang, H.-H.; Li, L.-H.; Lin, Y.-T.; Yang, T.-C. Molecular characterization of three tandemly located flagellin genes of *Stenotrophomonas maltophilia*. *Int. J. Mol. Sci.* **2022**, *23*, 3863, doi:10.3390/ijms23073863.
 53. de Oliveira-Garcia, D.; Dall’Agnol, M.; Rosales, M.; Azzuz, A.C.G.S.; Alcántara, N.; Martinez, M.B.; Girón, J.A. Fimbriae and adherence of *Stenotrophomonas maltophilia* to epithelial cells and to abiotic surfaces. *Cell. Microbiol.* **2003**, *5*, 625–636, doi:10.1046/j.1462-5822.2003.00306.x.

54. Nicoletti, M.; Iacobino, A.; Prosseda, G.; Fiscarelli, E.; Zarrilli, R.; De Carolis, E.; Petrucca, A.; Nencioni, L.; Colonna, B.; Casalino, M. *Stenotrophomonas maltophilia* strains from cystic fibrosis patients: Genomic variability and molecular characterization of some virulence determinants. *Int. J. Med. Microbiol.* **2011**, *301*, 34–43, doi:10.1016/j.ijmm.2010.07.003.
55. Giltner, C.L.; Nguyen, Y.; Burrows, L.L. Type IV pilin proteins: versatile molecular modules. *Microbiol. Mol. Biol. Rev.* **2012**, *76*, 740–772, doi:10.1128/MMBR.00035-12.
56. Kalidasan, V.; Neela, V.K. Twitching motility of *Stenotrophomonas maltophilia* under iron limitation: In-silico, phenotypic and proteomic approaches. *Virulence* **2020**, *11*, 104–112, doi:10.1080/21505594.2020.1713649.
57. Figueirêdo, P.M.S.; Furumura, M.T.; Santos, A.M.; Sousa, A.C.T.; Kota, D.J.; Levy, C.E.; Yano, T. Cytotoxic activity of clinical *Stenotrophomonas maltophilia*. *Lett. Appl. Microbiol.* **2006**, *43*, 443–449, doi:10.1111/j.1472-765X.2006.01965.x.
58. Windhorst, S.; Frank, E.; Georgieva, D.N.; Genov, N.; Buck, F.; Borowski, P.; Weber, W. The major extracellular protease of the nosocomial pathogen *Stenotrophomonas maltophilia*: Characterization of the protein and molecular cloning of the gene. *J. Biol. Chem.* **2002**, *277*, 11042–11049, doi:10.1074/jbc.M109525200.
59. DuMont, A.L.; Karaba, S.M.; Cianciotto, N.P. Type II secretion-dependent degradative and cytotoxic activities mediated by *Stenotrophomonas maltophilia* serine proteases StmPr1 and StmPr2. *Infect. Immun.* **2015**, *83*, 3825–3837, doi:10.1128/IAI.00672-15.
60. DuMont, A.L.; Cianciotto, N.P. *Stenotrophomonas maltophilia* serine protease StmPr1 induces matrilysis, anoikis, and protease-activated receptor 2 activation in human lung epithelial cells. *Infect. Immun.* **2017**, *85*, doi:10.1128/IAI.00544-17.
61. Karaba, S.M.; White, R.C.; Cianciotto, N.P. *Stenotrophomonas maltophilia* encodes a type II protein secretion system that promotes detrimental effects on lung epithelial cells. *Infect. Immun.* **2013**, *81*, 3210–3219, doi:10.1128/IAI.00546-13.
62. Nas, M.Y.; White, R.C.; DuMont, A.L.; Lopez, A.E.; Cianciotto, N.P. *Stenotrophomonas maltophilia* encodes a VirB/VirD4 type IV secretion system that modulates apoptosis in human cells and promotes competition against heterologous bacteria, including *Pseudomonas aeruginosa*. *Infect. Immun.* **2019**, *87*, doi:10.1128/IAI.00457-19.

63. Bayer-Santos, E.; Cenens, W.; Matsuyama, B.Y.; Oka, G.U.; Di Sessa, G.; Del Valle Mininel, I.; Alves, T.L.; Farah, C.S. The opportunistic pathogen *Stenotrophomonas maltophilia* utilizes a type IV secretion system for interbacterial killing. *PLoS Pathog.* **2019**, *15*, doi:10.1371/journal.ppat.1007651.
64. Costa, T.R.D.; Felisberto-Rodrigues, C.; Meir, A.; Prevost, M.S.; Redzej, A.; Trokter, M.; Waksman, G. Secretion systems in Gram-negative bacteria: Structural and mechanistic insights. *Nat. Rev. Microbiol.* **2015**, *13*, 343–359, doi:10.1038/nrmicro3456.
65. Barber, C.E.; Tang, J.L.; Feng, J.X.; Pan, M.Q.; Wilson, T.J.G.; Slater, H.; Dow, J.M.; Williams, P.; Daniels, M.J. A novel regulatory system required for pathogenicity of *Xanthomonas campestris* is mediated by a small diffusible signal molecule. *Mol. Microbiol.* **1997**, *24*, 555–566, doi:10.1046/j.1365-2958.1997.3721736.x.
66. An, S.Q.; Tang, J.L. Diffusible signal factor signaling regulates multiple functions in the opportunistic pathogen *Stenotrophomonas maltophilia*. *BMC Res. Notes* **2018**, *11*, 569, doi:10.1186/s13104-018-3690-1.
67. Alcaraz, E.; García, C.; Friedman, L.; De Rossi, B.P. The rpf/DSF signalling system of *Stenotrophomonas maltophilia* positively regulates biofilm formation, production of virulence-associated factors and β -lactamase induction. *FEMS Microbiol. Lett.* **2019**, *366*, 69, doi:10.1093/femsle/fnz069.
68. Yero, D.; Huedo, P.; Conchillo-Solé, O.; Martínez-Servat, S.; Mamat, U.; Coves, X.; Llanas, F.; Roca, I.; Vila, J.; Schaible, U.E.; et al. Genetic variants of the DSF quorum sensing system in *Stenotrophomonas maltophilia* influence virulence and resistance phenotypes among genotypically diverse clinical isolates. *Front. Microbiol.* **2020**, *11*, 1160, doi:10.3389/fmicb.2020.01160.
69. Huedo, P.; Yero, D.; Martínez-Servat, S.; Estibariz, I.; Planell, R.; Martínez, P.; Ruyra, À.; Roher, N.; Roca, I.; Vila, J.; et al. Two different *rpf* clusters distributed among a population of *Stenotrophomonas maltophilia* clinical strains display differential diffusible signal factor production and virulence regulation. *J. Bacteriol.* **2014**, *196*, 2431–2442, doi:10.1128/JB.01540-14.
70. Huedo, P.; Coves, X.; Daura, X.; Gibert, I.; Yero, D. Quorum sensing signaling and quenching in the multidrug-resistant pathogen *Stenotrophomonas maltophilia*. *Front. Cell.*

- Infect. Microbiol.* **2018**, *8*, 122, doi:10.3389/fcimb.2018.00122.
71. Devos, S.; Van Oudenhove, L.; Stremersch, S.; Van Putte, W.; De Rycke, R.; Van Driessche, G.; Vitse, J.; Raemdonck, K.; Devreese, B. The effect of imipenem and diffusible signaling factors on the secretion of outer membrane vesicles and associated Ax21 proteins in *Stenotrophomonas maltophilia*. *Front. Microbiol.* **2015**, *6*, 298, doi:10.3389/fmicb.2015.00298.
 72. Ferrer-Navarro, M.; Torrent, G.; Mongiardini, E.; Conchillo-Solé, O.; Gibert, I.; Daura, X. Proteomic analysis of outer membrane proteins and vesicles of a clinical isolate and a collection strain of *Stenotrophomonas maltophilia*. *J. Proteomics* **2016**, *142*, 122–129, doi:10.1016/j.jprot.2016.05.001.
 73. Kim, Y.J.; Jeon, H.; Na, S.H.; Kwon, H. Il; Selasi, G.N.; Nicholas, A.; Park, T.I.; Lee, S.H.; Lee, J.C. *Stenotrophomonas maltophilia* outer membrane vesicles elicit a potent inflammatory response in vitro and in vivo. *Pathog. Dis.* **2016**, *74*, 104, doi:10.1093/femspd/ftw104.
 74. An, S. qi; Tang, J. liang The Ax21 protein influences virulence and biofilm formation in *Stenotrophomonas maltophilia*. *Arch. Microbiol.* **2018**, *200*, 183–187, doi:10.1007/s00203-017-1433-7.
 75. Nikaido, H.; Vaara, M. Molecular basis of bacterial outer membrane permeability. *Microbiol. Rev.* **1985**, *49*, 1–32, doi:10.1128/mmbr.49.1.1-32.1985.
 76. Sánchez, M.B. Antibiotic resistance in the opportunistic pathogen *Stenotrophomonas maltophilia*. *Front. Microbiol.* **2015**, *6*, 658, doi:10.3389/fmicb.2015.00658.
 77. Li, X.Z.; Zhang, L.; Poole, K. SmeC, an outer membrane multidrug efflux protein of *Stenotrophomonas maltophilia*. *Antimicrob. Agents Chemother.* **2002**, *46*, 333–343, doi:10.1128/AAC.46.2.333-343.2002.
 78. Alonso, A.; Martinez, J.L. Cloning and characterization of SmeDEF, a novel multidrug efflux pump from *Stenotrophomonas maltophilia*. *Antimicrob. Agents Chemother.* **2000**, *44*, 3079–3086, doi:10.1128/aac.44.11.3079-3086.2000.
 79. Zhang, L.; Li, X.; Poole, K. SmeDEF multidrug efflux pump contributes to intrinsic multidrug resistance in *Stenotrophomonas maltophilia*. *Antimicrob. Agents Chemother.* **2001**, *45*, 3497–3503, doi:10.1128/AAC.45.12.3497.

80. Blanco, P.; Corona, F.; Martínez, J.L. Involvement of the RND efflux pump transporter SmeH in the acquisition of resistance to ceftazidime in *Stenotrophomonas maltophilia*. *Sci. Rep.* **2019**, *9*, doi:10.1038/s41598-019-41308-9.
81. Gould, V.C.; Okazaki, A.; Avison, M.B. Coordinate hyperproduction of SmeZ and SmeJK efflux pumps extends drug resistance in *Stenotrophomonas maltophilia*. *Antimicrob. Agents Chemother.* **2013**, *57*, 655–657, doi:10.1128/AAC.01020-12.
82. Lin, C.W.; Huang, Y.W.; Hu, R.M.; Yang, T.C. SmeOP-TolCSm efflux pump contributes to the multidrug resistance of *Stenotrophomonas maltophilia*. *Antimicrob. Agents Chemother.* **2014**, *58*, 2405–2408, doi:10.1128/AAC.01974-13.
83. Chen, C.H.; Huang, C.C.; Chung, T.C.; Hu, R.M.; Huang, Y.W.; Yang, T.C. Contribution of resistance-nodulation-division efflux pump operon *smeU1-V-W-U2-X* to multidrug resistance of *Stenotrophomonas maltophilia*. *Antimicrob. Agents Chemother.* **2011**, *55*, 5826–5833, doi:10.1128/AAC.00317-11.
84. Lin, Y.T.; Huang, Y.W.; Chen, S.J.; Chang, C.W.; Yang, T.C. The SmeYZ efflux pump of *Stenotrophomonas maltophilia* contributes to drug resistance, virulence-related characteristics, and virulence in mice. *Antimicrob. Agents Chemother.* **2015**, *59*, 4067–4073, doi:10.1128/AAC.00372-15.
85. Al-Hamad, A.; Upton, M.; Burnie, J. Molecular cloning and characterization of SmrA, a novel ABC multidrug efflux pump from *Stenotrophomonas maltophilia*. *J. Antimicrob. Chemother.* **2009**, *64*, 731–734, doi:10.1093/jac/dkp271.
86. Lin, Y.T.; Huang, Y.W.; Liou, R.S.; Chang, Y.C.; Yang, T.C. MacABCsm, an ABC-type tripartite efflux pump of *Stenotrophomonas maltophilia* involved in drug resistance, oxidative and envelope stress tolerances and biofilm formation. *J. Antimicrob. Chemother.* **2014**, *69*, 3221–3226, doi:10.1093/jac/dku317.
87. Huang, Y.W.; Hu, R.M.; Chu, F.Y.; Lin, H.R.; Yang, T.C. Characterization of a major facilitator superfamily (MFS) tripartite efflux pump EmrCABsm from *Stenotrophomonas maltophilia*. *J. Antimicrob. Chemother.* **2013**, *68*, 2498–2505, doi:10.1093/jac/dkt250.
88. Hu, R.M.; Liao, S.T.; Huang, C.C.; Huang, Y.W.; Yang, T.C. An inducible fusaric acid tripartite efflux pump contributes to the fusaric acid resistance in *Stenotrophomonas maltophilia*. *PLoS One* **2012**, *7*, doi:10.1371/journal.pone.0051053.

89. Gil-Gil, T.; Martínez, J.L.; Blanco, P. Mechanisms of antimicrobial resistance in *Stenotrophomonas maltophilia*: a review of current knowledge. *Expert Rev. Anti. Infect. Ther.* **2020**, *18*, 335–347, doi:10.1080/14787210.2020.1730178.
90. Okazaki, A.; Avison, M.B. Induction of L1 and L2 β -lactamase production in *Stenotrophomonas maltophilia* is dependent on an AmpR-type regulator. *Antimicrob. Agents Chemother.* **2008**, *52*, 1525–1528, doi:10.1128/AAC.01485-07.
91. Avison, M.B.; Von Heldreich, C.J.; Higgins, C.S.; Bennett, P.M.; Walsh, T.R. A TEM-2 Beta-lactamase encoded on an active Tn1-like transposon in the genome of a clinical isolate of *Stenotrophomonas maltophilia*. *J. Antimicrob. Chemother.* **2000**, *46*, 879–884.
92. Li, X.Z.; Zhang, L.; McKay, G.A.; Poole, K. Role of the acetyltransferase AAC(6')-Iz modifying enzyme in aminoglycoside resistance in *Stenotrophomonas maltophilia*. *J. Antimicrob. Chemother.* **2003**, *51*, 803–811, doi:10.1093/jac/dkg148.
93. Tada, T.; Miyoshi-Akiyama, T.; Dahal, R.K.; Mishra, S.K.; Shimada, K.; Ohara, H.; Kirikae, T.; Pokhrel, B.M. Identification of a novel 6'-N-aminoglycoside acetyltransferase, AAC(6')-Iak, from a multidrug-resistant clinical isolate of *Stenotrophomonas maltophilia*. *Antimicrob. Agents Chemother.* **2014**, *58*, 6324–6327, doi:10.1128/AAC.03354-14.
94. Okazaki, A.; Avison, M.B. Aph(3')-IIc, an aminoglycoside resistance determinant from *Stenotrophomonas maltophilia*. *Antimicrob. Agents Chemother.* **2007**, *51*, 359–360, doi:10.1128/AAC.00795-06.
95. Valdezate, S.; Vindel, A.; Antonio Saéz-Nieto, J.; Baquero, F.; Cantó, R. Preservation of topoisomerase genetic sequences during in vivo and in vitro development of high-level resistance to ciprofloxacin in isogenic *Stenotrophomonas maltophilia* strains. *J. Antimicrob. Chemother.* **2005**, *56*, 220–223, doi:10.1093/jac/dki182.
96. Shimizu, K.; Kikuchi, K.; Sasaki, T.; Takahashi, N.; Ohtsuka, M.; Ono, Y.; Hiramatsu, K. Smqnr, a new chromosome-carried quinolone resistance gene in *Stenotrophomonas maltophilia*. *Antimicrob. Agents Chemother.* **2008**, *52*, 3823–3825, doi:10.1128/AAC.00026-08.
97. Sánchez, M.B.; Martínez, J.L. SmQnr contributes to intrinsic resistance to quinolones in *Stenotrophomonas maltophilia*. *Antimicrob. Agents Chemother.* **2010**, *54*, 580–581,

doi:10.1128/AAC.00496-09.

98. García-León, G.; Salgado, F.; Oliveros, J.C.; Sánchez, M.B.; Martínez, J.L. Interplay between intrinsic and acquired resistance to quinolones in *Stenotrophomonas maltophilia*. *Environ. Microbiol.* **2014**, *16*, 1282–1296, doi:10.1111/1462-2920.12408.
99. García-León, G.; Ruiz de Alegría Puig, C.; García de la Fuente, C.; Martínez-Martínez, L.; Martínez, J.L.; Sánchez, M.B. High-level quinolone resistance is associated with the overexpression of *smeVWX* in *Stenotrophomonas maltophilia* clinical isolates. *Clin. Microbiol. Infect.* **2015**, *21*, 464–467, doi:10.1016/j.cmi.2015.01.007.
100. Hu, L.F.; Chang, X.; Ye, Y.; Wang, Z.X.; Shao, Y.B.; Shi, W.; Li, X.; Li, J. Bin *Stenotrophomonas maltophilia* resistance to trimethoprim/sulfamethoxazole mediated by acquisition of *sul* and *dfrA* genes in a plasmid-mediated class 1 integron. *Int. J. Antimicrob. Agents* **2011**, *37*, 230–234, doi:10.1016/j.ijantimicag.2010.10.025.
101. Barbolla, R.; Catalano, M.; Orman, B.E.; Famiglietti, A.; Vay, C.; Smayevsky, J.; Centrón, D.; Piñeiro, S.A. Class 1 integrons increase trimethoprim-sulfamethoxazole MICs against epidemiologically unrelated *Stenotrophomonas maltophilia* isolates. *Antimicrob. Agents Chemother.* **2004**, *48*, 666–669, doi:10.1128/AAC.48.2.666-669.2004.
102. Toleman, M.A.; Bennett, P.M.; Bennett, D.M.C.; Jones, R.N.; Walsh, T.R. Global emergence of trimethoprim/sulfamethoxazole resistance in *Stenotrophomonas maltophilia* mediated by acquisition of *sul* genes. *Emerg. Infect. Dis.* **2007**, *13*, 559–565.
103. Giles, A.; Foushee, J.; Lantz, E.; Gumina, G. Sulfonamide allergies. *Pharmacy* **2019**, *7*, 132, doi:10.3390/pharmacy7030132.
104. Abedon, S.T.; Kuhl, S.J.; Blasdel, B.G.; Kutter, E.M. Phage treatment of human infections. *Bacteriophage* **2011**, *1*, 66–85, doi:10.4161/bact.1.2.15845.
105. Chanishvili, N. Phage therapy-history from Twort and d’Herelle through Soviet experience to current approaches. In *Advances in Virus Research*; 2012; Vol. 83, pp. 3–40 ISBN 9780123944382.
106. Summers, W.C. The strange history of phage therapy. *Bacteriophage* **2012**, *2*, 130–133, doi:10.4161/bact.20757.
107. Burrowes, B.; Harper, D.R.; Anderson, J.; McConville, M.; Enright, M.C. Bacteriophage therapy: Potential uses in the control of antibiotic-resistant pathogens. *Expert Rev. Anti.*

- Infect. Ther.* **2011**, *9*, 775–785, doi:10.1586/eri.11.90.
108. Casjens, S. Prophages and bacterial genomics: What have we learned so far? *Mol. Microbiol.* **2003**, *49*, 277–300, doi:10.1046/j.1365-2958.2003.03580.x.
 109. Touchon, M.; Bernheim, A.; Rocha, E.P.C. Genetic and life-history traits associated with the distribution of prophages in bacteria. *ISME J.* **2016**, *10*, 2744–2754, doi:10.1038/ismej.2016.47.
 110. Ramisetty, B.C.M.; Sudhakari, P.A. Bacterial “grounded” prophages: Hotspots for genetic renovation and innovation. *Front. Genet.* **2019**, *10*, 12, doi:10.3389/fgene.2019.00065.
 111. Zhou, Y.; Liang, Y.; Lynch, K.H.; Dennis, J.J.; Wishart, D.S. PHAST: A fast phage search tool. *Nucleic Acids Res.* **2011**, *39*, W347–W352, doi:10.1093/nar/gkr485.
 112. Arndt, D.; Grant, J.R.; Marcu, A.; Sajed, T.; Pon, A.; Liang, Y.; Wishart, D.S. PHASTER: a better, faster version of the PHAST phage search tool. *Nucleic Acids Res.* **2016**, *44*, W16–W21, doi:10.1093/nar/gkw387.
 113. Patil, P.P.; Midha, S.; Kumar, S.; Patil, P.B. Genome sequence of type strains of genus *Stenotrophomonas*. *Front. Microbiol.* **2016**, *7*, 309, doi:10.3389/fmicb.2016.00309.
 114. Peters, D.L.; McCutcheon, J.G.; Stothard, P.; Dennis, J.J. Novel *Stenotrophomonas maltophilia* temperate phage DLP4 is capable of lysogenic conversion. *BMC Genomics* **2019**, *20*, 300, doi:10.1186/s12864-019-5674-5.
 115. McCutcheon, J.G.; Lin, A.; Dennis, J.J. Isolation and characterization of the novel bacteriophage AXL3 against *Stenotrophomonas maltophilia*. *Int. J. Mol. Sci.* **2020**, *21*, 1–20, doi:10.3390/ijms21176338.
 116. Brüssow, H.; Canchaya, C.; Hardt, W.-D. Phages and the evolution of bacterial pathogens: from genomic rearrangements to lysogenic conversion. *Microbiol. Mol. Biol. Rev.* **2004**, *68*, 560–602, doi:10.1128/mmbr.68.3.560-602.2004.
 117. Beres, S.B.; Sylva, G.L.; Barbian, K.D.; Lei, B.; Hoff, J.S.; Mammarella, N.D.; Liu, M.Y.; Smoot, J.C.; Porcella, S.F.; Parkins, L.D.; et al. Genome sequence of a serotype M3 strain of group A *Streptococcus*: Phage-encoded toxins, the high-virulence phenotype, and clone emergence. *Proc. Natl. Acad. Sci. U. S. A.* **2002**, *99*, 10078–10083, doi:10.1073/pnas.152298499.
 118. Hayashi, T.; Makino, K.; Ohnishi, M.; Kurokawa, K.; Ishii, K.; Yokoyama, K.; Han, C.G.;

- Ohtsubo, E.; Nakayama, K.; Murata, T.; et al. Complete genome sequence of enterohemorrhagic *Escherichia coli* O157:H7 and genomic comparison with a laboratory strain K-12. *DNA Res.* **2001**, *8*, 11–22, doi:10.1093/dnares/8.1.11.
119. Nakamura, K.; Murase, K.; Sato, M.P.; Toyoda, A.; Itoh, T.; Mainil, J.G.; Piérard, D.; Yoshino, S.; Kimata, K.; Isobe, J.; et al. Differential dynamics and impacts of prophages and plasmids on the pangenome and virulence factor repertoires of Shiga toxin-producing *Escherichia coli* O145:H28. *Microb. Genomics* **2020**, *6*, doi:10.1099/mgen.0.000323.
 120. Waldor, M.K.; Mekalanos, J.J. Lysogenic conversion by a filamentous phage encoding cholera toxin. *Science (80-.)*. **1996**, *272*, 1910–1914, doi:10.1126/science.272.5270.1910.
 121. Hendrix, R.W.; Smith, M.C.M.; Burns, R.N.; Ford, M.E.; Hatfull, G.F. Evolutionary relationships among diverse bacteriophages and prophages: All the world's a phage. *Proc. Natl. Acad. Sci. U. S. A.* **1999**, *96*, 2192–2197, doi:10.1073/pnas.96.5.2192.
 122. Ackermann, H.W.; Prangishvili, D. Prokaryote viruses studied by electron microscopy. *Arch. Virol.* **2012**, *157*, 1843–1849, doi:10.1007/s00705-012-1383-y.
 123. Roach, D.R.; Debarbieux, L. Phage therapy: awakening a sleeping giant. *Emerg. Top. Life Sci.* **2017**, *1*, 93–103, doi:10.1042/ETLS20170002.
 124. Loc-Carrillo, C.; Abedon, S.T. Pros and cons of phage therapy. *Bacteriophage* **2011**, *1*, 111–114, doi:10.4161/bact.1.2.14590.
 125. Yehl, K.; Lemire, S.; Yang, A.C.; Ando, H.; Mimee, M.; Torres, M.D.T.; de la Fuente-Nunez, C.; Lu, T.K. Engineering phage host-range and suppressing bacterial resistance through phage tail fiber mutagenesis. *Cell* **2019**, *179*, 459-469.e9, doi:10.1016/j.cell.2019.09.015.
 126. Lenneman, B.R.; Fernbach, J.; Loessner, M.J.; Lu, T.K.; Kilcher, S. Enhancing phage therapy through synthetic biology and genome engineering. *Curr. Opin. Biotechnol.* **2021**, *68*, 151–159, doi:10.1016/j.copbio.2020.11.003.
 127. Manrique, P.; Bolduc, B.; Walk, S.T.; Van Oost, J. Der; De Vos, W.M.; Young, M.J. Healthy human gut phageome. *Proc. Natl. Acad. Sci. U. S. A.* **2016**, *113*, 10400–10405, doi:10.1073/pnas.1601060113.
 128. Edwards, R.A.; Vega, A.A.; Norman, H.M.; Ohaeri, M.; Levi, K.; Dinsdale, E.A.; Cinek, O.; Aziz, R.K.; McNair, K.; Barr, J.J.; et al. Global phylogeography and ancient evolution

- of the widespread human gut virus crAssphage. *Nat. Microbiol.* **2019**, *4*, 1727–1736, doi:10.1038/s41564-019-0494-6.
129. Nguyen, S.; Baker, K.; Padman, B.S.; Patwa, R.; Dunstan, R.A.; Weston, T.A.; Schlosser, K.; Bailey, B.; Lithgow, T.; Lazarou, M.; et al. Bacteriophage transcytosis provides a mechanism to cross epithelial cell layers. *MBio* **2017**, *8*, doi:10.1128/mBio.01874-17.
 130. Bertozzi Silva, J.; Storms, Z.; Sauvageau, D. Host receptors for bacteriophage adsorption. *FEMS Microbiol. Lett.* **2016**, *363*, 1–11, doi:10.1093/femsle/fnw002.
 131. Gordillo Altamirano, F.L.; Barr, J.J. Unlocking the next generation of phage therapy: the key is in the receptors. *Curr. Opin. Biotechnol.* **2021**, *68*, 115–123, doi:10.1016/j.copbio.2020.10.002.
 132. Rakhuba D V; Kolomiets, E.I.; Sz wajcer Dey, E.; Novik, G.I. Bacteriophage receptors, mechanisms of phage adsorption and penetration into host cell. *Polish J. Microbiol.* **2010**, *59*, 145–155.
 133. Craig, L.; Pique, M.E.; Tainer, J.A. Type IV pilus structure and bacterial pathogenicity. *Nat. Rev. Microbiol.* **2004**, *2*, 363–378, doi:10.1038/nrmicro885.
 134. Burrows, L.L. *Pseudomonas aeruginosa* twitching motility: type IV pili in action. *Annu. Rev. Microbiol.* **2012**, *66*, 493–520, doi:10.1146/annurev-micro-092611-150055.
 135. Whitchurch, C.B.; Mattick, J.S. Characterization of a gene, *pilU*, required for twitching motility but not phage sensitivity in *Pseudomonas aeruginosa*. *Mol. Microbiol.* **1994**, *13*, 1079–1091, doi:10.1111/j.1365-2958.1994.tb00499.x.
 136. Bradley, D.E. A study of pili on *Pseudomonas aeruginosa*. *Genet. Res. (Camb)*. **1972**, *19*, 39–51.
 137. Kim, E.S.; Bae, H.W.; Cho, Y.H. A pilin region affecting host range of the *Pseudomonas aeruginosa* RNA phage, PP7. *Front. Microbiol.* **2018**, *9*, doi:10.3389/fmicb.2018.00247.
 138. Mutalik, V.K.; Adler, B.A.; Rishi, H.S.; Piya, D.; Zhong, C.; Koskella, B.; Kutter, E.M.; Calendar, R.; Novichkov, P.S.; Price, M.N.; et al. High-throughput mapping of the phage resistance landscape in *E. coli*. *PLoS Biol.* **2020**, *18*, doi:10.1371/JOURNAL.PBIO.3000877.
 139. Nobrega, F.L.; Vlot, M.; de Jonge, P.A.; Dreesens, L.L.; Beaumont, H.J.E.; Lavigne, R.; Dutilh, B.E.; Brouns, S.J.J. Targeting mechanisms of tailed bacteriophages. *Nat. Rev.*

- Microbiol.* **2018**, *16*, 760–773, doi:10.1038/s41579-018-0070-8.
140. Tu, J.; Park, T.; Morado, D.R.; Hughes, K.T.; Molineux, I.J.; Liu, J. Dual host specificity of phage SP6 is facilitated by tailspike rotation. *Virology* **2017**, *507*, 206–215, doi:10.1016/j.virol.2017.04.017.
 141. Schwarzer, D.; Buettner, F.F.R.; Browning, C.; Nazarov, S.; Rabsch, W.; Bethe, A.; Oberbeck, A.; Bowman, V.D.; Stummeyer, K.; Mühlenhoff, M.; et al. A multivalent adsorption apparatus explains the broad host range of phage phi92: a comprehensive genomic and structural analysis. *J. Virol.* **2012**, *86*, 10384–10398, doi:10.1128/jvi.00801-12.
 142. Le, S.; He, X.; Tan, Y.; Huang, G.; Zhang, L.; Lux, R.; Shi, W.; Hu, F. Mapping the tail fiber as the receptor binding protein responsible for differential host specificity of *Pseudomonas aeruginosa* bacteriophages PaP1 and JG004. *PLoS One* **2013**, *8*, e68562, doi:10.1371/journal.pone.0068562.
 143. Meyer, J.R.; Dobias, D.T.; Weitz, J.S.; Barrick, J.E.; Quick, R.T.; Lenski, R.E. Repeatability and contingency in the evolution of a key innovation in phage lambda. *Science* (80-.). **2012**, *335*, 428–432, doi:10.1126/science.1214449.
 144. de Jonge, P.A.; Nobrega, F.L.; Brouns, S.J.J.; Dutilh, B.E. Molecular and Evolutionary Determinants of Bacteriophage Host Range. *Trends Microbiol.* **2019**, *27*, 51–63, doi:10.1016/j.tim.2018.08.006.
 145. Luong, T.; Salabarria, A.C.; Roach, D.R. Phage therapy in the resistance era: where do we stand and where are we going? *Clin. Ther.* **2020**, *42*, 1659–1680, doi:10.1016/j.clinthera.2020.07.014.
 146. Aslam, S.; Lampley, E.; Wooten, D.; Karris, M.; Benson, C.; Strathdee, S.; Schooley, R.T. Lessons learned from the first 10 consecutive cases of intravenous bacteriophage therapy to treat multidrug-resistant bacterial infections at a single center in the United States. *Open Forum Infect. Dis.* **2020**, *7*, doi:10.1093/ofid/ofaa389.
 147. Chan, B.K.; Stanley, G.; Modak, M.; Koff, J.L.; Turner, P.E. Bacteriophage therapy for infections in CF. *Pediatr. Pulmonol.* **2021**, *56*, S4–S9, doi:10.1002/ppul.25190.
 148. Malik, D.J.; Sokolov, I.J.; Vinner, G.K.; Mancuso, F.; Cinquerrui, S.; Vladislavljevic, G.T.; Clokie, M.R.J.; Garton, N.J.; Stapley, A.G.F.; Kirpichnikova, A. Formulation,

- stabilisation and encapsulation of bacteriophage for phage therapy. *Adv. Colloid Interface Sci.* **2017**, *249*, 100–133, doi:10.1016/j.cis.2017.05.014.
149. Loh, B.; Gondil, V.S.; Manohar, P.; Khan, F.M.; Yang, H.; Leptihn, S. Encapsulation and delivery of therapeutic phages. *Appl. Environ. Microbiol.* **2021**, *87*, 1–13, doi:10.1128/AEM.01979-20.
 150. Rosner, D.; Clark, J. Formulations for bacteriophage therapy and the potential uses of immobilization. *Pharmaceuticals* **2021**, *14*, 359, doi:10.3390/ph14040359.
 151. Vinner, G.K.; Richards, K.; Leppanen, M.; Sagona, A.P.; Malik, D.J. Microencapsulation of enteric bacteriophages in a pH-responsive solid oral dosage formulation using a scalable membrane emulsification process. *Pharmaceutics* **2019**, *11*, doi:10.3390/pharmaceutics11090475.
 152. Singla, S.; Harjai, K.; Katare, O.P.; Chhibber, S. Encapsulation of bacteriophage in liposome accentuates its entry in to macrophage and shields it from neutralizing antibodies. *PLoS One* **2016**, *11*, doi:10.1371/journal.pone.0153777.
 153. Chadha, P.; Katare, O.P.; Chhibber, S. Liposome loaded phage cocktail: Enhanced therapeutic potential in resolving *Klebsiella pneumoniae* mediated burn wound infections. *Burns* **2017**, *43*, 1532–1543, doi:10.1016/j.burns.2017.03.029.
 154. Yang, Y.; Shen, W.; Zhong, Q.; Chen, Q.; He, X.; Baker, J.L.; Xiong, K.; Jin, X.; Wang, J.; Hu, F.; et al. Development of a bacteriophage cocktail to constrain the emergence of phage-resistant *Pseudomonas aeruginosa*. *Front. Microbiol.* **2020**, *11*, doi:10.3389/fmicb.2020.00327.
 155. Regeimbal, J.M.; Jacobs, A.C.; Corey, B.W.; Henry, M.S.; Thompson, M.G.; Pavlicek, R.L.; Quinones, J.; Hannah, R.M.; Ghebremedhin, M.; Crane, N.J.; et al. Personalized therapeutic cocktail of wild environmental phages rescues mice from *Acinetobacter baumannii* wound infections. *Antimicrob. Agents Chemother.* **2016**, *60*, 5806–5816, doi:10.1128/AAC.02877-15.
 156. Comeau, A.M.; Tétart, F.; Trojet, S.N.; Prère, M.F.; Krisch, H.M. Phage-antibiotic synergy (PAS): β -lactam and quinolone antibiotics stimulate virulent phage growth. *PLoS One* **2007**, *2*, 8–11, doi:10.1371/journal.pone.0000799.
 157. Kamal, F.; Dennis, J.J. *Burkholderia cepacia* complex phage-antibiotic synergy (PAS):

- Antibiotics stimulate lytic phage activity. *Appl. Environ. Microbiol.* **2015**, *81*, 1132–1138, doi:10.1128/AEM.02850-14.
158. Davis, C.M.; McCutcheon, J.G.; Dennis, J.J. Aztreonam lysine increases the activity of phages E79 and phiKZ against *Pseudomonas aeruginosa* PA01. *Microorganisms* **2021**, *9*, 1–19, doi:10.3390/microorganisms9010152.
 159. Rasko, D.A.; Sperandio, V. Anti-virulence strategies to combat bacteria-mediated disease. *Nat. Rev.* **2010**, *9*, 117–128, doi:10.1038/nrd3013.
 160. McCutcheon, J.G.; Peters, D.L.; Dennis, J.J. Identification and characterization of type IV pili as the cellular receptor of broad host range *Stenotrophomonas maltophilia* bacteriophages DLP1 and DLP2. *Viruses* **2018**, *10*, 338, doi:10.3390/v10060338.
 161. Gurney, J.; Brown, S.P.; Kaltz, O.; Hochberg, M.E. Steering phages to combat bacterial pathogens. *Trends Microbiol.* **2020**, *28*, 85–94, doi:10.1016/j.tim.2019.10.007.
 162. Gordillo Altamirano, F.; Forsyth, J.H.; Patwa, R.; Kostoulas, X.; Trim, M.; Subedi, D.; Archer, S.K.; Morris, F.C.; Oliveira, C.; Kielty, L.; et al. Bacteriophage-resistant *Acinetobacter baumannii* are resensitized to antimicrobials. *Nat. Microbiol.* **2021**, *6*, 157–161, doi:10.1038/s41564-020-00830-7.
 163. Gordillo Altamirano, F.L.; Kostoulas, X.; Subedi, D.; Korneev, D.; Peleg, A.Y.; Barr, J.J. Phage-antibiotic combination is a superior treatment against *Acinetobacter baumannii* in a preclinical study. *eBioMedicine* **2022**, *80*, 104045, doi:10.1016/j.
 164. Chan, B.K.; Sistro, M.; Wertz, J.E.; Kortright, K.E.; Narayan, D.; Turner, P.E. Phage selection restores antibiotic sensitivity in MDR *Pseudomonas aeruginosa*. *Sci. Rep.* **2016**, *6*, 26717, doi:10.1038/srep26717.
 165. Chan, B.K.; Turner, P.E.; Kim, S.; Mojibian, H.R.; Eleftheriades, J.A.; Narayan, D. Phage treatment of an aortic graft infected with *Pseudomonas aeruginosa*. *Evol. Med. Public Heal.* **2018**, *2018*, 60–66, doi:10.1093/emph/eoy005.
 166. Chung, I.-Y.; Jang, H.-J.; Bae, H.-W.; Cho, Y.-H. A phage protein that inhibits the bacterial ATPase required for type IV pilus assembly. *Proc. Natl. Acad. Sci.* **2014**, *111*, 11503–11508, doi:10.1073/pnas.1403537111.
 167. De Smet, J.; Wagemans, J.; Hendrix, H.; Staes, I.; Visnapuu, A.; Horemans, B.; Aertsen, A.; Lavigne, R. Bacteriophage-mediated interference of the c-di-GMP signalling pathway

- in *Pseudomonas aeruginosa*. *Microb. Biotechnol.* **2021**, *14*, 967–978, doi:10.1111/1751-7915.13728.
168. McCutcheon, J.G.; Lin, A.; Dennis, J.J. Characterization of *Stenotrophomonas maltophilia* phage AXL1 as a member of the genus *Pamexvirus* encoding resistance to trimethoprim–sulfamethoxazole. *Sci. Rep.* **2022**, *12*, 10299, doi:10.1038/s41598-022-14025-z.
 169. Moillo, A.M. Isolation of a transducing phage forming plaques on *Pseudomonas maltophilia* and *Pseudomonas aeruginosa*. *Genet. Res.* **1973**, *21*, 287–289, doi:10.1017/S0016672300013471.
 170. Chang, H.C.; Chen, C.R.; Lin, J.W.; Shen, G.H.; Chang, K.M.; Tseng, Y.H.; Weng, S.F. Isolation and characterization of novel giant *Stenotrophomonas maltophilia* phage Φ SMA5. *Appl. Environ. Microbiol.* **2005**, *71*, 1387–1393, doi:10.1128/AEM.71.3.1387-1393.2005.
 171. Chen, C.R.; Lin, C.H.; Lin, J.W.; Chang, C.I.; Tseng, Y.H.; Weng, S.F. Characterization of a novel T4-type *Stenotrophomonas maltophilia* virulent phage Smp14. *Arch. Microbiol.* **2007**, *188*, 191–197, doi:10.1007/s00203-007-0238-5.
 172. García, P.; Monjardín, C.; Martín, R.; Madera, C.; Soberón, N.; Garcia, E.; Meana, Á.; Suárez, J.E. Isolation of new *Stenotrophomonas* bacteriophages and genomic characterization of temperate phage S1. *Appl. Environ. Microbiol.* **2008**, *74*, 7552–7560, doi:10.1128/AEM.01709-08.
 173. Fan, H.; Huang, Y.; Mi, Z.; Yin, X.; Wang, L.; Fan, H.; Zhang, Z.; An, X.; Chen, J.; Tong, Y. Complete genome sequence of IME13, a *Stenotrophomonas maltophilia* bacteriophage with large burst size and unique plaque polymorphism. *J. Virol.* **2012**, *86*, 11392–11393, doi:10.1128/jvi.01908-12.
 174. Huang, Y.; Fan, H.; Pei, G.; Fan, H.; Zhang, Z.; An, X.; Mi, Z.; Shi, T.; Tong, Y. Complete genome sequence of IME15, the first T7-Like bacteriophage lytic to pan-antibiotic-resistant *Stenotrophomonas maltophilia*. *J. Virol.* **2012**, *86*, 13839–13840, doi:10.1128/jvi.02661-12.
 175. Zhang, J.; Li, X. [Biological characteristics of phage SM1 for *Stenotrophomonas maltophilia* and its effect in animal infection model]. *Zhejiang Da Xue Xue Bao Yi Xue*

- Ban* **2013**, *42*, 331–336.
176. Lee, C.-N.; Tseng, T.-T.; Chang, H.-C.; Lin, J.-W.; Weng, S.-F. Genomic sequence of temperate phage Smp131 of *Stenotrophomonas maltophilia* that has similar prophages in xanthomonads. *BMC Microbiol.* **2014**, *14*, 17, doi:10.1186/1471-2180-14-17.
 177. Peters, D.L.; Stothard, P.; Dennis, J.J. The isolation and characterization of *Stenotrophomonas maltophilia* T4-like bacteriophage DLP6. *PLoS One* **2017**, *12*, e0173341, doi:10.1371/journal.pone.0173341.
 178. Peters, D.L.; McCutcheon, J.G.; Dennis, J.J. Characterization of novel broad-host-range bacteriophage DLP3 specific to *Stenotrophomonas maltophilia* as a potential therapeutic agent. *Front. Microbiol.* **2020**, *11*, 1358, doi:10.3389/fmicb.2020.01358.
 179. Peters, D.L.; Dennis, J.J. Complete genome sequence of temperate *Stenotrophomonas maltophilia* bacteriophage DLP5. *Genome Announc.* **2018**, *6*, e00073-18, doi:10.1128/genomeA.00073-18.
 180. Pedramfar, A.; Maal, K.B.; Mirdamadian, S.H. Phage therapy of corrosion-producing bacterium *Stenotrophomonas maltophilia* using isolated lytic bacteriophages. *Anti-Corrosion Methods Mater.* **2017**, *64*, 607–612, doi:10.1108/ACMM-02-2017-1755.
 181. Damnjanović, D.; Vázquez-Campos, X.; Elliott, L.; Willcox, M.; Bridge, W.J. Characterisation of bacteriophage vB_SmaM_Ps15 infective to *Stenotrophomonas maltophilia* clinical ocular isolates. *Viruses* **2022**, *14*, 709, doi:10.3390/v14040709.
 182. Wu, H.; Zhang, Y.; Jiang, Y.; Wu, H.; Sun, W.; Huang, Y.-P. Characterization and genomic analysis of ϕ SHP3, a new transposable bacteriophage infecting *Stenotrophomonas maltophilia*. *J. Virol.* **2021**, *95*, doi:10.1128/jvi.00019-21.
 183. Hagemann, M.; Hasse, D.; Berg, G. Detection of a phage genome carrying a zonula occludens like toxin gene (zot) in clinical isolates of *Stenotrophomonas maltophilia*. *Arch. Microbiol.* **2006**, *185*, 449–458, doi:10.1007/s00203-006-0115-7.
 184. Liu, J.; Liu, Q.; Shen, P.; Huang, Y.P. Isolation and characterization of a novel filamentous phage from *Stenotrophomonas maltophilia*. *Arch. Virol.* **2012**, *157*, 1643–1650, doi:10.1007/s00705-012-1305-z.
 185. Liu, J.; Chen, P.; Zheng, C.; Huang, Y.P. Characterization of maltocin P28, a novel phage tail-like bacteriocin from *Stenotrophomonas maltophilia*. *Appl. Environ. Microbiol.* **2013**,

- 79, 5593–5600, doi:10.1128/AEM.01648-13.
186. Petrova, M.; Shcherbatova, N.; Kurakov, A.; Mindlin, S. Genomic characterization and integrative properties of phiSMA6 and phiSMA7, two novel filamentous bacteriophages of *Stenotrophomonas maltophilia*. *Arch. Virol.* **2014**, *159*, 1293–1303, doi:10.1007/s00705-013-1882-5.
 187. Roux, S.; Krupovic, M.; Daly, R.A.; Borges, A.L.; Nayfach, S.; Schulz, F.; Sharrar, A.; Matheus Carnevali, P.B.; Cheng, J.F.; Ivanova, N.N.; et al. Cryptic inoviruses revealed as pervasive in bacteria and archaea across Earth's biomes. *Nat. Microbiol.* **2019**, *4*, 1895–1906, doi:10.1038/s41564-019-0510-x.
 188. Burgener, E.B.; Sweere, J.M.; Bach, M.S.; Secor, P.R.; Haddock, N.; Jennings, L.K.; Marvig, R.L.; Johansen, H.K.; Rossi, E.; Cao, X.; et al. Filamentous bacteriophages are associated with chronic *Pseudomonas* lung infections and antibiotic resistance in cystic fibrosis. *Sci. Transl. Med.* **2019**, *11*, 9748, doi:10.1126/scitranslmed.aau9748.
 189. Sweere, J.M.; Van Belleghem, J.D.; Ishak, H.; Bach, M.S.; Popescu, M.; Sunkari, V.; Kaber, G.; Manasherob, R.; Suh, G.A.; Cao, X.; et al. Bacteriophage trigger antiviral immunity and prevent clearance of bacterial infection. *Science (80-.).* **2019**, *363*, doi:10.1126/science.aat9691.
 190. Secor, P.R.; Burgener, E.B.; Kinnersley, M.; Jennings, L.K.; Roman-Cruz, V.; Popescu, M.; Van Belleghem, J.D.; Haddock, N.; Copeland, C.; Michaels, L.A.; et al. Pf bacteriophage and their impact on *Pseudomonas* virulence, mammalian immunity, and chronic infections. *Front. Immunol.* **2020**, *11*, 244, doi:10.3389/fimmu.2020.00244.
 191. Hay, I.D.; Lithgow, T. Filamentous phages: masters of a microbial sharing economy. *EMBO Rep.* **2019**, *20*, 1–24, doi:10.15252/embr.201847427.
 192. Young, R. Phage lysis: three steps, three choices, one outcome. *J. Microbiol.* **2014**, *52*, 243–258, doi:10.1007/s12275-014-4087-z.
 193. Lee, C.N.; Lin, J.W.; Chow, T.Y.; Tseng, Y.H.; Weng, S.F. A novel lysozyme from *Xanthomonas oryzae* phage ϕ Xo411 active against *Xanthomonas* and *Stenotrophomonas*. *Protein Expr. Purif.* **2006**, *50*, 229–237, doi:10.1016/j.pep.2006.06.013.
 194. Dams, D.; Brøndsted, L.; Drulis-Kawa, Z.; Briers, Y. Engineering of receptor-binding proteins in bacteriophages and phage tail-like bacteriocins. *Biochem. Soc. Trans.* **2019**, *47*,

- 449–460, doi:10.1042/BST20180172.
195. Chen, J.; Zhu, Y.; Yin, M.; Xu, Y.; Liang, X.; Huang, Y.P. Characterization of maltocin S16, a phage tail-like bacteriocin with antibacterial activity against *Stenotrophomonas maltophilia* and *Escherichia coli*. *J. Appl. Microbiol.* **2019**, *127*, 78–87, doi:10.1111/jam.14294.
 196. Marquez, A.; Newkirk, H.; Moreland, R.; Gonzalez, C.F.; Liu, M.; Ramsey, J. Complete genome sequence of *Stenotrophomonas maltophilia* podophage Ponderosa. *Microbiol. Resour. Announc.* **2019**, *8*, e01032-19, doi:10.1128/MRA.01032-19.
 197. Hayden, A.; Martinez, N.; Moreland, R.; Liu, M.; Gonzalez, C.F.; Gill, J.J.; Ramsey, J. Complete genome sequence of *Stenotrophomonas* phage Pokken. *Microbiol. Resour. Announc.* **2019**, *8*, e01095-19, doi:10.1128/mra.01095-19.
 198. Vicary, A.; Newkirk, H.; Moreland, R.; Gonzalez, C.F.; Liu, M.; Ramsey, J.; Leavitt, J. Complete genome sequence of *Stenotrophomonas maltophilia* myophage Moby. *Microbiol. Resour. Announc.* **2020**, *9*, e01422-19, doi:10.1128/mra.01422-19.
 199. Garza, K.D.; Newkirk, H.; Moreland, R.; Gonzalez, C.F.; Liu, M.; Ramsey, J.; Leavitt, J. Complete genome sequence of *Stenotrophomonas* phage Mendera. *Microbiol. Resour. Announc.* **2020**, *9*, e01411-19, doi:10.1128/mra.01411-19.
 200. Zhang, W.; Zhang, R.; Hu, Y.; Liu, Y.; Wang, L.; An, X.; Song, L.; Shi, T.; Fan, H.; Tong, Y.; et al. Biological characteristics and genomic analysis of a *Stenotrophomonas maltophilia* phage vB_SmaS_BUCT548. *Virus Genes* **2021**, *57*, 205–216, doi:10.1007/s11262-020-01818-5.
 201. Han, P.; Hu, Y.; An, X.; Song, L.; Fan, H.; Tong, Y. Biochemical and genomic characterization of a novel bacteriophage BUCT555 lysing *Stenotrophomonas maltophilia*. *Virus Res.* **2021**, *301*, 198465, doi:10.1016/j.virusres.2021.198465.
 202. Jefferson, B.; Yao, G.; Clark, J.; Le, T.; Gonzalez, C.; Liu, M.; Burrowes, B. Complete genome sequence of *Stenotrophomonas maltophilia* siphophage Salva. *Microbiol. Resour. Announc.* **2021**, *10*, e00083-21, doi:1128/MRA.00083-21.
 203. Han, K.; He, X.; Fan, H.; Song, L.; An, X.; Li, M.; Tong, Y. Characterization and genome analysis of a novel *Stenotrophomonas maltophilia* bacteriophage BUCT598 with extreme pH resistance. *Virus Res.* **2022**, *314*, 198751, doi:10.1016/j.virusres.2022.198751.

204. Patel, J.; Godoy, B.; Clark, J.; Burrowes, B.; Young, R.; Liu, M. Complete genome sequence of *Stenotrophomonas maltophilia* myophage Marzo. *Microbiol. Resour. Announc.* **2022**, *11*, 1–3, doi:10.1128/mra.01422-19.
205. Wang, N.; Garcia, J.; Clark, J.; Le, T.; Burrowes, B.; Young, R.; Liu, M. Complete genome sequence of *Stenotrophomonas maltophilia* siphophage Silvanus. *Microbiol. Resour. Announc.* **2022**, *11*, doi:10.1128/mra.01210-21.
206. Vallavanatt, I.G.; Bartz, M.; Clark, J.; Le, T.; Burrowes, B.; Liu, M. Complete genome sequence of *Stenotrophomonas maltophilia* phage Philippe. *Microbiol. Resour. Announc.* **2022**, doi:10.1128/mra.00125-22.
207. Teve, M.; Clark, J.; Le, T.; Burrowes, B.; Liu, M. Complete genome sequence of *Stenotrophomonas maltophilia* siphophage Sonora. *Microbiol. Resour. Announc.* **2022**, *11*, doi:10.1128/mra.00167-22.
208. Marmion, J.; Tate, N.; Clark, J.; Le, T.; Burrowes, B.; Liu, M. Complete genome sequence of *Stenotrophomonas maltophilia* siphophage Siara. *Microbiol. Resour. Announc.* **2022**, doi:10.1128/mra.00177-22.
209. Lee, J.; Lo, J.; Clark, J.; Le, T.; Burrowes, B.; Liu, M. Complete genome sequence of *Stenotrophomonas maltophilia* podophage Pepon. *Microbiol. Resour. Announc.* **2022**, e00158-22, doi:10.1128/mra.00158-22.
210. Kirchhoff, M.; Ortega, C.; Clark, J.; Le, T.; Burrowes, B.; Liu, M. Complete genome sequence of *Stenotrophomonas maltophilia* podophage Piffle. *Microbiol. Resour. Announc.* **2022**, *11*, doi:10.1128/mra.00159-22.
211. Jeon, E.; Hudson, A.; Talcott, A.; Clark, J.; Le, T.; Burrowes, B.; Liu, M. Complete genome sequence of *Stenotrophomonas maltophilia* podophage Paxi. *Microbiol. Resour. Announc.* **2022**, doi:10.1128/mra.00179-22.
212. Berg, A.; Tate, N.; Clark, J.; Le, T.; Burrowes, B.; Liu, M. Complete genome sequence of *Stenotrophomonas maltophilia* podophage Ptah. *Microbiol. Resour. Announc.* **2022**, *11*, doi:10.1128/mra.00137-22.
213. Emilia, Q.; Groover, K.; Clark, J.; Le, T.; Burrowes, B.; Liu, M. Complete genome sequence of *Stenotrophomonas maltophilia* siphophage Suso. *Microbiol. Resour. Announc.* **2022**, *11*, doi:10.1128/mra.00117-22.

214. Bishop, A.; Zhang, X.-H.; Clark, J.; Le, T.; Burrowes, B.; Liu, M. Complete genome sequence of *Stenotrophomonas maltophilia* siphophage Summit. *Microbiol. Resour. Announc.* **2022**, *11*, doi:10.1128/mra.00089-22.
215. Sullivan, T.; Manuel, N.; Clark, J.; Liu, M.; Burrowes, B. Complete genome sequence of *Stenotrophomonas maltophilia* siphophage Suzuki. *Microbiol. Resour. Announc.* **2022**, *11*, doi:10.1128/mra.00136-22.
216. Nishimura, Y.; Yoshida, T.; Kuronishi, M.; Uehara, H.; Ogata, H.; Goto, S. ViPTree: The viral proteomic tree server. *Bioinformatics* **2017**, *33*, 2379–2380, doi:10.1093/bioinformatics/btx157.
217. McCutcheon, J.G.; Dennis, J.J. The potential of phage therapy against the emerging opportunistic pathogen *Stenotrophomonas maltophilia*. *Viruses* **2021**, *13*, 1057, doi:10.3390/v13061057.
218. Lewenza, S.; Falsafi, R.K.; Winsor, G.; Gooderham, W.J.; Mcphee, J.B.; Brinkman, F.S.L.; Hancock, R.E.W. Construction of a mini-Tn5-*luxCDABE* mutant library in *Pseudomonas aeruginosa* PAO1: A tool for identifying differentially regulated genes. *Genome Res.* **2005**, *15*, 583–589, doi:10.1101/gr.3513905.localization.
219. Jacobs, M.A.; Alwood, A.; Thaipisuttikul, I.; Spencer, D.; Haugen, E.; Ernst, S.; Will, O.; Kaul, R.; Raymond, C.; Levy, R.; et al. Comprehensive transposon mutant library of *Pseudomonas aeruginosa*. *Proc. Natl. Acad. Sci.* **2003**, *100*, 14339–14344, doi:10.1073/pnas.2036282100.
220. Held, K.; Ramage, E.; Jacobs, M.; Gallagher, L.; Manoil, C. Sequence-verified two-allele transposon mutant library for *Pseudomonas aeruginosa* PAO1. *J. Bacteriol.* **2012**, *194*, 6387–6389, doi:10.1128/JB.01479-12.
221. Holloway, B.W. Genetic recombination in *Pseudomonas aeruginosa*. *J. Gen. Microbiol* **1955**, *13*, 572–581.
222. Simon, R.; Priefer, U.; Puhler, A. A broad host range mobilization system for *in vivo* genetic engineering: transposon mutagenesis in gram negative bacteria. *Nat. Biotechnol.* **1983**, *1*, 784–791.
223. Hanahan, D.; Jessee, J.; Bloom, F.R. Plasmid transformation of *Escherichia coli* and other bacteria. *Methods Enzymol.* **1991**, *204*, 63–113.

224. Holloway, B.W.; Egan, J.B.; Monk, M. Lysogeny in *Pseudomonas aeruginosa*. *Aust. J. Exp. Biol. Med. Sci.* **1960**, *38*, 321–329, doi:10.1038/icb.1960.34.
225. Slayter, H.S.; Holloway, B.W.; Hall, C.E. The structure of *Pseudomonas aeruginosa* phages B3, E79, and F116. *J. Ultrastructure Res.* **1964**, *11*, 274–281, doi:10.1016/S0022-5320(64)90032-2.
226. Kovach, M.E.; Phillips, R.W.; Elzer, P.H.; Roop, R.M. 2nd; Peterson, K.M. pBBR1MCS: a broad-host-range cloning vector. *Biotechniques* **1994**, *16*, 800–802.
227. West, S.E.H.; Schweizer, H.P.; Dall, C.; Sample, A.K.; Runyen-Janecky, L.J. Construction of improved *Escherichia-Pseudomonas* shuttle vectors derived from pUC18/19 and sequence of the region required for their replication in *Pseudomonas aeruginosa*. *Gene* **1994**, *128*, 81–86.
228. Hoang, T.T.; Karkhoff-Schweizer, R.R.; Kutchma, A.J.; Schweizer, H.P. A broad-host-range Flp-FRT recombination system for site-specific excision of chromosomally-located DNA sequences: Application for isolation of unmarked *Pseudomonas aeruginosa* mutants. *Gene* **1998**, *212*, 77–86, doi:10.1016/S0378-1119(98)00130-9.
229. Kropinski, A.M.; Mazzocco, A.; Waddell, T.E.; Lingohr, E.; Johnson, R.P. Enumeration of bacteriophages by double agar overlay plaque assay. In *Bacteriophages: Methods and Protocols, Volume 1: Isolation, Characterization, and Interactions*; Clokie, M.R.J., Kropinski, A.M., Eds.; Humana Press: New Delhi, India, 2009; pp. 69–76.
230. Kearse, M.; Moir, R.; Wilson, A.; Stones-Havas, S.; Cheung, M.; Sturrock, S.; Buxton, S.; Cooper, A.; Markowitz, S.; Duran, C.; et al. Geneious Basic: an integrated and extendable desktop software platform for the organization and analysis of sequence data. *Bioinformatics* **2012**, *28*, 1647–1649, doi:10.1093/bioinformatics/bts199.
231. Edgar, R.C. MUSCLE: multiple sequence alignment with high accuracy and high throughput. *Nucleic Acids Res.* **2004**, *32*, 1792–1797, doi:10.1093/nar/gkh340.
232. Chojnacki, S.; Cowley, A.; Lee, J.; Foix, A.; Lopez, R. Programmatic access to bioinformatics tools from EMBL-EBI update: 2017. *Nucleic Acids Res.* **2017**, *45*, W550–W553, doi:10.1093/nar/gkx273.
233. Hmelo, L.R.; Borlee, B.R.; Almblad, H.; Love, M.E.; Randall, T.E.; Tseng, B.S.; Lin, C.; Irie, Y.; Storek, K.M.; Yang, J.J.; et al. Precision-engineering the *Pseudomonas*

- aeruginosa* genome with two-step allelic exchange. *Nat. Protoc.* **2015**, *10*, 1820–1841, doi:10.1038/nprot.2015.115.
234. Heckman, K.L.; Pease, L.R. Gene splicing and mutagenesis by PCR-driven overlap extension. *Nat. Protoc.* **2007**, *2*, 924–932, doi:10.1038/nprot.2007.132.
 235. Poole, K.; Heinrichs, D.E.; Neshat, S. Cloning and sequence analysis of an EnvCD homologue in *Pseudomonas aeruginosa*: regulation by iron and possible involvement in the secretion of the siderophore pyoverdine. *Mol. Microbiol.* **1993**, *10*, 529–544, doi:10.1111/j.1365-2958.1993.tb00925.x.
 236. Choi, K.H.; Kumar, A.; Schweizer, H.P. A 10-min method for preparation of highly electrocompetent *Pseudomonas aeruginosa* cells: Application for DNA fragment transfer between chromosomes and plasmid transformation. *J. Microbiol. Methods* **2006**, *64*, 391–397, doi:10.1016/j.mimet.2005.06.001.
 237. Ye, X.; Dong, H.; Huang, Y.P. Highly efficient transformation of *Stenotrophomonas maltophilia* S21, an environmental isolate from soil, by electroporation. *J. Microbiol. Methods* **2014**, *107*, 92–97, doi:10.1016/j.mimet.2014.09.010.
 238. Turnbull, L.; Whitchurch, C.B. Motility assay: Twitching motility. In *Pseudomonas Methods and Protocols*; Filloux, A., Ramos, J.-L., Eds.; Humana Press: New York, NY, 2014; Vol. 1149, pp. 73–86 ISBN 978-1-4939-0472-3.
 239. Schneider, C.A.; Rasband, W.S.; Eliceiri, K.W. NIH Image to ImageJ: 25 years of image analysis. *Nat. Methods* **2012**, *9*, 671–675, doi:10.1038/nmeth.2089.
 240. Burrows, L.L. Weapons of mass retraction. *Mol. Microbiol.* **2005**, *57*, 878–888, doi:10.1111/j.1365-2958.2005.04703.x.
 241. Nguyen, Y.; Sugiman-Marangos, S.; Harvey, H.; Bell, S.D.; Charlton, C.L.; Junop, M.S.; Burrows, L.L. *Pseudomonas aeruginosa* minor pilins prime type IVa pilus assembly and promote surface display of the PilY1 adhesin. *J. Biol. Chem.* **2015**, *290*, 601–611, doi:10.1074/jbc.M114.616904.
 242. Kus, J. V.; Tullis, E.; Cvitkovitch, D.G.; Burrows, L.L. Significant differences in type IV pilin allele distribution among *Pseudomonas aeruginosa* isolates from cystic fibrosis (CF) versus non-CF patients. *Microbiology* **2004**, *150*, 1315–1326, doi:10.1099/mic.0.26822-0.
 243. Giltner, C.L.; Rana, N.; Lunardo, M.N.; Hussain, A.Q.; Burrows, L.L. Evolutionary and

- functional diversity of the *Pseudomonas* type IVa pilin island. *Environ. Microbiol.* **2011**, *13*, 250–264, doi:10.1111/j.1462-2920.2010.02327.x.
244. Elleman, T.C.; Hoyne, P.A.; Stewart, D.J.; Mckern, N.M.; Peterson², J.E. Expression of pili from *Bacteroides nodosus* in *Pseudomonas aeruginosa*. *J. Bacteriol.* **1986**, *168*, 574–580.
 245. Beard, M.K.M.; Mattick, J.S.; Moore, L.J.; Mott, M.R.; Marrs, C.F.; Egerton², J.R. Morphogenetic expression of *Moraxella bovis* fimbriae (pili) in *Pseudomonas aeruginosa*. *J. Bacteriol.* **1990**, *172*, 2601–2607.
 246. Hoyne, P.A.; Haas, R.; Meyer, T.F.; Davies, J.K.; Elleman, T.C. Production of *Neisseria gonorrhoeae* pili (fimbriae) in *Pseudomonas aeruginosa*. *J. Bacteriol.* **1992**, *174*, 7321–7327.
 247. Sauvonnnet, N.; Gounon, P.; Pugsley, A.P. PpdD type IV pilin of *Escherichia coli* K-12 can be assembled into pili in *Pseudomonas aeruginosa*. *J. Bacteriol.* **2000**, *182*, 848–854.
 248. Aas, F.E.; Wolfgang, M.; Frye, S.; Dunham, S.; Løvold, C.; Koomey, M. Competence for natural transformation in *Neisseria gonorrhoeae*: components of DNA binding and uptake linked to type IV pilus expression. *Mol. Microbiol.* **2002**, *46*, 749–760, doi:10.1046/j.1365-2958.2002.03265.x.
 249. Roine, E.; Raineri, D.M.; Romantschuk, M.; Wilson, M.; Nunn, D.N. Characterization of type IV pilus genes in *Pseudomonas syringae* pv. *tomato* DC3000. *Mol. Plant-Microbe Interact.* **1998**, *11*, 1048–1056.
 250. Watson, A.A.; Mattick, J.S.; Aim, R.A. Functional expression of heterologous type 4 fimbriae in *Pseudomonas aeruginosa*. *Gene* **1996**, *175*, 143–150.
 251. Winther-Larsen, H.C.; Wolfgang, M.C.; Van Putten, J.P.M.; Roos, N.; Aas, F.E.; Egge-Jacobsen, W.M.; Maier, B.; Koomey, M. *Pseudomonas aeruginosa* type IV pilus expression in *Neisseria gonorrhoeae*: Effects of pilin subunit composition on function and organelle dynamics. *J. Bacteriol.* **2007**, *189*, 6676–6685, doi:10.1128/JB.00407-07.
 252. Haley, C.L.; Kruczek, C.; Qaisar, U.; Colmer-Hamood, J.A.; Hamood, A.N. Mucin inhibits *Pseudomonas aeruginosa* biofilm formation by significantly enhancing twitching motility. *Can. J. Microbiol.* **2014**, *60*, 155–166, doi:10.1139/cjm-2013-0570.
 253. Harvey, H.; Bondy-Denomy, J.; Marquis, H.; Sztanko, K.M.; Davidson, A.R.; Burrows,

- L.L. *Pseudomonas aeruginosa* defends against phages through type IV pilus glycosylation. *Nat. Microbiol.* **2018**, *3*, 47–52, doi:10.1038/s41564-017-0061-y.
254. Bradley, D.E. A pilus-dependent *Pseudomonas aeruginosa* bacteriophage with a long noncontractile tail. *Virology* **1973**, *51*, 489–492.
 255. Pemberton, J.M. F116: A DNA bacteriophage specific for the pili of *Pseudomonas aeruginosa* strain PAO. *Virology* **1973**, *55*, 558–560, doi:10.1016/0042-6822(73)90203-1.
 256. Budzik, J.M.; Rosche, W.A.; Rietsch, A.; O’toole, G.A. Isolation and characterization of a generalized transducing phage for *Pseudomonas aeruginosa* strains PAO1 and PA14. *J. Bacteriol.* **2004**, *186*, 3270–3273, doi:10.1128/JB.186.10.3270–3273.2004.
 257. Heo, Y.-J.; Chung, I.-Y.; Choi, K.B.; Lau, G.W.; Cho, Y.-H. Genome sequence comparison and superinfection between two related *Pseudomonas aeruginosa* phages, D3112 and MP22. *Microbiology* **2007**, *153*, 2885–2895, doi:10.1099/mic.0.2007/007260-0.
 258. Bae, H.-W.; Cho, Y.-H. Complete genome sequence of *Pseudomonas aeruginosa* podophage MPK7, which requires type IV pili for infection. *Genome Announc.* **2013**, *1*, e00744-13, doi:10.1128/genomeA.00744-13.
 259. Leon, M.; Bastias, R. Virulence reduction in bacteriophage resistant bacteria. *Front. Microbiol.* **2015**, *6*, 343, doi:10.3389/fmicb.2015.00343.
 260. Mirzaei, M.K.; Nilsson, A.S. Isolation of phages for phage therapy: a comparison of spot tests and efficiency of plating analyses for determination of host range and efficacy. *PLoS One* **2015**, *10*, e0118557, doi:10.1371/journal.pone.0118557.
 261. *Current protocols in molecular biology*; Ausubel, F.M., Brent, R., Kingston, R.E., Moore, D.D., Seidman, J.G., Smith, J.A., Struhl, K., Eds.; Greene Publishing and Wiley-Interscience: New York, NY, 1987; ISBN 047150338X.
 262. Afgan, E.; Baker, D.; Batut, B.; Van Den Beek, M.; Bouvier, D.; Ech, M.; Chilton, J.; Clements, D.; Coraor, N.; Grüning, B.A.; et al. The Galaxy platform for accessible, reproducible and collaborative biomedical analyses: 2018 update. *Nucleic Acids Res.* **2018**, *46*, W537–W544, doi:10.1093/nar/gky379.
 263. Seemann, T. Prokka: Rapid prokaryotic genome annotation. *Bioinformatics* **2014**, *30*, 2068–2069, doi:10.1093/bioinformatics/btu153.

264. Altschul, S.F.; Gish, W.; Miller, W.; Myers, E.W.; Lipman, D.J. Basic local alignment search tool. *J. Mol. Biol.* **1990**, *215*, 403–410, doi:10.1016/S0022-2836(05)80360-2.
265. Lu, S.; Wang, J.; Chitsaz, F.; Derbyshire, M.K.; Geer, R.C.; Gonzales, N.R.; Gwadz, M.; Hurwitz, D.I.; Marchler, G.H.; Song, J.S.; et al. CDD/SPARCLE: the conserved domain database in 2020. *Nucleic Acids Res.* **2020**, *48*, D265–D268, doi:10.1093/nar/gkz991.
266. Gilchrist, C.L.M.; Chooi, Y.H. Clinker & clustermap.js: Automatic generation of gene cluster comparison figures. *Bioinformatics* **2021**, *37*, 2473–2475, doi:10.1093/bioinformatics/btab007.
267. Seed, K.D.; Dennis, J.J. Development of *Galleria mellonella* as an alternative infection model for the *Burkholderia cepacia* complex. *Infect. Immun.* **2008**, *76*, 1267–1275, doi:10.1128/IAI.01249-07.
268. Kamal, F.; Peters, D.L.; McCutcheon, J.G.; Dunphy, G.B.; Dennis, J.J. Use of greater wax moth larvae (*Galleria mellonella*) as an alternative animal infection model for analysis of bacterial pathogenesis. In *Methods in Molecular Biology*; 2019; Vol. 1898, pp. 163–171.
269. Thomson, E.L.S.; Dennis, J.J. Common duckweed (*Lemna minor*) is a versatile high-throughput infection model for the *Burkholderia cepacia* Complex and other pathogenic bacteria. *PLoS One* **2013**, *8*, e80102, doi:10.1371/journal.pone.0080102.
270. Abedon, S.T. Lysis from without. *Bacteriophage* **2011**, *1*, 46–49, doi:10.4161/bact.1.1.13980.
271. Pirnay, J.P.; Verbeken, G.; Rose, T.; Jennes, S.; Zizi, M.; Huys, I.; Lavigne, R.; Merabishvili, M.; Vanechoutte, M.; Buckling, A.; et al. Introducing yesterday's phage therapy in today's medicine. *Future Virol.* **2012**, *7*, 379–390, doi:10.2217/FVL.12.24/ASSET/IMAGES/LARGE/FIGURE2.JPEG.
272. Dunger, G.; Llontop, E.; Guzzo, C.R.; Farah, C.S. The *Xanthomonas* type IV pilus. *Curr. Opin. Microbiol.* **2016**, *30*, 88–97, doi:10.1016/j.mib.2016.01.007.
273. Burdman, S.; Bahar, O.; Parker, J.K.; de la Fuente, L. Involvement of type IV pili in pathogenicity of plant pathogenic bacteria. *Genes (Basel)*. **2011**, *2*, 706–735, doi:10.3390/genes2040706.
274. Riechmann, L.; Holliger, P. The C-terminal domain of TolA is the coreceptor for filamentous phage infection of *E. coli*. *Cell* **1997**, *90*, 351–360, doi:10.1016/S0092-

8674(00)80342-6.

275. Karlsson, F.; Borrebaeck, C.A.K.; Nilsson, N.; Malmberg-Hager, A.C. The mechanism of bacterial infection by filamentous phages involves molecular interactions between TolA and phage protein 3 domains. *J. Bacteriol.* **2003**, *185*, 2628–2634, doi:10.1128/JB.185.8.2628-2634.2003.
276. Dennis, J.J.; Zylstra, G.J. Plasposons: Modular self-cloning minitransposon derivatives for rapid genetic analysis of Gram-negative bacterial genomes. *Appl. Environ. Microbiol.* **1998**, *64*, 2710–2715, doi:10.1128/aem.64.7.2710-2715.1998.
277. Llontop, E.E.; Cenens, W.; Favaro, D.C.; Sgro, G.G.; Salinas, R.K.; Guzzo, C.R.; Farah, C.S. The PilB-PilZ-FimX regulatory complex of the Type IV pilus from *Xanthomonas citri*. *PLoS Pathog.* **2021**, *17*, doi:10.1371/journal.ppat.1009808.
278. Liew, K.W.; Alvarez, A.M. Biological and morphological characterization of *Xanthomonas campestris* bacteriophages. *Phytopathology* **1981**, *71*, 269–273.
279. Nakayinga, R.; Makumi, A.; Tumuhaise, V.; Tinzaara, W. *Xanthomonas* bacteriophages: a review of their biology and biocontrol applications in agriculture. *BMC Microbiol.* **2021**, *21*, 1–20.
280. Dunger, G.; Guzzo, C.R.; Andrade, M.O.; Jones, J.B.; Farah, C.S. *Xanthomonas citri* subsp. *citri* type IV pilus is required for twitching motility, biofilm development, and adherence. *Mol. Plant-Microbe Interact.* **2014**, *27*, 1132–1147, doi:10.1094/MPMI-06-14-0184-R.
281. Ahern, S.J.; Das, M.; Bhowmick, T.S.; Young, R.; Gonzalez, C.F. Characterization of novel virulent broad-host-range phages of *Xylella fastidiosa* and *Xanthomonas*. *J. Bacteriol.* **2014**, *196*, 459–471, doi:10.1128/JB.01080-13.
282. Das, M.; Bhowmick, T.S.; Ahern, S.J.; Young, R.; Gonzalez, C.F. Control of Pierce's Disease by phage. *PLoS One* **2015**, *10*, e0128902, doi:10.1371/journal.pone.0128902.
283. Jacques, M.A.; Arlat, M.; Boulanger, A.; Boureau, T.; Carrère, S.; Cesbron, S.; Chen, N.W.G.; Cociancich, S.; Darrasse, A.; Denancé, N.; et al. Using ecology, physiology, and genomics to understand host specificity in *Xanthomonas*. *Annu. Rev. Phytopathol.* **2016**, *54*, 163–187, doi:10.1146/annurev-phyto-080615-100147.
284. Tambong, J.T.; Xu, R.; Cuppels, D.; Chapados, J.; Gerdis, S.; Eyres, J.; Koziol, A.;

- Dettman, J. Whole genome resources and species-level taxonomic validation of 89 plant pathogenic *Xanthomonas* strains isolated from various host plants. *Plant Dis.* **2022**, doi:10.1094/pdis-11-21-2498-sc.
285. Jaenicke, S.; Bunk, B.; Wibberg, D.; Spröer, C.; Hersemann, L.; Blom, J.; Winkler, A.; Schatschneider, S.; Albaum, S.P.; Kölliker, R.; et al. Complete genome sequence of the barley pathogen *Xanthomonas translucens* pv. *translucens* DSM 18974T (ATCC 19319T). *Genome Announc.* **2016**, *4*, 1334–1350, doi:10.1128/genomeA.01334-16.
 286. Buttner, C.; McAuliffe, O.; Ross, R.P.; Hill, C.; O'Mahony, J.; Coffey, A. Bacteriophages and bacterial plant diseases. *Front. Microbiol.* **2017**, *8*.
 287. Betts, J.W.; Phee, L.M.; Woodford, N.; Wareham, D.W. Activity of colistin in combination with tigecycline or rifampicin against multidrug-resistant *Stenotrophomonas maltophilia*. *Eur. J. Clin. Microbiol. Infect. Dis.* **2014**, *33*, 1565–1572, doi:10.1007/s10096-014-2101-3.
 288. Melloul, E.; Roisin, L.; Durieux, M.F.; Woerther, P.L.; Jenot, D.; Risco, V.; Guillot, J.; Dannaoui, E.; Decousser, J.W.; Botterel, F. Interactions of *Aspergillus fumigatus* and *Stenotrophomonas maltophilia* in an in vitro mixed biofilm model: Does the strain matter? *Front. Microbiol.* **2018**, *9*, 2850, doi:10.3389/fmicb.2018.02850.
 289. Tsai, C.J.Y.; Loh, J.M.S.; Proft, T. *Galleria mellonella* infection models for the study of bacterial diseases and for antimicrobial drug testing. *Virulence* **2016**, *7*, 214–229, doi:10.1080/21505594.2015.1135289.
 290. Seed, K.D.; Dennis, J.J. Experimental bacteriophage therapy increases survival of *Galleria mellonella* larvae infected with clinically relevant strains of the *Burkholderia cepacia* complex. *Antimicrob. Agents Chemother.* **2009**, *53*, 2205–2208, doi:10.1128/AAC.01166-08.
 291. Cutuli, M.A.; Petronio Petronio, G.; Vergalito, F.; Magnifico, I.; Pietrangelo, L.; Venditti, N.; Di Marco, R. *Galleria mellonella* as a consolidated in vivo model hosts: New developments in antibacterial strategies and novel drug testing. *Virulence* **2019**, *10*, 527–541, doi:10.1080/21505594.2019.1621649.
 292. Buchanan, S.K.; Lukacik, P.; Grizot, S.; Ghirlando, R.; Ali, M.M.U.; Barnard, T.J.; Jakes, K.S.; Kienker, P.K.; Esser, L. Structure of colicin I receptor bound to the R-domain of

- colicin Ia: Implications for protein import. *EMBO J.* **2007**, 26, 2594–2604, doi:10.1038/sj.emboj.7601693.
293. Killmann, H.; Videnov, G.; Jung, G.; Schwarz, H.; Braun, V. Identification of receptor binding sites by competitive peptide mapping: Phages T1, T5, and ϕ 80 and colicin M bind to the gating loop of FhuA. *J. Bacteriol.* **1995**, 177, 694–698, doi:10.1128/jb.177.3.694-698.1995.
 294. Troxell, B.; Hassan, H.M. Transcriptional regulation by Ferric Uptake Regulator (Fur) in pathogenic bacteria. *Front. Cell. Infect. Microbiol.* **2013**, 3, 59, doi:10.3389/fcimb.2013.00059.
 295. García, C.A.; Alcaraz, E.S.; Franco, M.A.; De Rossi, B.N.P. Iron is a signal for *Stenotrophomonas maltophilia* biofilm formation, oxidative stress response, OMPs expression, and virulence. *Front. Microbiol.* **2015**, 6, 1–14, doi:10.3389/fmicb.2015.00926.
 296. Bonnain, C.; Breitbart, M.; Buck, K.N. The Ferrojan horse hypothesis: Iron-virus interactions in the ocean. *Front. Mar. Sci.* **2016**, 3, doi:10.3389/fmars.2016.00082.
 297. Ito, A.; Sato, T.; Ota, M.; Takemura, M.; Nishikawa, T.; Toba, S.; Kohira, N.; Miyagawa, S.; Ishibashi, N.; Matsumoto, S.; et al. In vitro antibacterial properties of cefiderocol, a novel siderophore cephalosporin, against Gram-negative bacteria. *Antimicrob. Agents Chemother.* **2018**, 62, e01454-17, doi:10.1128/AAC.01454-17.
 298. McElheny, C.L.; Fowler, E.L.; Iovleva, A.; Shields, R.K.; Doi, Y. In Vitro evolution of cefiderocol resistance in an NDM-producing *Klebsiella pneumoniae* due to functional loss of CirA. *Microbiol. Spectr.* **2021**, 9, e01779-21, doi:10.1128/spectrum.01779-21.
 299. Kiljunen, S.; Datta, N.; Dentovskaya, S. V.; Anisimov, A.P.; Knirel, Y.A.; Bengoechea, J.A.; Holst, O.; Skurnik, M. Identification of the lipopolysaccharide core of *Yersinia pestis* and *Yersinia pseudotuberculosis* as the receptor for bacteriophage ϕ A1122. *J. Bacteriol.* **2011**, 193, 4963–4972, doi:10.1128/JB.00339-11.
 300. Carlson, K. Working with bacteriophages: common techniques and methodological approaches. In *Bacteriophages: Biology and Applications*; Kutter, E.M., Sulakvelidze, A., Eds.; CRC Press: Boca Raton, Florida, 2005; pp. 437–494.
 301. Andrews, S. FastQC: a quality control tool for high throughput sequence data Available

- online: <http://www.bioinformatics.babraham.ac.uk/projects/fastqc/>.
302. Bolger, A.M.; Lohse, M.; Usadel, B. Trimmomatic: a flexible trimmer for Illumina sequence data. *Bioinformatics* **2014**, *30*, 2114–2120, doi:10.1093/bioinformatics/btu170.
 303. Bankevich, A.; Nurk, S.; Antipov, D.; Gurevich, A.A.; Dvorkin, M.; Kulikov, A.S.; Lesin, V.M.; Nikolenko, S.I.; Pham, S.; Prjibelski, A.D.; et al. SPAdes: a new genome assembly algorithm and its applications to single-cell sequencing. *J. Comput. Biol.* **2012**, *19*, 455–477, doi:10.1089/cmb.2012.0021.
 304. Delcher, A.L.; Bratke, K.A.; Powers, E.C.; Salzberg, S.L. Identifying bacterial genes and endosymbiont DNA with Glimmer. *Bioinformatics* **2007**, *23*, 673–679, doi:10.1093/bioinformatics/btm009.
 305. Besemer, J.; Lomsadze, A.; Borodovsky, M. GeneMarkS: a self-training method for prediction of gene starts in microbial genomes. Implications for finding sequence motifs in regulatory regions. *Nucleic Acids Res.* **2001**, *29*, 2607–2618, doi:10.1093/nar/29.12.2607.
 306. Hyatt, D.; Chen, G.L.; LoCascio, P.F.; Land, M.L.; Larimer, F.W.; Hauser, L.J. Prodigal: prokaryotic gene recognition and translation initiation site identification. *BMC Bioinformatics* **2010**, *11*, 119, doi:10.1186/1471-2105-11-119.
 307. Krogh, A.; Larsson, B.; Von Heijne, G.; Sonnhammer, E.L.L. Predicting transmembrane protein topology with a hidden Markov model: application to complete genomes. *J. Mol. Biol.* **2001**, *305*, 567–580, doi:10.1006/jmbi.2000.4315.
 308. Juncker, A.S.; Willenbrock, H.; Von Heijne, G.; Brunak, S.; Nielsen, H.; Krogh, A. Prediction of lipoprotein signal peptides in Gram-negative bacteria. *Protein Sci.* **2003**, *12*, 1652–1662, doi:10.1110/ps.0303703.
 309. Chan, P.P.; Lowe, T.M. tRNAscan-SE: searching for tRNA genes in genomic sequences. In *Gene Prediction: Methods and Protocols, Methods in Molecular Biology*; Kollmar, M., Ed.; Humana: New York, NY, 2019; Vol. 1962, pp. 1–14.
 310. Laslett, D.; Canback, B. ARAGORN, a program to detect tRNA genes and tmRNA genes in nucleotide sequences. *Nucleic Acids Res.* **2004**, *32*, 11–16, doi:10.1093/nar/gkh152.
 311. Bin Jang, H.; Bolduc, B.; Zablocki, O.; Kuhn, J.H.; Roux, S.; Adriaenssens, E.M.; Brister, J.R.; Kropinski, A.M.; Krupovic, M.; Lavigne, R.; et al. Taxonomic assignment of

- uncultivated prokaryotic virus genomes is enabled by gene-sharing networks. *Nat. Biotechnol.* **2019**, *37*, 632–639, doi:10.1038/s41587-019-0100-8.
312. Shannon, P.; Markiel, A.; Ozier, O.; Baliga, N.S.; Wang, J.T.; Ramage, D.; Amin, N.; Schwikowski, B.; Ideker, T. Cytoscape: A software environment for integrated models of biomolecular interaction networks. *Genome Res.* **2003**, *13*, 2498–2504, doi:10.1101/gr.1239303.
 313. Ackermann, H.W.; Eisenstark, A. The present state of phage taxonomy. *Intervirology* **1974**, *3*, 201–219, doi:10.1159/000149758.
 314. Turner, D.; Kropinski, A.M.; Adriaenssens, E.M. A roadmap for genome-based phage taxonomy. *Viruses* **2021**, *13*, 506, doi:10.3390/v13030506.
 315. Dion, M.B.; Oechslin, F.; Moineau, S. Phage diversity, genomics and phylogeny. *Nat. Rev. Microbiol.* **2020**, *18*, 125–138, doi:10.1038/s41579-019-0311-5.
 316. Faux, N.G.; Bottomley, S.P.; Lesk, A.M.; Irving, J.A.; Morrison, J.R.; De La Banda, M.G.; Whisstock, J.C. Functional insights from the distribution and role of homopeptide repeat-containing proteins. *Genome Res.* **2005**, *15*, 537–551, doi:10.1101/gr.3096505.
 317. Chou, C.C.; Wang, A.H.J. Structural D/E-rich repeats play multiple roles especially in gene regulation through DNA/RNA mimicry. *Mol. Biosyst.* **2015**, *11*, 2144–2151, doi:10.1039/c5mb00206k.
 318. Maley, F.; Maley, G.F. A tale of two enzymes, deoxycytidylate deaminase and thymidylate synthase. *Prog. Nucleic Acid Res. Mol. Biol.* **1990**, *39*, 49–80, doi:10.1016/S0079-6603(08)60623-6.
 319. Hardy, L.W.; Finer-Moore, J.S.; Montfort, W.R.; Jones, M.O.; Santi, D. V; Stroud, R.M. Atomic structure of thymidylate synthase: target for rational drug design. *Science (80-.).* **1987**, *235*, 448–455, doi:10.1126/science.3099389.
 320. Mathews, I.I.; Deacon, A.M.; Canaves, J.M.; McMullan, D.; Lesley, S.A.; Agarwalla, S.; Kuhn, P. Functional analysis of substrate and cofactor complex structures of a thymidylate synthase-complementing protein. *Structure* **2003**, *11*, 677–690, doi:10.1016/S0969-2126(03)00097-2.
 321. Koch, H.; Lückner, S.; Albertsen, M.; Kitzinger, K.; Herbold, C.; Spieck, E.; Nielsen, P.H.; Wagner, M.; Daims, H. Expanded metabolic versatility of ubiquitous nitrite-oxidizing

- bacteria from the genus *Nitrospira*. *Proc. Natl. Acad. Sci. U. S. A.* **2015**, *112*, 11371–11376, doi:10.1073/pnas.1506533112.
322. Zhang, J.; Kasciukovic, T.; White, M.F. The CRISPR associated protein Cas4 is a 5' to 3' DNA exonuclease with an iron-sulfur cluster. *PLoS One* **2012**, *7*, e47232, doi:10.1371/journal.pone.0047232.
 323. Hooton, S.P.T.; Connerton, I.F. *Campylobacter jejuni* acquire new host-derived CRISPR spacers when in association with bacteriophages harboring a CRISPR-like Cas4 protein. *Front. Microbiol.* **2015**, *5*, 744, doi:10.3389/fmicb.2014.00744.
 324. Hudaiberdiev, S.; Shmakov, S.; Wolf, Y.I.; Terns, M.P.; Makarova, K.S.; Koonin, E. V Phylogenomics of Cas4 family nucleases. *BMC Evol. Biol.* **2017**, *17*, 232, doi:10.1186/s12862-017-1081-1.
 325. Crippen, C.S.; Lee, Y.-J.; Hutinet, G.; Shajahan, A.; Sacher, J.C.; Azadi, P.; de Crécy-Lagard, V.; Weigele, P.R.; Szymanski, C.M. Deoxyinosine and 7-deaza-2-deoxyguanosine as carriers of genetic information in the DNA of *Campylobacter* viruses. *J. Virol.* **2019**, *93*, e01111-19, doi:10.1128/jvi.01111-19.
 326. Tsai, R.; Corrêa, I.R.; Xu, M.Y.; Xu, S.Y. Restriction and modification of deoxyarchaeosine (dG⁺)-containing phage 9 g DNA. *Sci. Rep.* **2017**, *7*, 8348, doi:10.1038/s41598-017-08864-4.
 327. Hatfull, G.F. Bacteriophage genomics. *Curr. Opin. Microbiol.* **2008**, *11*, 447–453, doi:10.1016/j.mib.2008.09.004.
 328. Loessner, M.J.; Wendlinger, G.; Scherer, S. Heterogeneous endolysins in *Listeria monocytogenes* bacteriophages: a new class of enzymes and evidence for conserved holin genes within the siphoviral lysis cassettes. *Mol. Microbiol.* **1995**, *16*, 1231–1241, doi:10.1111/j.1365-2958.1995.tb02345.x.
 329. Mikoulinskaia, G. V.; Odinkova, I. V.; Zimin, A.A.; Lysanskaya, V.Y.; Feofanov, S.A.; Stepnaya, O.A. Identification and characterization of the metal ion-dependent l-alanoyl-d-glutamate peptidase encoded by bacteriophage T5. *FEBS J.* **2009**, *276*, 7329–7342, doi:10.1111/j.1742-4658.2009.07443.x.
 330. Sepúlveda-Robles, O.; Kameyama, L.; Guarneros, G. High diversity and novel species of *Pseudomonas aeruginosa* bacteriophages. *Appl. Environ. Microbiol.* **2012**, *78*, 4510–

- 4515, doi:10.1128/AEM.00065-12.
331. Besemer, J.; Lomsadze, A.; Borodovsky, M. GeneMarkS: a self-training method for prediction of gene starts in microbial genomes. Implications for finding sequence motifs in regulatory regions. *Nucleic Acids Res.* **2001**, *29*, 2607–2618, doi:10.1093/nar/29.12.2607.
 332. Naville, M.; Ghuillot-Gaudeffroy, A.; Marchais, A.; Gautheret, D. ARNold: a web tool for the prediction of rho-independent transcription terminators. *RNA Biol.* **2011**, *8*, 11–13, doi:10.4161/rna.8.1.13346.
 333. Ramsey, J.; Rasche, H.; Maughmer, C.; Criscione, A.; Mijalis, E.; Liu, M.; Hu, J.C.; Young, R.; Gill, J.J. Galaxy and Apollo as a biologist-friendly interface for high-quality cooperative phage genome annotation. *PLOS Comput. Biol.* **2020**, *16*, e1008214, doi:10.1371/JOURNAL.PCBI.1008214.
 334. Yang, J.; Zhang, Y. I-TASSER server: new development for protein structure and function predictions. *Nucleic Acids Res.* **2015**, *43*, W174–W181, doi:10.1093/nar/gkv342.
 335. Yang, J.; Roy, A.; Zhang, Y. BioLiP: a semi-manually curated database for biologically relevant ligand-protein interactions. *Nucleic Acids Res.* **2013**, *41*, D1096–D1103, doi:10.1093/nar/gks966.
 336. Roy, A.; Yang, J.; Zhang, Y. COFACTOR: an accurate comparative algorithm for structure-based protein function annotation. *Nucleic Acids Res.* **2012**, *40*, W471–W477, doi:10.1093/nar/gks372.
 337. Clavijo-Coppens, F.; Ginet, N.; Cesbron, S.; Briand, M.; Jacques, M.A.; Ansaldi, M. Novel virulent bacteriophages infecting mediterranean isolates of the plant pest *Xylella fastidiosa* and *Xanthomonas albilineans*. *Viruses* **2021**, *13*, doi:10.3390/v13050725.
 338. Flodman, K.; Corrêa, I.R.; Dai, N.; Weigle, P.; Xu, S.Y. In vitro Type II restriction of bacteriophage DNA With modified pyrimidines. *Front. Microbiol.* **2020**, *11*, 604618, doi:10.3389/fmicb.2020.604618.
 339. Dong, Z.; Xing, S.; Liu, J.; Tang, X.; Ruan, L.; Sun, M.; Tong, Y.; Peng, D. Isolation and characterization of a novel phage Xoo-sp2 that infects *Xanthomonas oryzae* pv. *oryzae*. *J. Gen. Virol.* **2018**, *99*, 1453–1462, doi:10.1099/jgv.0.001133.
 340. Andrade-Domínguez, A.; Kolter, R. Complete genome sequence of *Pseudomonas*

- aeruginosa* phage AAT-1. *Genome Announc.* **2016**, *4*, 165–181, doi:10.1128/genomeA.00165-16.
341. Ravichandran, K.; Olshansky, L.; Nocera, D.G.; Stubbe, J.A. Subunit interaction dynamics of class Ia ribonucleotide reductases: in search of a robust assay. *Biochemistry* **2020**, *59*, 1442–1453, doi:10.1021/acs.biochem.0c00001.
 342. Raimondi, M.V.; Randazzo, O.; Franca, M. La; Barone, G.; Vignoni, E.; Rossi, D.; Collina, S. DHFR inhibitors: reading the past for discovering novel anticancer agents. *Molecules* **2019**, *24*, 1140, doi:10.3390/molecules24061140.
 343. Iyer, L.M.; Babu, M.M.; Aravind, L. The HIRAN domain and recruitment of chromatin remodeling and repair activities to damaged DNA. *Cell Cycle* **2006**, *5*, 775–782, doi:10.4161/cc.5.7.2629.
 344. Simon, N.C.; Aktories, K.; Barbieri, J.T. Novel bacterial ADP-ribosylating toxins: structure and function. *Nat. Rev. Microbiol.* **2014**, *12*, 599–611, doi:10.1038/nrmicro3310.
 345. Jacobs-Sera, D.; Abad, L.A.; Alvey, R.M.; Anders, K.R.; Aull, H.G.; Bhalla, S.S.; Blumer, L.S.; Bollivar, D.W.; Alfred Bonilla, J.; Butela, K.A.; et al. Genomic diversity of bacteriophages infecting *Microbacterium* spp. *PLoS One* **2020**, *15*, e0234636, doi:10.1371/journal.pone.0234636.
 346. Jamet, A.; Touchon, M.; Ribeiro-Gonçalves, B.; Carriço, J.A.; Charbit, A.; Nassif, X.; Ramirez, M.; Rocha, E.P.C. A widespread family of polymorphic toxins encoded by temperate phages. *BMC Biol.* **2017**, *15*, 75, doi:10.1186/s12915-017-0415-1.
 347. Wilkens, K.; Tiemann, B.; Bazan, F.; Rüger, W. ADP-ribosylation and early transcription regulation by bacteriophage T4. *Adv. Exp. Med. Biol.* **1997**, *419*, 71–82, doi:10.1007/978-1-4419-8632-0_8.
 348. Chen, L.; Yang, J.; Yu, J.; Yao, Z.; Sun, L.; Shen, Y.; Jin, Q. VFDB: a reference database for bacterial virulence factors. *Nucleic Acids Res.* **2005**, *33*, D325–D328, doi:10.1093/nar/gki008.
 349. Liu, M.; Deora, R.; Doulatov, S.R.; Gingery, M.; Eiserling, F.A.; Preston, A.; Maskell, D.J.; Simons, R.W.; Cotter, P.A.; Parkhill, J.; et al. Reverse transcriptase-mediated tropism switching in *Bordetella* bacteriophage. *Science (80-.).* **2002**, *295*, 2091–2094, doi:10.1126/science.1067467.

350. Inoue, T.; Shingaki, R.; Hirose, S.; Waki, K.; Mori, H.; Fukui, K. Genome-wide screening of genes required for swarming motility in *Escherichia coli* K-12. *J. Bacteriol.* **2007**, *189*, 950–957, doi:10.1128/JB.01294-06.
351. Souza, R.F. de; Aravind, L. Identification of novel components of NAD-utilizing metabolic pathways and prediction of their biochemical functions. *Mol. Biosyst.* **2012**, *8*, 1661–1677, doi:10.1039/C2MB05487F.
352. Frelin, O.; Huang, L.; Hasnain, G.; Jeffries, J.G.; Ziemak, M.J.; Rocca, J.R.; Wang, B.; Rice, J.; Roje, S.; Yurgel, S.N.; et al. A directed-overflow and damage-control N-glycosidase in riboflavin biosynthesis. *Biochem. J* **2015**, *466*, 137–145, doi:10.1042/BJ20141237.
353. Young, R.; Wang, I.N.; Roof, W.D. Phages will out: strategies of host cell lysis. *Trends Microbiol.* **2000**, *8*, 120–128, doi:10.1016/S0966-842X(00)01705-4.
354. Shan, J.; Korbsrisate, S.; Withatanung, P.; Adler, N.L.; Clokie, M.R.J.; Galyov, E.E. Temperature dependent bacteriophages of a tropical bacterial pathogen. *Front. Microbiol.* **2014**, *5*, 599, doi:10.3389/fmicb.2014.00599.
355. Egilmez, H.I.; Morozov, A.Y.; Clokie, M.R.J.; Shan, J.; Letarov, A.; Galyov, E.E. Temperature-dependent virus lifecycle choices may reveal and predict facets of the biology of opportunistic pathogenic bacteria. *Sci. Rep.* **2018**, *8*, 1–13, doi:10.1038/s41598-018-27716-3.
356. Gleckman, R.; Blagg, N.; Joubert, D.W. Trimethoprim: mechanisms of action, antimicrobial activity, bacterial resistance, pharmacokinetics, adverse reactions, and therapeutic indications. *Pharmacother. J. Hum. Pharmacol. Drug Ther.* **1981**, *1*, 14–19, doi:10.1002/j.1875-9114.1981.tb03548.x.
357. Bushby, S.R.M. Synergy of trimethoprim sulfamethoxazole. *Can. Med. Assoc. J.* **1975**, *112*, 63–66, doi:1093654.
358. Kutter, E. Phage host range and efficiency of plating. In *Bacteriophages: Methods and Protocols, Volume 1: Isolation, Characterization, and Interactions*; Clokie, M.R.J., Kropinski, A.M., Eds.; Humana Press, 2009; Vol. 501, pp. 141–149.
359. Enault, F.; Briet, A.; Bouteille, L.; Roux, S.; Sullivan, M.B.; Petit, M.A. Phages rarely encode antibiotic resistance genes: a cautionary tale for virome analyses. *ISME J.* **2017**

- III* **2016**, *11*, 237–247, doi:10.1038/ismej.2016.90.
360. Torres-Barceló, C. The disparate effects of bacteriophages on antibiotic-resistant bacteria. *Emerg. Microbes Infect.* **2018**, *7*, 168, doi:10.1038/s41426-018-0169-z.
 361. Waterhouse, A.; Bertoni, M.; Bienert, S.; Studer, G.; Tauriello, G.; Gumienny, R.; Heer, F.T.; De Beer, T.A.P.; Rempfer, C.; Bordoli, L.; et al. SWISS-MODEL: homology modelling of protein structures and complexes. *Nucleic Acids Res.* **2018**, *46*, W296–W303, doi:10.1093/nar/gky427.
 362. Zimmermann, L.; Stephens, A.; Nam, S.Z.; Rau, D.; Kübler, J.; Lozajic, M.; Gabler, F.; Söding, J.; Lupas, A.N.; Alva, V. A completely reimplemented MPI bioinformatics toolkit with a new HHpred server at its core. *J. Mol. Biol.* **2018**, *430*, 2237–2243, doi:10.1016/j.jmb.2017.12.007.
 363. Craig, L.; Volkmann, N.; Arvai, A.S.; Pique, M.E.; Yeager, M.; Egelman, E.H.H.; Tainer, J.A. Type IV pilus structure by cryo-electron microscopy and crystallography: implications for pilus assembly and functions. *Mol. Cell* **2006**, *23*, 651–662, doi:10.1016/j.molcel.2006.07.004.
 364. Schrodinger, L. The PyMOL molecular graphics system.
 365. Dunne, M.; Prokhorov, N.S.; Loessner, M.J.; Leiman, P.G. Reprogramming bacteriophage host range: design principles and strategies for engineering receptor binding proteins. *Curr. Opin. Biotechnol.* **2021**, *68*, 272–281, doi:10.1016/j.copbio.2021.02.006.
 366. Simpson, D.J.; Sacher, J.C.; Szymanski, C.M. Development of an assay for the identification of receptor binding proteins from bacteriophages. *Viruses* **2016**, *8*, 1–9, doi:10.3390/v8010017.
 367. Tisi, D.; Talts, J.F.; Timpl, R.; Hohenester, E. Structure of the C-terminal laminin G-like domain pair of the laminin alpha2 chain harbouring binding sites for alpha-dystroglycan and heparin. *EMBO J.* **2000**, *19*, 1432–1440, doi:10.1093/emboj/19.7.1432.
 368. Monteiro, R.; Pires, D.P.; Costa, A.R.; Azeredo, J. Phage therapy: Going temperate? *Trends Microbiol.* **2019**, *27*, 368–378, doi:10.1016/j.tim.2018.10.008.
 369. Pires, D.P.; Cleto, S.; Sillankorva, S.; Azeredo, J.; Lu, T.K. Genetically engineered phages: a review of advances over the last decade. *Microbiol. Mol. Biol. Rev.* **2016**, *80*, 523–543, doi:10.1128/MMBR.00069-15.Address.

370. Dedrick, R.M.; Guerrero-Bustamante, C.A.; Garlena, R.A.; Russell, D.A.; Ford, K.; Harris, K.; Gilmour, K.C.; Soothill, J.; Jacobs-Sera, D.; Schooley, R.T.; et al. Engineered bacteriophages for treatment of a patient with a disseminated drug-resistant *Mycobacterium abscessus*. *Nat. Med.* **2019**, *25*, 730–733, doi:10.1038/s41591-019-0437-z.
371. Mageeney, C.M.; Sinha, A.; Mosesso, R.A.; Medlin, D.L.; Lau, B.Y.; Rokes, A.B.; Lane, T.W.; Branda, S.S.; Williams, K.P. Computational basis for on-demand production of diversified therapeutic phage cocktails. *mSystems* **2020**, *5*, doi:10.1128/msystems.00659-20.
372. Pires, D.P.; Monteiro, R.; Mil-Homens, D.; Fialho, A.; Lu, T.K.; Azeredo, J. Designing *P. aeruginosa* synthetic phages with reduced genomes. *Sci. Rep.* **2021**, *11*, 1–10, doi:10.1038/s41598-021-81580-2.
373. Liu, J.; Dehbi, M.; Moeck, G.; Arhin, F.; Banda, P.; Bergeron, D.; Callejo, M.; Ferretti, V.; Ha, N.; Kwan, T.; et al. Antimicrobial drug discovery through bacteriophage genomics. *Nat. Biotechnol.* **2004**, *22*, 185–191, doi:10.1038/nbt932.
374. Wan, X.; Hendrix, H.; Skurnik, M.; Lavigne, R. Phage-based target discovery and its exploitation towards novel antibacterial molecules. *Curr. Opin. Biotechnol.* **2021**, *68*, 1–7, doi:10.1016/j.copbio.2020.08.015.
375. Martel, B.; Moineau, S. CRISPR-Cas: an efficient tool for genome engineering of virulent bacteriophages. *Nucleic Acids Res.* **2014**, *42*, 9504–9513, doi:10.1093/nar/gku628.
376. Lemay, M.L.; Tremblay, D.M.; Moineau, S. Genome engineering of virulent lactococcal phages using CRISPR-Cas9. *ACS Synth. Biol.* **2017**, *6*, 1351–1358, doi:10.1021/acssynbio.6b00388.
377. Guan, J.; Bosch, A.O.; Mendoza, S.D.; Karambelkar, S.; Berry, J.; Bondy-Denomy, J. RNA targeting with CRISPR-Cas13a facilitates bacteriophage genome engineering. *bioRxiv* **2022**, 2022.02.14.480438, doi:10.1101/2022.02.14.480438.
378. Adler, B.A.; Hessler, T.; Cress, B.F.; Mutalik, V.K.; Barrangou, R.; Banfield, J.; Doudna, J.A. RNA-targeting CRISPR-Cas13 provides broad-spectrum phage immunity. *bioRxiv* **2022**, 2022.03.25.485874, doi:10.1101/2022.03.25.485874.
379. Burrowes, B.H.; Molineux, I.J.; Fralick, J.A. Directed in vitro evolution of therapeutic

- bacteriophages: The Appelmans protocol. *Viruses* **2019**, *11*, doi:10.3390/v11030241.
380. Favor, A.H.; Llanos, C.D.; Youngblut, M.D.; Bardales, J.A. Optimizing bacteriophage engineering through an accelerated evolution platform. *Sci. Rep.* **2020**, *10*, doi:10.1038/s41598-020-70841-1.
 381. Millman, A.; Melamed, S.; Leavitt, A.; Doron, S.; Bernheim, A.; Hör, J.; Lopatina, A.; Ofir, G.; Hochhauser, D.; Stokar-Avihail, A.; et al. An expanding arsenal of immune systems that protect bacteria from phages. *bioRxiv* **2022**, doi:10.1101/2022.05.11.491447.
 382. Vassallo, C.; Doering, C.; Littlehale, M.L.; Teodoro, G.; Laub, M.T. Mapping the landscape of anti-phage defense mechanisms in the *E. coli* pangenome. *bioRxiv* **2022**, doi:10.1101/2022.05.12.491691.
 383. Payne, L.J.; Todeschini, T.C.; Wu, Y.; Perry, B.J.; Ronson, C.W.; Fineran, P.C.; Nobrega, F.L.; Jackson, S.A. Identification and classification of antiviral defence systems in bacteria and archaea with PADLOC reveals new system types. *Nucleic Acids Res.* **2021**, *49*, 10868–10878, doi:10.1093/nar/gkab883.
 384. LeRoux, M.; Srikant, S.; Littlehale, M.L.; Teodoro, G.; Doron, S.; Badiie, M.; Leung, A.; Sorek, R.; Laub, M.T. The DarTG toxin-antitoxin system provides phage defense by ADP-ribosylating viral DNA. *bioRxiv* **2021**, 2021.09.27.462013, doi:10.1101/2021.09.27.462013.
 385. Dy, R.L.; Przybilski, R.; Semeijn, K.; Salmond, G.P.C.; Fineran, P.C. A widespread bacteriophage abortive infection system functions through a Type IV toxin-antitoxin mechanism. *Nucleic Acids Res.* **2014**, *42*, 4590–4605, doi:10.1093/nar/gkt1419.
 386. Doron, S.; Melamed, S.; Ofir, G.; Leavitt, A.; Lopatina, A.; Keren, M.; Amitai, G.; Sorek, R. Systematic discovery of antiphage defense systems in the microbial pangenome. *Science* (80-.). **2018**, *359*, eaar4120, doi:10.1126/science.aar4120.
 387. Bondy-Denomy, J.; Pawluk, A.; Maxwell, K.L.; Davidson, A.R. Bacteriophage genes that inactivate the CRISPR/Cas bacterial immune system. *Nature* **2013**, *493*, 429–432, doi:10.1038/nature11723.
 388. Shah, M.; Taylor, V.L.; Bona, D.; Tsao, Y.; Stanley, S.Y.; Pimentel-Elardo, S.M.; McCallum, M.; Bondy-Denomy, J.; Howell, P.L.; Nodwell, J.R.; et al. A phage-encoded anti-activator inhibits quorum sensing in *Pseudomonas aeruginosa*. *Mol. Cell* **2021**, *81*,

- 571-583.e6, doi:10.1016/J.MOLCEL.2020.12.011.
389. Chibeu, A.; Ceyssens, P.J.; Hertveldt, K.; Volckaert, G.; Cornelis, P.; Matthijs, S.; Lavigne, R. The adsorption of *Pseudomonas aeruginosa* bacteriophage phiKMV is dependent on expression regulation of type IV pili genes. *FEMS Microbiol. Lett.* **2009**, *296*, 210–218, doi:10.1111/j.1574-6968.2009.01640.x.
390. Plackett, B. No money for new drugs. *Nat. Outlook* **2020**, *586*, S50–S52.
391. McKenna, M. The antibiotic gamble. *Nature* **2020**, *584*, 338–341.